Antimicrobial Adaptation in Uropathogenic *Escherichia coli*

Emma Louise Henly

A thesis submitted in partial fulfilment of the requirements of
Sheffield Hallam University
for the degree of Doctor of Philosophy

October 2019

Candidate Declaration

I hereby declare that:

1. I have not been enrolled for another award of the University, or other academic or professional organisation, whilst undertaking my research degree.

2. None of the material contained in the thesis has been used in any other submission for an academic award.

3. I am aware of and understand the University's policy on plagiarism and certify that this thesis is my own work. The use of all published or other sources of material consulted have been properly and fully acknowledged.

4. The work undertaken towards the thesis has been conducted in accordance with the SHU Principles of Integrity in Research and the SHU Research Ethics Policy.

5. The word count of the thesis is 50,991.

Name	*Emma Louise Henly*
Date	*October 2019*
Award	*PhD*
Faculty	*Health and Wellbeing*
Director(s) of Studies	*Dr Sarah Forbes*

Abstract

Catheter-associated urinary tract infections (CAUTIs) make up the largest proportion of hospital acquired infections. Uropathogenic *Escherichia coli* (UPEC) are a major causative agent of CAUTI partially due to the bacteria's ability to form biofilms on the catheter surface in addition to their extensive array of virulence factors that facilitate infection. Anti-infective coatings for urinary catheters are a promising strategy to prevent bacterial attachment and subsequent biofilm formation on the catheter thus helping to prevent CAUTI. Concerns have been raised that exposure to biocides may select for biocide resistant populations of bacteria in addition to promoting cross-resistance with third part agents such as antibiotics. This, in addition to further concerns over biocide cytotoxicity, has led to the search for alternative anti-infective coating agents that exhibit long-term antimicrobial activity and low-level cytotoxicity. Quorum sensing inhibitors (QSIs) have emerged as potential candidates to prevent such biofilm associated infections, however the long-term effects of QSIs and biocides in uropathogens is poorly understood.

In this investigation, the impact of repeated exposure of eight UPEC strains to four biocides (PHMB, triclosan, BAC, silver nitrate) and three QSIs (cinnamaldehyde, furanone C30 and F-DPD) were evaluated. Antimicrobial susceptibility in planktonic (MIC and MBC) and biofilm (MBEC) states were determined before and after repeated exposure to each antimicrobial. Changes in pathogenicity were assessed in a *Galleria mellonella* waxworm model and through the use of cell invasion assays (SMC and HUEPC cell lines). Antimicrobial activity and cytotoxicity of antimicrobial impregnated polymers was assessed via inhibition assays and through agar overlay tests. After the initial assessment, the sol gel coating was determined to have the highest biocompatibility, and was assessed for antimicrobial activity in a continuous culture drip-flow biofilm reactor. In an attempt to understand the mechanisms that govern antimicrobial adaptation in UPEC, strain EC958 was subjected to full genome and RNA-sequencing and differential expression gene analysis.

The results of these experiments show the multiple and varied effects that occur after exposure to broad-spectrum antimicrobials must be taken into consideration when developing a new antimicrobial coating as these effects have impacts on resistance, virulence, biofilm formation, and antibiotic resistance.

Table of Contents

List of Figures

List of Tables

List of Abbreviations

BAC	Benzalkonium Chloride
CAUTI	Catheter Associated Urinary Tract Infection
CFU	Colony Forming Unit
F-DPD	4-fluoro-5-hydroxypentane-2,3-dione
Furanone C30	(Z)-4-Bromo-5(bromomethylene)-2(5H)-furanone
MIC	Minimum Inhibitory Concentration
MBC	Minimum Bactericidal Concentration
MBEC	Minimum Biofilm Eradication Concentration
MA	Marine Agar
MB	Marine Broth
MHA	Muller Hinton Agar
MHB	Muller Hinton Broth
PEG	Poly(ethylene glycol)
pHEMA	Poly(hydroxyethymethacrylate)
PHMB	Polyhexamethylene Biguanide
QS	Quorum Sensing
QSI	Quorum Sensing Inhibitor
UPEC	Uropathogenic *Escherichia coli*
w/v	Weight by volume
XTT	Sodium 3,3′-[1(phenylamino)carbonyl]-3,4-tetrazolium]-3is(4-methoxy-6-nitro) benzene sulfonic acid hydrate

Chapter 1

General Introduction

1.1.0 Introduction

Urinary catheterisation is a technique for bladder emptying by employing a catheter (flexible tube) to drain the bladder or urinary reservoir [1]. Catheterisation is used to treat urinary retention resulting from a wide variety of conditions including: spinal cord injury, multiple sclerosis, neurological disorders, diabetes, injury to the bladder region or bladder cancer [2]. There are many complications associated with catheterisation largely due to contamination of the catheter surface during insertion with commensal bacteria leading to infection. Catheterisation may result in urinary tract infection (UTI), potentially leading to pyelonephritis (infection of the kidney), and eventual bacteraemia (bacteria in the blood) [3]. These complications can lead to septicaemia, which can be fatal [3]. Bacterial infections are normally treated with courses of antibiotics, however, many uropathogenic bacteria are now developing resistance to multiple antibiotics [4]. Further complicating treatment is the formation of bacterial biofilms on the catheter surface which poses challenges in terms of recalcitrance and persistence resulting in difficult to eradicate infections.

A bacterial biofilm is a coherent cluster of bacterial cells embedded in a gel-like matrix of extracellular polymeric substances (EPS) which includes polysaccharides, proteins and DNA [5]. Biofilms have been shown to be recalcitrant to many antimicrobial agents in addition to the actions of the host immune system making them far less susceptible to antimicrobials compared with their planktonic counterparts [5]. Biofilms show decreased susceptibility to antibiotics due to the shielding effect of the EPS, low metabolic activity of the cells within the biofilm and due to the actions of membrane-bound efflux pumps that actively expel antimicrobial compounds from the cell [5]. Also, antibiotic-resistance genes are readily transferred between bacteria in a biofilm by horizontal gene transfer allowing the dissemination of resistance through a bacterial population [6]. Antibiotic treatment of catheter-associated urinary tract infections (CAUTIs) is often ineffective due to the antimicrobial recalcitrance of the biofilm and the potential for the generation of antibiotic resistance. It is therefore important that preventative treatments for these catheter-associated complications are investigated; this will reduce the financial burden on the healthcare system in terms of hospital admissions and treatment costs, and greatly improve patient health.

Biocides are broad-spectrum antimicrobial chemicals whose purpose is to inhibit the growth of or kill microorganisms [7]. Catheters have been developed that have been coated with biocides [8] in order to reduce bacterial contamination of the catheter surface. However, previous research has suggested that long-term exposure to certain biocides can cause certain bacterial species to become more resistant to biocides in addition to third party agents such as antibiotics due to the presence of shared target sites between the antibiotic and biocide in addition to the activation of broad-range defence mechanisms such as increased efflux activity or decreased cell permeability [9]. This is termed 'cross-resistance' and is a cause for concern when considering the impact of biocide coated catheters on the antimicrobial susceptibility profiles of uropathogens. Furthermore, biocides may be associated with cytotoxicity in the host, especially at concentrations that would be required to fully eradicate a bacterial biofilm.

A novel approach in the production of anti-infective catheter coatings is to use quorum sensing inhibitors (QSIs). Quorum sensing (QS) is a process by which bacteria produce and detect signalling molecules and thereby coordinate their behaviour in a cell density dependent manner [10]. Quorum sensing it is an important contributor to the formation of bacterial biofilms in certain bacterial species. QSIs act to disrupt this communication between bacteria and provide a potential treatment option to prevent the establishment of bacterial biofilms and reduce biofilm formation. By combining quorum sensing inhibitors with traditional biocides it may be possible to prevent the formation of mature biofilms allowing eradication of the residual contaminating bacteria at lower concentrations of biocide than would be required to eradicate an established biofilm.

The development of an anti-infective catheter coating which offers anti-biofilm and antibacterial and activity would therefore improve the outcome of antimicrobial treatment and help to prevent the establishment of CAUTIs.

1.2.0 Catheter-associated UTI

1.2.1 Financial cost of CAUTI on the NHS

It is estimated that UTIs affect around 150 million people per year globally [11]. The NHS in England spent £434 million in 2013/14 treating 184,000 hospital admissions for a UTI [12]; 80% of these infections are associated with indwelling urinary catheters [13]. Catheterisation is, therefore, one of the most important risk factors for developing

a UTI and as such it has been shown that there is a 5-8% increase in risk of developing bacteriuria (bacteria in the urine) for every day that a catheter is inserted and almost all catheterised patients will have bacteriuria after four weeks of insertion [14]. It is therefore unsurprising that UTI's make up the largest proportion (45%) of hospital acquired infections (HAI) posing an impending infection risk to the populace and a financial burden on healthcare service providers [15]. It is estimated that approximately 3% of people over the age of 65 require a catheter and, with an aging population, this figure is likely to increase [16]. With the treatment of CAUTI's costing the NHS on average £2000 per episode [16] it has become vital to prevent these infections before they become serious enough for hospitalisation.

1.2.2 Other diseases associated with catheterisation

Not only does insertion of a urinary catheter greatly increase the risk of developing a UTI but there are also many other complications associated with damage to the urinary tract as a result of catheterisation e.g. pyelonephritis, bacteraemia, carcinoma of the bladder, local periurinary tract infections, infection stones, blockage of catheter [1]. These complications can be serious and, in vulnerable patients, fatal. Currently *Escherichia coli (E. coli)* is the leading cause of blood stream infection in the UK with 40,580 cases reported in 2016–17 and a mortality rate of 14.8% [17]. Of these cases, 21% are linked to the presence of an indwelling urinary catheter [17].

Long-term catheterisation is a commonly used management option for elderly patients, where alternative treatments for bladder dysfunction are inappropriate or unsuccessful [18]. These patients are at an increased risk of developing CAUTI and associated secondary infections due to the hormonal, physiological and immunological effects of aging [18]. This has a detrimental impact on their quality of life and leads to a substantially increased morbidity and mortality rate.

1.2.3 Antibiotic resistance in uropathogens

It has become common practice to give catheterised patients prophylactic antibiotics however antibiotic resistance among uropathogens has become a substantial cause for concern. As such, the National Institute for Health and Care Excellence (NICE) has recently recommended that antibiotics should not be used to treat asymptomatic bacteriuria in adults with catheters and non-pregnant women, or to be used

prophylactically for patients with catheters [19]. Research carried out by Dewar *et al.* [20] has shown that antibiotic resistance has become very prevalent particularly among Gram-negative bacteria due to the production of extended-spectrum β-lactamases (ESBLs). Examples of antibiotics that Gram-negative bacteria isolated from community patients are resistant to include cephalosporins, penicillins, fluoroquinolones and trimethoprim [20].

1.2.4 Uropathogenic *Escherichia coli* (UPEC)

E.coli is the most common causative agent of UTI, accounting for 80-90% of all reported uncomplicated UTI cases [21], 50% of nosocomial [22] and 65% of all complicated UTI infections (including CAUTI) [23]. UPEC are classified as the O (semantic) and K (capsular) serotypes and are distinct from the gastrointestinal serotypes as UPEC have extra genes that encode P fimbriae/ pyelonephritis associated pili (PAP) [24]. These genes are found in mobile genetic elements known as pathogenicity islands [21]. Other key virulence factors in UPEC include: Type 1 pili, lipopolysaccharide (LPS), flagella, curli, secreted toxins, secretion systems, and TonB-dependent iron-uptake receptors [25].

Type 1 pili terminate at the FimH adhesin which binds to mannosylated glycoproteins on human bladder epithelium [26] and other cell surfaces. PAP are homologous to type 1 pili in that they share evolutionary origin therefore have a similar structure but not necessarily function [27]. The adhesin at the end of P fimbriae is called PapG and specifically binds to the globoside, galabiose 4 (GBO4), on the uroepithelium of the human kidney [28] and other cell surfaces. These unique structures make UPEC highly virulent urinary pathogens as they are able to adhere to the uroepithelia against the flow of urine facilitating colonisation of the host. PapG adhesins have been found in up to 100% of strains causing UTI showing the clinical relevance of this virulence factor [29].

Other bacterial surface appendages have been associated with UPEC virulence - such as curli and flagella [25]. Curli secrete soluble monomers that are alike in characteristics to amyloid fibrils, which are associated with many human degenerative disorders such as Parkinson's disease [30]. These bacterial amyloids are involved in adhesion to surfaces, cell aggregation, host cell adhesion and invasion [31]. It has also been shown that curli play an important role in biofilm formation and are potent inducers of the host inflammatory response [31]. Flagella are organelles that provide motive force for

bacterial cells but they have also been implicated in cell invasion and infection of the urinary tract [32].

LPS molecules are found on the bacterial cell surface and consist of fatty acids lined to an oligosaccharide core, which in turn is bound to a long polysaccharide chain commonly called O antigen [25]. Mutations to genes encoding LPS have affected UPEC's susceptibility to detergents, and the ability to adhere to and invade urothelial cells [33]. When the *waaL* gene (O-antigen ligase gene) was deleted proinflammatory cytokine secretion was enhanced [33] indicating the role of LPS in evoking host immune response.

UPEC are also able to secrete toxins, adhesins and enzymes via membrane vesicles which provide a way of delivering these elements to host cells without them being degraded by the extracellular environment [34]. Toxins that have been associated with UPEC strains are: α-hemolysin, cytotoxic necrotizing factor 1, vacuolating autotransporter toxin, and secreted autotransporter toxin [35].

Iron is a key nutrient for UPEC as it is required for cell division and pathogenesis [36]. As the urinary tract is an iron-limited environment, UPEC have numerous iron transport and iron chelating mechanisms such as yersiniabactin, salmochelin, aerobactin, and siderophores [25]. Siderophore receptors require the TonB cytoplasmic membrane-localized complex which has been shown, in gene deletion mutants, to be critical for UPEC virulence [37].

1.3.0 Bacterial Biofilms in Catheter-associated UTI

The formation of a bacterial biofilm can be divided into three stages: attachment, maturation, and dispersal [38] and can be seen in Figure 1.1. After the formation of a conditioning film, the bacterial cells attach to the surface due to the actions of reversible attracting forces such as electrostatic interactions and van der Walls forces. Irreversible attachment follows due to the binding of cell surface appendages such as bacterial pili to the underlying substratum. Following adhesion is the formation of microcolonies, the production of extracellular polymeric substance and the maturation of the biofilm. This maturation process is governed through the actions of quorum sensing between the bacterial cells. Once the biofilm has matured it will enter a phase of dispersal, whereby planktonic cells will be shed from the biofilm surface and will travel to a new site to

initiate the formation of a new biofilm [39]. It has been shown that biofilm development is dependent on environmental cues e.g. the availability of nutrients [39] in addition to the actions of quorum sensing molecules [5].

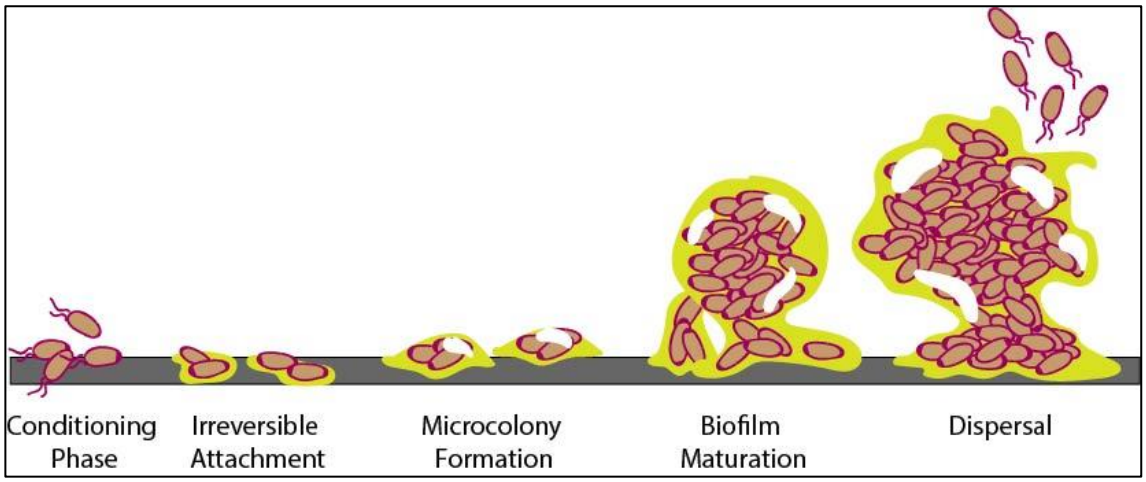

Figure 1.1 Biofilm formation on a solid surface. Biofilm formation is divided into three stages: attachment, maturation, and dispersal [38].

1.3.1 Intracellular biofilm communities

During the first stages of infection and biofilm formation UPEC transition from reversible to irreversible binding to cell surface. It is this stage when the bacteria undergo genetic change to produce adhesins and pili structures (e.g. PAP and type 1 - see above) that allow this binding to cells [40].

Not only do these structures allow attachment to the substratum of the urinary tract and therefore subsequent infection but they also allow the internalisation of UPEC into host cells to form intracellular biofilms (or intracellular bacterial communities [IBCs]) which can cause infection relapse in the form of recurrent UTI [40]. In the bladder, these intracellular biofilms have been shown to become encapsulated in a uroplakin shell that would protect the bacteria from antibiotics in the urine and the actions of the host inflammatory responses - allowing the bacteria within to proliferate, re-invade uroepithelia, and form a persistent reservoir [41].

1.3.2 Quorum sensing and bacterial biofilms

Quorum sensing is density dependent bacterial communication whereby bacterial cells sense the concentration of signal molecules and activate QS-controlled genes in response [42]. As bacterial density increases the biofilm develops new characteristics

that are different to their planktonic bacterial counterparts, specifically the biofilm tends to be more virulent and less susceptible to antimicrobial drugs.

Quorum sensing in UPEC is mediated by acyl-homoserine lactone (AHL) and autoinducer-2 (AI-2) (Figure 1.2) [43]. In Gram-negative bacteria, AHLs are the most common class of autoinducers [43]. They have a core *N*-acylated homoserine-lactone ring and can freely diffuse across the cell membrane [43]. There are three families of AHL synthases: LuxI, HdtS, and LuxM [44]. The LuxI family is the most comprehensively studied. This enzyme family uses *S*-adenosyl-methionine (SAM) and acyl-acyl-carrier-protein (acyl-ACP) as substrates to produce AHL and 5'-methyl-thioadenosine [44]. *E.coli* cannot produce AHL as it does not have an AHL synthase gene [45]. However, it can respond to AHL because the bacteria produce SdiA which is a homologue of LuxR an AHL signal receptor [45]. LuxR receptors possess an amino-terminal AHL-binding domain and a carboxy-terminal DNA-binding domain and are transcription factors for a range of QS controlled genes [44]. SdiA detects a broad range of AHLs and in the absence of AHLs, the protein is degraded [46].

AI-2 consists of derivatives of 4,5-dihydroxy-2,3-pentanedione (DPD) [47]. It has been shown that AI-2 production is directly correlated to biofilm production in *E.coli* [48]. S-ribosylhomocysteine lyase (LuxS), the AI-2 synthase, is known to be present in more than 500 bacterial species [43]. The production of DPD is catalysed by LuxS although the enzyme also forms an integral part of the activated methyl cycle (AMC), which is an important metabolic pathway that serves to recycle homocysteine. During the second product of this reaction DPD undergoes spontaneous cyclization to form a mixture of different furanones collectively known as AI-2 [47]. At high cell densities, the AI-2 molecules are actively transported into the cell by association of receptor LsrB in *E.coli* [49]. The AI-2 is then imported by the LsrABC transport system where it is phosphorylated by LsrK and is thought to interact with LsrR, relieving the repression of the *lsr* operon [46]. The resulting downstream reactions activate the transcription of target genes to produce a particular QS response [50]. It has been shown that AI-2 controls 166 to 404 genes, including those for chemotaxis, flagellar synthesis, motility, and virulence factors in *E. coli* [48]. The LuxS/AI-2 system, or homologues of it, is found in both Gram negative and Gram positive bacteria [48].

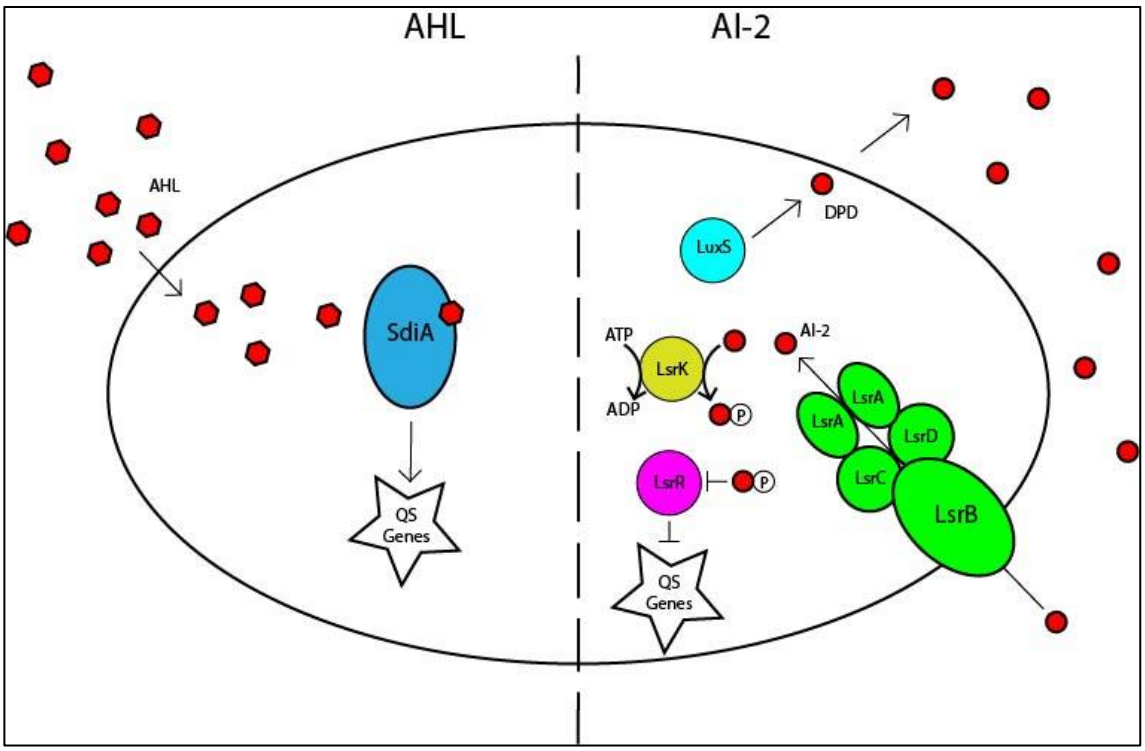

Figure 1.2 Quorum sensing systems in *E.coli*. AHL is the most common system in Gram negative bacteria, *E. coli* express SdiA which recognises AHL and initiates transcription of QS controlled genes. AI-2 is the system that *E. coli* mostly uses, LuxS synthesises AI-2 and is recognised by LsrB. The phosphorylated AI-2 inhibits LsrR repression of QS controlled genes.

1.3.3 Biofilm resistance

Bacterial biofilms show tolerance or resistance to antimicrobial agents through a variety of mechanisms. The structure of the biofilm itself can cause antimicrobials to become less effective due to the shielding effect of the surrounding matrix. Subpopulations within the bacteria are slow growing or even dormant due to limited nutrients [51] or oxygen gradients [52] in the center of the biofilm which results in antibiotics that target active biological processes being less effective on these populations [53]. Also conditions within the biofilm (i.e. differences in pH and CO_2) can affect the action of some antimicrobials e.g. the activity of tetracyclines are compromised at low pH [54]. Quorum sensing also has a role to play in biofilm antimicrobial tolerance, for example eDNA release is regulated by quorum sensing and this is known to be a chelator of aminoglycosides [55]. Activity of the bacterial cells, such as actively expelling antimicrobials through increased efflux pump activity also promotes the reduced susceptibility phenotype of biofilms [5]. In addition, bacteria are in closer proximity to each other so there is a higher chance of genetic transfer of resistance genes between

bacterial cells in a biofilm promoting the spread of antibiotic resistance throughout the biofilm community [6]. Additionally, when a selection pressure is introduced (such as antibiotics) the high density of bacterial cells induces increased competition and therefore selection for mutator phenotypes which means that there is a higher mutation rate within a biofilm compared to planktonic communities [56].

Another mechanism of biofilm resistance is the propagation of persister cells. Persister cells do not undergo a genetic change nor do they grow in the presence of antibiotics like resistant cells [57]. However, persister cells are essentially dormant, and therefore multidrug resistant, which are able to re-establish biofilm after the treatment has ended [58]. In biofilms, persister cells make up around 1% of the population providing a reservoir of resistance [57].

1.3.3 Biofilm associated infections

Biofilms are associated with chronic infection which persists despite immune response/antibiotic therapy [5]. The surface of a catheter provides an optimum surface for a biofilm to form and the subsequent dispersion of viable planktonic bacteria from the biofilm can lead to bacteria infecting the bladder, kidneys and becoming systemic. Not only does the formation of a biofilm produce a reservoir for bacteria to infect the patient but the mass of the biofilm may even occlude the catheter lumen and obstruct urine outflow which could cause septicemia due to a back-flow of bacterial filled urine within the urethra. This is a particular problem in biofilms incorporating urease producing bacteria, such as *Proteus mirabilis,* as this species forms crystalline biofilms which occlude the catheter lumen [59].

1.4.0 Quorum Sensing Inhibitors

Quorum sensing inhibitors act by targeting the generation, dissemination, or reception of the QS signal [60]. There is now an interest in developing pharmaceuticals based on disrupting QS to treat or prevent chronic infections. Targeting the enzymes involved in synthesising AI-2 is a promising strategy. Lux-S is an attractive target as it is only found in bacteria [10] and several Lux-S inhibitors have been synthesised [61]. Inhibiting Lux-S has been shown to limit biofilm formation [62], however it has also been shown that inhibition of Lux-S may lead to increased mutation rate plasticity, as demonstrated by increased resistance to rifampicin in *E.coli* [63].

1.4.1 Dihydroxypentanedione

Blocking the QS signal is primarily achieved by synthetically creating analogues that act as competitive inhibitors of the AI-2-binding site [60]. Dihydroxypentanedione (DPD) has been used to prevent AI-2 binding to the periplasmic receptor [64]. Isobutyl-DPD and phenyl-DPD inhibited *E. coli* and *P. aeruginosa* biofilm formation and resulted in a removal of preformed biofilms in a microfluidics biofilm reactor [65].

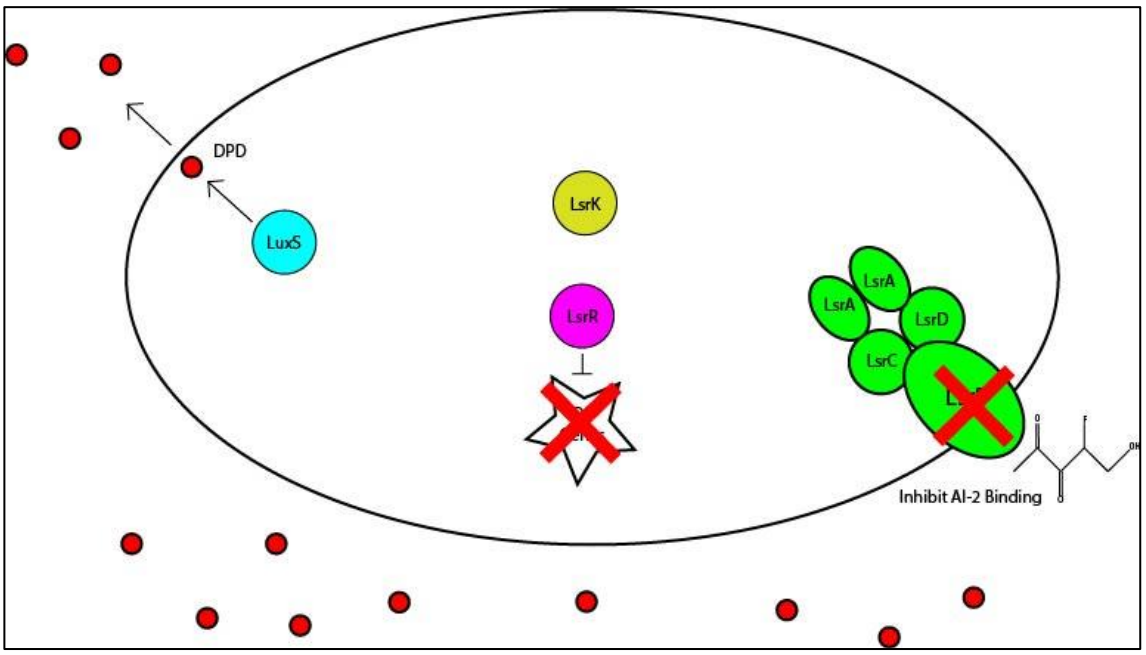

Figure 1.3 Mechanism of action of DPD. The DPD molecule acts as a competitive inhibitor of the AI-2 binding site thereby inhibiting quorum sensing.

1.4.2 Furanone

A small variety of compounds including furanone, have been shown to inhibit AI-2 signal transduction. Furanones, are natural compounds produced naturally in the environment by the red alga *Delisea pulchra* [10]. Furanone has been shown to inhibit AI-2 QS in *Vibrio harveyi* by decreasing the DNA binding ability of the response regulator LuxR [10]. In addition, the natural furanone covalently modifies and inactivates LuxS and accelerates LuxR turnover [66]. *E.coli* biofilm formation is inhibited by furanone as shown in previous studies [67, 68], which is in part due to the repression of AI-2 induced genes involved in chemotaxis, flagella, and motility [69].

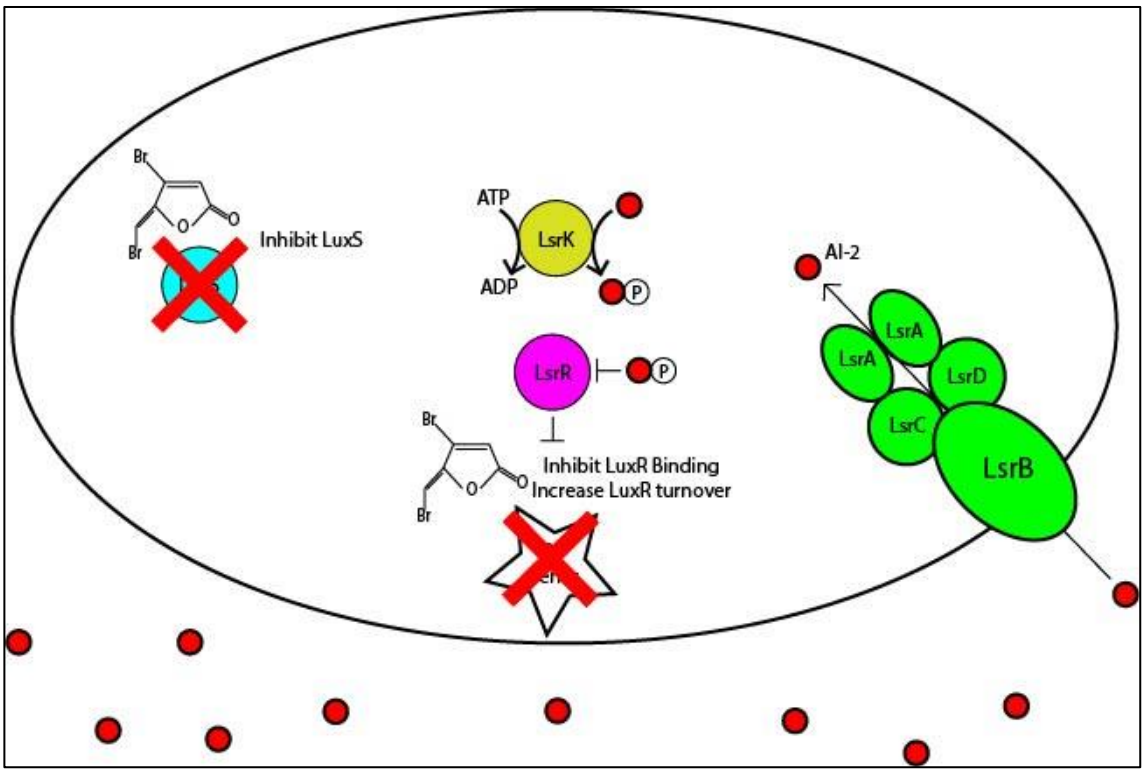

Figure 1.4 Mechanism of action of furanone. Quorum sensing inhibition is achieved by inhibition of LuxS and LuxR binding to target genes. Furanone also increases LuxR turnover.

1.4.3 Cinnamaldehyde

Cinnamaldehyde is a natural product from the bark of the cinnamon tree, and has been observed to inhibit AI-2 based quorum sensing in *Vibrio spp*. [49]. Cinnamaldehyde elucidates its quorum sensing inhibition by blocking the DNA binding ability of response regulator LuxR and can disrupt biofilm formation by reducing formation/accumulation of EPS [70]. Cinnamaldehyde treatment has been shown to affect biofilm formation and to increase biofilm susceptibility towards antibiotic treatment in *P. aeruginosa* [71].

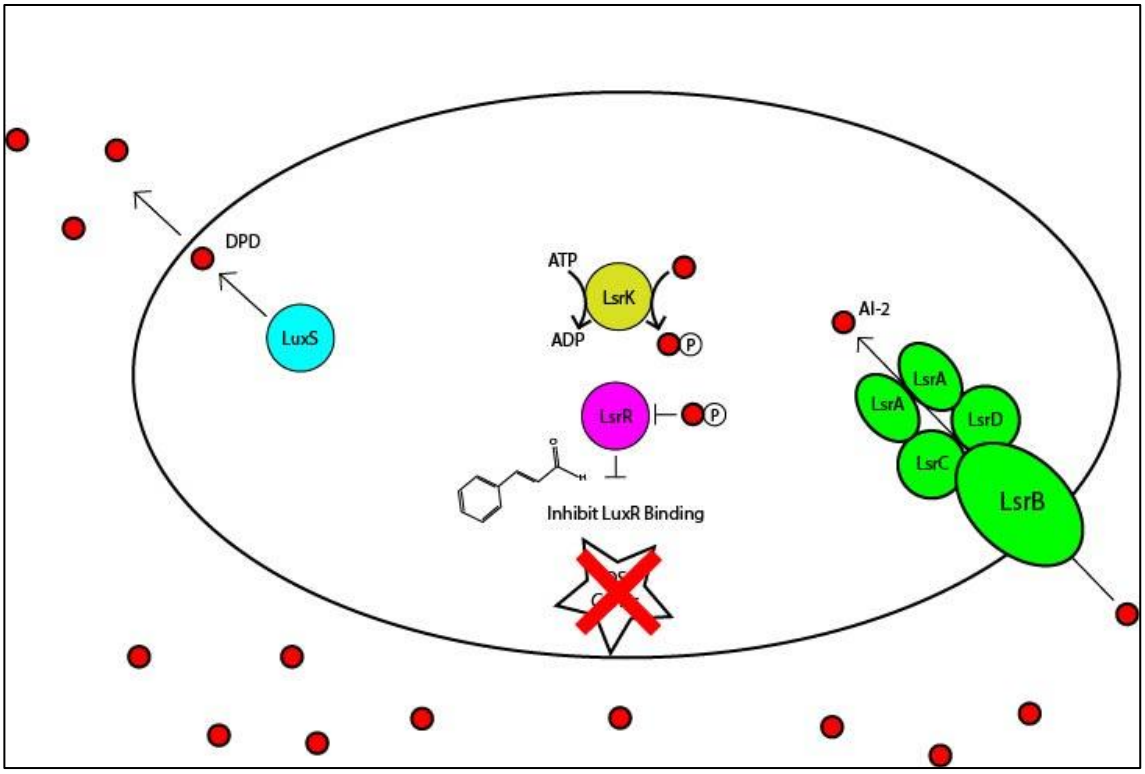

Figure 1.5 Mechanism of action of cinnamaldehyde. Cinnamaldehyde inhibits quorum sensing through inhibition of LuxR binding.

1.5.0 Biocides

Biocides have been used for many years being incorporated into soaps, cosmetics and disinfectants [72]. There are a variety of different types of biocide that are being investigated for use in humans, all have a very broad mechanism of action primarily focussing on the bacterial cell membrane. Therefore the composition of the bacterial cell membrane can have a significant impact on the efficacy of a particular biocide. A representation of a Gram-negative cell membrane is shown in Figure 1.6.

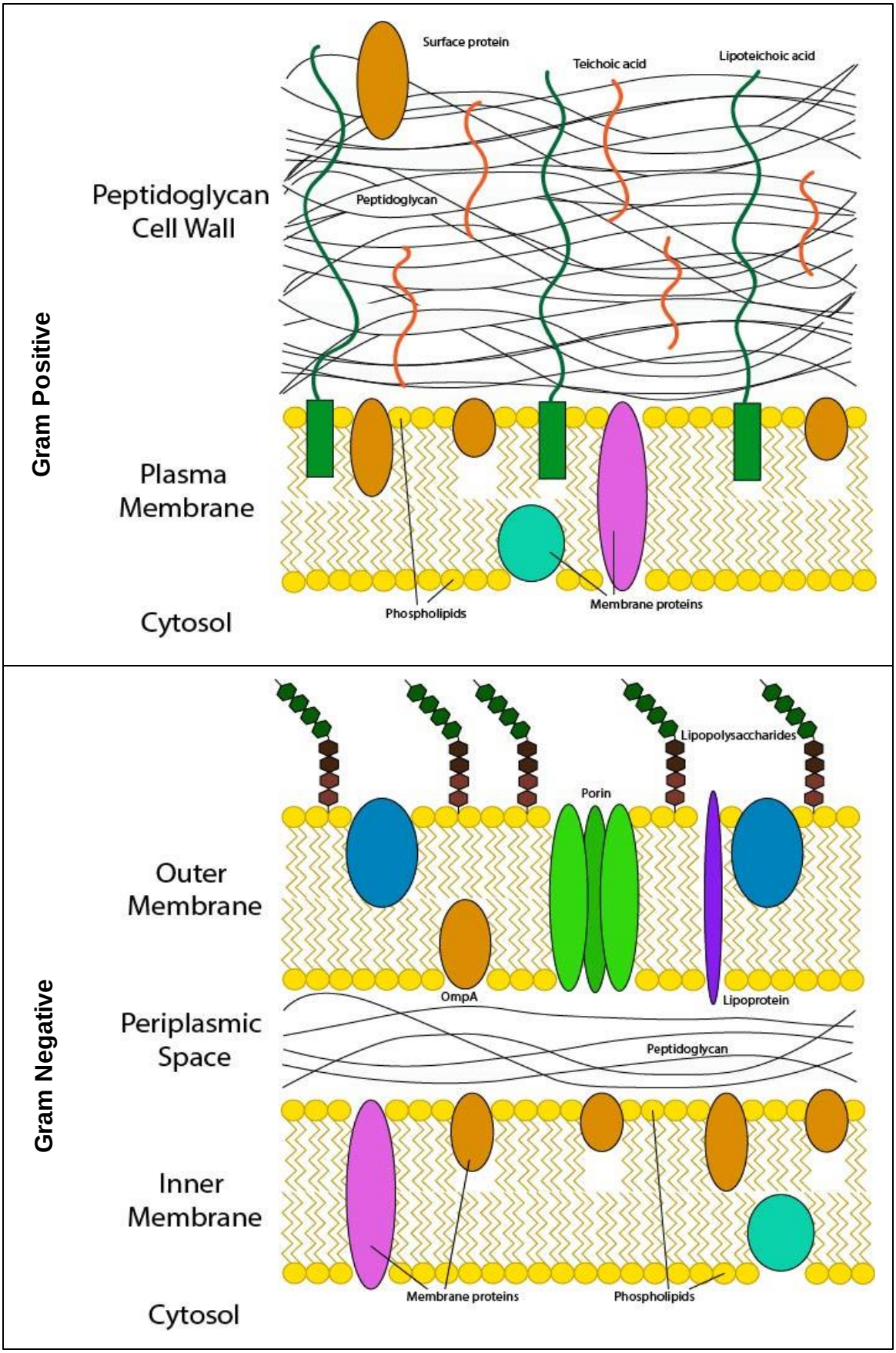

Figure 1.6 The Gram-negative cell and Gram-positive cell membranes. The Gram-negative membrane is composed of the outer phospholipid membrane, periplasmic space, and the inner phospholipid membrane. The Gram-positive cell membrane differs in the thicker peptidoglycan layer and only one plasma membrane.

1.5.1 PHMB

Cationic biocides, such as polyhexamethylene biguanide (PHMB) and chlorhexidine, often rely on an initial attraction between the biocide and anionic bacterial membrane in order to exhibit their antimicrobial effect. PHMB, a polymeric biguanide, is a general disinfecting agent utilised by the food industry, used to disinfect swimming pools and can be found in in contact lens solution. PHMB is a polycationic linear polymer with a hydrophobic backbone and multiple cationic groupings separated by hexamethylene chains [73]. PHMB largely acts by displacing cations, such as calcium, in the bacterial outer membrane because it competes for negatively charged sites on the peptidoglycan underneath [74]. This disrupts the outer membrane and allows the PHMB molecules to further act on the inner membrane. Here PHMB bridges with acidic phospholipids in the inner membrane causing membrane rigidity and resulting membrane fissures [75], this is followed by loss of K^+ ions, and possible impairment of the function of neighboring proteins. This destroys the membrane integrity which causes leakage of intracellular components, affects the function of cell membrane associated proteins and causes eventual cell lysis [76]. The bacteria may be able to recover and reform the membrane at bacteriostatic concentrations but at lethal concentrations the cytoplasm coagulates as nucleic acids react with PHMB, the membrane precipitates and the cell undergoes lysis [75].

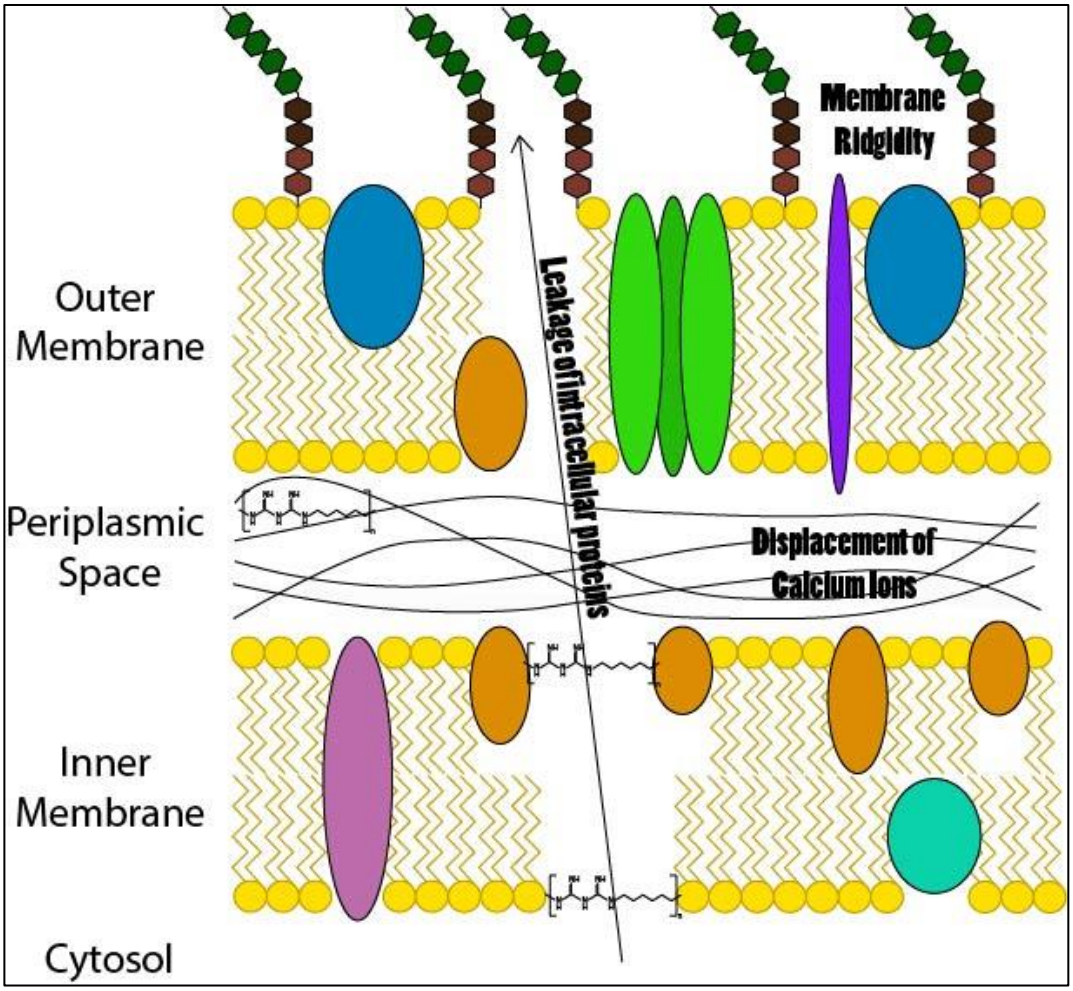

Figure 1.7 Mechanism of action of the cationic biocide, PHMB. PHMB displaces cations in the outer membrane and bridges with acidic phospholipids in the inner membrane causing membrane rigidity, leakage of intracellular proteins, and cell lysis.

1.5.2 Triclosan

Triclosan (2,4,4′-trichloro-2′-hydroxydiphenyl ether) is a bis-phenol commonly used in hand soaps [77]. In studies with *E. coli*, triclosan at subinhibitory concentrations inhibited the uptake of essential nutrients due to its disruptive effects on the bacterial cytoplasmic membrane, whilst at higher, bactericidal concentrations resulted in the rapid release of cellular components and cell death [78]. Triclosan directly damages the cell membrane by solubilising lipids within the membrane which disrupts the membrane structure leading to leakage and lysis [79]. At bacteriostatic concentrations, triclosan inhibits lipid biosynthesis via targeting ENR (enoyl-acyl carrier protein reductase) encoded by gene *fabI* [80]. Triclosan inhibits this enzyme by interacting with ENR and increasing its binding affinity to the cofactor NAD+ [81]. When triclosan, enzyme and cofactor are bound together this forms a stable ternary complex that cannot catalyse the reaction [79]. When the cell cannot synthesise fatty acids growth is inhibited. Triclosan also acts by disrupting the glycolysis pathway by inhibiting a number of the enzymes involved (pyruvate kinase, lactic dehydrogenase, aldolase) and increasing the sensitivity of the pathway to acid inhibition [82].

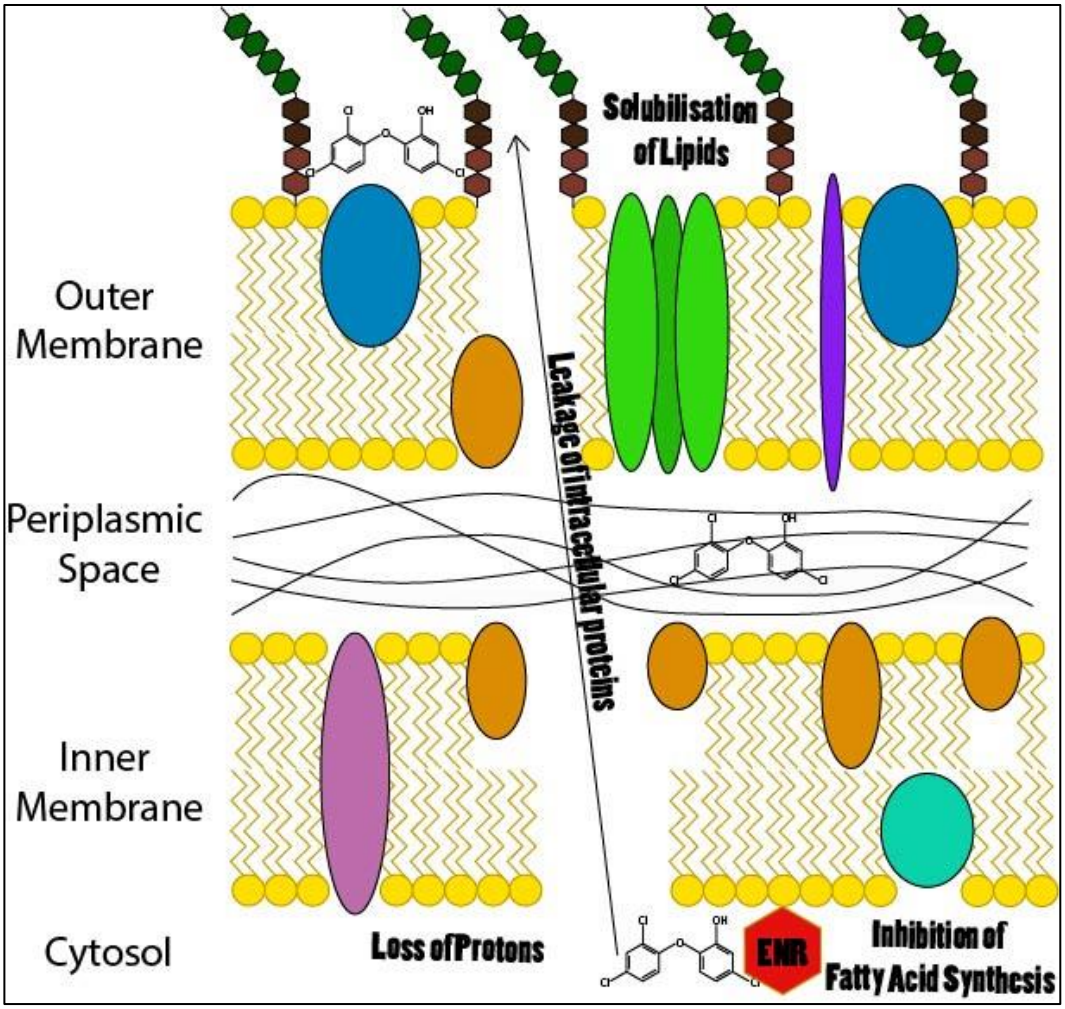

Figure 1.8 Mechanism of action of the biocide, triclosan. Triclosan directly damages the cell membrane by solubilising lipids within the membrane, and inhibits lipid biosynthesis via targeting ENR (enoyl-acyl carrier protein reductase).

1.5.3 Benzalkonium chloride

Benzalkonium chloride (BAC) is a quaternary ammonium compound (QAC). QACs are often monocationic surfactants generally containing one quaternary nitrogen associated with at least one major hydrophobic component [73]. The proposed mechanism of action of BAC against microorganisms is: (i) adsorption to and penetration of the cell wall; (ii) binding of the polar head group to phospholipids within the cytoplasmic membrane (lipid or protein), followed by membrane disorganization due to interdigitation of the alkyl tail into the membrane core; (iii) leakage of intracellular lower-weight material; (iv) degradation of proteins and nucleic acids; and (v) cell wall lysis caused by autolytic enzymes [83]. BAC will disrupt the phospholipid bilayer, proteins in the cytoplasmic membrane, and nucleic acids in cytoplasm [84]. BAC can also damage the outer membrane of Gram-negative bacteria, thereby promoting its own uptake [77]. Self-promoted uptake has been seen in other cationic biocides (such as PHMB and chlorhexidine) where the cation interacts with cross-linked cations in the outer membrane which causes structural and functional changes to the outer membrane and loss of the previously associated cations causing a reduction of electostatic charge. This leads an increase in outer membrane permeability to hydrophobic (cationic) compounds and a stronger electrostatic interaction between the cationic biocide and the anionic cell [85].

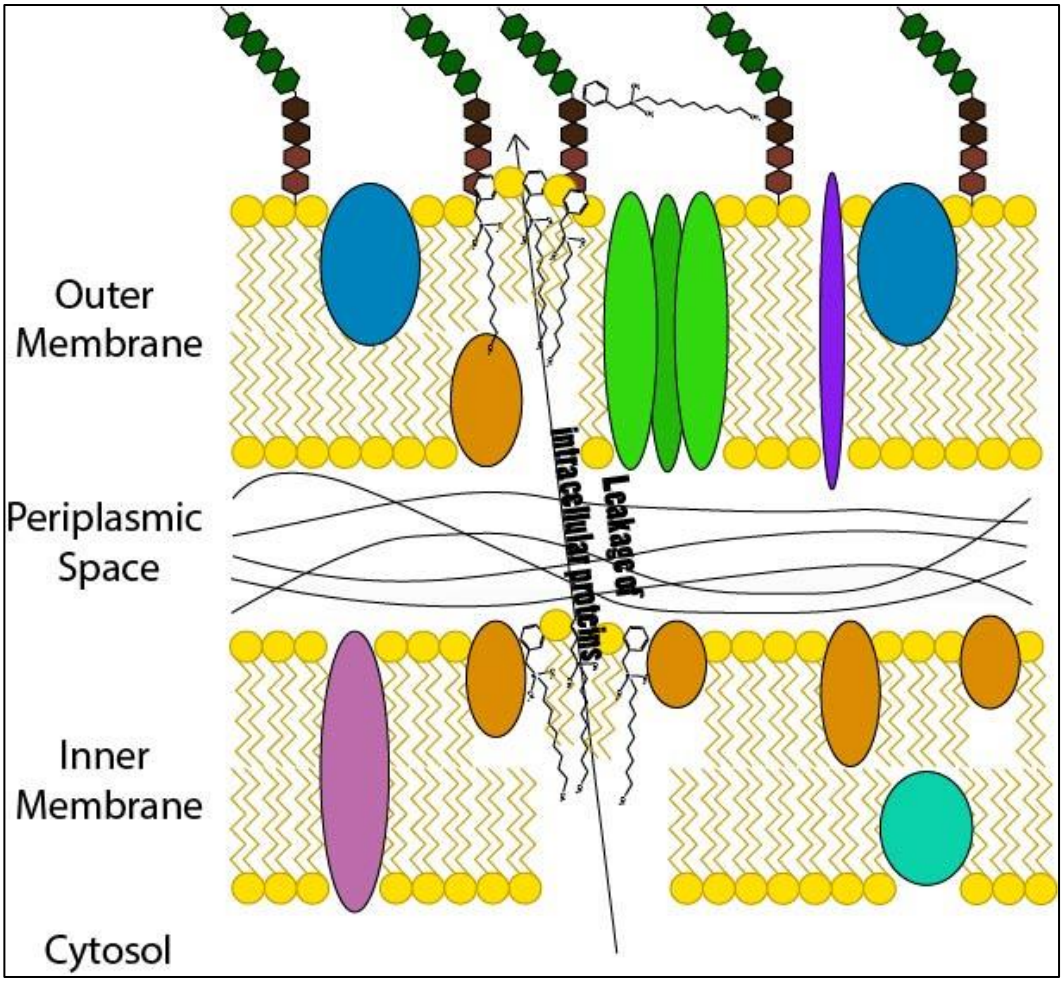

Figure 1.9 Mechanism of action of the biocide, BAC. BAC binds to phospholipid head groups in the outer cell membrane, leading to membrane disorganisation, leakage of intracellular proteins, and cell wall lysis.

1.5.4 Silver Nitrate

Silver has been used for antimicrobial benefits for many years. Silver ions interact with thiol (sulfydryl, —SH) groups [86] which has been implicated in damaging the cytoplasmic membrane, intracellular proteins and DNA [77]. Silver has been found to inhibit the respiratory chain in *E.coli* by interacting with cytochrome a_2 [87] and inhibiting phosphate uptake and exchange [88]. Silver ions also form complexes with DNA bases in preference to phosphate groups [89]. Silver ions inhibit several functions in the cell and this leads to the generation of reactive oxygen species, which are produced possibly through the inhibition of a respiratory enzyme by silver ions and attack the cell itself [90]. Utilising silver in medical applications has seen some success such as incorporation into antimicrobial impregnated wounds dressings [91].

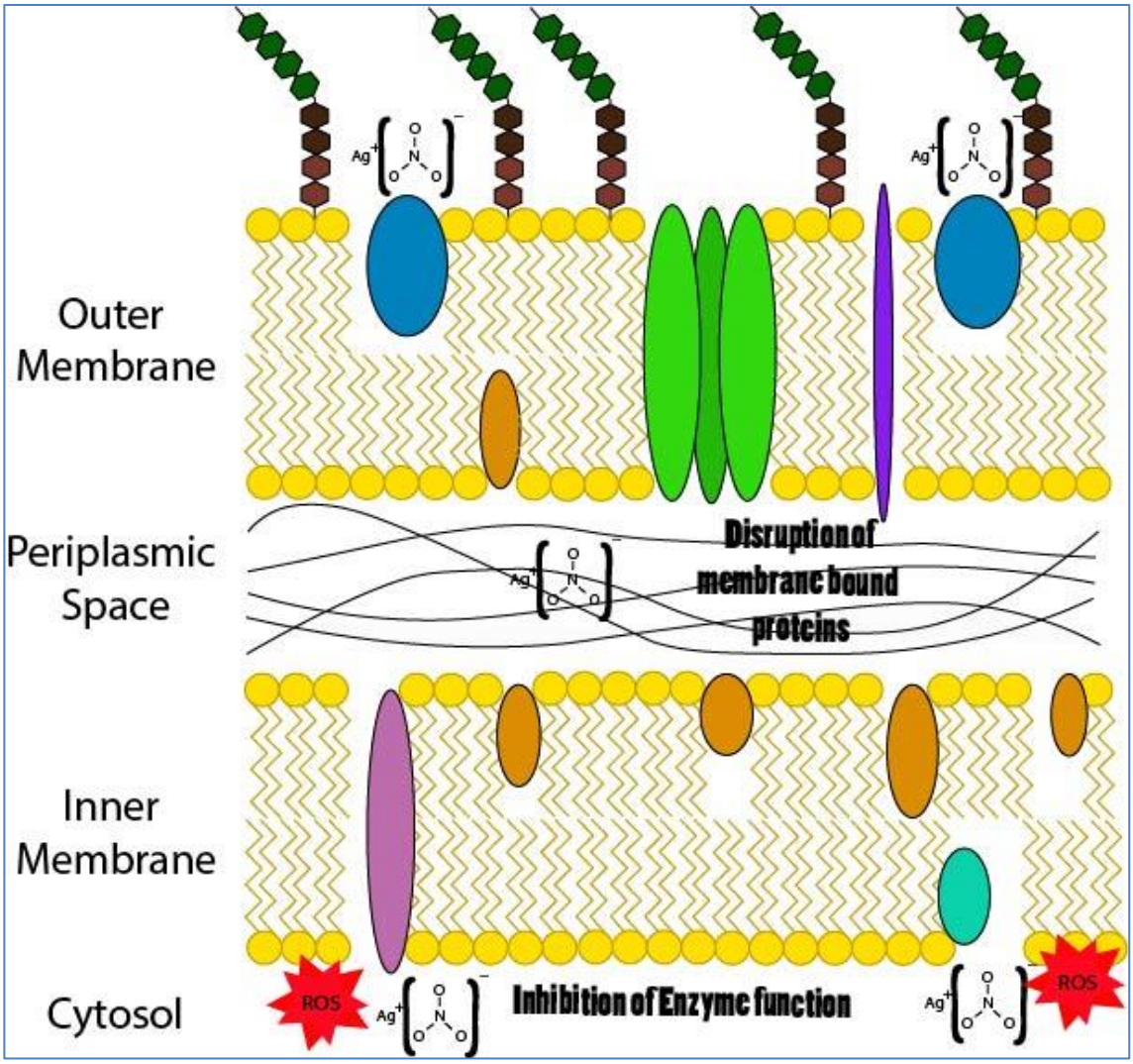

Figure 1.10 Mechanism of action of the biocide, silver nitrate. Silver interacts with thiol (sulfydryl, SH) groups on both extracellular and intracellular proteins, and generation of reactive oxygen species causes cell death.

1.5.5 Biocide resistance

As with antibiotics, the indiscriminate use of biocides has caused concern about the selection of biocide resistant bacteria [92]. Biocides have a broad spectrum of action therefore they act on multiple non-specific targets. With multiple targets, there is a lower chance that a single mutation will lead to resistance [93]. Despite this there are still multiple documented cases of biocide resistance in bacteria. Furthermore, there is concern that the development of resistance to biocides may also confer resistance to antibiotics due to the presence of shared target sites or due to phenotypic alterations in the bacteria physiology that alter electrostatic charge, decrease cell permeability or increase efflux. This has been shown to occur in *Pseudomonas aeruginosa* by mutation in the regulator gene controlling multidrug efflux pumps when exposed to triclosan [94].

Gilbert *et al.* found that whilst the concentration exponent for PHMB was significantly different between planktonic and biofilm populations of *E.coli* [76] there was no evidence of acquired resistance to PHMB within the bacterial population [75]. However there are many changes that have been observed in *E.coli* when exposed to PHMB, these include: Loss of flagella, *RbsD* downregulation (ribose transporter), cell-cell aggregation, and *tnaA* downregulation (*tnaA* can signal biofilm formation) [95] indicating that biocide adaptation may have multiple consequences on the bacterial cell aside from the generation of insusceptability.

It has been previously documented that significant decreases in BAC susceptibility after long-term bacterial exposure have not been detected [96]. However, QAC resistance has become an increasing area of concern since the use of these disinfectants have become more widespread [97]. As such, QAC resistance genes have been found in *E.coli* recovered from retail meat [98]. Changes in gene expression have been identified in BAC adapted *E.coli* including *tolC*, an efflux pump, and OmpA, porins [99]. A study by McCay *et al* [100] found that *P. aeruginosa* exposed to sub-inhibitory concentrations of BAC showed increased expression of multidrug efflux genes *mexB, mexD, mexF* and *mexY*. This increase in expression would decrease susceptibility to antimicrobials due to increased efflux.

Previous investigations corroborate the selection of silver resistance in other Gram negative pathogens including *E.coli* [101], and high levels of silver resistance are already being documented in invasive *Enterobacteriaceae* [102] possibly due to active

efflux and loss of outer membrane porins [103]. Indeed, silver-resistant *E.coli* have been shown to have acquired mutations in *ompR* and *cusS* [103]. These mutations caused the loss of ompC/F porins and derepression of the CusCFBA efflux transporter. The combined effect of decreased cell wall permeability and increased efflux resulted in reduced concentrations of intracellular silver.

Despite the previously mentioned evidence on the induction of biocide resistance in bacteria, understanding the real-world impact of bacterial resistance to biocides may be more complicated than previously thought. Forbes *et al.* [80] induced resistance to triclosan in *Staphylococcus aureus* (*S. aureus*) and this resulted in an increased susceptibility to antibiotics, reduced planktonic and biofilm growth, impaired haemolysis, coagulase and DNase activity, decreased competitive fitness and relative pathogenicity. The triclosan adapted strain demonstrated impaired cross-wall formation partially explaining growth deficits and also showed reduction in multiple cell surface adhesins potentially explaining decreased virulence [104]. This shows that biocide resistance may be associated with other functional deficits which brings into question how biocide adapted bacteria behave during infection. These previous data only concerned *S. aureus* so research into the effects of biocide resistance on other bacterial pathogens, such as *E.coli*, should be investigated. Yu *et al.* [93] discovered many genes were upregulated in triclosan resistant *E.coli* however they did not investigate whether these genes conferred resistance or perhaps had other effects. It is known that overexpression of *sdiA* is known to change cell morphology to rounder and shorter forms and can affect the expression of efflux pump proteins, it has also been linked to resistance to other drugs.

Another important consideration is the formulation of biocides used. Most *in vitro* experiments use biocide in aqueous solution however in consumer products the biocide would be formulated with surfactants and sequestrants. Experiments to compare formulated with unformulated biocides revealed that formulated biocides were more potent and induced resistance was less significant compared with unformulated biocides, likely due to their multiple-target site mode of action [105]. *In vitro* studies that used unformulated biocides should therefore be viewed critically when discussing biocide resistance.

1.6.0 Current anti-infective catheter coatings

Coating a catheter with an antimicrobial has become an increasingly popular area of research. Recently a coating was developed with immobilised acylase which was reported to reduce *P. aeruginosa* biofilm formation by 60% [106]. Acylase catalyses the degradation of AHL molecules and so inhibits quorum sensing by bacteria that use this system [107]. This is one of the first coatings that have been developed to incorporate quorum sensing inhibitors. Biocide catheter coatings have shown promising results [108] with triclosan being effective against *E. coli* and *P. mirabilis* biofilms [109, 110]. PLGA coatings containing cinnamaldehyde have been shown to be effective against *E. coli* biofilms [111, 112].

There are anti-infective catheter coatings already in clinical use. Silver coated catheters were among the first to be developed and two types of coating, silver oxide and silver alloy, were used [113]. Now a hydrogel silver alloy-coated latex catheter (CR Bard Inc.) is amongst the most popular used in practice, however results into the efficacy of this coating have been variable [114]. In certain investigations, silver coated catheters have been shown to be no more effective at preventing infections than non-coated catheters [113]. Devak *et al.* reported that the anti-attachment effect apparently seen in silver coatings was actually an effect of the hydrogel rather than the silver itself [115]. In a trial recruiting 6394 catheterised patients, it was found that there was no evidence to suggest that silver coated catheters benefited patients compared to non-coated catheters [114]. Considering the large body of evidence on the development of silver resistance in bacteria [116] this may be a consequence of adaptation of the bacteria to prolonged silver exposure causing a reduction in susceptibility. This would be particularly problematic when considering long-term catheterisation.

Two further antimicrobial catheter coatings have been developed and evaluated in clinical studies, these are Nitrofurazone and aminocycline/rifampicin mixture [117]. The minocycline/rifampicin coating was not taken past the initial trial stages but nitrofurazone-impregnated urethral catheters are currently commercially available (Rochester Medical Corp) [114]. Trial data suggest that nitrofurazone coated catheters may be effective for the first 3 days after insertion but after that time there was no significant difference in incidence of CAUTI compared to non-coated catheters [114] highlighting the short-lived activity of certain coating agents.

1.6.1 Modified surface coatings

A 'passive' coating is when the physicochemical properties of a surface is altered so bacterial attachment to the surface is prevented [118]. These types of coatings can be limited due to the surfaces being modified after implantation, often as a consequence of a conditioning layer of host proteins adhering to the device providing sites for bacterial adherence. Kingshott *et al* found that PEG modified stainless steel had no effect on bacterial attachment but PEG modified carboxylated poly(ethylene terephthalate) (PET−COOH) reduced bacterial attachment [119]. Silicone modified with polyethylene oxide (PEO) and polypropylene oxide (PPO) brushes showed limited effectiveness at reducing biofilm adherence and high variability between bacterial strains (adhesion, growth, and detachment of *Staphylococcus* species were affected but *Pseudomonas aeruginosa* was not) [120].

1.6.2 Active release coatings

'Active' release coatings incorporate antimicrobials that are released over a period of time to reduce bacterial attachment to the surface [118]. Compounds that have been incorporated into active release coatings include silver [121], antibiotics [122], nitric oxide [123], and antibodies [124]. Schierholz *et al* found that the hydrophobicity of both the compound and the polymer matrix determines the release profile of the antimicrobial [125]. For example, hydrophilic molecules incorporated into hydrophobic polymers leached via an initial "burst" followed by substantially lower levels of release at extended periods. However, when molecule and polymer are both hydrophobic, there is a less significant initial release and a more sustained release over longer periods of time.

Antibiotics have been incorporated into a variety of polymers including hydroxyapatite [122], polyurathane [126], and biodegradable polymers such as polylactide-co-glycolide (PLGA) [127]. Initial coatings with incorporated silver were shown to have limited efficacy *in vivo* [128]. It is thought that the reason for this is that the oxidised, active form of the silver ion (Ag^+) is not released in metallic surface coatings [118]. Research has been done to develop coatings that actively release oxidised silver ions. Silver nanoparticles have become an increasing area of interest in this field. Yu *et al* have developed a poly(L-lactic acid) (PLLA) coating containing silver nanoparticles that

showed antibacterial activity and favourable biocompatibility [129]. A silver nanoparticle poly (lactic-co-glycolic acid) (PLGA) coating was developed for urinary catheters and showed enhanced resistance to encrustation compared with non-coated catheters, however the coating also contained norfloxacin (an antibiotic) [130] so it is unclear if the anti-infective properties of this coating can be solely attributed to the silver nanoparticles or are due to this combinatorial effect.

1.6.3 Coatings with covalently bonded antimicrobials

For some applications, the antimicrobials are incorporated directly onto the surface of medical devices by covalent bonds. Covalent bonds occur between atoms that share a pair of electrons and the attractive and repulsive forces between them form a stable bond [131]. The benefit of this method is that the antibacterial effect for the implant or device would be permanent rather than leaching out over time [132]. However there are limited numbers of compounds that can be incorporated in this way because the active site of molecules may be masked by the covalent attachment [133]. Furthermore, deposition of host proteins on the device surface may shield the effect of the adhered antimicrobial.

Catheters are commonly made from silicone, polyethylene, polyurethane, or latex, all of which are hydrophobic and therefore can't bind molecules with much stability. The catheter material is 'functionalised' first (introduction of polar, ionic, or radical groups on the surface) to allow the binding of the antimicrobial molecules. This is usually done with plasma, gamma, or ultraviolet radiation [134].

Antimicrobial compounds that have been covalently bound to silicon previously include quaternary ammonium silane (QAS), which has been incorporated onto silicon discs by oxidisation of the silicon with argon plasma, coating with QAS, and drying at 80ºC [135]. The coated silicon was implanted into rats and there were significantly fewer cases of infection with the coated sections compared with uncoated sections [135]. The nitrofurazone coating for urinary catheters is an example of covalently attached coatings. Nitrofurazone is a nitrofuran derivative chemically related to nitrofurantoin. The nitrofurazone is incorporated in a silicone matrix on the surface of the catheter [136].

1.6.4 Hydrogels

Hydrogels are polymer networks with hydrophilic structures, meaning they are able to retain large amounts of water [137]. The nature of hydrogels being wet and slippery is advantageous for use in a catheter since this helps prevent damage to the urethral mucosa when inserted, *in situ*, and removed [134]. Vimala, *et al* created a hydrogel-based coating that releases silver nanoparticles [138]. The hydrogels were shown to be antimicrobial with potency increasing with smaller nanoparticle size. Hydrogels are increasingly being used to create nanoparticles as the free spaces within them can be used to synthesise and contain the nanoparticles [139].

A study by Ahearn *et al.* [140] compared the anti-adhesion properties of hydrogel/silver-all-silicone-, and hydrogel/silver-latex-Foley urinary catheters compared with non-coated catheters. Interestingly, results varied depending on the bacteria tested, for example: there was a greater reduction in adhesion of *E.coli* to the coated latex catheter than the coated silicone catheter, whereas for *P. aeruginosa* it was the coated silicone catheter that showed the greater reduction. This could be due to the properties of the material itself or the modification process.

1.6.5 Sol-Gel

The sol–gel process involves the formation of an inorganic colloidal suspension (sol) and gelation of the sol in a continuous liquid phase (gel) to form a 3D network structure [141]. An advantage to the sol-gel manufacturing process over other glassy coating processes is that it can be conducted at much lower temperatures, such as room temperature [142]. Formation of sol-gel starts with simultaneous hydrolysis and condensation of monomers to form particles, growth of particles, and finally agglomeration of polymers networks within the liquid [142]. Active agents can be added to the porous sol-gel to be eluted out.

Research has been carried out on the application of sol-gel coatings for medical devices and the results are promising. Nablo *et al* investigated the efficacy of stainless steel orthopedic implants coated in sol-gel [143]. The sol-gel was infused with nitric oxide (NO) donors which was shown to inhibit bacterial attachment to the implant over a range of temperatures and bacterial species [143]. This NO releasing sol-gel was also incorporated onto silicone elastomer and was shown to inhibit *S. aureus* biofilm

formation on the coated silicone [123]. This implies that the sol-gel can be successfully used to coat silicone catheters.

1.7.0 Summary and Aims

CAUTI's are becoming an increasing problem within hospitals and communities, contributing substantially to patient morbidity and mortality rates. The increasing threat of antibiotic resistance, and the ability of bacteria to form biofilms in the catheter, means that these infections are becoming increasingly difficult to treat. New therapies must be developed not only for the treatment of CAUTIs but to curb the increase in antibiotic resistance in uropathogens by reducing the need for antibiotic treatment and by providing alterative therapeutic strategies. The most common causative agent of CAUTIs is uropathogenic *E.coli* and it has been shown that when UPEC form a biofilm within the catheter it becomes less susceptible to antibiotics and shows increased virulence and pathogenicity. It is the action of AI-2 that mediates the formation of the UPEC biofilm and activates the genes responsible for the biofilm and virulence associated phenotypes.

Quorum sensing inhibitors act to block the communication between bacteria in a biofilm by blocking the synthesis, dissemination, or reception of AI-2, thereby disrupting the biofilm establishment and making the infection easier to resolve. Biocides have a broad mechanism of action but issues with cytotoxicity at high biocide concentrations have been reported. By using combinations of biocides and QSIs it may be possible to disrupt biofilm formation and allow bacterial eradication at lower biocide concentrations than would be required to eradicate an established biofilm. Whilst there is evidence of the emergence of biocide insusceptibility in bacteria, the phenotypic adaptations exhibited by UPEC in response to biocides and QSIs has received little investigation. In order to develop a long-lasting anti-infective coating we need to initially understand the long-term effects of these agents in relevant pathogenic microorganisms.

The aim of this project is to evaluate the impact of prolonged biocide and QSI exposure in a panel of UPEC isolates. These isolates comprise of two laboratory characterised strains (EC958 and CFT073) and six clinical isolates (EC1, EC2, EC11, EC26, EC28, and EC34) previously isolated from urinary tract infections (Stepping Hill Hospital, Stockport, UK). The isolates EC2, EC26, and EC34 have been previously identified as

ESBL producers. The biocides under investigation are PHMB, triclosan, BAC, and silver nitrate and the QSIs are cinnamaldehyde, (Z)-4-Bromo-5(bromomethylene)-2(5H)-furanone (C30) and 4-fluoro-5-hydroxypentane-2,3-dione (F-DPD). Comprehensive screening of these potential coating agents will include detailed analysis of (i) the broad-range antimicrobial activity against UPEC in planktonic and biofilm growth, (ii) the effects that long-term antimicrobial exposure has on bacterial susceptibility and physiology (iii) the antimicrobials' biocompatibility with a mammalian cell line and (v) the association of the test compounds with different biomaterial polymers and their resulting antimicrobial efficacy and cytotoxicity.

Chapter 2

Biocide Exposure Induces Changes in Susceptibility, Pathogenicity and Biofilm Formation in Uropathogenic *Escherichia coli*.

I acknowledge the following people for contributing to the work presented in this chapter: J Dowling and J Maingay (undergraduate project students) who conducted the antibiotic cross resistance experiments.

2.1.0 Abstract

Background: Uropathogenic *Escherichia coli* (UPEC) are a frequent cause of catheter associated urinary tract infection (CAUTI). Biocides have been incorporated into catheter-coatings to inhibit bacterial colonisation whilst ideally exhibiting low cytotoxicity and mitigating the selection of resistant bacterial populations. The effects of long-term biocide exposure on susceptibility, biofilm-formation and relative-pathogenicity were compared between eight UPEC isolates. **Methods:** Minimum inhibitory concentrations (MIC), minimum bactericidal concentrations (MBC), minimum biofilm eradication concentrations (MBEC) and antibiotic susceptibilities were determined before and after long-term exposure to triclosan, polyhexamethylene biguanide (PHMB), benzalkonium chloride (BAC) and silver nitrate. Biofilm-formation was quantified using a crystal violet assay, and relative-pathogenicity was assessed via a *Galleria mellonella* waxworm model and cell invasion assays using bladder smooth muscle (SMC) and urothelial cells (HUEPC). Cytotoxicity and resulting biocompatibility index values were determined against an L929 murine fibroblast cell line. **Results:** Biocide exposure resulted in multiple decreases in biocide susceptibility in planktonic and biofilm associated UPEC. Triclosan exposure induced the largest frequency and magnitude of susceptibility decreases at MIC, MBC and MBEC, which correlated to an increase in biofilm biomass in all isolates. Induction of antibiotic-cross-resistance occurred in 6/84 possible combinations of bacteria, biocide and antibiotic. Relative-pathogenicity significantly decreased after triclosan exposure (5/8 isolates), increased after silver nitrate exposure (2/8 isolates) and varied between isolates for PHMB and BAC. Biocompatibility index ranked antiseptic potential as PHMB>triclosan>BAC>silver nitrate. **Conclusion:** Biocide exposure in UPEC may lead to reductions in biocide and antibiotic susceptibility, changes in biofilm-formation and alterations in relative-pathogenicity. These data indicate the multiple consequences of biocide adaptation that should be considered when selecting an anti-infective catheter-coating agent.

2.2.0 Introduction

Catheter-associated urinary tract infections (CAUTI) are amongst the most commonly acquired healthcare associated infections contributing considerably to patient morbidity and posing an economic burden on healthcare service providers [144]. Complications

associated with catheterisation often arise due to contamination of the catheter surface with uropathogenic *Escherichia coli* (UPEC) during catheter insertion, leading to the formation of bacterial biofilms and subsequent infection. Patients undergoing long-term catheterisation are at a particular risk of acquiring CAUTI, with studies indicating a 5-8% increase in the risk of developing bacteriuria for every day that the catheter remains inserted [14]. The majority of patients will exhibit bacteriuria after four weeks of catheterisation, potentially leading to further complications such as pyelonephritis and septicaemia [3, 14].

Bacterial biofilms are often recalcitrant to antimicrobial chemotherapy and to the actions of the host immune system, making biofilm associated infections such as CAUTIs difficult to treat [5]. Biofilms show decreased susceptibility to antibiotics, partially due to the shielding effect of the extracellular polymeric substance (EPS) encasing the bacterial cells [145], the low metabolic activity of the cells within the biofilm [146] and the activity of membrane-bound efflux pumps that actively expel antimicrobial compounds from the bacterial cell [5]. Furthermore, antibiotic-resistance genes are frequently transferred between bacteria within a biofilm by horizontal gene transfer allowing the dissemination of resistance through a bacterial population [6]. Antibiotic treatment of CAUTIs is therefore often ineffective due to the recalcitrance of the biofilm in addition to the increasing prevalence of antibiotic resistant uropathogens [147]. There is considerable interest in developing anti-infective catheter coatings that are refractory to microbial colonisation and subsequent biofilm formation in an attempt to prevent the establishment of CAUTI.

Biocides are broad-spectrum antimicrobial chemicals that inhibit the growth of, or kill microorganisms [7]. Biocide coated urinary catheters have been developed incorporating biocides such as silver nitrate and nitrofurazone that are eluted from the surface of the catheter providing an antimicrobial gradient and a potential selective pressure for biocide resistant populations of bacteria [8]. Current clinical trial data has highlighted the limited antimicrobial efficacy of silver-impregnated catheters when compared to those without an antimicrobial coating, whilst nitrofurazone-containing coatings have been shown to exhibit only short-term antimicrobial activity and may therefore be ineffective in patients undergoing long-term catheterisation [114, 115]. This has fuelled the search for further anti-infective coating agents that display broad-spectrum activity which is maintained after prolonged use.

Long-term exposure of certain bacterial species to biocides may cause the induction of biocide insusceptibility either through the selection of intrinsically resistant mutants or through induced phenotypic adaptations, bringing into question the long-term antimicrobial activity of various biocide containing coatings [148]. Concerns have also been raised that long-term biocide exposure may promote cross-resistance to antibiotics through the acquisition of mutations in shared target sites or through the activation of broad-range defence mechanisms [149], such as increased cellular efflux activity [150] or decreased cell permeability [77]. It can, however, be argued that whilst long-term biocide exposure may lead to reductions in biocide or antibiotic susceptibility in bacteria, these reductions are small and would not impact on the susceptibility of bacteria to the concentrations of biocide used in practice. Furthermore, such changes in biocide susceptibility may be accompanied with functional deficits impacting biofilm formation, pathogenicity and competitive fitness in bacteria [80]. Therefore in order to develop an effective anti-infective catheter coating the multiple long-term effects of the biocide used within the coating must be taken into consideration.

Whilst previous investigations have evaluated the impact of long-term biocide exposure on the antimicrobial susceptibility of many clinically relevant bacteria, there is no current investigation into the multiple phenotypic consequences that may occur due to long-term biocide exposure in UPEC. The current study therefore aims to quantify the effects of long-term biocide exposure in eight UPEC isolates. The commonly used biocides PHMB, triclosan, BAC and silver nitrate were evaluated for their long-term antibacterial and anti-biofilm activity and their potential to induce antibiotic cross-resistance. The impact that biocide exposure has on bacterial relative pathogenicity was assessed using a *Galleria mellonella* waxworm model and the biocides antiseptic potential was determined via calculating cytotoxicity in an L929 murine fibroblast cell line allowing the determination of a biocompatibility index value [151].

2.3.0 Aims and objectives

The purpose of this chapter was to evaluate the effects of long term biocide exposure on eight UPEC isolates. Previous studies have indicated biocide exposure impacts antimicrobial resistance, biofilm formation, and fitness in bacteria [80]. Biocides have a broad mechanism of action therefore it is posited that adaptation to biocide exposure would have multiple effects on the exposed bacteria.

The specific aims of the chapter were to:

- Evaluate biocide susceptibility before and after biocide exposure using MIC, MBC, and MBEC assays.
- Determine antibiotic cross resistance against biocide exposed UPEC.
- Evaluate the ability of UPEC to form biofilms before and after biocide exposure using crystal violet assay.
- Investigate the pathogenicity of UPEC before and after biocide exposure using *Galleria mellonella* model and primary cell invasion assays.
- Determine the biocompatibility of the four biocides against an L929 cell line.

2.4.0 Methods

2.4.1 Bacteria and chemicals Six UPEC clinical isolates (EC1, EC2, EC11, EC26, EC28 and EC34) previously isolated from urinary tract infections (Stepping Hill Hospital, Stockport, UK) and two laboratory characterised UPEC strains EC958 and CFT073 were used in the investigation. Bacteria were cultured on Muller-Hinton agar (MHA; Oxoid, UK) and Muller-Hinton broth (MHB; Oxoid, UK) and incubated aerobically at 37 °C for 18 h, unless otherwise stated. Biocides were formulated as follows: triclosan solubilised in 5% (v/v) ethanol. Polyhexamethylene biguanide (PHMB) (LONZA, Blackley, UK), benzalkonium chloride (BAC) and silver nitrate were prepared at 1 mg/ml in water and filter sterilised prior to use. All chemicals were purchased from Sigma–Aldrich (Poole, UK) unless otherwise stated.

2.4.2 Long-term exposure of bacteria to biocides Bacteria were repeatedly exposed to biocides using an antimicrobial gradient plating system adapted from McBain *et al* [152]. In brief, 100 µl of a 5 × MBC concentration solution of biocide was added to an 8 x 8 mm well in the centre of a 90 mm agar plate. Bacterial pure cultures were radially inoculated in duplicate from the edge of the plate to the centre, prior to incubation for 2 days aerobically at 37°C. Biomass from the inner edge of the annulus of bacterial growth representative of the highest biocide concentration at which growth could occur was removed and used to inoculate a new biocide containing plate, as outlined above. This process was repeated for 12 passages. Control isolates passaged 12 times on biocide free media were also included. Bacteria were archived at -80 °C before and after biocide passage for subsequent testing.

2.4.3 Minimum inhibitory and minimum bactericidal concentration Minimum inhibitory concentration (MIC) and minimum bactericidal concentration (MBC) were determined as described previously [80]. In brief, 2 × 5 ml overnight cultures of test bacteria were prepared in MHB prior to overnight incubation (18-24 h) at 37ºC and 100 rpm. Cultures were diluted to an OD_{600} of 0.008 in 20 ml of sterile MHB to produce a bacterial inoculum for biocide susceptibility testing. Doubling dilutions (150 µl) of each test biocide were prepared in sterile MHB in a 96-well microtiter plate prior to addition of bacterial inoculum (150 µl). Plates were incubated overnight (18-24 h) at 37ºC and 100 rpm. The MIC was defined as the lowest concentration of biocide for which growth was completely inhibited (viewed as turbidity relative to a sterile negative control). To determine MBC aliquots (5 µl) were taken from the wells of the MIC plate and were spot plated onto Muller Hinton Agar (MHA) in triplicate. The plates were incubated statically for 18-24 h at 37ºC. The lowest test concentration for which visible bacterial growth was completely inhibited was deemed the MBC.

2.4.4 Minimum biofilm eradication concentration Minimum biofilm eradication concentrations were determined using the Calgary biofilm device (CBD) as described previously [105]. Briefly, 2 × 5 ml overnight cultures of test bacteria were prepared in MHB and were incubated for 18-24 h at 37ºC and 100 rpm before being diluted to an OD_{600} of 0.008 in MHB to create a bacterial inoculum for biofilm susceptibility testing. 100 µl of bacterial inoculum was added to each well of the CBD base, plates were incubated at 37ºC for 48 h to allow biofilm formation on the pegs. Doubling dilutions of biocides were prepared in sterile broth across a 96-well microtiter plate. Biofilms were exposed to antimicrobial compounds and incubated for 24 h at 37°C and 100 rpm. After incubation, the pegged lid was transferred to a 96-well plate containing 200 µl of sterile broth and was incubated for 24 h at 37°C and 100 rpm. MBEC was defined as the lowest concentration of biocide for which re-growth was completely inhibited (viewed as turbidity relative to a sterile negative control) indicating complete biofilm eradication.

2.4.5 Crystal violet bacterial attachment assay 2 × 5 ml overnight cultures of test bacteria were diluted to an OD_{600} of 0.008 in MHB after incubation for 18-24h at 37º C and 100 rpm. 150 µl of diluted overnight bacterial culture was added to the wells of a sterile 96-well microtiter plate. Plates were incubated statically for 48 h at 37ºC. Media was removed from wells and replaced with 180 µl of crystal violet solution. The plate was left at room temperature for 30 minutes, crystal violet solution was decanted and

the wells were rinsed with 3 × 200 µl of PBS prior to drying for 1 h at 37ºC. The remaining crystal violet was solubilised in 250 µl of 100% ethanol. The A_{600} of the solubilised crystal violet solution was determined and compared to a sterile MHB negative control.

2.4.6 *Galleria mellonella* pathogenicity assay The pathogenesis model was adapted from that of Peleg *et al* [153]. Final larval-stage *G. mellonella* (Live Foods Direct, Sheffield, UK) were stored in the dark at 4°C for up to 7 days, before randomly assigning 24 to each treatment group and incubating at 37°C for 30 min. Overnight suspensions of *E. coli* were pelleted via centrifugation at 13,000 rpm, washed twice in 1 ml of PBS and then diluted appropriately to achieve an OD_{600} of 0.1 (5×10^5 - 8×10^5 CFU/ml, as confirmed by colony counts on MHA). Aliquots of each suspension (5 µl) were injected into the hemocele of each larva via the last left proleg using a Hamilton syringe. Larvae were incubated in a petri dish at 37°C and the number of surviving individuals was recorded daily. An untreated group and a group injected with sterile PBS were used as controls. The experiment was terminated when at least two individuals in a control group had died or after 7 days of incubation. Two independent bacterial replicates were used to inoculate 24 caterpillars (12 per replicate) and significance in death rate was calculated using a log-rank reduction test ($p \leq 0.01$).

2.4.7 Biocompatibility index Calculation of biocompatibility index (BI) was performed as described by Muller and Kramer [151]. To determine cytotoxicity, Neutral Red (NR) (3-amino- 7-dimethylamino-2-methylphenazine hydrochloride) assays and MTT [3-(4,5-dimethylthiazol-2-yl)-2, 5-diphenyltetra-zolium bromide] assays were performed on an L929 cell line to establish IC_{50}. Procedures for the NR assay and the MTT test have been described in detail elsewhere [151]. The bacterial quantitative suspension tests were done in accordance with the guidelines for testing disinfectants and antiseptics of the European Committee for Standardization [154]. Suspension tests were performed in the presence of serum to determine the rf value, defined as the concentration of biocide that achieved a reduction in bacterial load of at least $3\log_{10}$ (99.9%). Suspension tests were conducted as follows, overnight bacterial cultures were diluted to 10^8-10^9 CFU/ml as determined by colony counts on MHA. Aliquots of 15 µl of inoculum were then transferred into 135 µl of biocide containing cell culture medium prior to incubation for 30 min at 37ºC. For PHMB, BAC, and triclosan, the biocide was subsequently inactivated by transfer of 15 µl of the suspension into 135 µL of TSHC

(3% (w/v) Tween 80, 3% (w/v) saponin, 0.1% (w/v) histidine and 0.1% (w/v) cysteine). Silver nitrate was inactivated using TLA-thio (3% [w/v] Tween 80, 0.3% lecithin from soy bean, 0.1% [w/v] histidine and 0.5% [w/v] sodium thiosulphate). After 30 min of inactivation, 5 µl aliquots were spot plated onto MHA in triplicate. The plates were incubated statically for 18-24 h at 37ºC and CFU/ml was determined. The lowest test concentration which achieved at least a $3\log_{10}$ (99.9%) reduction in bacterial load was deemed the rf value. BI is calculated as IC50/rf for each combination of biocide and isolate and indicates the antiseptic potential of the test compound.

2.4.8 Antibiotic susceptibility Bacterial susceptibility was determined for trimethoprim sulfamethoxazole (25 µg), nitrofurantoin (50 µg), ciprofloxacin (10 µg), and gentamicin (200 µg). Antibiotic susceptibility tests were performed according to the standardized British Society for Antimicrobial Chemotherapy (BSAC) disc diffusion method for antimicrobial susceptibility testing [155].

2.4.9 Determination of mutation rate frequency Mutation rate frequency was determined as described by Miller *et al* [156]. In brief, 100 µl aliquots of diluted overnight culture obtained from single bacterial colonies were plated onto antibiotic free MHA plates and MHA plates containing 50µg/ml rifampicin in triplicate. Plates were incubated for 24h at 37ºC prior to determination of viable count. Mutation frequencies were expressed as the number of resistant mutants recovered as a fraction of total viable bacteria.

2.4.10 Cell Invasion Assay Evaluation of % invasion was performed on primary normal bladder smooth muscle cells (SMC) and human urothelial epithelial cells (HUEPC). SMCs were grown in Vascular Cell Basal Medium supplemented with the Vascular Smooth Muscle Cell Growth Kit (ATCC, UK). HUEPCs were grown in urothelial cell growth medium supplemented with serum free supplements (Provitro, Germany). Cells were seeded in 24 well plates at a concentration of $8x10^4$ cells/ml, with 1ml of cell suspension per well. Plates were incubated at 37ºC, 5% CO_2 for 48h. Cells were incubated with 500µl 2% Bovine Serum Albumin for 1 hour, at 37ºC, 5% CO_2. Overnight bacterial cultures were diluted to 200x the number of host cells per ml in cell culture medium. Host cells were washed twice with PBS and 500µl bacterial suspension was added. Wells of bacterial suspension that did not contain host cells were also included ('survival' plate). All plates were incubated for 90 mins at 37ºC, 5% CO_2.The

invasion plate was washed three times with PBS before 500µl media with 200µg/ml metronidazole was added. The plate was incubated for a further 60 mins at 37ºC, 5% CO_2. The attach plate was washed three times with PBS. Cells of each well were lysed in the presence of 200µl dH_2O for 1 minute per well. Lysate was removed and serial dilutions were carried out in PBS. Dilutions were plated out in triplicate onto MHA. This was repeated for the invasion plate and the 'survival' wells. Agar plates were incubated at 37ºC for 1 overnight and cfu/ ml were counted.

2.5.0 Results

2.5.1 Biocide susceptibility of UPEC in planktonic and biofilm states MIC (Table 2.1), MBC (Table 2.2) and MBECs (Table 2.3) were determined for all test isolates before (P0) and after repeated passage either in the absence (C12) or presence of a specific biocide (P12). Change in biocide susceptibility after exposure was calculated as fold-change relative to the control (C12) (Table 2.4). Data indicates both the frequency of susceptibility change (≥2 fold) and the average magnitude of susceptibility change for each biocide.

In terms of MIC, after repeated biocide exposure there was a ≥2 fold increase in 4/8 isolates for BAC, 8/8 for silver nitrate and 8/8 for triclosan compared to the respective bacteria passaged in a biocide free environment (Table 2.1). In contrast 4/8 isolates showed a ≥2 fold decrease in MIC after exposure to PHMB. The average fold-change for MIC (C12 to P12) across the test panel of UPEC was 1.5 for BAC, 0.7 for PHMB, 2 for silver nitrate and 807.1 for triclosan (Table 2.4). For MBC in the biocide exposed isolates (Table 2.2) there was a ≥2 fold increase in 4/8 isolates after BAC exposure, 8/8 for silver nitrate and 5/8 for triclosan. In contrast 1 isolate showed a decrease in MBC after PHMB exposure. The average fold change in MBC after biocide exposure was 1.5 for BAC, 0.8 for PHMB, 3.8 for silver nitrate and 5.4 for triclosan (Table 2.4). In terms of MBEC (Table 2.3), after repeated biocide exposure there was a ≥2 fold increase in 7/8 isolates for BAC, 8/8 for PHMB and 8/8 for triclosan. Silver nitrate exposure led to a 1 increase in MBEC and 1 decrease. The average fold change in MBEC after biocide exposure was 4.5 for BAC, 29.2 for PHMB, 832.7 for triclosan and 7.8 for silver nitrate (Table 2.4). We observed a number of changes in MIC, MBC and MBEC after the passage of bacteria solely in a biocide free-environment when compared to the unpassaged parent isolate. We did not, however see any incidence of a control passaged

isolate (C12) exhibiting a significantly higher MIC, MBC or MBEC ($P<0.05$) than the respective biocide passaged isolate (P12) with the exception of PHMB where the biocide exposed isolates frequently exhibited a lower MIC and MBC than the unexposed parent strain and the control passaged isolate subsequently matched the susceptibility of the parent strain.

	PHMB			Triclosan			BAC			Silver Nitrate		
Isolate	**P0**	**P12**	**C12**	**P0**	**P12**	**C12**	**P0**	**P12**	**C12**	**P0**	**P12**	**C12**
EC1	0.5	0.2	0.5	0.00001	2	0.02 (0.01)	15.6	15.6	15.6	31.3	62.5	31.3
EC2	0.2	0.2	0.2	0.1	15.6	0.05 (0.02)	15.6	31.3	15.6	31.3	62.5	31.3
EC11	0.2	0.2	0.2	0.1	2	0.05 (0.02)	15.6	31.3	15.6	31.3	62.5	31.3
EC26	0.5	0.2	0.5	0.2	125	0.03	15.6	31.3	15.6	31.3	62.5	31.3
EC28	0.5	0.5	0.5	0.2	3.9	0.2 (0.06)	15.6	15.6	15.6	31.3	62.5	31.3
EC34	0.2	0.2	0.2	0.03	15.6	0.02	15.6	15.6	15.6	31.3	62.5	31.3
EC958	1	0.2	1	0.1	7.8	0.03	15.6	31.3	15.6	31.3	62.5	31.3
CFT073	1	0.2	1	0.1	15.6	0.02	15.6	15.6	15.6	31.3	31.3	15.6

Table 2.1 Minimum inhibitory concentrations (µg/ml) for UPEC before exposure to biocide (P0), after 12 passages in the presence of the same biocide (P12), and after 12 passages in a biocide free environment (C12). Data represent mean MICs taken from two separate experiments each with four technical replicates.

	PHMB			Triclosan			BAC			Silver Nitrate		
Isolate	**P0**	**P12**	**C12**	**P0**	**P12**	**C12**	**P0**	**P12**	**C12**	**P0**	**P12**	**C12**
EC1	1	0.5	0.7 (0.3)	0.002	7.8	7.8	15.6	31.3	15.6	31.3	62.5	31.3
EC2	1	0.5	1	7.8	31.3	7.8	31.3	31.3	15.6	31.3	62.5	31.3
EC11	1	0.5	0.5	7.8	7.8	7.8	15.6	31.3	15.6	31.3	62.5	31.3
EC26	0.5	0.5	0.5	7.8	125	7.8	62.5	31.3	15.6	31.3	62.5	31.3
EC28	1	1	1	7.8	7.8	7.8	31.3	15.6	19.5 (8)	31.3	62.5	31.3
EC34	1	0.5	0.7 (0.3)	7.8	62.5	7.8	15.6	15.6	15.6	31.3	62.5	31.3
EC958	2	1	1.1 (0.5)	7.8	62.5	7.8	62.5	15.6	15.6	31.3	500	31.3
CFT073	15.6	1	1.1 (0.5)	7.8	31.3	7.8	15.6	15.6	15.6	31.3	31.3	15.6

Table 2.2 Minimum bactericidal concentrations (µg/ml) for UPEC before exposure to biocide (P0), after 12 passages in the presence of the same biocide (P12), and after 12 passages in a biocide free environment (C12). Data represent mean MBCs taken from two separate experiments each with four technical replicates.

	PHMB			Triclosan			BAC			Silver Nitrate		
Isolate	**P0**	**P12**	**C12**	**P0**	**P12**	**C12**	**P0**	**P12**	**C12**	**P0**	**P12**	**C12**
EC1	31.3	2000	93.8 (36)	7.8	31.3	0.5	250	500	125	2000	3000	3000
EC2	31.3	2000	93.8 (36)	3.9	250	2	125	500	62.5	3000	3000	3000
EC11	31.3	250	7.8	2	125	0.06	125	125	13.7 (4)	3000	3000	54.7 (16)
EC26	31.3	500	78.1 (31)	1	5000	2	250	250	93.8 (36)	2500	3000	3000
EC28	62.5	2000	62.5	3.9	125	7.8	125	125	125	4000	3000	2750 (500)
EC34	15.6	500	7.8	1	250	0.2 (0.07)	62.5	62.5	11.7 (5)	3000	3000	1750 (975)
EC958	62.5	1000	23.5 (9)	7.8	125	1	250	250	62.5	4000	4000	3000
CFT073	31.3	500	35.2 (20)	2	500	1	62.5	250	62.5	2000	500	1500 (577)

Table 2.3 Minimum biofilm eradication concentrations (μg/ml) for UPEC before exposure to biocide (P0), after 12 passages in the presence of the same biocide (P12), and after 12 passages in a biocide free environment (C12). Data represent mean MBECs taken from two separate experiments each with four technical replicates.

	MIC				MBC				MBEC			
Isolate	**PHMB**	**Triclosan**	**BAC**	**Silver nitrate**	**PHMB**	**Triclosan**	**BAC**	**Silver nitrate**	**PHMB**	**Triclosan**	**BAC**	**Silver nitrate**
EC1	**-2.5**	**97.7**	1	**2**	-1.4	1	**2**	**2**	**21.3**	**62.6**	**2**	1
EC2	1	**312.5**	**2**	**2**	**-2**	**4**	**2**	**2**	**21.3**	**125**	**8**	1
EC11	1	**39.1**	**2**	**2**	1	1	**2**	**2**	**32**	**2083.3**	**9.1**	**54.8**
EC26	**-2.5**	**4166.7**	**2**	**2**	1	**16**	**2**	**2**	**6.4**	**2500**	**2.7**	1
EC28	1	**19.5**	1	**2**	1	1	-1.25	**2**	**32**	**16**	1	1.1
EC34	1	**781.3**	1	**2**	-1.4	**8**	1	**2**	**64**	**1250**	**5.3**	1.7
EC958	**-5**	**260**	**2**	**2**	-1.1	**8**	1	**16**	**42.5**	**125**	**4**	1.3
CFT073	**-5**	**780**	1	**2**	-1.1	**4**	1	**2**	**14.2**	**500**	**4**	**-3**

Table 2.4 Fold changes are indicated for MIC, MBC, and MBEC in UPEC isolates after long-term biocide exposure compared with the respective isolate passaged in a biocide free-environment (C12). Changes (≥2 fold-change) are shown in bold.

2.5.2 The impact of biocide exposure on UPEC biofilm formation Biofilm formation was determined via a crystal violet biofilm assay for each UPEC isolate before and after repeated biocide exposure and after passage in a biocide free media (Figure 2.11). Unexposed isolates displayed varying biofilm forming capabilities prior to biocide exposure with EC2 showing the highest level of biofilm formation followed by EC1>CFT073>EC11>EC28>EC34>EC26 and EC958. When repeatedly exposed to triclosan, all isolates (with the exception of CFT073) demonstrated a significant (ANOVA $p \leq 0.05$) increase in biofilm formation relative to the respective control. All isolates demonstrated a significant increase in biofilm formation after BAC exposure with the exception of EC2. For PHMB and silver nitrate, EC1 showed a significant increase in biofilm formation after repeated exposure to either biocide. PHMB exposure also induced decreases in biofilm formation in EC2 and CFT073. Differences in biofilm formation were determined to be irrespective of growth rate as we did not observe any significant (ANOVA $p<0.05$) change in growth rate or overall growth productivity when in binary culture (Figure 2.12).

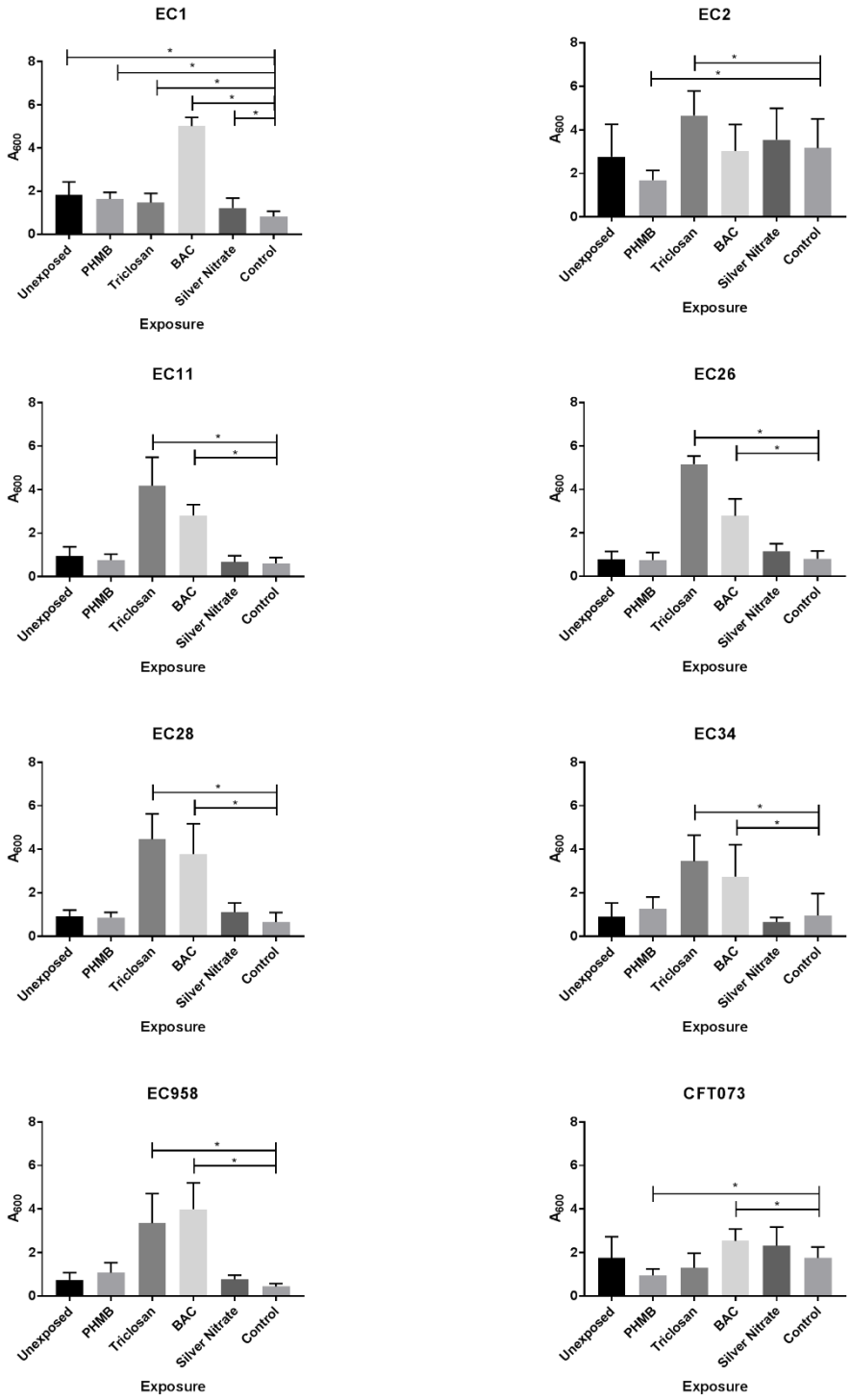

Figure 2.1 Crystal violet biofilm assay indicating the effect of previous biocide exposure on biofilm formation in eight isolates of UPEC. Data shows the mean absorbance (A_{600}) representative of biofilm formation for individual bacteria before and after long-term exposure to PHMB, triclosan, BAC or silver nitrate or after passage on a biocide free media (C12). Data represent samples taken from two separate experiments each with four technical replicates. For data that varied between replicates, SDs are given as error bars. Significance was determined using ANOVA; * $p \leq 0.05$.

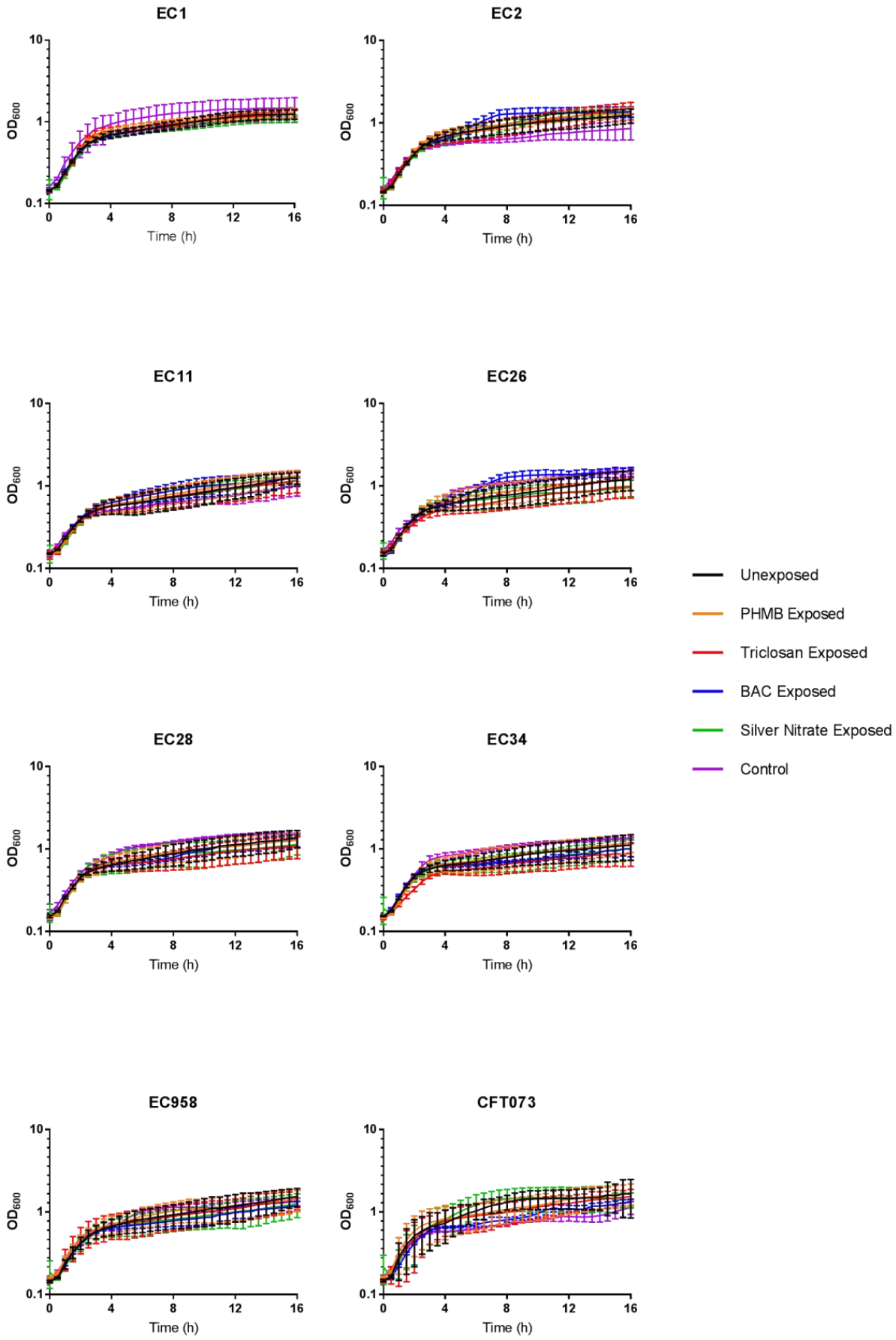

Figure 2.2 Planktonic growth for eight UPEC isolates after exposure to four biocides. Control isolates passaged without biocide (C12) are also shown.

2.5.3 Relative pathogenicity of UPEC after long-term biocide exposure A *G. mellonella* waxworm model was used to determine relative pathogenicity in UPEC isolates (Figure 2.3). Data indicate that prior to biocide exposure, EC2 was the least pathogenic and EC1 and EC958 were the most pathogenic isolates. PHMB exposure induced significantly (log-rank $p \leq 0.05$) decreased relative pathogenicity in 3/8 isolates (EC11, EC34 and EC958) and a significant increase in pathogenicity for EC2 when compared to the respective control isolate (C12). BAC exposure induced significantly decreased pathogenicity in 6/8 isolates (EC1, EC11, EC26, EC28, EC34 and EC958) and significantly increased pathogenicity in EC2. Silver nitrate was the only biocide to only induce significant increases in pathogenicity which occurred in 2/8 isolates (EC11 and EC28) and triclosan was the only biocide to induce only significant decreases in pathogenicity which occurred in 5/8 isolates (EC11, EC26, EC34, EC958 and CFT073).

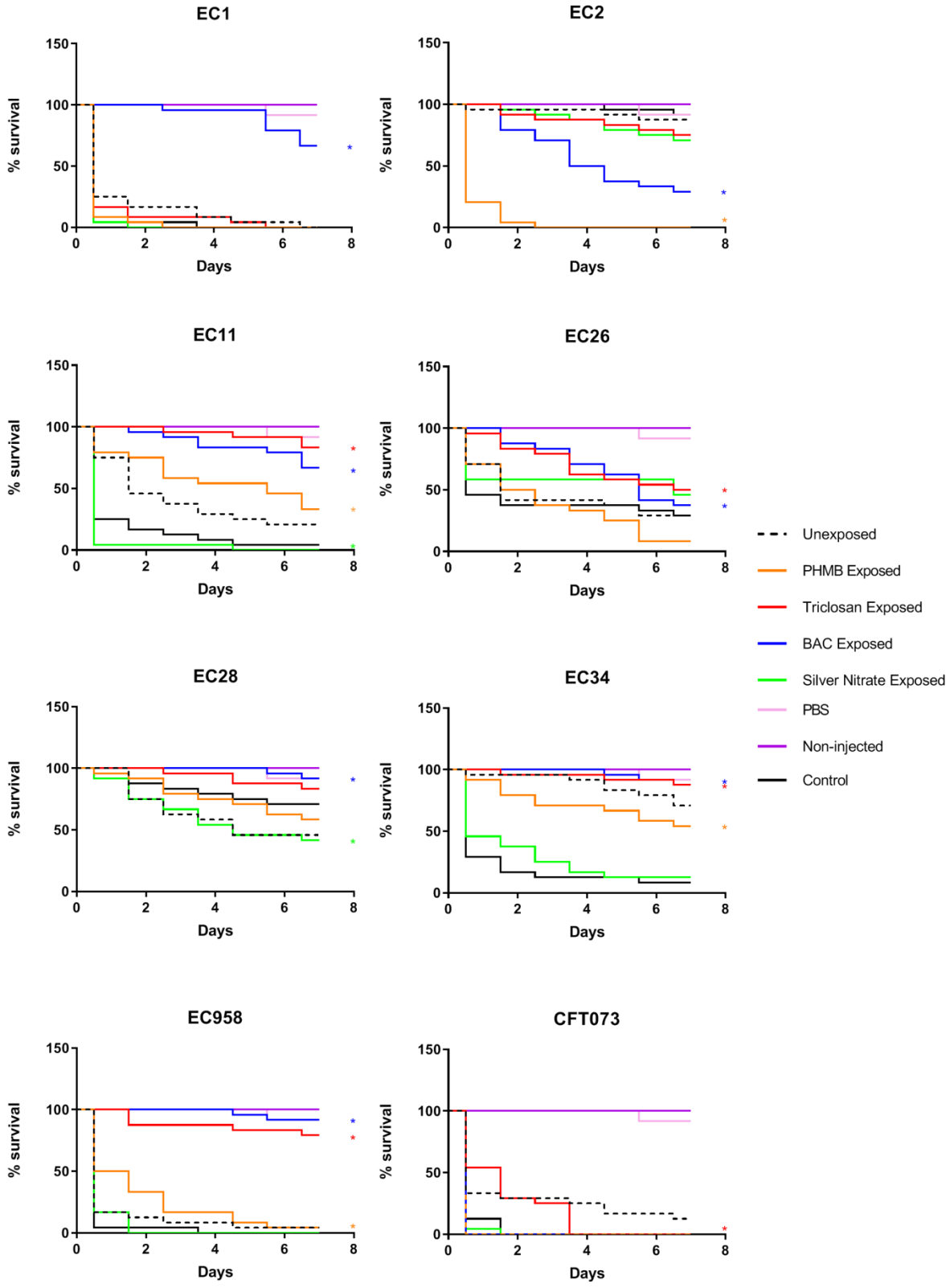

Figure 2.3 *G. mellonella* survival curves for larvae injected with unexposed and biocide-exposed UPEC. Data represents 24 biological replicates. Control data from non-injected larvae, larvae injected with PBS alone, and larvae injected with control isolates passaged on a biocide free media (Control) are also shown. * indicates a significant difference in pathogenicity when comparing biocide adapted isolates to the respective control strain ($p \leq 0.05$, log-rank reduction test).

2.5.4 Cell invasion Bacterial invasion of human cells was determined by cell invasion assay with each UPEC isolate before and after exposure for bladder smooth muscle (Figure 2.4) and urothelial cells (Figure 2.5). For the unexposed isolates, EC1 showed the highest percentage of invasion followed by EC11, EC2, EC28, EC34, EC958, CFT073 and EC26 in SMC. When exposed to PHMB, EC1, EC2, EC11, EC28, and EC34 showed an increase in SMC invasion. Exposure to BAC induced an increase in SMC invasion in EC958. Exposure to triclosan and silver nitrate had no significant effect on SMC invasion.

For HUEPC, EC958 showed the highest rate of invasion of the unexposed isolates, followed by, CFT073, EC1, EC26, EC11, EC34, EC28, and EC2. Exposure to PHMB induced significantly increased cell invasion in EC26. Triclosan exposure induced increased invasion in EC1 and EC28. BAC exposure induced increases in cell invasion for EC26 and EC34. Exposure to silver nitrate induced increases in cell invasion for CFT073.

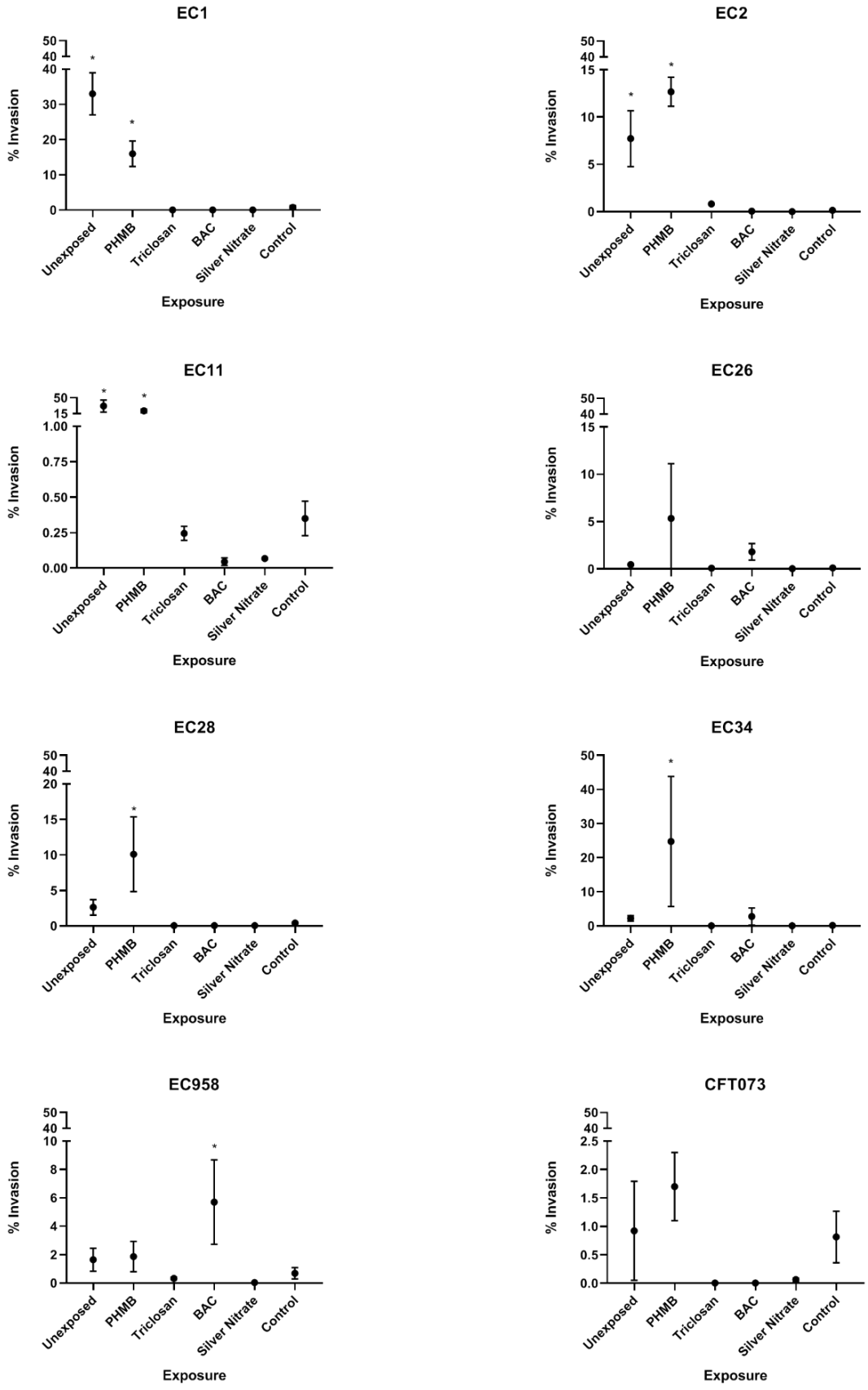

Figure 2.4 SMC invasion of eight strains of unexposed and biocide adapted UPEC. * indicates significant (ONE –WAY ANOVA $p<0.05$) change in cell invasion compared with relative control.

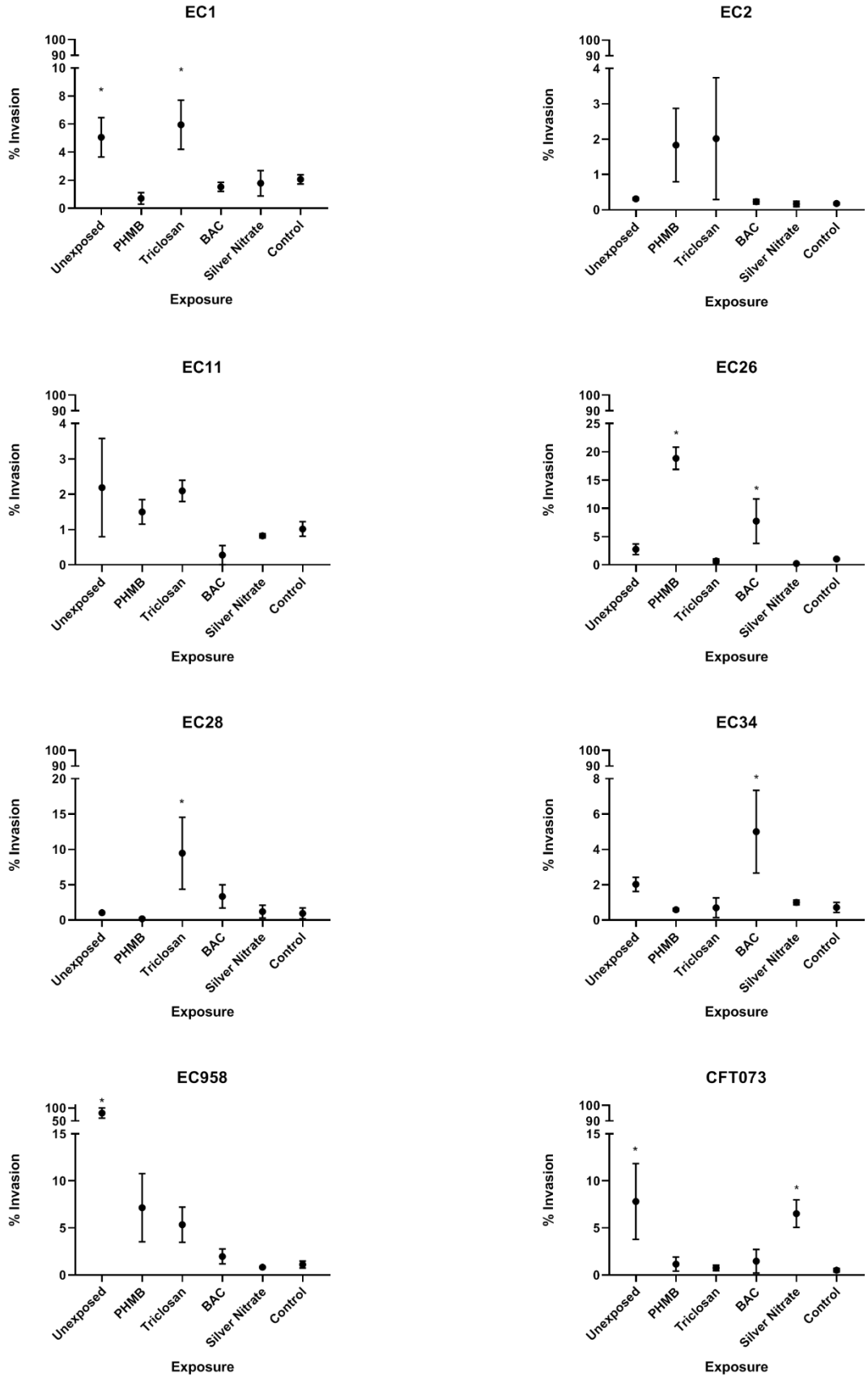

Figure 2.5 HUEPC invasion of eight strains of unexposed and biocide adapted UPEC. * indicates significant (ONE –WAY ANOVA $p<0.05$) change in cell invasion compared with relative control.

2.5.5 Changes in antibiotic susceptibility after biocide exposure Isolates were classed as resistant or sensitive to each antibiotic as defined by BSAC breakpoints [155]. Antibiotic susceptibility was determined for UPEC isolates before and after exposure to each biocide (Table 2.5). Data indicate that PHMB exposure induced CFT073 to become resistant to trimethoprim sulfamethoxazole and EC26 to become resistant to gentamicin. Exposure to triclosan induced nitrofurantoin resistance in EC958 and ciprofloxacin resistance in EC2. Triclosan exposure also induced intermediate resistance to gentamicin in EC2. Silver nitrate exposure induced EC2 to become resistant to ciprofloxacin as did BAC exposure. There were cases where isolates that were initially resistant to trimethoprim sulfamethoxazole became more susceptible after biocide exposure. This occurred in EC2 after exposure to PHMB, BAC, or silver nitrate and in EC11 after exposure to triclosan or BAC. This was also observed in EC11 for ciprofloxacin after triclosan exposure and CFT073 after BAC, triclosan or silver nitrate exposure.

Antibiotic	Exposure	EC1	EC2	EC11	EC26	EC28	EC34	EC958	CFT073
Trimethoprim Sulfamethoxazole	Unexposed	31.8 (1.3) S	0 **R**	0 **R**	0 **R**	0 **R**	0 **R**	0 **R**	30 (0.6) S
	PHMB	31.7 (0.8) S	30.3 (0.6) S	0 **R**	0 **R**	0 **R**	0 **R**	0 **R**	0 **R**
	Triclosan	31.5 (0.6) S	0 **R**	32.3 (0.3) S	0 **R**	0 **R**	0 **R**	0 **R**	28.8 (0.4) S
	BAC	29.7 (3.6) S	26 S	31 (0.6) S	0 **R**	0 **R**	0 **R**	0 **R**	28.8 (1.3) S
	Silver Nitrate	32.7 (0.6) S	25.5 (0.5) S	0 **R**	0 **R**	0 **R**	0 **R**	0 **R**	29.5 (0.5) S
Nitrofurantoin	Unexposed	20.3 (0.3) S	20.7 (0.3) S	23.7 (0.3) S	21.2 (1.5) S	19.7 (0.5) S	16.3 (1.2) S	20.4 (1.4) S	18 (0.6) S
	PHMB	20.3 (0.9) S	19.5 (0.5) S	25 (1) S	23.2 (3.1) S	19.2 (0.4) S	15 (0.6) S	19.8 (0.25) S	17.8 (0.8) S
	Triclosan	20 (0.6) S	20.5 (0.6) S	24.7 (0.3) S	24.2 (1.5) S	18.7 (1.4) S	18 (0.6) S	0 **R**	21.2 (0.4) S
	BAC	19.3 (0.3) S	18.5 (0.5) S	23.8 (0.3) S	23.3 (3.1) S	19.5 (1.5) S	15.2 (1.2) S	20.4 (0.1) S	17.2 (0.4) S
	Silver Nitrate	20.3 (0.3) S	18.8 (0.3) S	23.5 (1.6) S	23.3 (2.1) S	21.3 (0.5) S	15.8 (0.8) S	20 S	17.2 (0.4) S
Ciprofloxacin	Unexposed	31.2 (0.8) S	34 (0.6) S	13.8 (0.6) **R**	0 **R**	30 S	0 **R**	0 **R**	0 **R**
	PHMB	31.3 (0.8) S	35 (0.6) S	0 **R**	0 **R**	30 S	0 **R**	0 **R**	0 **R**
	Triclosan	32.5 (0.5) S	0 **R**	29.5 (0.8) S	0 **R**	30.7 (1) S	0 **R**	0 **R**	33.2 (1.9) S
	BAC	30 (0.3) S	0 **R**	0 **R**	0 **R**	29.7 (0.8) S	0 **R**	0 **R**	31.2 (1.8) S
	Silver Nitrate	31.2 (0.3) S	0 **R**	0 **R**	0 **R**	29.7 (0.8) S	0 **R**	0 **R**	31.7 (2.1) S
Gentamicin	Unexposed	26 (0.5) S	27.7 (0.3) S	25.5 (0.6) S	14.3 (1.2) **I**	18.2 (1) S	16.5 (0.5) **I**	26 S	24.8 (0.4) S
	PHMB	25.5 (0.6) S	28.1 (0.4) S	27.3 (0.3) S	11.8 (0.8) **R**	18.5 (1.6) S	16.2 (1.2) **I**	26.4 (0.5) S	25 S
	Triclosan	25.8 (0.3) S	16 **I**	23.5 (0.6) S	15.8 (3.5) **I**	20.8 (1) S	20 (0.9) S	27 (0.6) S	28.3 (1.4) S
	BAC	26.5 (0.5) S	25.8 (0.8) S	25.3 (0.3) S	16.8 (0.8) **I**	18.8 (0.8) S	18 S	26.7 (0.6) S	24.7 (0.5) S
	Silver Nitrate	27.8 (0.3) S	27.2 (0.1) S	27 (0.3) S	15.2 (1.5) **I**	18.7 (0.8) S	17 (1.3) S	26.2 (0.3) S	24 S

Table 2.5 Data show the mean antibiotic inhibition zones (mm) or UPEC before and after biocide exposure (mm) and represent samples taken from two separate experiments each with three technical replicates. For data that varied between replicates, SDs are given in parentheses. S = Sensitive, I = Intermediate, R = Resistant, as defined by BSAC breakpoint (23).

2.5.6 Biocompatibility Index Cytotoxicity data for the four biocides against an L929 cell line are shown in Table 2.6, rf values, indicating antimicrobial activity, and the corresponding BI values, highlighting the antiseptic potential of the compounds, are shown in Table 2.7. The order of cytotoxicity in relation to the biocide concentration was silver nitrate>PHMB>BAC>triclosan. The only isolate for which an rf value could be determined for silver nitrate was CFT073 as the rf values for the other isolates exceeded the maximum solubility of the biocide. Similarly, an rf value could not be determined in EC28 and CFT073 for triclosan as the rf value was greater than the highest achievable test concentration. BI values for the eight isolates were averaged for each biocide and the final ranked order of BI was PHMB>triclosan>BAC>silver nitrate indicating the antiseptic potential of the biocides.

Biocide	NR IC_{50}	MTT IC_{50}	m.w.	Mean IC_{50}	
				mg/ ml	mmol/ ml
PHMB	0.02	0.03	2800	0.026	0.000009
Triclosan	0.19	0.14	289.54	0.16	0.00057
BAC	0.07	0.03	340	0.047	0.00014
Silver Nitrate	0.002	0.003	169.87	0.0027	0.000016

Table 2.6 Mean concentration of biocides allowing 50% survival (IC_{50}) of murine fibroblasts after 30 min at 37ºC as determined via Neutral Red (NR) and [3-(4,5-dimethylthiazol-2-yl)-2, 5-diphenyltetra-zolium bromide] (MTT) assays. Mean IC_{50} based on mass and molecular weight (m.w.). Data indicates two separate experiments each with six replicates.

Biocide	EC1		EC2		EC11		EC26		EC28		EC34		EC958		CFT073	
	rf	BI	rf	BI	rf	BI	rf	BI	rf	BI	rf	BI	rf	BI	rf	BI
PHMB	0.02	1.6	0.06	0.4	0.01	1.6	0.02	1.6	0.3	0.1	0.1	0.2	0.5	0.05	0.02	1.6
Triclosan	0.2	0.7	1.1	0.1	0.2	0.7	1.1	0.1	NC	NC	0.6	0.3	2.3	0.07	NC	NC
BAC	0.07	0.7	0.2	0.2	0.2	0.2	0.2	0.2	0.1	0.3	0.2	0.2	0.6	0.08	0.07	0.7
Silver Nitrate	NC	NC	NC	NC	NC	NC	NC	NC	NC	NC	NC	NC	NC	NC	0.01	0.2

Table 2.7 Data shows the concentration of biocide (mg/l) producing 3 $\log_{10}$ reduction (rf) after 30 min of exposure at 37ºC on eight isolates of UPEC and the resulting BI value. NC- not calculable, for certain combination of biocide and bacterial isolate the rf value exceeded the maximum solubility of the biocide. Data represent mean rf values taken from two separate experiments each with four technical replicates.

2.5.7 Mutation rate frequency in UPEC isolates Mutation rate frequency was determined with regards to rifampicin resistance. We observed rifampicin resistant mutants from all UPEC isolates (Table 2.8). Mutation frequencies varied from 1.7×10^{-8} for CFT073 up to 3×10^{-7} for EC2 with an overall mutation frequency rank order of EC2>EC28>EC11>EC1>EC34>EC958>EC26>CFT073.

Isolate	**Mutation Rate**
EC1	7.97×10^{-8}
EC2	3×10^{-7}
EC11	1.36×10^{-7}
EC26	3.41×10^{-8}
EC28	1.86×10^{-7}
EC34	6.81×10^{-8}
EC958	3.49×10^{-8}
CFT073	1.69×10^{-8}

Table 2.8 Mutation rate frequencies of eight strains of UPEC for rifampicin resistance given as a fraction of the population.

2.6.0 Discussion

The current investigation aimed to explore the phenotypic changes that occur in genetically mixed populations of UPEC as a result of long-term biocide exposure. Susceptibility of eight UPEC isolates to a panel of test biocides was determined in planktonic and biofilm states before and after long-term biocide exposure. Changes that biocide exposure had on biofilm formation, relative pathogenicity and antibiotic susceptibility were assessed. Furthermore, cytotoxicity and the corresponding BI values were determined for each biocide against an L929 murine fibroblast cell line indicating the antiseptic potential of the test agents.

2.6.1 Biocide exposure induces changes in antimicrobial susceptibility in planktonic UPEC The data in this investigation highlights that long-term exposure to biocides may influence biocide susceptibility in UPEC. Bacterial susceptibility to biocides can be markedly affected by structural variations in the bacterial cell that (i) impact attraction of the biocide to the cell [77] (ii) lead to changes in cell permeability to the biocide [157] and (iii) cause modification in efflux activity allowing the bacteria to expel the biocide from the cell [158]. These modifications may account for some of the changes in biocide susceptibility observed in the current study, however the exact mechanisms that govern each specific adaptation depends upon a multitude of factors inherent to both the particular biocide and the bacterium [77]. Furthermore, previous studies have indicated that biocide exposure in bacteria may result in reversible phenotypic adaptations that occur as a consequence of temporary changes in gene expression, for instance the induction of stress responses [95]. In contrast, other investigations highlight that biocide exposure may lead to the selection of biocide resistant mutants with stable phenotypes that do not revert in the absence of the biocide [159]. This may reflect diversity within the mechanisms of action of biocides particularly with regards to target site specificity. Bacterial exposure to target site specific biocides such as triclosan readily appears to lead to the selection of mutations in target enzyme FabI [159] whilst induced insusceptibility towards membrane active compounds such as biguanides (PHMB) and quaternary ammonium compounds (BAC) is often associated with the induction of stress responses [160, 161].

In terms of initial antimicrobial efficacy, silver nitrate demonstrated the lowest activity against planktonic UPEC when compared with other test biocides at MIC and MBC.

We observed a high frequency of small magnitude decreases (≤2-fold) in silver nitrate susceptibility after long-term exposure resulting in comparatively high MIC and MBC values. Silver is widely considered as an effective anti-infective urinary catheter coating agent and is used in currently marketed anti-infective urinary catheters [113]. However, previous investigations have also documented the selection of silver resistance in Gram negative pathogens [101] including *E. coli* and other invasive *Enterobacteriaceae* [102]. This resistance has been correlated to increased efflux activity [103] or a loss of outer membrane porins [116] thereby decreasing cell permeability, which may explain the induced reductions in silver nitrate susceptibility observed in our UPEC isolates.

PHMB exposure induced a high frequency of small magnitude (≤2-fold) increases in susceptibility in planktonic UPEC at MIC and MBC. Previous data indicate that changes in bacterial susceptibility in response to membrane active compounds, such as biguanides, is usually attributed to alterations in the structural integrity of the bacterial cell envelope impacting cell permeability, modifications in the structure of LPS interfering in electrostatic interactions between the cationic biocide and cell envelope and due to increased cellular efflux activity, expelling the biocide from the cell [95], these mechanisms of resistance are in contrast with the data in the current investigation. Whilst other studies have also highlighted increases in PHMB susceptibility in bacteria after long-term exposure the underlying mechanisms that govern this adaptation remains unknown. It has been suggested that long-term exposure to biocides in bacteria may result in cumulative cellular damage and a resulting loss of fitness increasing bacterial susceptibility over time [148].

Triclosan was the most potent antimicrobial before repeated biocide exposure in planktonic UPEC. However triclosan induced the largest frequency and magnitude of susceptibility decreases in MIC and MBC. Resistance of *E. coli* to triclosan has been widely documented and is believed to be due to a mutation in the target enzyme FabI [159], due to increased cellular efflux [150] and changes in the cell membrane composition that reduce permeability [162]. Triclosan-impregnated catheters have demonstrated marked efficacy in *in vitro* studies [108], and show little reduction in antimicrobial activity even after long-term use [163]. This may be due to the fact that whilst large susceptibility changes may occur in bacteria following triclosan exposure, as indicated in our data, the initial potency of triclosan means that the catheter maintains

a high level of antimicrobial activity even after the bacteria adapt to the presence of the biocide likely due to its multi-target site mode of action.

BAC demonstrated lower initial antimicrobial activity against planktonic UPEC compared to triclosan and PHMB (MIC and MBC) and only induced minor reductions (≤2-fold) in susceptibility after long-term exposure. Changes in gene expression in BAC adapted *E. coli* have been previously identified revealing an upregulation of efflux pump membrane transporter *yhiV* and downregulation of the outer membrane porin *ompA* thereby increasing cellular efflux of BAC and reducing cell permeability towards the biocide [99].

Repeated passage of bacteria on a biocide free media occasionally led to changes in biocide susceptibility within planktonic culture, however these changes occurred at a substantially lower magnitude and frequency than those observed after biocide adaptation and were predominantly increases in susceptibility. This potentially reemphasises the fitness costs associated with repeated culture. Significantly, we observed only five cases of significant reduction in biocide susceptibility when comparing the isolate passaged in the absence of biocide to the unexposed parent strain. This reduction in susceptibility could be attributed to the stress of repeated passage leading to protective stress responses. For example, reduced amino acid availability leading to the stringent response has been shown to cause reduced penicillin susceptibility in *E.coli* [164].

2.6.2 Biofilm formation and susceptibility in UPEC after biocide exposure Bacteria that have adapted to the presence of biocides may exhibit further phenotypic alterations such as changes in growth rate, biofilm formation and competitive fitness, which may influence pathogenicity [13, 17]. After biocide exposure several UPEC isolates in the current study exhibited significant changes in biofilm formation. Whilst this biofilm formation is a complex multifactorial process, these changes could potentially be attributed to the selection of mutants with alterations in factors involved in the establishment of biofilms, such as adhesion, EPS production or maturation.

Biocide exposure largely led to increases in biofilm formation particularly after exposure to BAC and triclosan. Of the 7 UPEC isolates that demonstrated an increase in biofilm formation after BAC exposure 6 had a corresponding increase in MBEC. All 7 isolates that increased in biofilm formation after triclosan exposure also exhibited an

elevation in MBEC. PHMB exposure led to a significant decrease in biofilm formation for EC2 and CFT073 which did not correspond with decreases in MBEC, possibly indicating the recalcitrance of persister populations within the biofilm irrespective of biofilm biomass [165].

BAC adaptation has been previously correlated to an increase in biofilm biomass in *E. coli* which is believed to be due to an increase in protein and polysaccharide content within the extracellular polymeric substance (EPS) [166]. This change in EPS composition may lead to reduced BAC susceptibility, as observed in our BAC adapted isolates.

Yu *et al.* [93] utilised a genome-wide enrichment screen to demonstrate the genes involved in triclosan adaptation in *E. coli.* Microarray analysis revealed that triclosan exposure resulted in an increase in *fimDFHI* which encodes proteins involved in fimbrial biosynthesis, that have been shown to be positively associated with an increase in biofilm formation [167]. This may provide a potential link between the increase in biofilm formation and thus resistance caused by triclosan exposure in the UPEC isolates used in the current investigation.

2.6.3 Changes in antibiotic susceptibility after biocide exposure in UPEC Concerns have been raised that biocide exposure may induce cross-resistance to clinically relevant antibiotics**.** In the current study we observed the generation of antibiotic resistance in 7 out of a possible 84 combinations of bacteria, biocide and antibiotic. The biocide that induced the highest number of cases of cross-resistance in a previously susceptible or intermediate isolate was triclosan, which was to nitrofurantoin, gentamicin and ciprofloxacin. PHMB exposure led to trimethoprim sulfamethoxazole and gentamicin cross resistance. BAC and silver nitrate exposure led to one observed case of cross-resistance each which was towards ciprofloxacin.

There have been previous reports into efflux mediated cross-resistance between antibiotics and to triclosan reportedly due to upregulation of *acrAB,* encoding the AcrAB efflux pump [168]. Efflux pumps have also been correlated to observed cross-resistance to between quaternary ammonium compounds and antibiotics in *E. coli*. Bore *et al* observed reduced antibiotic susceptibility in BAC-adapted *E. coli* which also coincided with an increase in the expression of *acrAB* and a downregulation in multiple outer membrane porins including OmpA, OmpF and OmpT [99]. Whilst there is

relatively sparse evidence on the generation of antibiotic cross-resistance due to PHMB exposure in bacteria, the mechanisms of uptake of PHMB is similar to that of aminoglycosides involving destabilisation of the bacterial cell membrane and LPS reorganisation [169]. Interaction between LPS and PHMB is known to be a key step in the initial interaction of the biocide with the bacterial cell in *E. coli* (31). This may suggest why an induced reduction in PHMB susceptibility in our UPEC isolates also led to a similar reduction in susceptibility towards gentamicin. Studies on silver resistance in *E. coli* have revealed acquired low-level cross-resistance to cephalosporins, similarly due to increased efflux and reduced porin expression [116]. In this study, there were 10 cases of biocide exposure eliciting increased susceptibility to antibiotics namely towards trimethoprim sulfamethoxazole and ciprofloxacin. This display of "cross-protection" has been noted in previous studies and has been suggested to be due to a potential increase in cell permeability in response to biocide adaptation however the underlying mechanisms remain unclear [80].

2.6.4 Biocompatibility of test biocides in an L929 cell line To assess the suitability of an antiseptic agent both the antimicrobial activity and cytotoxicity must be considered. Silver nitrate showed the highest level of cytotoxicity in an L929 cell line and the lowest antimicrobial efficacy in the corresponding quantitative suspension test (rf value). Reduced activity of silver when in the presence of serum has been previously attributed to binding of the silver cations to the electronegative serum components, which may explain the low level of antimicrobial activity in silver nitrate observed in the quantitative suspension test in the current study [170]. Silver ions have been demonstrated to interact with components of mammalian cells including the mitochondria, nuclei, endoplasmic reticulum and the cell membrane [171]. Interaction of silver ions with mitochondria reportedly causes mitochondrial damage and the release of reactive oxygen species (ROS) resulting in apoptosis suggesting a mechanism of silver-mediated cytotoxicity [172]. Whilst PHMB was shown to be the second most cytotoxic biocide tested, it exhibited a relatively low rf value resulting in the highest BI value out of all the test biocides. PHMB has previously shown low level cytotoxicity towards mammalian cells, including L929 cells, which is suggested to be due to the interaction of the biocide with the mammalian cell membrane leading to membrane damage [173]. BAC was the second least cytotoxic biocide tested and the showed the second highest level of antimicrobial activity in the presence of serum in the

quantitative suspension tests. BAC has been shown to interact with guanine nucleotide triphosphate-binding proteins (G proteins) impacting cell signalling transduction in mammalian cells and causing DNA damage [174]. Cytotoxicity data indicated triclosan to be the least cytotoxic of all the test biocides. However the rf values were high resulting in the second highest BI value. Triclosan has previously shown reduced antimicrobial efficacy in the presence of serum, this is believed to be due to the bacteria's ability to gain an exogenous supply of fatty acids from the serum, thereby bypassing the inhibitory effects of the biocide [175]. Additionally, previous studies report on triclosan interference with mitochondrial respiration [176] in addition a damaging effect on the plasma membrane and induced apoptotic cell death [177] suggesting a potential mechanism of cytotoxicity.

2.6.5 Altered relative pathogenicity in biocide adapted UPEC Repeated biocide exposure to silver nitrate induced an increase in relative pathogenicity in 2/8 isolates of UPEC whilst PHMB exposed isolates exhibited a decrease in pathogenicity in 3/8 and an increase in pathogenicity in 1/8 isolates respectively. A decrease in pathogenicity was observed after triclosan exposure in 5/8 isolates and in 6/8 isolates after exposure to BAC. BAC also induced an increase in pathogenicity in 1 further isolate. Triclosan exposure has previously been shown to reduce relative pathogenicity in a *G. mellonella* waxworm model in certain bacterial species [104]. These pathogenicity changes were suggested to be due to changes in virulence factor production, specifically reduced DNase activity and a down-regulation in cell surface adhesins [178]. It has been shown that triclosan exposure specifically downregulates genes encoding the outer membrane proteins P-fimbriae and protein X in *E. coli* [179] which are integral for UPEC attachment to cell surfaces [180] and entry into host cells [181]. Isolates of *E. coli* that have been exposed to BAC have been shown to have increased hemolysin activity and enhanced virulence [182] which may explain the increase in pathogenicity for the BAC exposed isolates in the current study. To our knowledge there are no current studies regarding the effects of silver or PHMB exposure on bacterial virulence factor production and resulting pathogenicity.

2.6.6 UPEC invasion into human cells after exposure to biocides It was observed that, on average, invasion was higher in HUEPC than in SMC. This would make sense as UPEC express genes that encode P fimbriae/ pyelonephritis associated pili (PAP) [24] and type 1 pili which both adhere specifically to uroepithelium [26, 183].When

exposed to PHMB, 5/8 showed an increase in SMC invasion. For HUEPC, exposure to PHMB induced increased invasion in 1/8 isolates. Exposure to PHMB has been shown to induce expression of adhesion gene *ycgV* and increase production of pili which are used as adherence factors [95]. This would explain increases in cell invasion.

For HUEPC invasion triclosan exposure induced increased invasion in 2/8 isolates. Triclosan exposure has previously been shown to specifically downregulate genes encoding outer membrane proteins (P-fimbriae and protein X in *E. coli*) [179] which are integral for UPEC attachment to cell surfaces [180] and entry into host cells [181]. This data is therefore in contrast to what we see in the current investigation.

Exposure to BAC induced an increase in invasion in 1/8 isolates for SMC. BAC exposure induced increases in HUEPC invasion for 2/8 isolates. BAC exposure has been shown to increase expression of efflux pumps [100] and decrease expression of motility associated genes [184]. But to our knowledge there are no studies that have investigated the effects of BAC on *E.coli* cell invasion or have identified genes associated with invasion/adhesion that are associated with BAC exposure.

When exposed to silver nitrate, 1/8 isolates showed increases in HUEPC invasion. A study into the effects of ionic silver on *E.coli* found an upregulation of *ydeS,R* which is putatively involved in cell adhesion [185]. Bacteria first have to adhere to cells before being able to invade so an increase in cell adhesion could explain the increased invasion seen in this study.

2.6.7 Consequence of variance in mutation rate frequency in UPEC Elevated mutation rates have been previously reported in *E. coli* strains [186]. Furthermore, the adapting populations generated in the current investigation may lead to the selection of hypermutators due to the selective pressures created during biocide exposure. We evaluated the mutation frequencies in our parent isolates to determine whether this correlated to a higher frequency of phenotypic adaptations after biocide exposure. Mutation rate frequency was determined to be ordered EC2>EC28>EC11>EC1>EC34>EC958>EC26>CFT072. When comparing mutation rate to incidences of biocide susceptibility change (MIC, MBC and MBEC) EC11 and CFT073 showed the highest frequency of changes in biocide susceptibility whilst EC28 showed the least. We observed two cases of significant change in biofilm formation for each isolate with the exception of EC1 for which we observed four. In terms of

significant changes in relative pathogenicity, EC11 demonstrated four significant changes after biocide exposure, EC34 and EC958 showed three, EC2, EC26 and EC28 showed 2 and EC1 and CFT073 showed one. These data indicate a lack of correlation between the frequency of mutation rate in the parent strain and the rate of phenotypic adaptation in the respective isolate after biocide exposure.

2.7.0 Conclusion

The use of biocides for the purpose of antisepsis has led to concern over the selection of biocide resistance in clinically relevant pathogens. Here it is demonstrated that long-term exposure of UPEC to commonly used biocides can result in changes in biocide susceptibility which may be accompanied by further phenotypic alterations impacting biofilm formation, antibiotic susceptibility and relative pathogenicity. The multiple consequences of bacterial adaptation towards biocides should therefore be evaluated when considering a potential anti-infective catheter coating agent.

Chapter 3

Impact of long-term quorum sensing inhibition in uropathogenic *Escherichia coli*

I acknowledge the following people for contributing to the work presented in this chapter: L Jaques (MSci student) who helped with the MIC, MBC, MBEC, pathogenicity, and antibiotic sensitivity experiments for the cinnamaldehyde and furanone C30 exposed isolates. P.G Chirila (PhD student) and C Whiteoak (academic) who synthesised the furanone C30. M Kadirvel (academic) who synthesised the F-DPD.

3.1.0 Abstract

Background: Quorum sensing is a cell-cell communication system utilised in the density-dependent regulation of gene expression in bacteria and the subsequent development of biofilms. Biofilm-formation has been implicated in the establishment of catheter-associated urinary tract infections (CAUTIs) therefore quorum sensing inhibitors (QSIs) have been suggested as anti-biofilm catheter coating agents to prevent CAUTI. The long-term effects of QS inhibition in uropathogens are, however, not clearly understood. The effects of long-term exposure to potential QSIs cinnamaldehyde, (Z)-4-Bromo-5(bromomethylene)-2(5H)-furanone (C30) and 4-fluoro-5-hydroxypentane-2,3-dione (F-DPD) were evaluated on susceptibility, biofilm-formation and relative-pathogenicity in eight uropathogenic *Escherichia coli* (UPEC) isolates. **Methods:** Minimum inhibitory, bactericidal and biofilm eradication concentrations were determined before and after QSI exposure. Biofilm-formation was quantified using crystal-violet and relative-pathogenicity was assessed in a *Galleria mellonella* model. Cytotoxicity and resulting biocompatability index values were determined in an L929 murine fibroblast cell line. Cell invasion assays were performed against bladder smooth muscle (SMC) and urothelial (HUEPC) cell lines. **Results:** Cinnamaldehyde and furanone C30 led to multiple increases in susceptibility in planktonic and biofilm-associated UPEC. Relative pathogenicity increased after cinnamaldehyde exposure (4/8 isolates), decreased after furanone C30 exposure (6/8 isolates) and varied after F-DPD exposure (2/8 increases and 2/8 decreases). Cinnamaldehyde and furanone C30 both induced 1/8 increase in HUEPC invasion whilst F-DPD induced 1/8 decrease in SMC invasion. 9 out of 21 possible cases of antibiotic cross-resistance were generated. The order of biocompatibility was furanone C30 > cinnamaldehyde > F-DPD. **Conclusion:** The impact of long-term QS inhibition in UPEC should be considered when selecting an anti-infective catheter coating agent.

3.2.0 Introduction

Urinary tract infection (UTI) is the most common healthcare associated infection (HCAI), with between 43% and 56% of cases associated with the presence of an indwelling urethral catheter [15]. Long-term catheterisation carries a significant risk of symptomatic catheter associated urinary tract infection (CAUTI), which can lead to complications such as pylonephritis and subsequent blood stream infection [14].

Uropathogenic *Escherichia coli* (UPEC) is a frequent cause of catheter-associated urinary tract infection (CAUTI). Currently *E. coli* is the leading cause of blood stream infection in the UK with a mortality rate of 14.8% [17]. Of these cases, 21% are linked to urethral catheterisation [17]. With an ageing population in the UK it is likely that the need for urinary catheters will continue to rise resulting in an increasing risk to health and an escalating cost for healthcare service providers.

The treatment of CAUTI is complicated by the emergence of UPEC exhibiting multiple antibiotic resistances. In Europe and the US 50,000 people a year lose their lives due to antibiotic resistant pathogens with that number rising to 700,000 worldwide [187]. This number is predicted to reach 10 million deaths by 2050 if alternative therapies are not found [187]. There has therefore been significant interest in the development of strategies to help prevent infection that avoids the use of antibiotics. A novel approach in the production of anti-infective catheter coatings is to use quorum sensing inhibitors (QSIs).

Quorum sensing (QS) is a process by which bacteria produce and detect signalling molecules and thereby coordinate their behaviour in a cell density dependent manner [10]. It has been shown to be an important contributor to the formation of a bacterial biofilms in certain bacterial species and may be involved in the expression of various virulence factors [5]. QSIs act to disrupt this communicative process and provide a potential strategy to prevent the establishment of biofilm associated infections such as CAUTI, whilst exhibiting limited cytotoxic effects due to their bacterial target site specific mode of action.

Quorum sensing in UPEC is mediated by acyl-homoserine lactone (AHL) and autoinducer-2 (AI-2) [43]. AI-2 consists of derivatives of 4,5-dihydroxy-2,3-pentanedione (DPD) [47] with LuxS, the DPD synthase, present in more than 500 bacterial species [43]. It has been shown that AI-2 production is directly correlated to biofilm production in *E.coli* [48]. DPD analogues have been used to prevent AI-2 binding to the periplasmic receptor LsrB [64] and disrupt AI-2 based transduction. 4-fluoro-5-hydroxypentane-2,3-dione (F-DPD) a fluoro DPD analogue has been shown to disrupt AI-2 based QS and biofilm formation in *Vibrio harveyi*. A small variety of naturally produced compounds have also been shown to inhibit AI-2 based signalling. Cinnamaldehyde is a natural product from the bark of the cinnamon tree and furanone is

a naturally produced QSI produced by red algae *Delisea pulchra* [10]. Both furanone C30 and cinnamaldehyde have been suggested to inhibit AI-2 based QS by decreasing the DNA binding ability of the response regulator LuxR [10]. Both compounds have been shown to affect biofilm-formation and increase biofilm susceptibility towards antibiotic treatment in a range of bacterial species *in vivo* [71]. As well as demonstrating QSI activity these compounds have also shown bacteriostatic and bactericidal effects [188, 189].

The gradient created by the release of an antimicrobial agent from a coated medical device creates a selective pressure that may induce phenotypic adaptations within individual bacterial cells or select for intrinsically resistant mutants altering both the bacteria itself and the surrounding microbial community composition. The risks associated with long-term exposure of bacteria to broad-spectrum antimicrobials has been extensively studied [9, 83], however there has been significantly lesser research into the long-term impact of QSIs. The current study therefore aimed to quantify the effects of QSI exposure in eight UPEC isolates. Specifically we will determine impact on antimicrobial and anti-biofilm susceptibility, the induction of antibiotic cross-resistance, level of biocompatibility in addition to changes in biofilm-formation, relative pathogenicity and capacity for cell invasion.

3.3.0 Aims and objectives

Quorum sensing inhibitor treatment has been shown to reduce biofilm formation in *E.coli* by inhibiting the cell signalling required to initiate the genetic switch to biofilm growth [190]. There have also been reports of other effects of QSI treatment, for example increased antibiotic resistance [63]. There have not been any major studies into the impact of long term exposure to QSIs on bacteria. As quorum sensing is involved in the control of hundreds of genes in *E.coli* it is hypothesised that UPEC adaptation to QSI exposure will result in multiple phenotypic changes.

The specific aims of this chapter were to:

- Determine the efficacy of the QSIs cinnamaldehyde, furanone C30, and F-DPD in a *Vibrio harveyi* reporter system.
- Evaluate QSI susceptibility before and after QSI exposure using MIC, MBC, and MBEC assays.

- Determine antibiotic cross resistance against QSI exposed UPEC.
- Evaluate the ability of UPEC to form biofilms before and after QSI exposure using crystal violet assay.
- Investigate the pathogenicity of UPEC before and after QSI exposure using *Galleria mellonella* model and primary cell invasion assays.
- Determine the biocompatibility of the three QSIs against an L929 cell line.

3.4.0 Methods

3.4.1 Bacteria and chemical reagents Six UPEC clinical isolates (EC1, EC2, EC11, EC26, EC28 and EC34) previously isolated from urinary tract infections (Stepping Hill Hospital, UK) and two laboratory characterised UPEC isolates (EC958 and CFT073) were used in the investigation. Bacteria were cultured onto Muller-Hinton agar (MHA; Oxoid, UK) or Muller-Hinton broth (MHB; Oxoid, UK) and incubated aerobically at 37 °C for 18 h unless otherwise stated. Furanone C30, cinnamaldehyde and F-DPD were prepared at 1 mg/ml in water and filter sterilised prior to use. Cinnamaldehyde was purchased from Sigma–Aldrich (Poole, UK). (Z)-4-Bromo-5(bromomethylene)-2(5H)-furanone C30 (furanone C30) was synthesised at Sheffield Hallam University by P.G Chirila and C. Whiteoak as described previously [191]. 4-fluoro-5-hydroxypentane-2,3-dione (F-DPD) was synthesised at University of Manchester by M. Kadirvel as described previously [192].

3.4.2 *Vibrio* model for determination of QSI activity Overnight cultures of *Vibrio harveyi BB170* were grown in 20ml marine broth (Difco) at 37ºC 200rpm prior to dilution to OD_{600} 0.008 and exposure to doubling dilutions of QSI in a 96-well microtitre plate. Plates were incubated at 37ºC for 40 h at 200rpm in a ClarioStar plate reader (BMG Labtech). Bioluminescence and the corresponding OD_{600} were recorded every 30 minutes.

3.4.3 Long-term exposure of bacteria to quorum sensing inhibitors Bacteria were repeatedly exposed to QSIs using an antimicrobial gradient plating system as described in McBain *et al* [152]. In brief, 100 µl of a 5 × MBC concentration solution of QSI was added to an 8 x 8 mm well in the centre of a 90 mm agar plate. Bacterial pure cultures were radially inoculated in duplicate from the edge of the plate to the centre, prior to incubation for 2 days aerobically at 37°C. Biomass from the inner edge of the annulus

of bacterial growth representative of the highest QSI concentration at which growth could occur was removed and used to inoculate a new QSI containing plate, as outlined above. This process was repeated for 12 passages. Control isolates passaged 12 times on QSI free media were also included. Bacteria were archived at -80 °C before and after QSI passage for subsequent testing.

3.4.4 Minimum inhibitory and minimum bactericidal concentration Minimum inhibitory concentration (MIC) and minimum bactericidal concentration (MBC) were determined as described previously [80]. The MIC was defined as the lowest concentration of QSI for which growth was completely inhibited (viewed as turbidity relative to a sterile negative control). To determine MBC aliquots (5 µl) were taken from the wells of the MIC plate and were spot plated onto Muller Hinton Agar (MHA) in triplicate. The plates were incubated statically for 18-24 h at 37ºC. The lowest test concentration for which visible bacterial growth was completely inhibited was deemed the MBC.

3.4.5 Minimum biofilm eradication concentration Minimum biofilm eradication concentrations were determined using the Calgary biofilm device (CBD) as described previously [105]. MBEC was defined as the lowest concentration of QSI for which re-growth was completely inhibited (viewed as turbidity relative to a sterile negative control) indicating complete biofilm eradication.

3.4.6 Crystal violet bacterial attachment assay 2 × 5 ml overnight cultures of test bacteria were diluted to an OD_{600} of 0.008 in MHB after incubation for 18-24h at 37º C and 100 rpm. 150 µl of diluted overnight bacterial culture was added to the wells of a sterile 96-well microtiter plate. Plates were incubated statically for 48 h at 37ºC. Media was removed from wells and replaced with 180 µl of crystal violet solution. Plates were left to dry at room temperature for 30 minutes, crystal violet solution was decanted and the wells were rinsed with 3 × 200 µl of PBS prior to drying for 1 h at 37ºC. The remaining crystal violet was solubilised in 250 µl of 100% ethanol. The A_{600} of the solubilised crystal violet solution was determined and compared to a sterile negative control.

3.4.7 *Galleria mellonella* pathogenicity assay The pathogenesis model was performed as described in Peleg *et al* [153]. Final larval-stage *G. mellonella* were obtained from Live Foods Direct, Sheffield, UK. Treated larvae were incubated in a petri dish at 37°C

and the number of surviving individuals was recorded daily. An untreated group and a group injected with sterile PBS were used as controls. The experiment was terminated when at least two individuals in a control group had died or after 7 days of incubation. Two independent bacterial replicates were used to inoculate 24 caterpillars (12 per replicate) and significance in death rate was calculated using a log-rank reduction test ($p \leq 0.05$).

3.4.8 Biocompatibility index Calculation of biocompatibility index (BI) was performed as described by Muller and Kramer [151]. To determine cytotoxicity, Neutral Red (NR) (3-amino- 7-dimethylamino-2-methylphenazine hydrochloride) assays and MTT [3-(4,5-dimethylthiazol-2-yl)-2, 5-diphenyltetra-zolium bromide] assays were performed on an L929 cell line to establish IC_{50}. Procedures for the NR assay and the MTT test have been described in detail elsewhere [151]. The bacterial quantitative suspension tests were done in accordance with the guidelines for testing disinfectants and antiseptics of the European Committee for Standardization [154]. Suspension tests were performed in the presence of serum to determine the rf value, defined as the concentration of QSI that achieved a reduction in bacterial load of at least $3\log_{10}$ (99.9%). BI is calculated as IC50/rf for each combination of QSI and isolate and indicates the antiseptic potential of the test compound.

3.4.9 Antibiotic susceptibility Bacterial susceptibility was determined for trimethoprim sulfamethoxazole (25 µg), nitrofurantoin (50 µg), ciprofloxacin (10 µg), and gentamicin (200 µg). Antibiotic susceptibility tests were performed according to the standardized British Society for Antimicrobial Chemotherapy (BSAC) disc diffusion method for antimicrobial susceptibility testing [155].

3.4.10 Cell Invasion Assay Evaluation of % invasion was performed on primary normal bladder smooth muscle cells (SMC) and human urothelial epithelial cells (HUEPC). SMCs were grown in Vascular Cell Basal Medium supplemented with the Vascular Smooth Muscle Cell Growth Kit (ATCC, UK). HUEPCs were grown in urothelial cell growth medium supplemented with serum free supplements (Provitro, Germany). Cells were seeded in 24 well plates at a concentration of $8x10^4$ cells/ml, with 1ml of cell suspension per well. Plates were incubated at 37ºC, 5% CO_2 for 48h. Cells were incubated with 500µl 2% Bovine Serum Albumin for 1 hour, at 37ºC, 5% CO_2. Overnight bacterial cultures were diluted to 200x the number of host cells per ml in cell

culture medium. Host cells were washed twice with PBS and 500µl bacterial suspension was added. Wells of bacterial suspension that did not contain host cells were also included ('survival' plate). All plates were incubated for 90 mins at 37ºC, 5% CO_2.The invasion plate was washed three times with PBS before 500µl media with 200µg/ml metronidazole was added. The plate was incubated for a further 60 mins at 37ºC, 5% CO_2. The attach plate was washed three times with PBS. Cells of each well were lysed in the presence of 200µl dH_2O for 1 minute per well. Lysate was removed and serial dilutions were carried out in PBS. Dilutions were plated out in triplicate onto MHA. This was repeated for the invasion plate and the 'survival' wells. Agar plates were incubated at 37ºC for 1 overnight and cfu/ ml were counted.

3.5.0 Results

3.5.1 Efficacy of QSI's QS reporter strain *Vibrio harveyi BB170* was used to determine QS inhibitory activity of furanone C30, F-DPD and cinnamaldehyde. The lowest concentration of QSI where bioluminescence was significantly (One-Way ANOVA) reduced without significantly reducing planktonic growth was termed the minimum quorum sensing inhibitory concentration (MQSIC). The MQSICs for the three test QSI's were: 39.06 µg/ml for cinnamaldehyde, 0.098 µg/ml for furanone C30 and 31.2 µg/ml for F-DPD (Figure 3.1).

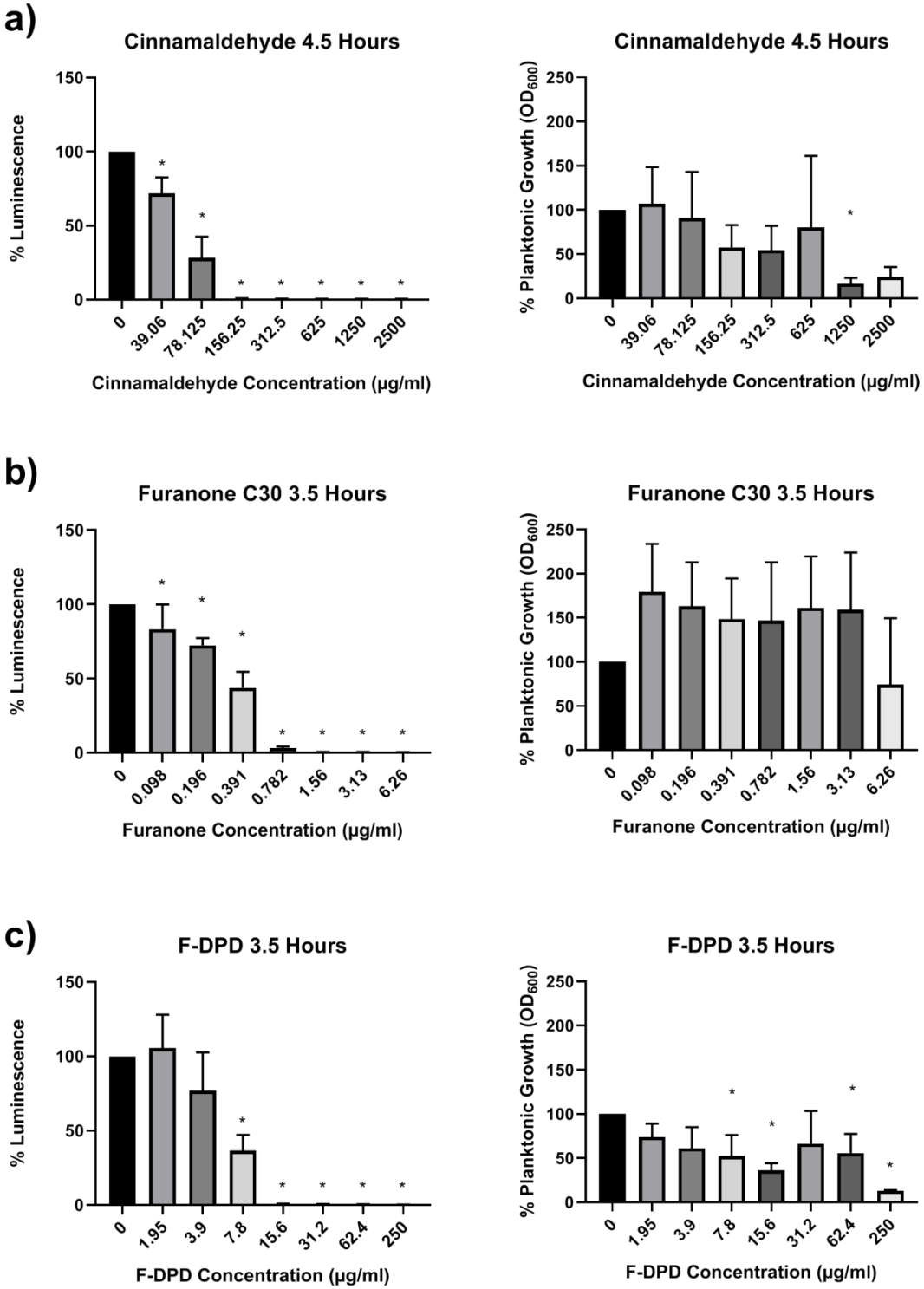

Figure 3.1 Graphs showing the planktonic growth (absorbance) and QSI activity (luminescence) of *Vibrio harveyi BB170* in the presence of increasing concentrations of a) cinnamaldehyde, b) furanone C30, and c) F-DPD as a % relative to the negative control (0 µg/ml). The lowest concentration where QS was significantly (* $p < 0.05$, n=3) reduced without significantly reducing growth was termed the minimum quorum sensing inhibition concentration (MQSIC).

3.5.2 QSI susceptibility of UPEC in planktonic and biofilm states MIC (Table 3.1), MBC (Table 3.2) and MBECs (Table 3.3) were determined for all test isolates before and after repeated QSI exposure and were compared to the respective control passaged on QSI free media. Change in QSI susceptibility after exposure was calculated as fold-change relative to the control (Table 3.4). Data indicates both the frequency of susceptibility change (≥2 fold) and the average magnitude of susceptibility change for each QSI.

After repeated cinnamaldehyde exposure there was a ≥2 fold-decrease in MIC in 8/8 isolates for cinnamaldehyde indicating an increase in susceptibility (Table 3.1). The same results for furanone C30 susceptibility were seen after furanone C30 exposure. There were no significant changes in MIC induced by F-DPD exposure. The average fold-change in MIC was -2.5 for cinnamaldehyde and -3 for furanone C30 (Table 3.4). For MBC (Table 3.2) QSI exposure led to a ≥2 fold-decrease in 8/8 isolates for cinnamaldehyde and 6/8 isolates for furanone C30. In contrast 1/8 isolates showed a ≥2 fold-increase in MBC after exposure to F-DPD indicating reduced susceptibility. The average fold-change in MBC was -2.56, -2.59, and 2 for cinnamaldehyde, furanone C30 and F-DPD respectively. In terms of MBEC (Table 3.3) there was a ≥2 fold-decrease in 8/8 isolates for cinnamaldehyde and 6/8 isolates for furanone C30. There were no significant changes in MBEC induced by F-DPD exposure. The average fold-change in MBEC was -3.5 for cinnamaldehyde and -2.56 for furanone C30 (Table 3.4).

	Cinnamaldehyde			Furanone C30			F-DPD		
Isolate	**P0**	**P12**	**C12**	**P0**	**P12**	**C12**	**P0**	**P12**	**C12**
EC1	250	125	500	125	125	500	125	125	125
EC2	250	250	500	125	125	375 (144)	125	125	125
EC11	250	250	500	125	125	375 (144)	62.5	125	125
EC26	250	125	500	125	125	313 (125)	62.5	125	125
EC28	250	250	500	125	125	500	62.5	125	125
EC34	250	250	500	125	125	313 (125)	62.5	125	125
EC958	250	250	500	125	125	375 (144)	62.5	125	125
CFT073	250	250	500	125	125	250	125	250	250

Table 3.1 Minimum inhibitory concentrations (μg/ml) for UPEC before exposure to QSI (P0), after 12 passages in the presence of the same QSI (P12), and after 12 passages in a QSI free environment (C12). Data represent mean MICs taken from two separate experiments each with four technical replicates. SDs are given in parentheses.

	Cinnamaldehyde			Furanone C30			F-DPD		
Isolate	**P0**	**P12**	**C12**	**P0**	**P12**	**C12**	**P0**	**P12**	**C12**
EC1	1000	500	1750 (500)	250	250	500	250	500	500
EC2	1000	1000	2000	250	125	500	250	500	500
EC11	250	1000	2000	125	250	437.5 (125)	250	500	500
EC26	250	1000	2000	125	125	375 (144)	250	250	250
EC28	250	1000	2000	250	125	500	250	500	500
EC34	250	1000	2000	125	125	312.5 (125)	250	250	125
EC958	250	1000	2000	250	250	375 (144)	250	500	500
CFT073	250	250	1250 (500)	125	125	250	250	500	500

Table 3.2 Minimum bactericidal concentrations (μg/ml) for UPEC before exposure to QSI (P0), after 12 passages in the presence of the same QSI (P12), and after 12 passages in a QSI free environment (C12). Data represent mean MBCs taken from two separate experiments each with four technical replicates. SDs are given in parentheses.

	Cinnamaldehyde			Furanone C30			F-DPD		
Isolate	**P0**	**P12**	**C12**	**P0**	**P12**	**C12**	**P0**	**P12**	**C12**
EC1	250	250	1000	250	250	312.5 (125)	500	500	500
EC2	250	250	1000	250	250	437.5 (125)	250	250	250
EC11	250	250	500	125	125	437.5 (375)	62.5	15.6	15.6
EC26	250	250	1000	125	250	500	250	250	250
EC28	250	250	1000	250	125	500	500	250	250
EC34	250	250	1000	125	93.75 (44.2)	187.5 (72.2)	62.5	62.5	62.5
EC958	250	250	1000	250	125	500	500	500	500
CFT073	250	250	500	250	125	250	500	500	500

Table 3.3 Minimum biofilm eradication concentrations (μg/ml) for UPEC before exposure to QSI (P0), after 12 passages in the presence of the same QSI (P12), and after 12 passages in a QSI free environment (C12). Data represent mean MBECs taken from two separate experiments each with four technical replicates. SDs are given in parentheses.

	MIC			MBC			MBEC		
Isolate	**Cinnamaldehyde**	**Furanone C30**	**F-DPD**	**Cinnamaldehyde**	**Furanone C30**	**F-DPD**	**Cinnamaldehyde**	**Furanone C30**	**F-DPD**
EC1	**-4**	**-4**	0	**-3.5**	**-2**	0	**-4**	-1.25	0
EC2	**-2**	**-3**	0	**-2**	**-4**	0	**-4**	-1.75	0
EC11	**-2**	**-3**	0	**-2**	-1.75	0	**-2**	**-3.5**	0
EC26	**-4**	**-2.5**	0	**-2**	**-3**	0	**-4**	**-2**	0
EC28	**-2**	**-4**	0	**-2**	**-4**	0	**-4**	**-4**	0
EC34	**-2**	**-2.5**	0	**-2**	**-2.5**	**2**	**-4**	**-2**	0
EC958	**-2**	**-3**	0	**-2**	-1.5	0	**-4**	**-4**	0
CFT073	**-2**	**-2**	0	**-5**	**-2**	0	**-2**	**-2**	0

Table 3.4 Fold changes are indicated for MIC (Table 3.9), MBC (Table 3.10), and MBEC (Table 3.11) in UPEC isolates after long-term QSI exposure compared with the respective isolate passaged in a QSI free-environment (C12). Changes (≥2 fold-change) are shown in bold.

3.5.3 The impact of QSI exposure on UPEC biofilm-formation Biofilm formation was determined via a crystal violet biofilm assay for each UPEC isolate before and after repeated QSI exposure (Figure 3.2). Unexposed isolates displayed varying biofilm forming capabilities with EC2 showing the highest level of biofilm-formation followed by EC1>CFT073>EC11>EC28>EC34>EC26 and EC958. When repeatedly exposed to cinnamaldehyde, 6/8 isolates (EC1, EC11, EC26, EC28, EC34, EC958) demonstrated a significant (ANOVA $p \leq 0.05$) increase in biofilm-formation relative to the respective control. Exposure to furanone C30 induced one significant increase in biofilm-formation (EC958) and one decrease (EC26). When exposed to F-DPD, EC1 showed a significant increase in biofilm-formation. Differences in biofilm-formation were determined to be irrespective of growth rate as we did not observe any significant change in rate or overall growth productivity when in binary culture (Figure 3.3; ANOVA $p<0.05$).

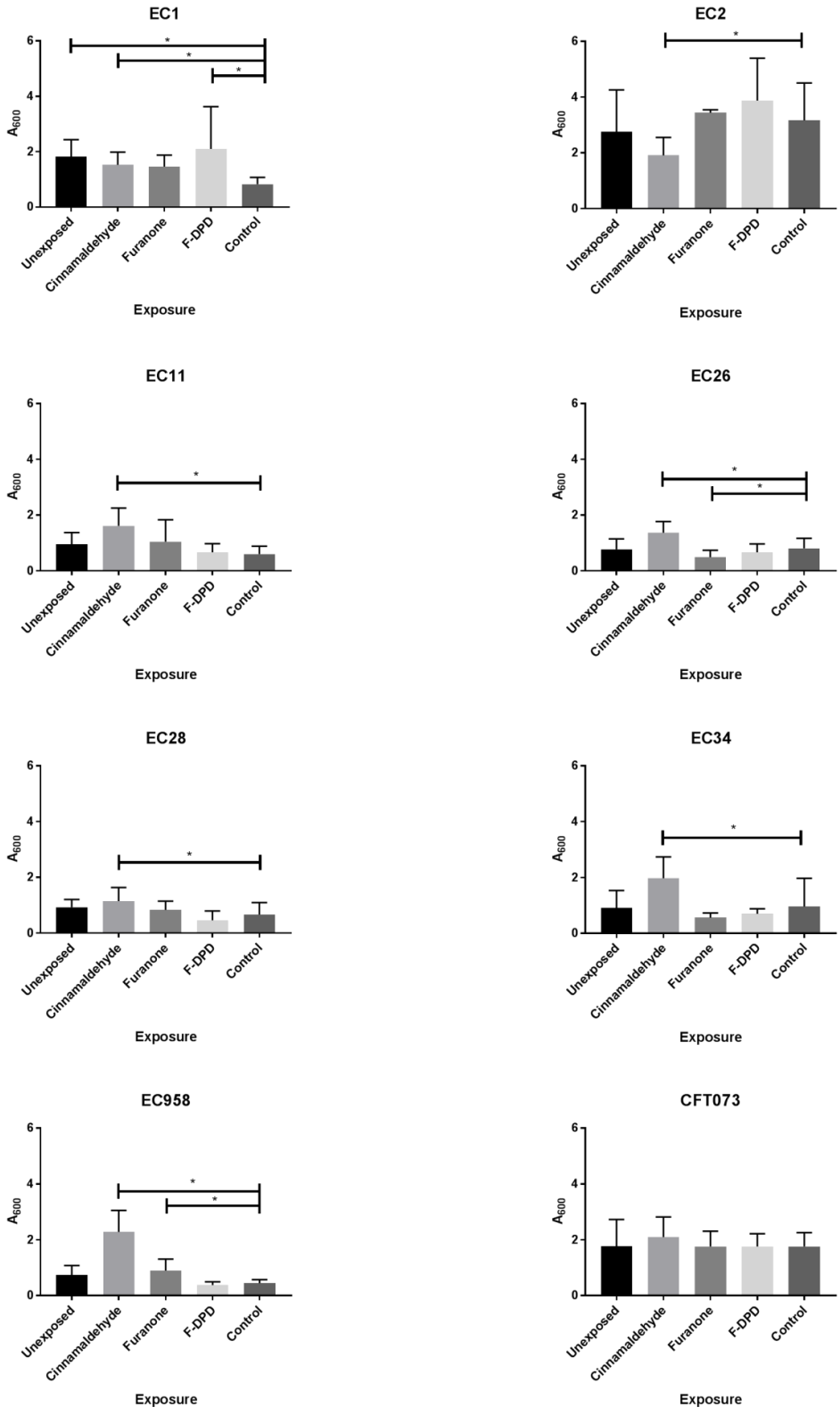

Figure 3.2 Crystal violet biofilm assay indicating the effect of previous QSI exposure on biofilm-formation in eight isolates of UPEC. Data shows the mean absorbance (A_{600}) representative of biofilm-formation for individual bacteria before and after long-term exposure to cinnamaldehyde, furanone C30, and F-DPD or after passage on a QSI free media (C12). Data represent samples taken from two separate experiments each with four technical replicates. For data that varied between replicates, SDs are given as error bars. Significance was determined using ANOVA; * $p \leq 0.05$.

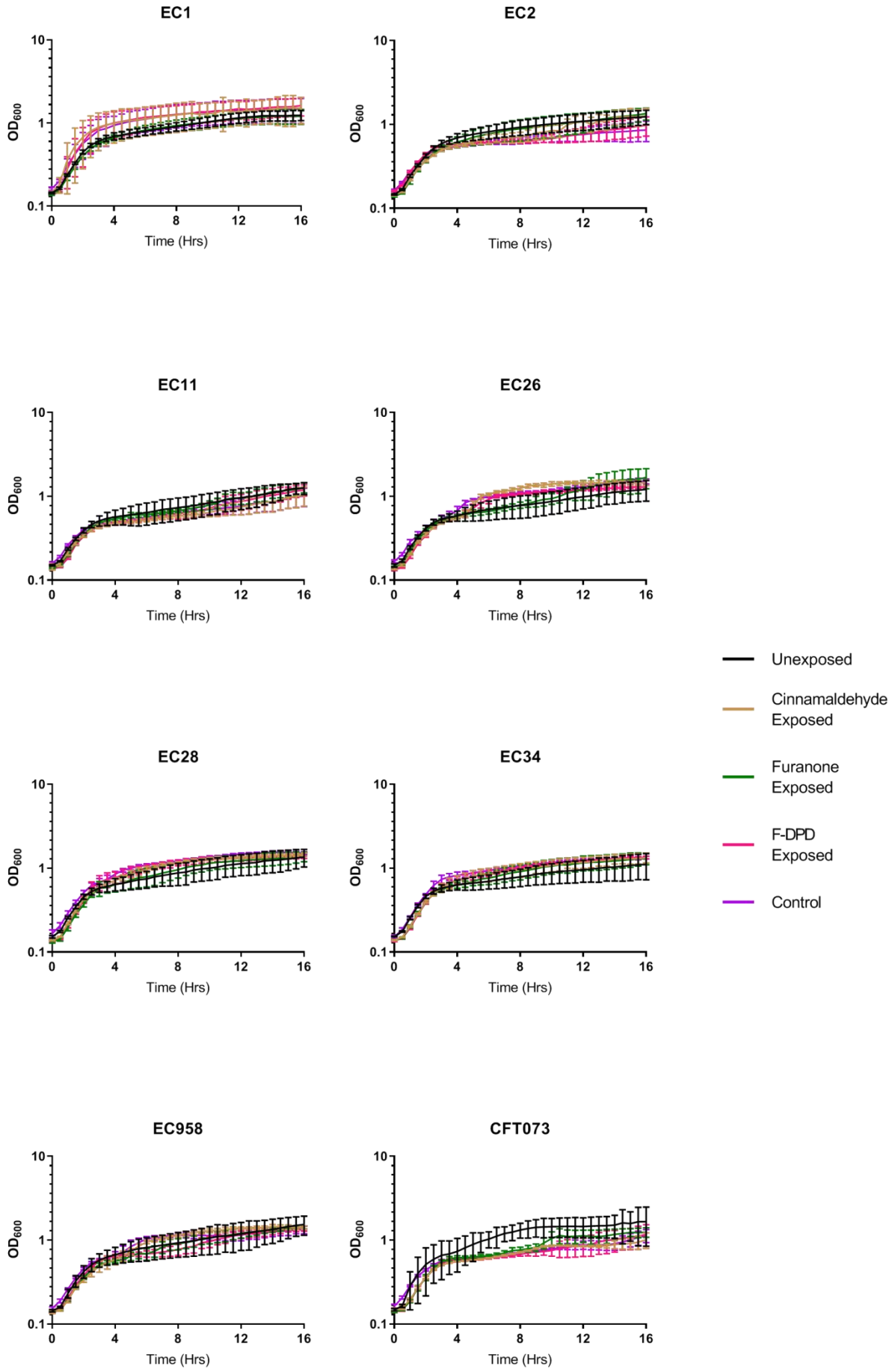

Figure 3.3 Planktonic growth for eight UPEC isolates after exposure to three QSIs. Control isolates passaged without QSI (C12) are also shown.

3.5.4 Relative pathogenicity of UPEC after long-term QSI exposure A *G. mellonella* waxworm model was used to determine relative pathogenicity in UPEC isolates (Figure 3.4). Data indicate that prior to QSI exposure, EC2 was the least pathogenic and EC1 and EC958 were the most pathogenic isolates. Cinnamaldehyde exposure induced significantly (log-rank $p \leq 0.05$) increased relative pathogenicity in 4/8 isolates (EC2, EC11, EC26, EC28) when compared to the respective control isolate. F-DPD exposure induced significantly increased pathogenicity in 2/8 isolates (EC11, EC26) and significantly decreased pathogenicity in 2/8 isolates (EC34, CFT073). Furanone C30 was the only QSI to induce only significant decreases in pathogenicity which occurred in 6/8 isolates (EC1, EC11, EC26, EC34, EC958, and CFT073).

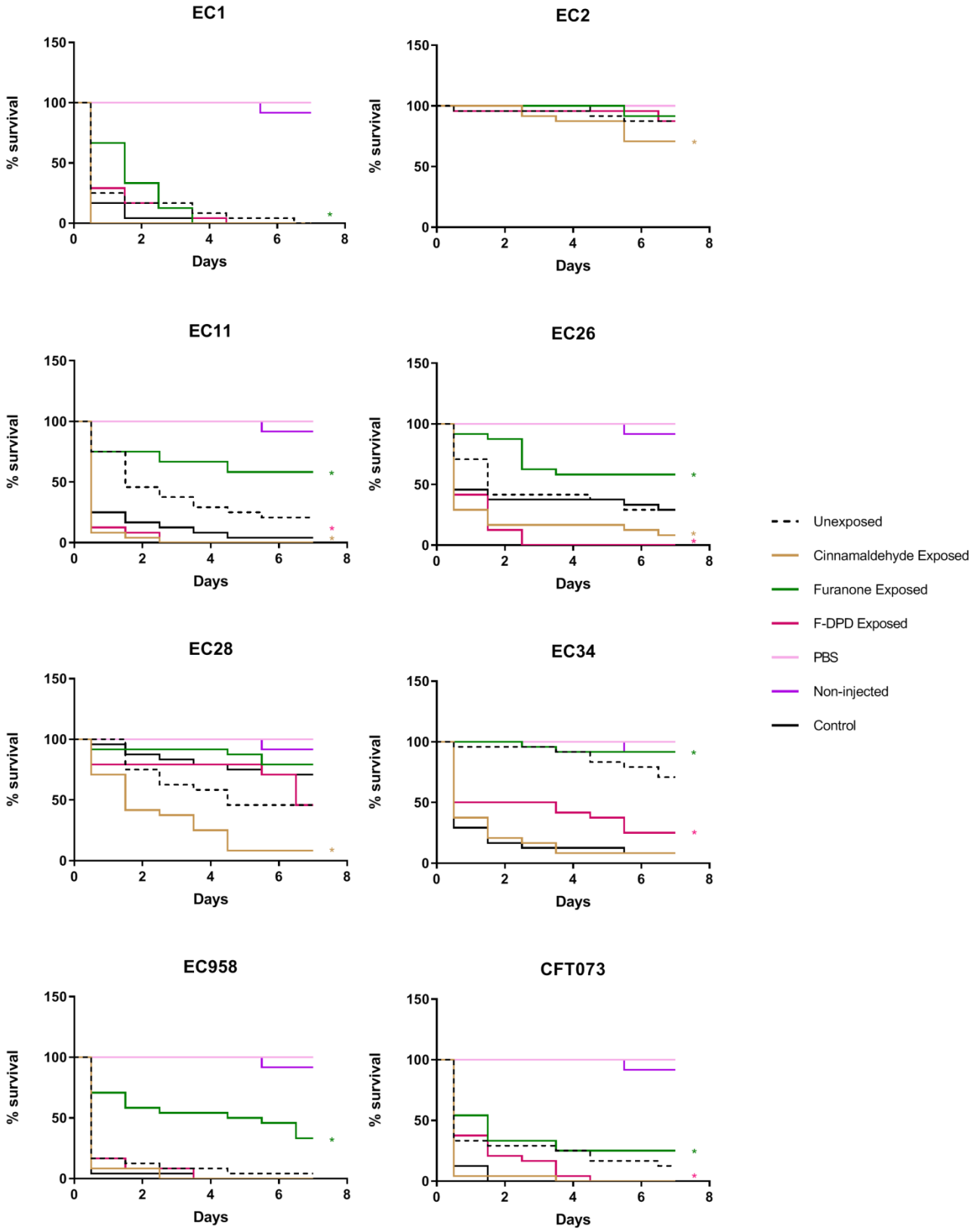

Figure 3.4 *G. mellonella* survival curves for larvae injected with QSI-exposed and -unexposed UPEC. Data represents 24 biological replicates. Control data from non-injected larvae, larvae injected with PBS alone, and larvae injected with control isolates passaged on a QSI free media (Control) are also shown. * indicates a significant difference in pathogenicity when comparing QSI adapted isolates to the respective control strain ($p \leq 0.05$, log-rank reduction test).

3.5.5 Cell invasion Bacterial invasion of human cells was determined via cell invasion assay for bladder smooth muscle (SMC) (Figure 3.5) and urothelial cells (HUEPC) (Figure 3.6). For the unexposed isolates, EC1 showed the highest percentage of invasion followed by EC11, EC2, EC28, EC34, EC958, CFT073 and EC26 in SMC. F-DPD induced a decrease in SMC invasion in EC26 when compared to the respective control. For HUEPC, EC958 showed the highest rate of invasion of the unexposed isolates, followed by, CFT073, EC1, EC26, EC11, EC34, EC28, and EC2. Cinnamaldehyde led to increased HUEPC cell invasion in EC26 whilst furanone C30 exposure induced increased cell invasion in EC34.

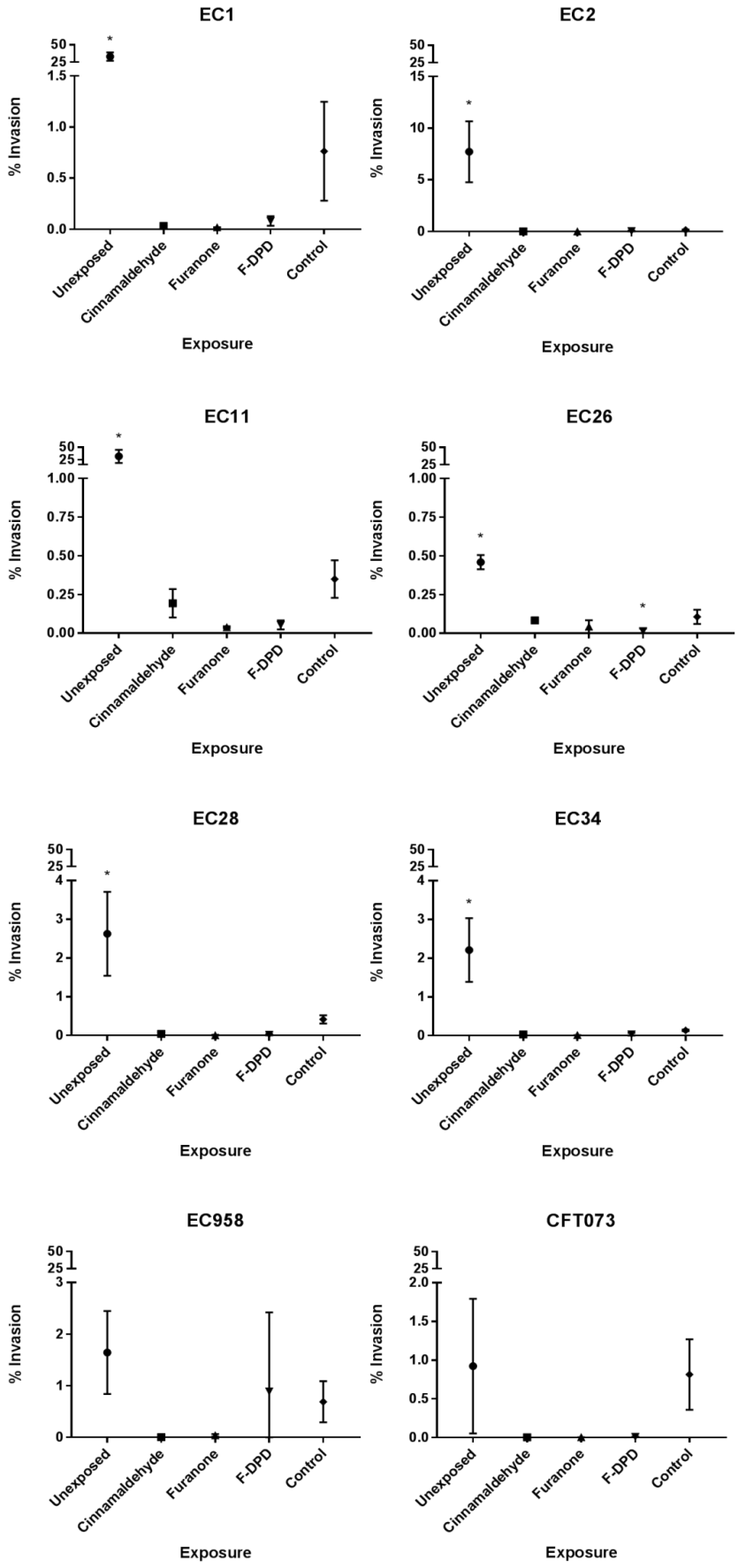

Figure 3.5 Data show the % invasion of eight UPEC isolates before and after exposure to three QSIs (Cinnamaldehyde, Furanone C30, F-DPD) into SMCs. Control isolates passaged on QSI free media are also shown. * indicates a significant difference in pathogenicity when comparing QSI adapted isolates to the respective control strain ($p \leq 0.05$, ANOVA).

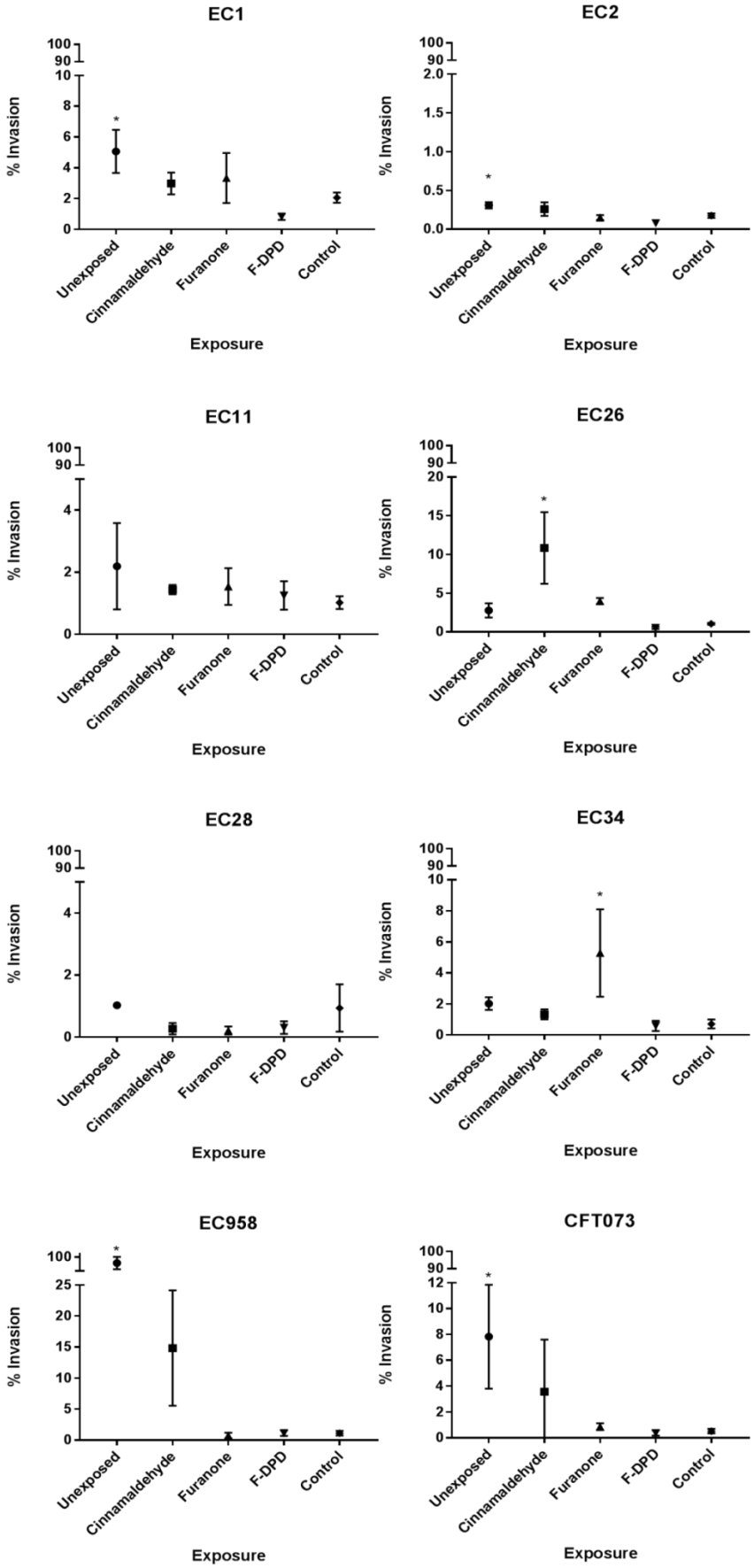

Figure 3.6 Data show the % invasion of eight UPEC isolates before and after exposure to three QSIs (Cinnamaldehyde, Furanone C30, F-DPD) into HUEPCs. Control isolates passaged on QSI free media are also shown. * indicates a significant difference in pathogenicity when comparing QSI adapted isolates to the respective control strain ($p \leq 0.05$, ANOVA).

3.5.6 Changes in antibiotic susceptibility after QSI exposure Isolates were classed as resistant, intermediate, or sensitive to each antibiotic as defined by EUCAST breakpoints [155]. Antibiotic susceptibility was determined for UPEC isolates before and after exposure to each QSI (Table 3.5). Data indicate that cinnamaldehyde exposure induced EC26 to become resistant to gentamicin and EC28 to become intermediately resistant to gentamicin. Exposure to furanone C30 induced gentamicin resistance in EC26 and EC34 and intermediate resistance in EC28. F-DPD exposure induced gentamicin resistance in EC26 and EC28. Cinnamaldehyde exposure induced CFT073 to become intermediately resistant to trimethoprim sulfamethoxazole as did furanone C30 exposure. There were cases where isolates that were initially resistant to trimethoprim sulfamethoxazole became more susceptible after QSI exposure. This occurred in EC2 after exposure to furanone C30 and F-DPD. This was also observed in EC28 for ciprofloxacin after cinnamaldehyde and F-DPD exposure.

Antibiotic	Exposure	EC1	EC2	EC11	EC26	EC28	EC34	EC958	CFT073
Trimethoprim Sulfamethoxazole	Unexposed	14.4 (1.8) S	0 **R**	0 **R**	0 **R**	0 **R**	0 **R**	0 **R**	15.3 (1) S
	Cinnamaldehyde	14.3 (0.8) S	11 (5.5) **R**	0 **R**	0 **R**	0 **R**	0 **R**	0 **R**	12.8 (1.9) **I**
	Furanone C30	14.2 (1.5) S	11.3 (1.4) **I**	0 **R**	0 **R**	0 **R**	0 **R**	0 **R**	13 (3.5) **I**
	F-DPD	29.7 (0.5) S	29 (0.6) S	0 **R**	3.7 (4) **R**	0 **R**	0 **R**	0 **R**	36.7 (0.8) S
Nitrofurantoin	Unexposed	20.3 (0.3) S	20.7 (0.3) S	23.7 (0.3) S	21.2 (1.5) S	19.7 (0.5) S	16.3 (1.2) S	20.4 (1.4) S	18 (0.6) S
	Cinnamaldehyde	23 (1) S	22.3 (1.5) S	26.7 (1.2) S	25 (1) S	20.3 (4.7) S	18 (3) S	20.7 (0.6) S	22 (1) S
	Furanone C30	24 (1) S	24.7 (0.6) S	22.3 (0.6) S	21.7 (0.6) S	18.3 (2.1) S	17.3 (0.6) S	19.7 (1.5) S	17.7 (2.3) S
	F-DPD	22.3 (0.6) S	24.7 (0.6) S	23.7 (1.2) S	26.3 (2.5) S	19.3 (0.6) S	18.7 (1.5) S	21.7 (2.1) S	19.7 (0.6) S
Ciprofloxacin	Unexposed	33 (0.6) S	0 **R**	0 **R**	0 **R**	25 (0.9) **I**	0 **R**	0 **R**	35 (1.3) S
	Cinnamaldehyde	35.5 (0.8) S	0 **R**	0 **R**	0 **R**	29 (1.3) S	1.7 (4.1) **R**	0 **R**	33.3 (1) S
	Furanone C30	29.9 (1) S	0 **R**	0 **R**	0 **R**	25 (2.5) **I**	0 **R**	0 **R**	32.2 (1.2) S
	F-DPD	33 (1.3) S	0 **R**	0 **R**	0 **R**	27.5 (1.4) S	0 **R**	0 **R**	47.7 (2.5) S
Gentamicin	Unexposed	26 (0.5) S	27.7 (0.3) S	25.5 (0.6) S	14.3 (1.2) **I**	18.2 (1) S	16.5 (0.5) **I**	26 S	24.8 (0.4) S
	Cinnamaldehyde	20.2 (0.8) S	20.2 (1) S	20.2 (1) S	12.3 (0.8) **R**	15 **I**	14.3 (0.8) **I**	20 S	21.8 (1.8) S
	Furanone C30	19 (1.1) S	19.8 (0.4) S	20 S	11 (0.9) **R**	14.5 (0.8) **I**	13.3 (1.5) **R**	20.7 (1.6) S	23.9 (2.1) S
	F-DPD	17.5 (0.5) S	19 (0.6) S	19 (0.9) S	13.7 (0.5) **R**	13.3 (0.8) **R**	14.3 (0.8) **I**	19.2 (1) S	23 (1.7) S

Table 3.5 Data show the mean antibiotic inhibition zones (mm) for UPEC before and after QSI exposure (mm) and represent samples taken from two separate experiments each with three technical replicates. For data that varied between replicates, SDs are given in parentheses. S = Sensitive, I = Intermediate, R = Resistant, as defined by BSAC breakpoint.

3.5.7 Biocompatibility Index Cytotoxicity data for the three QSIs against an L929 cell line are shown in Table 3.6. rf values indicating antimicrobial activity and corresponding BI values, highlighting the antiseptic potential of the compounds, are shown in Table 3.7. The order of cytotoxicity in relation to the QSI concentration was F-DPD > cinnamaldehyde > furanone C30. BI values for the eight isolates were averaged for each QSI and the final ranked order of BI was furanone C30 > cinnamaldehyde > F-DPD indicating the antiseptic potential of the QSIs.

QSI	NR IC_{50}	MTT IC_{50}	m. w.	Mean IC_{50}	
				mg/ ml	mmol/ ml
Cinnamaldehyde	0.28	0.0115	132.16	0.1458	0.0011
Furanone C30	0.5735	0.0217	253.877	0.2976	0.0012
F-DPD	0.06495	0.0003	134.04	0.0326	0.0002

Table 3.6 Mean concentration of QSIs allowing 50% survival (IC_{50}) of murine fibroblasts after 30 min at 37ºC as determined via Neutral Red (NR) and [3-(4,5-dimethylthiazol-2-yl)-2, 5-diphenyltetra-zolium bromide] (MTT) assays. Mean IC_{50} based on mass and molecular weight (m.w.). Data indicates two separate experiments each with six replicates.

QSI	EC1		EC2		EC11		EC26		EC28		EC34		EC958		CFT073	
	rf	BI	rf	BI	rf	BI	rf	BI	rf	BI	rf	BI	rf	BI	rf	BI
Cinnamaldehyde	0.23	0.63	0.23	0.63	0.23	0.63	0.23	0.63	0.23	0.63	0.23	0.63	6.48 (1.85)	0.022	0.23	0.63
Furanone C30	0.38	0.79	0.5	0.60	0.38	0.79	0.5	0.60	1	0.30	0.5	0.60	0.5	0.60	0.5	0.60
F-DPD	0.5	0.07	0.5	0.07	0.5	0.07	0.5	0.07	1	0.04	0.5	0.07	0.5	0.07	0.5	0.07

Table 3.7 Data shows the concentration of QSI (mg/ml) producing 3 $\log_{10}$ reduction (rf) after 30 min of exposure at 37ºC on eight isolates of UPEC and the resulting BI value. Data represent mean rf values taken from two separate experiments each with four technical replicates. Standard deviation is given in parentheses.

3.6.0 Discussion

3.6.1 QSI activity in a *V. harveyi* reporter system Blocking the AI-2 based signaling pathway is often primarily achieved by synthetically creating analogues that act as competitive inhibitors of the AI-2-binding site [60]. F-DPD is a 4-fluoro analogue of the AI-2 precursor (S)-4,5-Dihydroxypentane-2,3-dione (S)-DPD and has been previously shown to inhibit AI-2 based QS systems through such competitive inhibition[192]. Both furanone C30 and cinnamaldehyde reportedly inhibit AI-2 QS in *Vibrio harveyi* by decreasing the DNA binding ability of a response regulator LuxR [10]. In addition, the natural furanone C30 covalently modifies and inactivates LuxS and accelerates LuxR turnover [66]. All test compounds showed QSI activity at concentrations below that required for growth inhibition. Our data suggests that furanone C30 displayed the highest level of QS inhibitory activity whilst cinnamaldehyde displayed the least. This may be due to the multiple proposed mechanisms of QS disruption exhibited by furanone C30 leading to a combinatorial effect.

3.6.2 QSI exposure induces changes in susceptibility in planktonic UPEC Exposure to QSI's was performed using a previously validated gradient plating system [193], simulating the selective conditions that may be experienced during leaching of an antimicrobial coating agent from a catheter surface. Cinnamaldehyde induced a high frequency of >2-fold increases in susceptibility at MIC, MBC, and MBEC. Cinnamaldehyde has been previously shown to cause oxidative damage to and alter the fatty acid composition of the *E.coli* cell membrane [194]. This compromised the structural integrity of the membrane and increased cell permeability [195]. This would explain the increased susceptibility seen here as, with the cell wall more permeable, more cinnamaldehyde can penetrate the cell wall and cause damage.

There were increases in susceptibility for all of the UPEC isolates when exposed to furanone C30 at MIC and 6 increases observed at MBC. A previous investigation assessing the effects of furanone C30 on *B. subtilis* found that furanone C30 treatment increased the permeability of the cell plasma membrane [189], which could consequentially result in increased antimicrobial susceptibility, however there is no previous report of the response of *E. coli* to furanone C30 treatment outside of its immediate inhibitory influence on QS and biofilm formation [196].

F-DPD induced 1 decrease in susceptibility at MBC for EC34. F-DPD has been shown to increase mutation rate in *E.coli* leading to rifampicin resistance [63] by modulating LuxS dependant methylases. This same mechanism could lead decreases in susceptibility to other antimicrobials so this could explain the decreased susceptibility to F-DPD seen here.

3.6.3 Biofilm-formation and susceptibility in UPEC after QSI exposure QS in *E.coli* is mediated by AI-2 and it has been shown that AI-2 production is directly correlated to biofilm production [48].Cinnamaldehyde is widely believed to elucidate its quorum sensing inhibition by blocking the binding of LuxR to its transcriptional regulator and can reportedly disrupt biofilm-formation by reduced formation/accumulation of EPS [70]. There was an increase in biofilm susceptibility for all isolates after cinnamaldehyde exposure in the current investigation however this was associated with 6/8 increases in biofilm formation. Genes for biofilm cell signaling protein (*bhsA*) have been shown to become upregulated in *E.coli* after sub-lethal exposure to cinnamaldehyde [197]. In the same study, long term exposure to cinnamaldehyde caused increased expression of type 1 fimbriae which would increase cell adhesion [197]. Increases in cell signaling and cell adhesion would increase biofilm formation, this could be the explanation for the results seen in this study.

Furanone C30 also reportedly decreases the DNA binding activity of LuxR [198] and was the most potent quorum sensing inhibitor within the *V. harveyi* reporter system. Small magnitude increases in biofilm susceptibility were observed in 6/8 isolates and the effect on biofilm formation was variable (one increase and one decrease). *E.coli* biofilm formation has been shown previously to be inhibited by furanone C30 [67, 68] partially due to a down regulation in genes associated with chemotaxis, flagella synthesis, and motility. These are examples of immediate effects so not necessarily indicative of the adaptive responses that have been observed in the work reported in this chapter.

F-DPD is an analogue of AI-2 and inhibits quorum sensing by blocking the AI-2 receptor [192]. Isobutyl-DPD has been shown to inhibit biofilm-formation in *E.coli* [65]. In this study, exposure to F-DPD did not induce any increase or decrease in biofilm susceptibility and only one significant increase in biofilm-formation.

3.6.4 Changes in antibiotic susceptibility after QSI exposure in UPEC Cross-resistance to antibiotics occurred in 9 out of a possible 63 cases. Previous studies have shown that exposure to cinnamaldehyde upregulated the expression of several antibiotic resistance genes including *marRAB* and *mdtEF* in *E.coli* [197]. Furanone C30 exposure has been shown to reduce expression of *AmpC* (beta-lactamase) [199] and caused increased antibiotic resistance to 10 antibiotics in *P. aeruginosa* due to overexpression of multidrug efflux pumps [200]. Treatment with F-DPD has been previously shown to increase rifampicin resistance in *E.coli* [63]. Inhibition of the QS pathway by F-DPD increased mutation rate plasticity via increased modulation of mutational hotspots by Dam methylase (which itself is modulated by LuxS) [63]. There were also 4 cases where exposure to the QSI increased the susceptibility of certain isolates (EC2, and EC28) to certain antibiotics (trimethoprim and ciprofloxacin). Antibiotic cross protection after antimicrobial exposure has been demonstrated previously [193], and is likely to be caused due to increased membrane permeability. Exposure to F-DPD induced the most increases in antibiotic susceptibility. Other AI-2 analogues have been shown to increase bacterial susceptibility to antibiotics when used in combination (e.g phenyl-DPD combined with gentamicin was more effective at clearing *P.aeruginosa* biofilms than gentamicin alone [201]). Also, LuxS mutants have been shown to have increased susceptibility to antibiotics [202], it was hypothesised that AI-2 QS is associated with the ability to cope with environmental stress and so inhibition of this communication increased bacterial sensitivity to antibiotics.

3.6.5 Biocompatibility of test QSIs in an L929 cell line To assess the suitability of an antiseptic agent both the antimicrobial activity and cytotoxicity must be considered. F-DPD was shown to be the most cytotoxic compound followed by cinnamaldehyde and furanone C30. Cinnamaldehyde has been shown to upregulate Fas/CD95 expression and decrease mitochondrial transmembrane potential ($\Delta\psi m$) [203]. Fas/FasL is an important death receptor pathway and induces apoptosis by activation of caspase 8 [204]. The activation of subsequent processes by caspase 8 induce apoptosis in cells causing nuclear degradation and cellular morphological change [204].The cytotoxic mechanisms of furanone compounds have been shown to be the production of reactive oxygen species and breakage of DNA, in a study by Murakami *et al.* (5H)-Furanone (structurally similar to furanone C30) did not inhibit aconitase and so was concluded to not have superoxide radical generation activity [205]. This would explain why furanone

C30 was the least cytotoxic QSI tested. F-DPD was the most cytotoxic QSI tested and also had the lowest calculated BI value. To our knowledge, there are no previous studies into the cytotoxicity of DPD associated analogues.

3.6.6 Altered relative pathogenicity in QSI adapted UPEC Many virulence factors, such as flagellar motility, surface adhesion and toxin production have been shown to be regulated by QS in *E.coli* [206]. Exposure to cinnamaldehyde induced increased pathogenicity in 4 UPEC isolates. Cinnamaldehyde treatment has been also been associated with reduced virulence in *Vibrio spp* towards *Artemia franciscana* shrimp , possibly due to reduced protease expression [70]. Furanone C30 was the only QSI to induce only decreases in pathogenicity. Furanone C30 has been shown to repress major virulence factors (proteasases (*lasA* and *lasB*), chitinase (*chiC*), and pyocyanine synthesis (*phzABCDEFG*)) in *P.aeruginosa* [207], 80% of the genes that were downregulated by furanone C30 were controlled by QS. Experiments with *Vibrio spp.* show that exposure to furanone C30 decreases the virulence of the bacteria towards *A. franciscana* [208]. This was hypothesised to occur due to reduced virulence factor production such as proteases, haemolysin, and siderophores [209]. Increases in relative pathogenicity were observed in 2/8 isolates (EC11 and EC26) when exposed to F-DPD. DPD has been shown to upregulate QS associated virulence factors *lasB* encoding elastase and *xcpP* encoding a type II protein secretion apparatus in *P. aeruginosa* but there is no previous investigation in *E. coli* [210].

3.6.7 UPEC invasion into human cells after exposure QSIs It was observed that, on average, invasion was higher in HUEPC than in SMC. This is likely due to UPEC expressing genes that encode P fimbriae/ pyelonephritis associated pili (PAP) [24] and type 1 pili which both adhere specifically to uroepithelium [26, 183]. Cinnamaldehyde induced increases in HUEPC invasion in 1/8 isolates. In contrast, in previous studies, cinnamaldehyde exposure has been associated with reduced virulence in UPEC due to decreased expression in cell surface adhesins fimA, fimH, and papG [211] impacting adhesion to the cell.

Furanone C30 induced increased HUEPC invasion in 1/8 isolates. Furanone C30 has been shown to repress major virulence factors (proteasases (*lasA* and *lasB*), chitinase (*chiC*), and pyocyanine synthesis (*phzABCDEFG*)) in *P.aeruginosa* [207]. These reductions were proposed to be directly controlled by inhibition of QS. Again this

demonstrates that the effects of short term exposure can be very different to those seen after long term exposure. F-DPD induced decreases in SMC invasion in 1/8 isolates. As far as we are aware, there have been no studies into the effect of F-DPD exposure on UPEC virulence.

3.7.0 Conclusion

Quorum sensing inhibitors (QSIs) are a novel class of anti-biofilm agents and are being increasingly studied to investigate their potential uses in medical device coatings. Uropathogenic *E.coli* is the major causative of CAUTI so it is important to research the effects of QSIs on this pathogen to be able to develop a catheter coating. In this study, the long term effects of three QSIs were tested on eight strains of UPEC. The changes in susceptibility, biofilm-formation, pathogenicity, and virulence were varied between each QSI and each UPEC isolate indicating the complex responses to these agents. It is therefore very important to continue to research the long term effects of these compounds to properly evaluate the suitability of these antimicrobials for use in a catheter coating.

Chapter 4

Evaluation of Biocidal Coating Agents in Uropathogenic *Escherichia coli* Urinary Catheter Biofilms

I acknowledge the following people for contributing to the work presented in this chapter: P.G Chirila (PhD student) and C Whiteoak (academic) who synthesised the furanone C30. M Kadirvel (academic) who synthesised the F-DPD.

4.1.0 Abstract

Background: Catheter associated urinary tract infections (CAUTIs) are an increasing burden on healthcare providers and a substantial risk to the health of the population. As antibiotic resistance in uropathogens in on the rise, a new approach is needed to help prevent these infections and reduce the need to further antibiotic treatment. One such approach is to use antimicrobial impregnated catheters to reduce bacterial contamination and subsequent biofilm formation on the catheter surface. **Methods:** In this study seven antimicrobial agents (PHMB, triclosan, benzalkonium chloride (BAC), silver nitrate, cinnamaldehyde, furanone C30, and F-DPD) were incorporated into three coating agents (sol gel, polyethylene glycol diacrylate (PEG), and Poly(hydroxyethymethacrylate) (pHEMA). The biocompatibilities of the coatings were determined by comparing antimicrobial activity to cytotoxicity in an L929 murine fibroblast cell line. After this initial screen, the sol gel coating was determined to have the best biocompatibility. In order to evaluate the sol gel coating combinations further, we determined the antimicrobial efficacy of urinary catheter segments coated with sol gel against uropathogenic *E. coli* in a continuous culture drip-flow reactor. In order to determine the long-term efficacy of the antimicrobials used within the catheter coating, 8 strains of uropathogenic *E.coli* (UPEC) were repeatedly exposed to the antimicrobials to simulate long-term adaptation to the coating agent. The subsequent effects of antimicrobial exposure on biofilm formation on the catheter surface were evaluated in a catheter biofilm model. Biofilm biomass was determined using crystal violet and metabolic activity was determined using XTT. **Results:** In the antimicrobial inhibition assay, the coating agent with the highest average antimicrobial efficacy when impregnated with the seven antimicrobials, was PEG followed by sol gel and pHEMA, whereas cytotoxicity was ordered PEG > sol gel > pHEMA indicating the different release strategies of these polymers. Therefore, the coating agent with the highest biocompatibility was sol gel followed by PEG and pHEMA. In the drip flow reactor, the order of antimicrobial efficacy for the sol gel coated catheter segments was found to be PHMB > furanone C30 > silver nitrate > F-DPD > cinnamadlehyde > BAC > triclosan. With regard to the effects of long-term exposure to the test compounds, we saw a number of isolates that reduced in their ability to form biofilms on the catheter surface, however the biofilm that did form was often highly metabolically active as determined through the use of XTT. **Conclusion:** This study highlights the importance of assessing

the biocompatibility and antimicrobial efficacy of coating agents in a range of experimental systems and investigating the long term effects of the coating agents on relevant bacteria.

4.2.0 Introduction

Catheter associated urinary tract infections (CAUTIs) account for the highest proportion of hospital acquired infections [15] with uropathogenic *Escherichia coli* (UPEC) reportedly responsible for 65% of complicated UTI cases [23]. CAUTIs often show recalcitrance to antimicrobial treatment due to the formation of bacterial biofilms within the catheter in addition to the increasing prevalence of antibiotic resistance in uropathogens [3, 4]. Biofilms are adhered microbial communities encased in a protective gel like matrix of extracellular polymeric substance secreted from the bacterial cell and are frequently associated with chronic infection that persists despite immune response or antibiotic therapy [5]. The catheter provides the surface for the initiation of biofilm formation which following maturation may occlude the central lumen of the catheter obstructing urine outflow in addition to providing a continuous reservoir for infection.

In order to reduce the incidence of CAUTI approaches for the production of anti-infective catheter coatings have been developed including (i) surfaces containing antimicrobials that may be eluted into the surrounding environment [125] (ii) surfaces containing covalently bound antimicrobials [132] and (iii) surfaces coated in an anti-adhesive material to reduce bacterial attachment [118]. Biocides are often considered as anti-infective coating agents due to their broad-spectrum of antimicrobial activity and their multiple site-targeted mode of action [105], meaning the risk of selecting resistant microorganisms is comparatively low when compared to antibiotics. Biocide coated urinary catheters incorporating biocides such as silver nitrate and nitrofurazone have been developed but have shown limited efficacy during clinical trial partly due to their short lived antimicrobial activity resulting in low efficacy in patients undergoing long-term catheterisation [114]. This has fuelled the search for further anti-infective catheter coating agents that display broad -spectrum activity which is maintained after prolonged use.

A novel approach in the production of anti-infective catheter coatings is to use quorum sensing inhibitors (QSIs). Quorum sensing (QS) is a extracellular signalling process

utilised by bacteria to coordinate their behaviour through cell density dependent gene expression [10]. QS involves the production and detection of autoinducer molecules that can be divided into Autoinducer-1 (AI-1) and Autoinducer 2 (AI-2). AI-1 type QS molecules are acyl homoserine lactones produced by LuxI- like synthases and detected by a LuxR transcriptional regulator [43]. In comparison AI-2 are DPD-derived molecules dependent on LuxS-like synthases, detected by a LuxPQ receptor and regulatory complex [47]. Two quorum sensing systems in *E. coli*, AI-2/LsrR and AHL/SdiA, have been shown to play a role in both biofilm formation and virulence factor production [48].

'Active' release coatings incorporate antimicrobials that are released over a period of time to reduce bacterial attachment to the surface [118]. Compounds that have been incorporated into active release coatings include conventional antibiotics [122] in addition to broad-spectrum antimicrobials such as silver [121] and nitric oxide [123] as well as antibodies [124]. Antibiotics have been incorporated into a variety of polymers including hydroxyapatite [122], polyurathane [126], and biodegradable polymers such as polylactide-co-glycolide (PLGA) [127]. Hydrogels are polymer networks with hydrophilic structures, meaning they are able to retain large amounts of water [137]. The nature of hydrogels being wet and slippery is advantageous for use in a catheter as this helps prevent damage to the urethral mucosa when inserted, and removed, *in situ* [134]. The sol gel process involves the formation of an inorganic colloidal suspension (sol) and gelation of the sol in a continuous liquid phase (gel) to form a 3D network structure [141]. An advantage to the sol gel manufacturing process over other coating processes is that it can be conducted at much lower temperatures such as room temperature [142], facilitating mass-production. Materials can be designed to elute incorporated antimicrobials using either instant or sustained release strategies. Instant release will deliver a higher dose of antimicrobial over a short period of time, whereas sustained release will deliver lower levels of antimicrobial over longer periods of time [118]. Using a sustained release strategy provides advantages with regards to long-term antimicrobial activity but concerns have been raised that this strategy increases the likelihood of exposing bacteria to sub-lethal concentrations of antimicrobials promoting the selection of antimicrobial resistance populations.

Drip flow biofilm reactors are designed for the study of biofilms grown under low shear conditions and are ideal for medical material evaluations and indwelling medical device

testing [212]. The drip flow reactor has been used to model environments such as catheters, cystic fibrosis lung, and the oral cavity [213]. The reactor consists of 4 chambers that each have their own influent and effluent ports to allow the continuous flow of media through the reactor. The benefit of a drip flow reactor is that the experimental conditions can mimic that of clinical infections more closely than standard biofilm assays [212].

The phenotypic adaptations that may occur in a panel of UPEC clinical isolates as a consequence of long-term biocide exposure in bacteria have been demonstrated in previous chapters [193]. The current investigation aims to determine the efficacy of antimicrobial impregnated catheter coating polymers by assessing their antimicrobial and cytotoxic effects. The long-term effects of the antimicrobials on both biofilm formation and biofilm viability on the catheter surface will be evaluated utilising high-throughput biofilm formation assays.

4.3.0 Aims and objectives

The previous chapters detail the phenotypic changes observed in eight strains of UPEC after long term exposure to seven antimicrobials (PHMB, triclosan, BAC, silver nitrate, cinnamaldehyde, furanone C30, and F-DPD). These effects are important to consider when selecting for potential catheter coating agents. How these changes impact the bacteria in a catheter infection must be investigated. It is also important to assess the performance of these antimicrobials when incorporated into coatings in conditions that are comparable to an *in vivo* infection.

The specific aims of this chapter were to:

- Determine the effects of antimicrobial exposure on UPEC biofilm formation and viability grown on urinary catheters using crystal violet and XTT assays.
- Evaluate antimicrobial efficacy of the seven antimicrobials when incorporated into three different coatings (sol gel, PEG, and pHEMA) against UPEC isolate EC958.
- Determine the biocompatibility of these coatings against an L929 cell line.
- Select the most promising coating and evaluate the anti-biofilm capabilities using the drip flow biofilm reactor.

4.4.0 Methods

4.4.1 Bacteria and antimicrobials Six UPEC clinical isolates (EC1, EC2, EC11, EC26, EC28 and EC34) previously isolated from urinary tract infections (Stepping Hill Hospital, UK) and two laboratory characterised UPEC isolates (EC958 and CFT073) were used in the investigation. Bacteria were cultured onto Muller-Hinton agar (MHA; Oxoid, UK) or Muller-Hinton broth (MHB; Oxoid, UK) and incubated aerobically at 37 °C for 18 h unless otherwise stated. Antimicrobials were formulated as follows: triclosan and furanone C30 solubilised in 5% (v/v) ethanol. Polyhexamethylene biguanide (PHMB) (LONZA, Blackley, UK), benzalkonium chloride (BAC), silver nitrate, cinnamaldehyde, and F-DPD were prepared at 1 mg/ml in water and filter sterilised prior to use. Furanone C30 and F-DPD were synthesised in-house. All chemicals were purchased from Sigma–Aldrich (Poole, UK) unless otherwise stated.

4.4.2 Long-term exposure of bacteria to biocides and quorum sensing inhibitors Bacteria were repeatedly exposed to antimicrobials using a gradient plating system adapted from Moore *et al* [152]. In brief, 100 µl of a 5 × MBC concentration solution of antimicrobial was added to an 8 x 8 mm well in the centre of a 90 mm agar plate. Bacterial pure cultures were radially inoculated in duplicate from the edge of the plate to the centre, prior to incubation for 2 days aerobically at 37°C. Biomass from the inner edge of the annulus of bacterial growth representative of the highest antimicrobial concentration at which growth could occur was removed and used to inoculate a new antimicrobial containing plate, as outlined above. This process was repeated for 12 passages. Bacteria were archived at -80 °C before and after antimicrobial passage for subsequent testing.

4.4.3 Catheter biofilm model Method adapted from Nweze *et al* [214]. 1cm catheter sections were cut with a hot scalpel lengthways and autoclaved. Overnight cultures of bacteria were made in MHB. In a 12 well plate, sections were pre-coated with 4ml FBS for 24 h at 37ºC and 30 rpm (3 sections per well). Bacteria were washed twice with PBS and resuspended in 5 ml PBS at OD_{600} 0.18 (10^7 cells/ml). FBS was removed from sections and 4 ml bacterial suspension was added. These were incubated for 90 min at 37ºC (Adhesion phase). Sections were removed with a sterile forceps and placed in a 12 well plate containing MHB. Plates were incubated for 48 h at 37ºC and 30 rpm (Biofilm

formation phase) the sections were moved to new plates containing sterile MHB after the first 24 h.

4.4.3.1 XTT A working solution containing XTT and menadione was prepared by adding 1200 µL of XTT from 1 mg/mL XTT stock and 88 µL of menadione from 1 mM menadione stock solution to 88 mL of PBS and mixing gently. MHB was carefully removed by aspiration from each well of the plate containing discs with formed biofilms and replaced with 3mL of the XTT/menadione mixture. The microtitre plates were covered with aluminium foil and incubated for 90mins at 37ºC. Blank wells containing 3mL of the XTT/menadione mixture with sections and no biofilm were prepared, covered with aluminium foil and incubated with the biofilm plate. Next, the catheter sections were carefully removed and the optical density (OD) read at 490 nm using a Microplate Reader.

4.4.3.2 Crystal violet Catheter sections that had grown biofilm were added to a 12 well plate. Then 3ml of crystal violet solution was added and left the plate at room temperature for 30 minutes. The crystal violet solution was carefully removed and replaced with 4ml of PBS. This rinse step was repeated three times with PBS. Plates were left to dry for 1h in a 37ºC incubator. The remaining crystal violet was solubilised in 4ml of 100 % ethanol and the catheter section was removed. The A_{600} of the solubilised crystal violet solution was measured using a microplate reader.

4.4.4 Evaluation of biocompatibility of catheter coatings Three polymer coatings were assessed: Polyethylene glycol diacrylate (PEG), Poly(hydroxyethymethacrylate) (pHEMA), and sol gel. The polymers were prepared as follows:

PEG was prepared using 6.57 ml PBS, 1.43 ml Polyethylene glycol and 48 µl 2-hydroxy-2-methyl-propiophenone (Darocur 1173). The reagents were combined in a 96 well plate with 6mm glass coverslips placed on the bottom of the wells. The plate was placed under a UV lamp for 90 seconds to induce polymerisation and the discs were stored for later use.

pHEMA gels containing 2% methacrylic acid were prepared using 9.78 ml 2-hydroxyethymethacrylate (HEMA), 19 µl ethylene glycol dimethacrylate (EGDMA), 50 µl Daracur 1173 and 0.2 ml methacrylic acid. The mixture was aliquoted into the wells of a 96-well microtiter plate with 6mm glass coverslips placed on the bottom of the

wells. Polymerisation was carried out under a UV lamp for 30 seconds. Discs were submerged in 70% ethanol for 48 h followed by 30% ethanol for 48 h. Gels were continuously washed in water for 24 h until transparent, and stored in water for later use.

Sol gel was prepared by first mixing 0.5 ml tetraethylorthosilicate, 1ml tetramethylorthosilicate, 2.18 ml Isopropanol (anhydrous) for 5 mins. Added to this mixture was 1ml trimethoxymethysilane slowly (5 x 200 µl). In a separate universal, 2.18 ml Isopropanol was added to 2.5 ml 0.07M Nitric acid. 2.35 ml of the acid/solvent mixture was added dropwise (approx 1 drop per second). 0.2 ml polydimethylsiloxane (mwt 162) was slowly (4 x 50 µl) added as was the remaining acid/solvent mix dropwise (approx 1 drop/sec). This was left stirring for 5 - 10 mins then a further 2.4 ml of Nitric acid was added dropwise (approx 1 drop/sec). Sol gel was aliquoted onto 6mm circular coverslips, left to dry, and stored in the fridge until needed.

4.4.4.1 Disc diffusion Overnight cultures of EC958 were diluted to OD_{600} 0.008 and were used to inoculate MHA plates. Polymer discs (as prepared above) containing concentrations of 10, 50, 100, 250 X MBC (determined previously) of antimicrobials were placed onto the inoculated plates and incubated at 37ºC for 24 h. Zones of inhibition were measured in mm. Untreated discs acted as negative controls.

4.4.4.2 Agar overlay To determine the direct cytotoxicity of antimicrobial impregnated polymers we performed an agar overlay assay using an L929 cell line according to ISO standards [215]. In brief, 2.4 x 10^6 cells in 10 ml of EMEM were seeded into 60 mm diameter cell culture plates. Cells were incubated for 48 h at 37ºC and 5% CO_2 to form a monolayer on the base of the dish. After incubation media was removed by aspiration and cells were washed twice in 10 ml of PBS. 10 ml of EMEM containing 1% agar was added to each dish and was allowed to solidify at room temperature.

After the agar set, 10 ml of a 0.1% neutral red solution was added to the centre of each plate, which was then rotated to evenly distribute the dye, left for 15 min, and excess solution was removed by aspiration. Three polymer discs were placed in an individual cell culture dish. Plates were incubated for 24 h at 37°C and 5% CO2 before being checked for cell lysis. Disc toxicity was characterised by a white colourless zone of dead cells around the implanted region. The diameter of the lysis zone was measured in mm. Untreated discs acted as negative controls.

4.4.5 Drip Flow Biofilm Reactor Sol gel was the best performing coating so the efficacy of this coating was evaluated in the drip flow biofilm reactor (BioSurface technologies). To mimic an *in vivo* catheter infection, artificial urine was pumped through the reactor, each chamber containing catheter pieces coated with sol gel, sol gel containing 1.25 mg/ml antimicrobials, and uncoated catheter controls. The protocol, in brief, consists of reactor assembly and sterilisation by autoclaving at 121ºC for 20 minutes. Artificial urine was prepared as described by Brooks and Keevil [216], briefly this is formulated as 1 g/L peptone L37, 0.005 g/L yeast extract, 0.1 g/L lactic acid, 0.4 g/L citric acid, 2.1 g/L sodium bicarbonate, 10 g/L urea, 0.07 g/L uric acid, 0.8 g/L creatinine, 0.37 g/L calcium chloride $2H_2O$, 5.2 g/L sodium chloride, 0.0012 g/L iron II sulphate $7H_2O$, 0.49 g/L magnesium sulphate $7H_2O$, 3.2 g/L sodium sulphate $10H_2O$, 0.95 g/L potassium dihydrogen phosphate, 1.2 g/L di-potassium hydrogen phosphate, 1.3 g/L ammonium chloride. Catheter sections are placed within the reactor and inoculated with 25 ml of bacterial culture (EC958) at OD_{600} 0.008. The reactor was incubated flat (batch phase) for 6 h at 37ºC. Then the reactor was angled 10º and sterile one inch 23 gauge needles were inserted into the injection port valve at the top of each chamber. The pump was turned on (continuous phase) and artificial urine was pumped into the chambers at 0.83 ml/min for 48 h at 37ºC. After continuous phase the catheter sections were removed with sterile forceps, rinsed and placed in sterile water and vortexed for 30 seconds. Biofilms were serially diluted and plated onto MHA plates in triplicate, plates were incubated for 24 h at 37ºC and cfu/ml were determined.

4.5.0 Results

4.5.1 Biofilm attachment to catheter service before and after exposure Biofilm formation was determined via a crystal violet biofilm assay for each UPEC isolate before and after repeated exposure (Figure 4.1). Unexposed isolates displayed varying biofilm forming capabilities prior to exposure with EC1 showing the highest level of biofilm formation followed by EC26 > EC11 > CFT073 > EC958 > EC2 > EC34 and EC28. When repeatedly exposed to PHMB, 4/8 isolates (EC11, EC28, EC34, and EC958) demonstrated a significant (ANOVA $p \leq 0.05$) decrease in biofilm formation when compared with the respective control (C12). Triclosan exposure induced significant decreases in biofilm formation for 3/8 isolates, EC11, EC34, and EC958. When exposed to BAC, 3/8 isolates showed a significant decrease in biofilm formation

(EC11, EC28, EC34) the same results were seen in these isolates when exposed to silver nitrate. When exposed to cinnamaldehyde, EC11 and EC34 showed a significant decrease in biofilm formation. The isolates EC28, EC34, and EC958 showed a significantly decreased biofilm formation when exposed to furanone C30. When exposed to F-DPD, 3/8 isolates (EC11, EC34, EC958) demonstrated a decreased biofilm formation. Triclosan was the only compound to induce a significantly increased biofilm formation in 1/8 isolates (EC26).

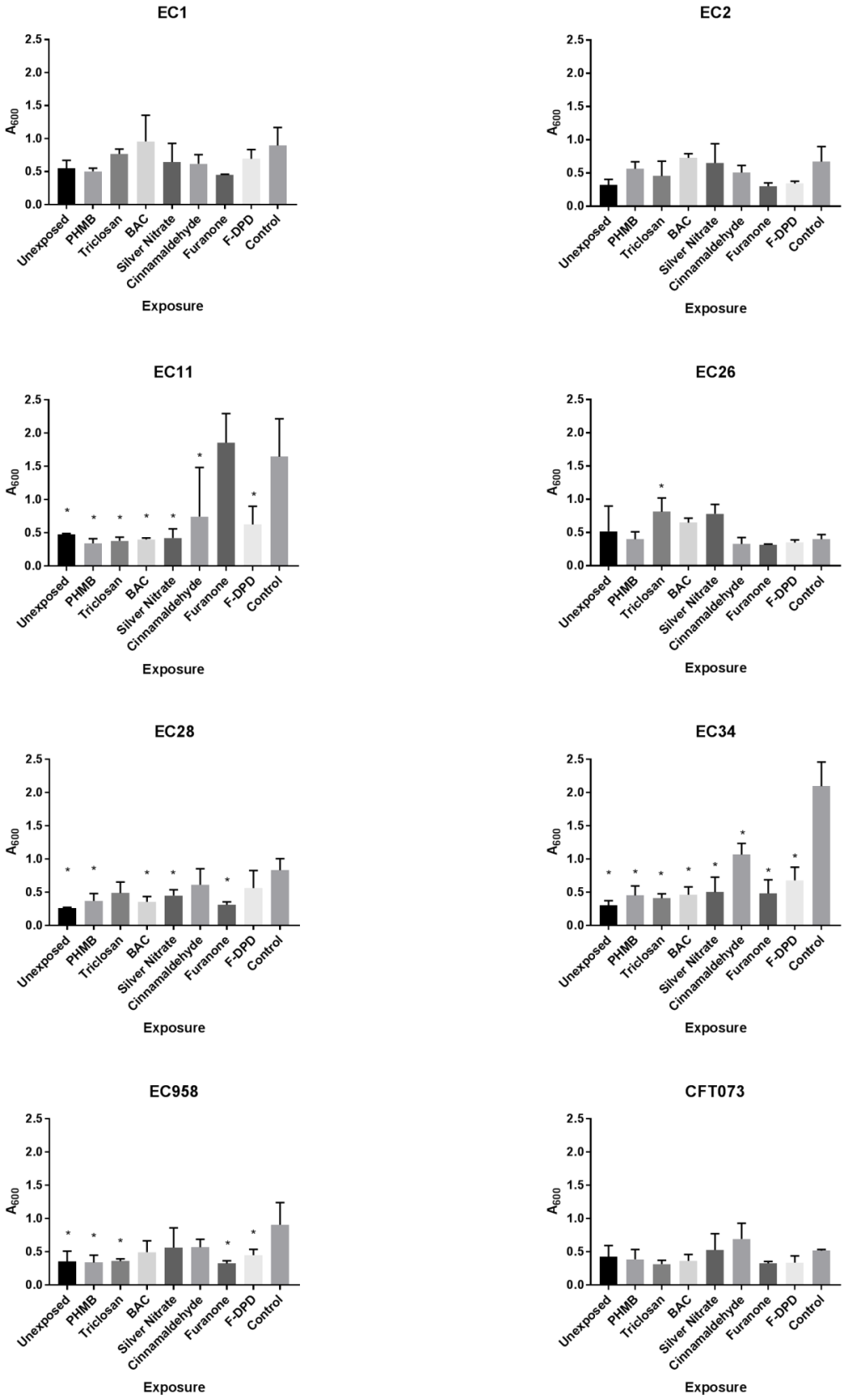

Figure 4.1 Crystal violet biofilm assay indicating the effect of previous biocide and QSI exposure on biofilm formation in eight isolates of UPEC. Data shows the mean absorbance (A_{600}) representative of biofilm formation for individual bacteria before and after long-term exposure to PHMB, triclosan, BAC, silver nitrate, cinnamaldehyde, furanone, and F-DPD. Data represent samples taken from experiments each with three technical replicates. For data that varied between replicates, SDs are given as error bars. Significance was determined using ANOVA; * $p \leq 0.05$ relative to the respective control.

4.5.2 Biofilm viability after repeated exposure to test compounds Biofilm viability on the catheter surface was determined for all isolates before and after repeated antimicrobial exposure by XTT assay. Before exposure, EC1 was shown to form the highest viability biofilm with the remaining isolates ranking as: EC28 > EC2 > EC26 > EC11 > EC958 > EC34 > CFT073 (Figure 4.2). PHMB exposure induced significant increases in biofilm viability in 4/8 isolates (EC2, EC11, EC958 and CFT073). Triclosan exposure induced significantly increased biofilm viability in 4/8 isolates (EC11, EC26, EC28 and EC958). Silver nitrate was induced significantly increased biofilm viability in EC26. There were no significant changes in biofilm viability after exposure to BAC, cinnamaldehyde, furanone or F-DPD.

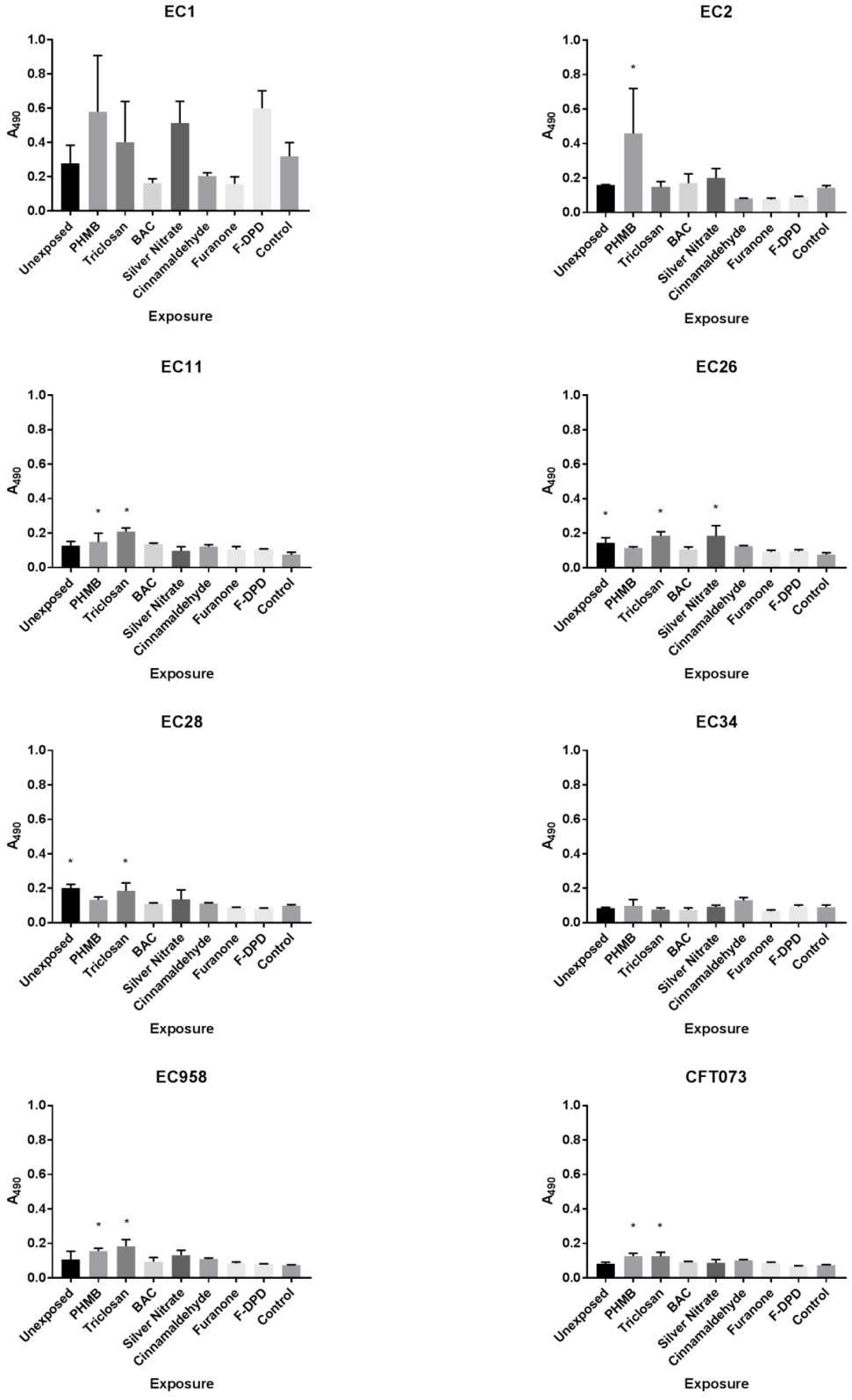

Figure 4.2 XTT biofilm assay indicating the effect of previous biocide and QSI exposure on biofilm viability in eight isolates of UPEC. Data shows the mean absorbance (A_{490}) representative of biofilm viability for individual bacteria before and after long-term exposure to PHMB, triclosan, BAC, silver nitrate, cinnamaldehyde, furanone, and F-DPD. Data represent samples taken from experiments with three technical replicates. For data that varied between replicates, SDs are given as error bars. Significance was determined using ANOVA; * $p \leq 0.05$ relative to the respective control.

4.5.3 Disc Diffusion Polymer discs were formulated containing antimicrobial agents at concentrations of 10, 50, 100, and 250 X the MBC. F-DPD could only be formulated at 10 X MBC due to limited availability of the compound. Polymer discs were assessed for their antibacterial efficacy against EC958 in disc diffusion experiments. Figure 4.3 shows the mean zones of inhibition (Sol gel, PEG, and pHEMA) for each of the 7 antimicrobials at increasing concentrations.

For PHMB, incorporation into sol gel resulted in a significantly (One Way ANOVA $p<0.05$) higher level of antimicrobial activity than when incorporated into PEG or pHEMA at 100 X MBC and pHEMA at 250 X MBC. In contrast, PHMB impregnated PEG was more antimicrobial than PHMB impregnated sol gel and pHEMA at 50 and 10 X MBC. PHMB impregnated PEG showed significantly higher antimicrobial activity than PHMB impregnated pHEMA at 250 and 100 X MBC.

For triclosan, incorporation into sol gel was significantly more potent than PEG at 100 X MBC and significantly more potent than pHEMA at 10 X MBC.

For BAC, incorporation into PEG resulted in significantly higher antimicrobial activity than incorporation into pHEMA at 250 X MBC.

For silver nitrate, incorporation into sol gel resulted in significantly higher microbial inhibition than pHEMA at 250, 100, and 50 X MBC. PEG was significantly more potent than pHEMA at 250 and 100 X MBC.

For cinnamaldehyde, incorporation into sol gel exhibited significantly higher antimicrobial activity than PEG at 250 X MBC and pHEMA at 250, 100 and 50 X MBC. PEG was also significantly more potent than pHEMA at 250, 100 and 50 X MBC. For Furanone C30, incorporation into sol gel showed significantly higher levels of inhibition than pHEMA at 250 X MBC. The only coating to show any antimicrobial activity after F-DPD incorporation was PEG (at 10 X MBC).

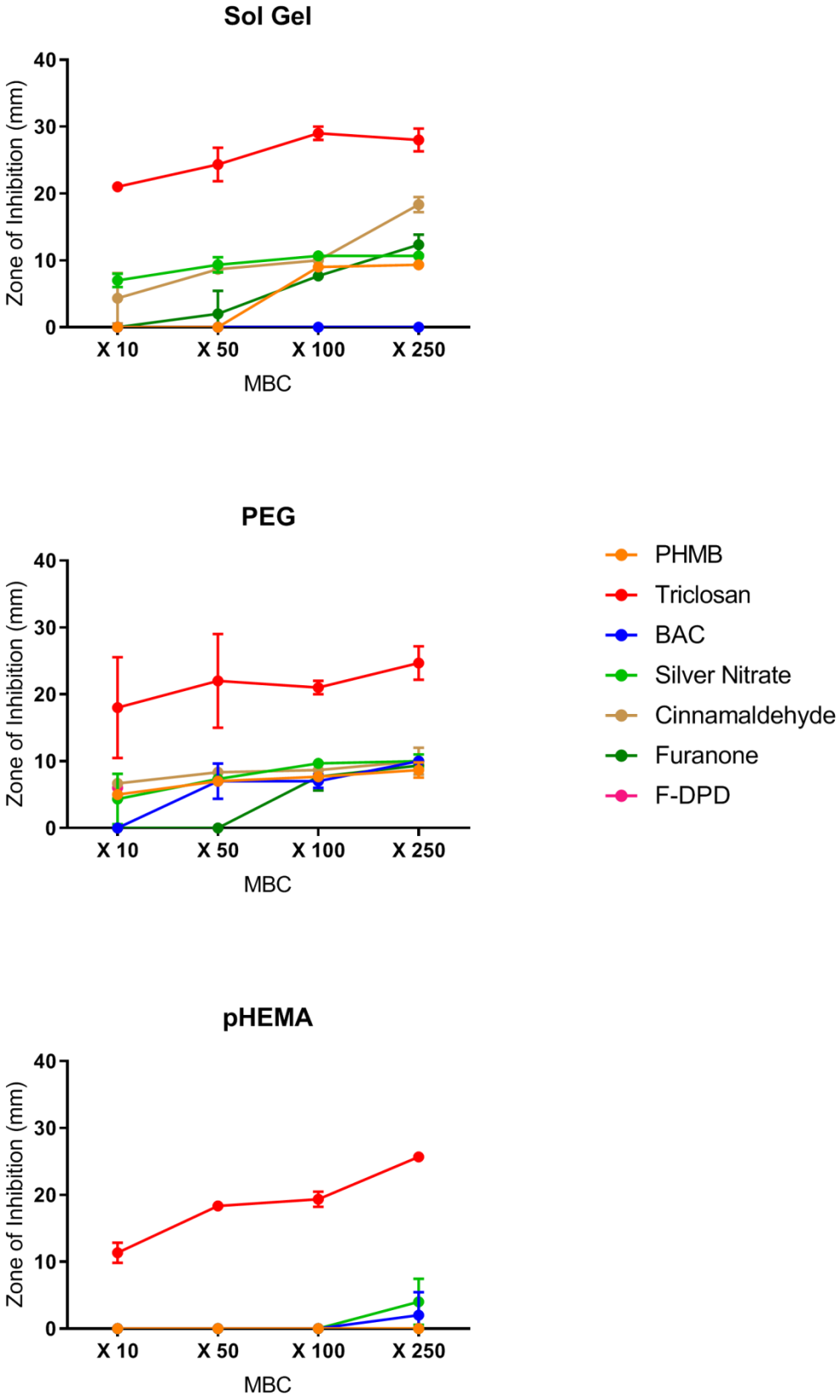

Figure 4.3 Disc diffusion assay for three polymer coatings containing seven antimicrobials at increasing concentrations. Antibacterial zone was measured in mm for each disc (n=3).

4.5.4 Agar overlay Polymer discs containing antimicrobial agents at concentrations of 10, 50, 100, and 250 X the MBC as determined previously were assessed for their cytotoxicity against L929 cells in agar overlay experiments. Figure 4.4 shows the mean zone of inhibition of the polymer disc (Sol gel, PEG, and pHEMA) for each of the 7 antimicrobials at increasing concentrations.

For PHMB, incorporation into pHEMA was significantly more cytotoxic than sol gel and PEG at 50 X MBC. For triclosan, PEG was significantly more cytotoxic than sol gel at 250, 100, and 50 X MBC. pHEMA was significantly more cytotoxic than sol gel at 250 and 50 X MBC.

For BAC, incorporation into PEG was significantly more cytotoxic than sol gel at 100, 50 and 10 X MBC. pHEMA was more cytotoxic than sol gel at 100 X MBC. There was no statistical significance between the polymer coatings for silver nitrate cytotoxicity.

For cinnamaldehyde, sol gel was significantly more cytotoxic than PEG at 10 X MBC. For furanone C30, both PEG and pHEMA were significantly more cytotoxic than sol gel at 250, 100, 50 and 10 X MBC. For F-DPD, PEG was significantly more cytotoxic than pHEMA (at 10 X MBC).

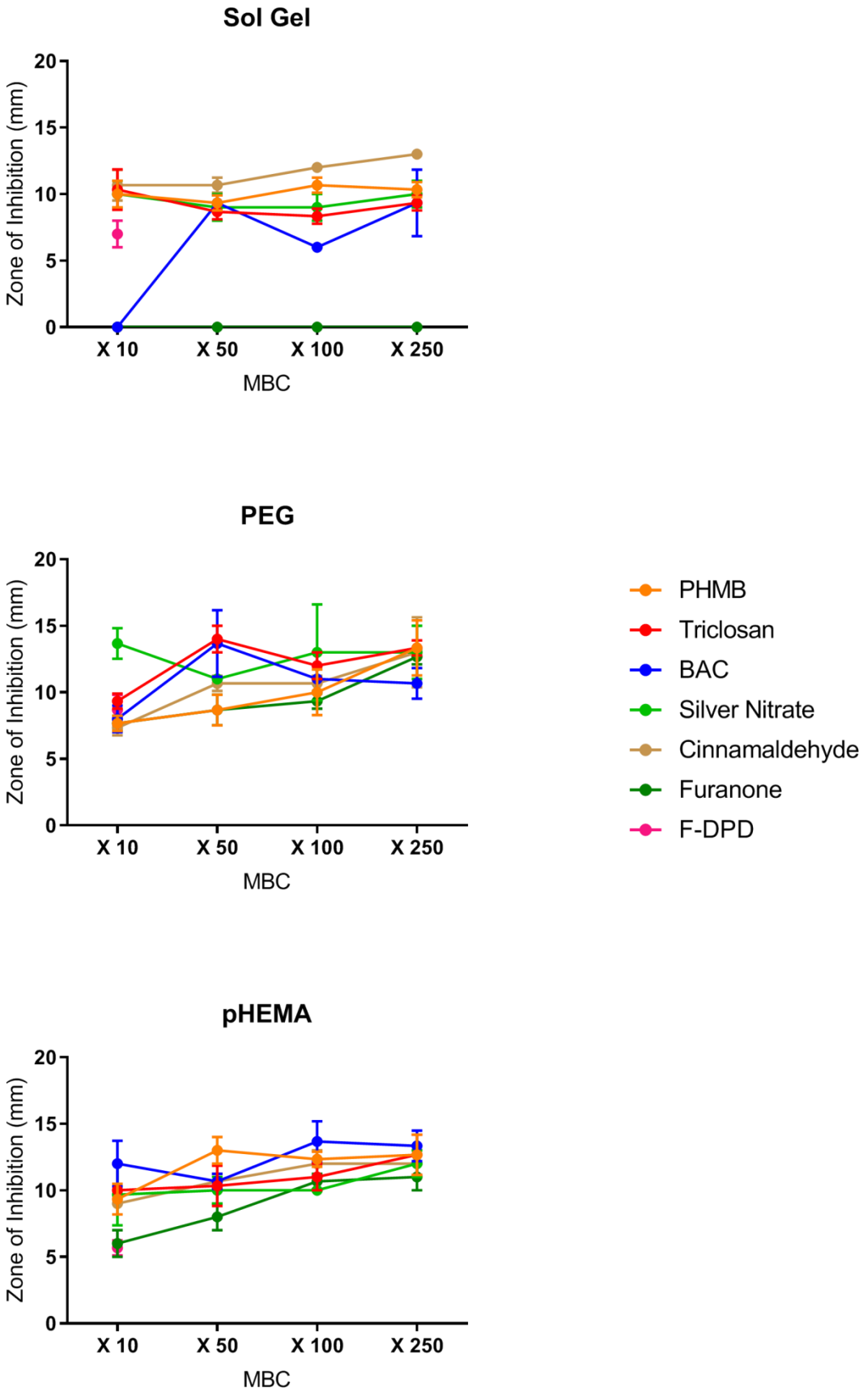

Figure 4.4 Agar overlay assay for three polymer coatings containing seven antimicrobials at increasing concentrations. Cytotoxic zone was measured in mm for each disc (n=3).

4.5.5 Biocompatibility The biocompatibility of the antimicrobials were calculated by dividing the mean antimicrobial diffusion zone by the mean cytotoxicity diffusion zone. A biocompatibility value of over 1 signifies higher levels of antibacterial action than cytotoxicity (Table 4.1).

For PHMB, the order of biocompatibility at both 250 and 100 X MBC was sol gel > PEG > pHEMA, whilst at 50 and 10 X MBC it was PEG > sol gel = pHEMA. For triclosan, the order of biocompatibility at 250 X MBC was sol gel > pHEMA > PEG. At 100 X MBC it was sol gel > PEG = pHEMA, at 50 X MBC it was sol gel > pHEMA > PEG, and at 10 X MBC it was sol gel > PEG > pHEMA.

For BAC, the order of biocompatibility at 250 X MBC was PEG > pHEMA > sol gel. At 100 X MBC it was PEG > sol gel = pHEMA, at 50 X MBC it was PEG > sol gel = pHEMA, and at 10 X MBC it was sol gel = PEG = pHEMA. For silver nitrate, the order of biocompatibility at 250 X MBC was sol gel > PEG > pHEMA. At 100 X MBC was sol gel > PEG > pHEMA, at 50 X MBC was sol gel > PEG > pHEMA, and at 10 X MBC was sol gel > PEG > pHEMA.

For cinnamaldehyde, the order of biocompatibility at 250 X MBC was sol gel > PEG > pHEMA. At 100 X MBC was sol gel > PEG > pHEMA, at 50 X MBC was sol gel > PEG > pHEMA, and at 10 X MBC was PEG > sol gel > pHEMA.

For furanone C30, the order of biocompatibility at 250 X MBC was sol gel > PEG > pHEMA. At 100 X MBC was sol gel > PEG > pHEMA, at 50 X MBC was sol gel > PEG > pHEMA, and at 10 X MBC was sol gel > PEG > pHEMA. For F-DPD, the order of biocompatibility (at 10 X MBC) was PEG > sol gel = pHEMA.

Coating	Sol gel				PEG				pHEMA			
Concentration (X MBC)	10	50	100	250	10	50	100	250	10	50	100	250
PHMB	0	0	0.85	0.91	0.66	0.81	0.76	0.65	0	0	0	0
Triclosan	2.04	2.83	3.49	3.01	1.94	1.57	1.75	1.85	1.13	1.78	1.75	2.03
BAC	0	0	0	0	0	0.51	0.64	0.94	0	0	0	0.15
Silver Nitrate	0.7	1.04	1.18	1.06	0.32	0.66	0.74	0.77	0	0	0	0.33
Cinnamaldehyde	0.41	0.81	0.83	1.41	0.9	0.78	0.81	0.77	0	0	0	0
Furanone C30	0	2	7.6	12.3	0	0	0.82	0.74	0	0	0	0
F-DPD	0	-	-	-	0.69	-	-	-	0	-	-	-

Table 4.1 Biocompatibility of seven antimicrobials at increasing concentrations for three coating agents. Biocompatibility was calculated by dividing the mean antimicrobial diffusion zone by the mean cytotoxicity diffusion zone (mean of n = 3 experiments). A value of 0 indicates no antimicrobial activity.

4.5.6 Biofilm formation in Drip Flow Biofilm Reactor Colony forming units (cfu) /ml were determined after growth on coated catheter pieces in the presence of a steady flow of artificial urine. The mean cfu/ml of biofilm formed on uncoated catheters was $2.77x10^7$ (Figure 4.5). There was a small but significant (One way ANOVA $p < 0.005$) reduction to $1.29x10^7$ cfu/ml when non antimicrobial containing sol gel was added to the catheter sections. All antimicrobial incorporated coatings induced significant ($p < 0.0001$) reductions in biofilm formation. The largest reduction occurred for PHMB which completely eradicated biofilm growth. The second most potent antimicrobial was furanone C30 which reduced biofilm growth to an average of $1.33x10^2$ cfu/ml. Silver nitrate reduced the biofilm growth to an average of $3.33x10^2$ cfu/ml. F-DPD incorporated sol gel gave a reduction to $9.56x10^4$ cfu/ml. When cinnamaldehyde was added to the sol gel coating the biofilm formation was reduced to $2.4x10^5$ cfu/ml and BAC incorporation reduced biofilm growth to $1.13x10^6$ cfu/ml. Triclosan incorporation was the least potent antimicrobial which reduced cfu/ml to $1.64x10^6$.

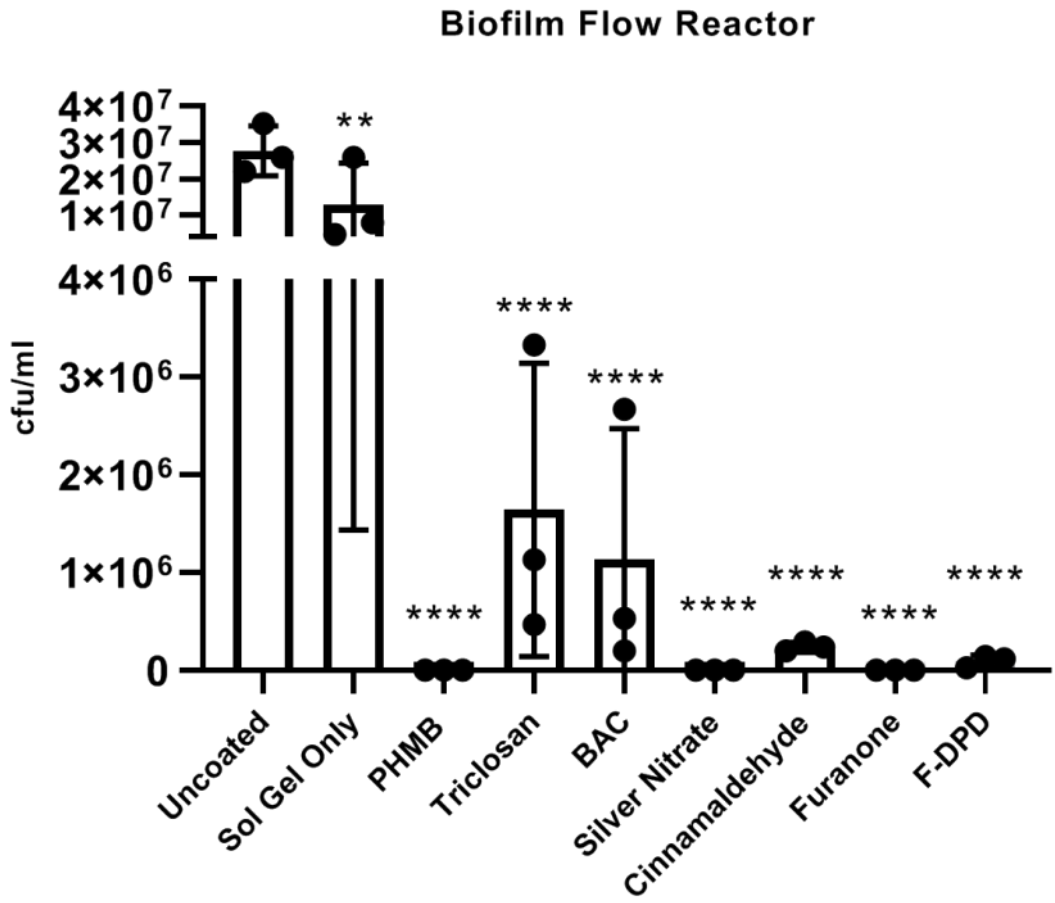

Figure 4.5 Biofilms of EC958 were grown on urinary catheter pieces coated in sol gel containing seven antimicrobials. Controls coated in sol gel only and uncoated catheters were also used. Colony forming units (cfu/ml) were evaluated after 48 hours and mean cfu/ml was calculated (n=3). Statistical analysis by One Way ANOVA: ** $p < 0.005$ and **** $p < 0.0001$.

4.6.0 Discussion

CAUTIs are becoming an increasing concern due to the aging population and the rise of antibiotic resistant uropathogens which has resulted in these infections becoming more difficult to treat [217]. Preventing these infections with the use of catheters coated with anti-infective agents is one area of research that has produced seemingly positive results *in vitro* [218] but has not been as successful in practice [114, 117]. It is clear that a more thorough screening of anti-infective agents needs to be employed when attempting to select for a novel coating for catheters to make sure that the components chosen will display long lasting efficacy. Three coating agents were screened in this study. PEG is a hydrogel based polymer that has been shown to elute antimicrobials in a sustained release profile [219]. pHEMA is also a hydrogel which, although has been used in controlled release of antimicrobials, exhibits an instant 'burst' release strategy when initially hydrated [220]. Sol gel coatings can vary in their properties depending on their preparation [221], the preparation used in this study has been shown to have a sustained release profile [222]. In this investigation we have exposed UPEC isolates to four biocides and three QSI's with the aim to assess which of these compounds would prove suitable as a catheter coating agent through the use of a series of high through put assays and a continuous culture catheter biofilm model.

4.6.1 Formation of bacterial biofilms grown on urinary catheters after long-term antimicrobial adaptation There was no significant effect on biofilm formation for the isolates EC1, EC2, CFT073 after exposure to any compound. In contrast, PHMB exposure decreased biofilm formation in 4/8 isolates (EC11, EC28, EC34, and EC958). Long term exposure to PHMB has been shown to reduce biofilm formation in UPEC previously [193]. It has been suggested that PHMB exposure induced downregulation of genes associated with flagella which are essential for initiation of biofilm formation [95]. If the PHMB exposed isolates have downregulated flagella this may impair the ability of those isolates to form biofilms, which may explain the reduction in overall biofilm found in the PHMB exposed isolates in the current investigation.

Triclosan exposure decreased biofilm formation in 3/8 (EC11, EC34, and EC958) isolates and increased biofilm formation in EC26. Sublethal exposure to triclosan has

been shown to impair biofilm formation in *S. aureus*, possibly due to repression of the extracellular matrix component PIA [104], a similar mechanism may occur in *E.coli*. Contrastingly, triclosan was also the only antimicrobial to induce any increase in biofilm formation after exposure. Studies on the effect of sub-lethal concentrations of triclosan on *S. mutans* biofilm formation showed that biofilm formation was increased by the upregulation of biofilm formation genes such as *gtfB*, *gtfC*, and *luxS* [223]. If a similar mechanism occurs in *E. coli* this could explain the increase in biofilm formation seen here. This demonstrates a strain specific response in the presence of triclosan.

When repeatedly exposed to BAC, 3/8 isolates (EC11, EC28, and EC34) demonstrated a significant decrease in biofilm formation. One possible explanation for a decrease in biofilm formation is a decrease in motility, as flagellar and chemotaxis proteins have been associated with biofilm initiation (attachment) [224]. Exposure to BAC has previously lead to a decrease in motility of *E.coli* [184], which RNA-sequencing revealed was due to a decrease in the expression of genes associated with flagella synthesis. A reduction in motility associated genes may explain the decreased biofilm formation in our BAC exposed isolates.

Silver Nitrate exposure decreased biofilm formation in 3/8 isolates (EC11, EC28, and EC34). It has been shown that bacteria that have been exposed to silver have downregulated adhesion factors and chemotaxis genes [225], further suggesting a possible mechanism for biofilm reduction.

Biofilm formation in EC11 and EC34 decreased when exposed to cinnamaldehyde. A study by Yuan *et al* [226] showed that exposure to cinnamaldehyde caused an upregulation in genes associated with metabolism but virulence genes associated with biofilm formation were repressed in *E.coli*. This could explain the decrease in biofilm formation after exposure to cinnamaldehyde. When exposed to furanone C30, EC28, EC34, and EC958 showed a significant decrease in biofilm formation. Genes for chemotaxis, flagella, and motility have been shown to be repressed by furanone C30 [69]. These genes are important for the initiation of biofilm formation [224]. If this has occurred in the furanone C30 exposed isolates then this could explain the decrease in biofilm formation seen here.

Exposure to DPD induced decreased biofilm formation in 3/8 isolates (EC11, EC34, and EC958). F-DPD is an AI-2 analogue and therefore inhibits quorum sensing by binding to the AI-2 receptor [64] and has been shown to inhibit biofilm formation in *E.coli* [65]. As far as we are aware there is no previous data on the effects of *E.coli* biofilm formation after adaptation to F-DPD.

Although these responses are not measuring the direct effect of the QSI on biofilm formation, undergoing long-term QS inhibition may have resulted in selecting for isolates with alterations in normal AI-2 based signalling, which are known to play a role in biofilm establishment [227].

4.6.2 Viability of bacterial biofilms grown on urinary catheters XTT assays were used to evaluate the viability of the UPEC biofilms grown in the catheter model. XTT is a redox dye that works by colour change due to the metabolisation of XTT to formazan in the presence of metabolic activity (mainly mitochondrial succinoxidase, cytochrome P450 systems, and flavoprotein oxidases) [228]. Exposure to PHMB caused increased biofilm viability in 4/8 isolates. A study by Allen *et al* examined the effects of PHMB exposure on *E.coli* and found upregulation of genes associated with energy and amino acid metabolism [95] if this has occurred in the PHMB exposed isolates this could explain the increase in viability seen in this study.

Triclosan exposure induced significantly increased biofilm viability in isolates EC11, EC26, EC28 and EC958. Triclosan has been shown to be effective at controlling *E.coli* infection in catheter models previously [229, 230]. *E.coli* that are tolerant to triclosan have been shown to have upregulated fatty acid, glyoxylate, dicarboxylate, and butanoate metabolism compared to the wild type [231]. This adaptive response likely occurs in an attempt to subvert the inhibitory effects of triclosan on fatty acid synthesis. If this has occurred in the triclosan exposed isolates, this upregulation in metabolism could increase the conversion of XTT to formazan and therefore show increased viability results for these isolates.

BAC exposure did not induce any changes in biofilm viability. In previous studies XTT assays were unaffected by previous BAC exposure in *E.coli* biofilms [166] which corroborates this study. Silver Nitrate induced one significant increase in biofilm viability (EC26). Silver has been shown to act on enzyme activity as one of the mechanisms of bactericide [232]. To adapt to the presence of silver, the bacteria

would have to overcome this enzyme inhibition, perhaps by attempting to increase enzymic activity. An increase in enzyme activity, especially respiratory enzymes, would cause increased metabolism of XTT to formazan which would lead to increased viability results seen here.

4.6.3 Biocompatibility of polymer coatings Out of the three coating agents tested, sol gel was calculated to have the highest biocompatibility values overall. Sol gel coatings are generally considered to have high biocompatibility [233] and are the subject of increasing interest in use for medical device coatings. For the most part, all polymer coatings were measured to have a similar level of cytotoxicity but the calculated BI score was mainly influenced by the variable antimicrobial activity of the coatings. pHEMA gels were observed to have the lowest antimicrobial activity for the majority of the antimicrobials tested and therefore lowest biocompatibility. Drug elution by pHEMA has been previously studied and it was found that unmodified pHEMA has poor capacity for drug loading and delivery [234].

As mentioned earlier, pHEMA hydrogels initially elute the majority of incorporated antimicrobial when first hydrated. Due to the method of synthesising pHEMA gels, the discs were washed in water for 24 hours before being used in experiments. It could be that the antimicrobials incorporated into these discs were partially eluted out during the washing process. This highlights the variability of pHEMA as a catheter coating agent. PEG and sol gel coatings both have a sustained release profile, sustained release is associated with higher biocompatibility [235] as the antimicrobial dose can be lower to avoid cytotoxicity and longer elution periods are beneficial if the medical device is *in situ* for a longer period of time [236]. The biocompatibility of furanone C30 when incorporated into sol gel were the highest values seen in this study, mainly due to the fact that there was no zone of cytotoxicity recorded for this coating combination. 5H-furanones have been shown to be less cytotoxic than other furanone derivatives possibly due to their inability to reduce transition metals and so cannot produce reactive oxygen species [205].

4.6.4 Evaluation using Drip Flow Biofilm Reactor Within the continuous culture system, the order of antimicrobial efficacy in terms of reduction in biofilm growth was found to be PHMB > furanone C30 > silver nitrate > F-DPD > cinnamadlehyde

> BAC > triclosan. The sol gel coating itself was also found to be mildly effective at reducing biofilm growth.

For the previous diffusion experiments triclosan performed the best out of the seven antimicrobials tested when incorporated into sol gel. However it performed the worst for the drip flow biofilm reactor, which was surprising considering the high concentration of triclosan in the biofilm reactor. Triclosan is a potent antimicrobial [193] but it is also a small, hydrophilic molecule which means that it can easily elute out of polymer gels [237]. It could be hypothesised that either all the triclosan eluted out of the sol gel in a short period of time and was washed away, allowing any residual bacteria to repopulate or that the bacteria quickly developed resistance to the triclosan coating. Triclosan is well documented to induce resistance in both planktonic and biofilm growth [193]. It could also be that triclosan is less effective against biofilms compared with planktonically growing cells, however triclosan has been shown to be effective against *E.coli* biofilms [230] so it is more likely that the results observed in the current investigation are due to rapid elution of triclosan from the coating or due to the selection of resistant bacterial populations, potentially having acquired mutations in the well document triclosan target enzyme FabI [80].

Conversely, BAC performed better in the flow reactor experiments than the disc diffusion (50, 100, and 250 X MBC are higher concentrations than 1.25mg/ml for BAC). BAC is a very large molecule and has both hydrophilic and hydrophobic regions [238] so it is less likely to be able to elute out of coatings easily when under static conditions such as found in the disc diffusion assay (which would explain the low biocompatibility values for BAC). It is possible that under continuous flow and increased polymer hydration that BAC was able to release more readily from the impregnated sol gel. It is also important to note, that the biocompatibility assays were only conducted over a period of 24 hours. Quaternary ammonium salts (which are similar to BAC) have been incorporated onto catheter coatings and were shown to have activity over longer periods of time [239] so it could be that BAC simply takes longer than 24 hours to elute out and therefore would show less activity in the inhibition assay experiments.

Cinnamaldehyde and F-DPD are both QSIs so it is likely that they were able to prevent biofilm formation on the coated catheters. We have previously tested the

potency of these QSIs in terms of antimicrobial and anti-biofilm activity and how they perform at disrupting AI-2 based signalling. These compounds possessed similar anti-biofilm activity in the drip flow reactor, however cinnamaldehyde was the least potent QSI overall. It may be that the QSIs performance as catheter coatings in this model is directly proportionate to their quorum sensing inhibitory activity.

The National Institute of Health and Care Excellence (NICE) recommends that cfu counts of > 10^3 of *E.coli* should be used to diagnose CAUTI in adults [19]. Sol gel coatings containing silver nitrate, furanone C30, and PHMB were able to reduce the cfu/ml to beneath this guideline. Silver nitrate was one of the best performing antimicrobials in the flow reactor system, however, in clinical practice silver coated catheters have been shown to not be any more effective than uncoated catheters [114]. It is our hypothesis that silver works for a short term *in vitro* however *in vivo* bacteria develop resistance to the coating [103], it is possible that the silver elutes out of the coating over a short period of time so is not suitable for long term catheterisation. It is also possible that sol gel is a more appropriate delivery system for silver than current coatings, hence the improved efficacy of the sol gel coating. More investigation would be needed before drawing these conclusions.

Furanone C30 was the best performing QSI and is also the most potent QSI with regards to dirupting AI-2 basted signalling (Chapter 3). Furanone C30 has been shown to be an effective antimicrobial when incorporated into coatings [240] and the results seen in this study corroborates that.

Sol gel containing PHMB was the best performing coating as it completely eradicated all biofilm in the flow reactor model. A study showed PEG containing PHMB coatings were also particularly effective at reduce biofilm formation [241]. PHMB did not exhibit high antimicrobial activity in the disc diffusion assays, however this shows the importance of evaluation using a model that more realistically mimics in-use conditions.

4.7.0 Conclusion

When evaluating antimicrobials to be used in medical device coatings it is important to not only assess the antimicrobial efficacy and biocompatibility of the coating but also the long term effects of exposure to the coating agent on the bacteria it will

encounter. In this study, PHMB was found to perform the best in an *in vitro* catheter biofilm model and induced the most decreases in biofilm formation after long term biocide exposure. However it was also observed that PHMB induced increases in biofilm viability and had generally low biocompatibility. When considering all experiments, furanone C30 was the best performing QSI, induced decreased biofilm formation in 3/8 isolates and had the highest biocompatibility values for sol gel. Further investigation is warranted to further evaluate the potential of these coatings.

Chapter 5

Genomic and transcriptomic analysis of antimicrobial exposed uropathogenic *Escherichia coli EC958*

I acknowledge the following people for contributing to the work presented in this chapter: K Norris and K Rawson (research assistants) who performed the RNA extraction and conducted integrity analysis before sending for sequencing. N Zoulias (academic) for assisting in data analysis. Genome sequencing was provided by MicrobesNG (http://www.microbesng.uk). RNA sequencing was provided by Genewiz (https://www.genewiz.com/en-GB/).

5.1.0 Abstract

Background: Catheter associated urinary tract infections (CAUTIs) are a major burden on healthcare providers and can lead to fatal complications such as pyelonephritis and bacteremia. The major causative agent of CAUTI is uropathogenic *E.coli* (UPEC) which forms biofilms on the catheter surface making the infection difficult to treat. Anti-infective coatings have been developed and are in clinical use however they demonstrate limited efficacy at preventing CAUTI during long term catheterisation due to the emergence of insusceptible bacterial populations. The genomic and transcriptomic changes that occur as a consequence of long term exposure to a panel of antimicrobials were characterised in UPEC strain EC958, a well characterised ESBL producing strain of the ST131 subgroup. **Methods:** Genome sequencing and RNA sequencing were performed before and after exposure to the biocides PHMB, triclosan, benzalkonium chloride (BAC), and silver nitrate, and the QSI's cinnamaldehyde, furanone C30, and F-DPD using an antimicrobial gradient plating system. Comparative genomics and differential gene expression analysis was utilised to evaluate the molecular mechanisms that govern antimicrobial adaptation in EC958. **Results:** Impaired motility by downregulation of flagella associated genes occurred after exposure to PHMB, BAC, cinnamaldehyde and F-DPD which correlated to a reduction in biofilm formation on the catheter surface for the PHMB and F-DPD exposed isolates. Multidrug efflux pumps were upregulated after exposure to PHMB (*mdtE*) and cinnamaldehyde (*marA* and *mdtN*). Triclosan exposure induced a mutation in *fabI* which conferred decreased susceptibility to triclosan. However antimicrobial susceptibility to PHMB, cinnamaldehyde, and furanone C30 increased potentially due to downregulation of murein transglycosylase *mltA*. *MltA* is is involved in peptidoglycan synthesis, reduced synthesis may impair the structure of the cell wall leading to increased membrane permeability and increased antimicrobial susceptibility. Multiple virulence factors were upregulated after exposure to triclosan (Type 1 fimbriae *fimA,C,D*) and cinnamaldehyde (*tonB* which is involved in iron transport) which did not correlate to changes in pathogenicity in this case. Antigen 43 (*ag43*) was upregulated after exposure to BAC and cinnamaldehyde which correlated with increased biofilm formation in these isolates. *Ag43* was downregulated after exposure to F-DPD which correlated to reduced biofilm formation on the catheter surface. **Conclusion:** The

multiple and varied effects that occur after exposure to broad-spectrum antimicrobials must be taken into consideration when developing a new antimicrobial coating as these effects have impacts on resistance, virulence, biofilm formation, and antibiotic resistance.

5.2.0 Introduction

Catheter associated urinary tract infections (CAUTIs) cause 20% of all episodes of health-care acquired bacteremia in acute care facilities, and over 50% in long term care facilities [242]. It is estimated that approximately 3% of people over the age of 65 will require a catheter and, with an aging population, this figure is likely to increase [16]. The major causative agent of CAUTI is uropathogenic *E.coli* which is distinct from the gastrointestinal serotypes of *E. coli* in its virulence factor production. UPEC encode P fimbriae/ pyelonephritis associated pili (PAP) [24] which facilitate attachment and invasion of the uroepithelia. P fimbriae mediate the internalisation of UPEC into host cells to form intracellular biofilm communities (IBCs) [40] allowing the bacteria within to proliferate inside the cell and form a persistent reservoir, often leading to recurrent UTI [41]. Other key virulence factors in UPEC may include: Type 1 pili, lipopolysaccharide (LPS), flagella, curli, secreted toxins, secretion systems, and tonB-dependent iron-uptake receptors [25].

EC958 is a UPEC isolate belonging to subgroup ST131 [243]. This bacteria was isolated from the urine of a patient presenting with a urinary tract infection in the Northwest region of England and is a leading contributor to urinary tract and bloodstream infections in clinical and community settings [243]. The *E.coli* ST131 subgroup is associated with resistance to fluoroquinolones, high virulence gene content, the possession of the type 1 fimbriae *FimH30*, and the production of the CTX-M-15 extended spectrum β-lactamase (ESBL) [244].

UPEC form biofilms on the surface of the catheter which exacerbates infection as biofilms are reportedly recalcitrant to many antimicrobial agents in addition to the actions of the host immune system making them far less susceptible compared to their planktonic counterparts [5]. Quorum sensing is density dependent bacterial communication whereby bacterial cells sense the concentration of signal molecules and activate QS-controlled genes in response [42]. As bacterial density increases the biofilm develops new characteristics that are different to the planktonic cells,

specifically the biofilm tends to be more virulent and less susceptible to antimicrobial treatment.

Antimicrobial catheter coatings have been developed as an attempt to prevent CAUTIs from occurring, with silver coated catheters currently in clinical use. However there is little evidence to suggest that the current coated catheters are any more effective at preventing bacterial growth than uncoated catheters [113]. A novel approach in the production of anti-infective catheter coatings is to use quorum sensing inhibitors (QSIs). These molecules disrupt the communication between bacterial cells and so inhibit biofilm formation. Another approach is to use biocides, broad-spectrum antimicrobial chemicals whose purpose is to inhibit the growth or kill microorganisms [7]. Catheters have been previously developed that have been coated with biocides [8] in order to reduce the bacterial contamination of the catheter but success has been limited, largely due to issue with cytotoxicity and the emergence of biocide resistance in bacteria during treatment.

It is hypothesised that current antimicrobial coatings become ineffective due to bacteria developing resistance to the coating over time [114]. It is important, then, that new coating agents should be assessed using long-term exposure to elucidate the effects of these antimicrobials over an extended amount of time. Research into the long-term effects of biocides has shown multiple phenotypic and genotypic changes occurring as bacteria respond to the antimicrobial challenge, which has been correlated with phenotypic effects such as changes in antimicrobial susceptibility, biofilm formation and relative pathogenicity [80, 184, 193].

The previous chapters have detailed the phenotypic changes that have occurred after exposure to the biocides PHMB, triclosan, benzalkonium chloride (BAC), and silver nitrate, and the QSI's cinnamaldehyde, furanone C30, and F-DPD in eight UPEC isolates. For the EC958 isolate these have included: decreased susceptibility after triclosan, BAC, and silver nitrate exposure, increased susceptibility after exposure to PHMB, cinnamaldehyde, and furanone C30, increased biofilm formation in 96 well plates after triclosan, BAC, cinnamaldehyde, and furanone C30 exposure, decreased biofilm formation on catheter surface after exposure to PHMB, triclosan, furanone C30, and F-DPD, and decreased pathogenicity after PHMB, triclosan, BAC, and furanone C30 exposure. In this chapter, we assess the genotypic and transcriptomic

changes that occur in UPEC isolate EC958 after long term exposure PHMB, triclosan, benzalkonium chloride (BAC), silver nitrate, cinnamaldehyde, furanone C30, and F-DPD.

5.3.0 Aims and objectives

In the previous chapters, multiple phenotypic changes have been observed in UPEC after exposure to seven antimicrobials (PHMB, triclosan, BAC, silver nitrate, cinnamaldehyde, furanone C30, and F-DPD). In light of the phenotypic data, there is a need for transcriptomic and genomic analysis to attempt to understand the mechanisms of UPEC adaptation to these antimicrobials. The isolate EC958 and the antimicrobial exposed strains of EC958 were selected for genome and RNA sequencing, the resulting data can be used to explain the corresponding phenotypic observations reported in previous chapters. As many phenotypic changes have been observed in this isolate, it is expected that there will also be a significant amount of genomic and transcriptomic changes revealed in the analysis of the sequencing data.

The specific aims of this chapter were to:

- Compare the genome sequencing data of EC958 and the antimicrobial exposed strains of EC958 to determine mutations that have occurred as a result of antimicrobial exposure.
- Compare the RNA sequencing data of EC958 and the antimicrobial exposed strains of EC958 to determine transcriptomic changes that have occurred as a result of antimicrobial exposure.
- Relate these genomic and transcriptomic changes to phenotypic observations.

5.4.0 Methods

5.4.1 Bacteria and chemical reagents Laboratory characterised UPEC isolate EC958 was used in the investigation. Bacteria were cultured onto Muller-Hinton agar (MHA; Oxoid, UK) or Muller-Hinton broth (MHB; Oxoid, UK) and incubated aerobically at 37 °C for 18 h unless otherwise stated. Furanone C30, cinnamaldehyde and F-DPD were prepared at 1 mg/ml in water and filter sterilised prior to use. Cinnamaldehyde was purchased from Sigma–Aldrich (Poole, UK). (Z)-4-Bromo-5(bromomethylene)-2(5H)-furanone C30 (furanone C30) was synthesised at

Sheffield Hallam University by P.G Chirila and Dr C. Whiteoak as described previously [191]. 4-fluoro-5-hydroxypentane-2,3-dione (F-DPD) was synthesised at University of Manchester by Dr M. Kadirvel as described previously [192].

5.4.2 Long-term exposure of bacteria to antimicrobials Bacteria were repeatedly exposed to antimicrobials using an antimicrobial gradient plating system as described in McBain *et al* [152]. In brief, 100 µl of a 5 × MBC concentration solution of antimicrobial was added to an 8 x 8 mm well in the centre of a 90 mm agar plate. Bacterial pure cultures were radially inoculated in duplicate from the edge of the plate to the centre, prior to incubation for 2 days aerobically at 37°C. Biomass from the inner edge of the annulus of bacterial growth representative of the highest antimicrobial concentration at which growth could occur was removed and used to inoculate a new antimicrobial containing plate, as outlined above. This process was repeated for 12 passages. Control isolates passaged 12 times on antimicrobial free media were also included. Bacteria were archived at -80 °C before and after antimicrobial passage for subsequent testing.

5.4.3 Whole genome sequencing Exposed isolates of EC958 and unexposed and control isolates were sent to MicrobesNG (Birmingham, UK) to be sequenced. MicrobesNG sequencing protocol is as follows:

Three beads were washed with extraction buffer containing lysozyme and RNase A, incubated for 25 min at 37ºC. Proteinase K and RNase A were added and incubated for 5 min at 65ºC. Genomic DNA was purified using an equal volume of SPRI beads and resuspended in EB buffer.

DNA was quantified in triplicates with the Quantit dsDNA HS assay in an Ependorff AF2200 plate reader. Genomic DNA libraries were prepared using Nextera XT Library Prep Kit (Illumina, San Diego, USA) following the manufacturer's protocol with the following modifications: two nanograms of DNA instead of one were used as input, and PCR elongation time was increased to 1 min from 30 seconds. DNA quantification and library preparation were carried out on a Hamilton Microlab STAR automated liquid handling system. Pooled libraries were quantified using the Kapa Biosystems Library Quantification Kit for Illumina on a Roche light cycler 96

qPCR machine. Libraries were sequenced on the Illumina HiSeq using a 250bp paired end protocol.

Reads were adapter trimmed using Trimmomatic 0.30 with a sliding window quality cutoff of Q15 [245]. De novo assembly was performed on samples using SPAdes version 3.7 [246], and contigs were annotated using Prokka 1.11 [247].

Each genome of exposed bacterial strain of EC958 was compared to the genome of EC958 prior to exposure with a minimum of 30 x genome coverage.

5.4.4 RNA sequencing RNA from each exposed strain of EC958 was extracted using the TRIzol plus RNA purification kit (Thermofisher, UK). RNA integrity and quality was assessed using the NanoDrop (Thermofisher, UK), Qubit fluorometer (Thermofisher, UK), and Affymetrix Genechip microarray system (Thermofisher, UK).

Library preparations, sequencing reactions, and bioinformatics analysis were conducted at GENEWIZ, LLC. (South Plainfield, NJ, USA). rRNA depletion was performed using Ribozero rRNA Removal Kit (Illumina, San Diego, CA, USA). RNA sequencing library preparation used NEBNext Ultra RNA Library Prep Kit for Illumina by following the manufacturer's recommendations (NEB, Ipswich, MA, USA). Briefly, enriched RNAs were fragmented for 15 minutes at 94 °C. First strand and second strand cDNA were subsequently synthesized. cDNA fragments were end repaired and adenylated at 3'ends, and universal adapter was ligated to cDNA fragments, followed by index addition and library enrichment with limited cycle PCR. Sequencing libraries were validated using the Agilent Tapestation 4200 (Agilent Technologies, Palo Alto, CA, USA), and quantified by using Qubit 2.0 Fluorometer (Invitrogen, Carlsbad, CA) as well as by quantitative PCR (Applied Biosystems, Carlsbad, CA, USA).

The sequencing libraries were multiplexed and clustered on one lane of a flowcell and loaded on the Illumina HiSeq instrument according to manufacturer's instructions. The samples were sequenced using a HiSeq 2x150 Paired End (PE) configuration. Image analysis and base calling were conducted by the HiSeq Control Software (HCS). Raw sequence data (.bcl files) generated from Illumina HiSeq was

converted into fastq files and de-multiplexed using Illumina's bcl2fastq 2.17 software. One mis-match was allowed for index sequence identification.

After demultiplexing, sequence data was checked for overall quality and yield. Then, sequence reads were trimmed to remove possible adapter sequences and nucleotides with poor quality using Trimmomatic v.0.36. The trimmed reads were mapped to the *Escherichia coli* reference genome available on ENSEMBL using the STAR aligner v.2.5.2b. The STAR aligner is a splice aware aligner that detects splice junctions and incorporates them to help align the entire read sequences. BAM files were generated as a result of this step. Unique gene hit counts were calculated by using featureCounts from the Subread package v.1.5.2. Only unique reads within exon regions were counted.

After extraction of gene hit counts, the gene hit counts table was used for downstream differential expression analysis. Using DESeq2, a comparison of gene expression between the groups of samples was performed. The Wald test was used to generate p-values and Log2 fold changes. Genes with adjusted p-values < 0.05 and absolute log2 fold changes > 1 were called as differentially expressed genes for each comparison. A gene ontology analysis was performed on the statistically significant set of genes by implementing the software GeneSCF v1.1. The GO list was used to cluster the set of genes based on their biological process and determine their statistical significance. A PCA analysis was performed using the "plotPCA" function within the DESeq2 R package. The plot shows the samples in a 2D plane spanned by their first two principal components. The top 500 genes, selected by highest row variance, were used to generate the plot. RNA expression of each exposed isolate was compared with the control isolate. Analysis of genes was conducted using PANTHER [248].

5.5.0 Results

5.5.1 Mutations in antimicrobial adapted UPEC isolate EC958

5.5.1.1 PHMB There were no genes that acquired mutations that were specific to PHMB exposure alone. All of the genes that acquired mutations after exposure to PHMB also acquired mutation after exposure to the other test antimicrobials (Table 5.1). These mutations were as follows: missense mutation in exodeoxyribonuclease 8

(*recE1*), missense mutation in 50S ribosome binding GTPase (*yeeP*), missense mutation in ISEc9 family transposase (*tnpA*), missense mutation in EntS/YbdA MFS transporter (*entS*), missense mutation in IS1 transposase (*insB*), missense mutation in increased serum survival gene (*iss*), missense mutation in putitative sulfertransferase (*yeeD*), missense mutation in positive regulator (*alpA*).

5.5.1.2 Triclosan Mutations that occurred after triclosan exposure (Table 5.1) include missense mutation in *fabI* enoyl-[acyl-carrier-protein] reductase (Table 5.2), nonsense mutation in *wbbL* rhamnosyltransferase (Table 5.18), missense mutation in lipid II flippase (*murJ*), and silent mutation in glutamate decarboxylase beta (*gadB*).

5.5.1.3 BAC Mutations that occurred after BAC exposure (Table 5.1) included missense mutation in *cspE* cold-shock like protein and missense mutation in *ldrD2* small toxic polypeptide. The BAC exposed isolate was one of the only isolates to not acquire a *yeeD* mutation.

5.5.1.4 Silver Nitrate Mutations that occurred after silver nitrate exposure (Table 5.1) included missense mutation in *fadA* (3 ketoacyl CoA thiolase) (Table 5.2) and a silent mutation in glutamate decarboxylase beta (*gadB*).

5.5.1.5 Cinnamaldehyde Mutations that occurred after cinnamaldehyde exposure (Table 5.1) include nonsense mutation in *proQ* RNA chaperone, frame shift mutation in dihydrolipoyl dehydrogenase (*ipd*), missense mutation in *dnaX* DNA polymerase III subunit tau (Table 5.2), missense mutation in TONB protein (*tonB*), and a silent mutation in glutamate decarboxylase beta (*gadB*).

5.5.1.6 Furanone C30 Mutations that occurred after furanone C30 exposure (Table 5.1) include silent mutation in probable manganese efflux pump (*mntP*), and silent mutation in glutamate decarboxylase beta (*gadB*).

5.5.1.7 F-DPD Mutations that occurred after F-DPD exposure (Table 5.1) include silent mutation in negative regulator (*rsxC*), missense mutation in uncharacterized HTH-type transcriptional regulator (*yfhH*), missense mutation in *ldrD3* small toxic polypeptide, and a silent mutation in glutamate decarboxylase beta (*gadB*). The F-DPD exposed isolate was one of the only isolates to not acquire a *yeeD* mutation.

Antimicrobial	Gene name	Type of mutation	Function
All	*recE1*	Missense	Exodeoxyribonuclease 8 hydrolyses phosphodiester bonds in DNA and is mainly involved in recombination and damage repair
All	*yeeP*	Missense	50S Ribosome binding GTPase. Era mutant era1 suppresses some temperature-sensitive mutations that affect DNA replication and chromosome partitioning and segregation
All	*tnpA*	Missense	ISEc9 family transposase. Transposase is an enzyme that binds to the end of a transposon and catalyzes its movement to another part of the genome
All	*entS*	Missense	EntS/YbdA MFS transporter. The transporter is mainly involved in efflux of enterobactin
All	*insB*	Missense	IS1 transposase. Transposase is an enzyme that binds to the end of a transposon and catalyzes its movement to another part of the genome
All	*iss*	Missense	ISS (increased serum survival gene). ISS has role in the complement resistance associated with a ColV plasmid and is an outer membrane protein
PHMB, triclosan, silver nitrate, cinnamaldehyde, furanone C30	*yeeD*	Missense	yeeD encodes a putitative sulfertransferase

All	*alpA*	Missense	*AlpA* is a positive regulator of the expression of the *slpA* gene. *SlpA* encodes surface layer protein A.
Triclosan	*fabI*	Missense	Enoyl-[acyl-carrier-protein] reductase is a key enzyme of the type II fatty acid synthesis (FAS) system
Triclosan	*wbbL*	Nonsense	Rhamnosyltransferase is involved bacterial outer membrane biogenesis (O antigen)
Triclosan	*murJ*	Missense	Lipid II flippase is involved in peptidoglycan biosynthesis
BAC	*cspE*	Missense	*cspE* encodes cold-shock like protein which regulates expression of genes encoding stress response proteins but can also perform an essential function during cold acclimation
BAC	*ldrD2*	Missense	Small toxic polypeptide is the toxic component of a type I toxin-antitoxin (TA) system
F-DPD	*ldrD3*	Missense	Small toxic polypeptide is the toxic component of a type I toxin-antitoxin (TA) system
Silver nitrate	*fadA*	Missense	3 ketoacyl CoA thiolase enzyme catalyzes the final step of fatty acid oxidation
Triclosan, silver nitrate, cinnamaldehyde, furanone C30, F-DPD	*gadB*	Silent	Glutamate decarboxylase beta converts glutamate to gamma-aminobutyrate (GABA)
Cinnamaldehyde	*proQ*	Nonsense	RNA chaperone with significant RNA binding, RNA strand exchange and RNA duplexing activities
Cinnamaldehyde	*ipd*	Frame Shift	Dihydrolipoamide dehydrogenase is a

			bacterial enzyme that is involved in the central metabolism and is a component of the glycine cleavage system as well as of the alpha-ketoacid dehydrogenase complexes
Cinnamaldehyde	*dnaX*	Missense	DNA polymerase III subunit tau. DNA polymerase III is a complex, multichain enzyme responsible for most of the replicative synthesis in bacteria
Cinnamaldehyde	*tonB*	Missense	TONB protein involved with the transport of iron-containing compounds and colicins into the cell
Furanone C30	*mntP*	Silent	Probable manganese efflux pump
F-DPD	*rsxC*	Silent	Negative regulator of *soxS* transcription
F-DPD	*yfhH*	Missense	Uncharacterized HTH-type transcriptional regulator

Table 5.1 Summary of genes that acquired mutations after antimicrobial exposure, type of mutation and brief overview of function.

5.5.2 Alterations in UPEC transcriptome after antimicrobial exposure

5.5.2.1 PHMB Following PHMB exposure 268 genes were significantly ($p<0.05$) upregulated and 137 genes were significantly downregulated compared to the control strain. The largest fold increase (3.82) was allantoin permease *ybbW* and the largest fold decrease (-4.93) was PTS trehalose transporter subunit IIBC (*treB*). PANTHER analysis revealed functional groups of genes that had altered expression in the PHMB exposed mutant. These were genes associated with TCA cycle such as *gltA* (1.26) and *fumC* (1.13). Genes associated with flagella structure (*flgB,C,D,E,F,G,H,I*) (-1.00 to -2.35) and function (*fliF,G,H,I,J,K,LM,N,P*) were all downregulated (-1.09 to -2.55). There were increases in the expression of genes associated with membrane transport such as *dppD* (2.75), *dppF* (2.17) and *sufA,B,C,E* (1.17 to 1.37). Changes were observed in the expression of genes associated with cell membrane synthesis such as *mltA* (-1.2) and *lysM* (1.21). Genes associated with DNA repair such as *recR* were downregulated (-1.17). *BolA*, a transcription factor associated with cellular stress response, was upregulated (1.24) (Table 5.2).

5.5.2.2 Triclosan Following triclosan exposure 172 genes were significantly ($p<0.05$) upregulated and 155 genes were significantly downregulated. The largest fold increase (5.48) was 2-hydroxy-3-oxopropionate reductase (*garR*) and the largest fold decrease was (-4.37 and -4.06) for nitrate reduction associated genes *napH* and *napG* respectively. PANTHER analysis revealed functional groups of genes that had altered expression in the triclosan exposed isolate. These were genes involved in purine biosynthesis such as *purH* (1.11) and *purE* (1.36) (Table 5.18). Genes that contribute to cellular transport systems such as *dppD* (3.34), *dppF* (2.44), *sufB,C,D,E* (1.08 to 1.25), *dcuC* (-1.12), *potE* (-1.66) and *malE,F,K* (-1.49 to -2.05) (Table 5.2). Genes associated with cell adhesion such as *fimA,C,D* were upregulated (1.25 to 2.2), and genes involved in the PTS system such as *srlE* (-2.08) and *srlA* (-2.03) were downregulated. Genes associated with cell wall synthesis such as *mltA* were downregulated (-1.22) (Table 5.2).

5.5.2.3 BAC Following BAC exposure 195 genes were significantly ($p<0.05$) upregulated and 248 genes were significantly downregulated. The largest fold increase (4.47) was antigen 43 (*ag43*) an autotransporter outer membrane protein

(Table 5.2) and the largest fold decrease (-6.48) was flagellin (*fliC*) (Table 5.2). PANTHER analysis revealed groups of genes that had altered expression in the BAC exposed isolate. These were genes involved in purine synthesis such as *purH* (1.49), *purN* (1.14), and *purE* (2.16) (Table 5.2). Genes associated with motility such as *fliA,D,F,G,H,I,J,K,L,M,N,O,P,R,S,T,Z* (-1.31 to -3.24), *flgC,D,E,G,H,I,J,K,L,N* (-1.06 to -3.83), *motA* (-2.97), *motB* (-3.38) and *cheA,R,W,Z* (-3.99 to -3.14) were downregulated. Genes involved in transport systems such as *dppD* (1.53), *dppF* (1.18) were upregulated and *potE* (-1.19) was downregulated.

5.5.2.4 Silver Nitrate Following silver nitrate exposure 225 genes were significantly ($p<0.05$) upregulated and 141 genes were significantly downregulated. The largest fold increase (4.8) was antigen 43 (*ag43*) (Table 5.2). The largest fold decrease (-5.43) was PTS trehalose transporter subunit IIBC (*treB*). PANTHER analysis revealed functional groups of genes that had altered expression in the silver nitrate exposed isolate. These were genes involved in purine synthesis such as *purH* (1.34), *purN* (1.1), and *purE* (1.34) (Table 5.2) and genes associated with the TCA cycle such as *gltA* (1.25) and *fumC* (1.07). Genes involved in fatty acid degradation such as *fadA* (1.13) and *fadB* (1.57) were upregulated. Genes associated with transport such as *dppD* (2.59), *actP* (1.59), *potG* (1.02), and *artP* (1.06) were upregulated, *malF* (-3.9) (Table 5.18) and *dcuC* (-1.55) were downregulated. Genes involved in cell wall synthesis such as *mltA* were downregulated (-1.84).

5.5.2.5 Cinnamaldehyde Following cinnamaldehyde exposure 368 genes were significantly ($p<0.05$) upregulated and 329 genes were significantly downregulated. The largest fold increase (4.64) was 2-hydroxy-3-oxopropionate reductase (*garR*) and the largest fold decrease (-5.74) was *mexE* family multidrug efflux RND transporter periplasmic adaptor subunit (Table 5.2). PANTHER analysis revealed groups of genes that had altered expression in the cinnamaldehyde exposed isolate. These were *gltA* (1), *fumC* (1.36), and *sucA* (1.14) involved in the TCA cycle. Genes involved in ribonucleotide synthesis *upp* (-1.31), *pyrG* (-1.17) and *carB* (-2.54), and purine synthesis *adk* (-1.29) and *guaA* (-1.32) were all downregulated. Flagella associated genes *flgB,C,D,E,H,I,J,K,L* (-1.09 to -2.64) and *fliA,D,F,G,H,J,K,L,M,N,P,S,T,Z* (-1.23 to -2.75) were downregulated. Genes associated with chemotaxis *cheA,R,W,Z* were downregulated (-2.13 to -2.61). Genes associated with transport such as *uhpT* (1.05) *tonB* (1.13), and *marA* (1.5) were

upregulated and *sufA,B,C,D* (Table 5.2) (-1.2 to -1.8) was downregulated. *MdtE* was downregulated (-2.73) whereas *mdtN* was upregulated (1.87). Genes associated with adhesion such as Antigen 43 (*ag43*) (1.14) and *yfcV* (1.83) were upregulated. Genes associated with DNA transcription and repair such as *proQ* (-1.44), *recR* (-1.62) and *dnaK* (-2.34) were downregulated. Genes associated with cell wall synthesis such as *mltA* (-1.02) were downregulated.

5.5.2.6 Furanone C30 Following furanone C30 exposure 122 genes were significantly ($p<0.05$) upregulated and 98 genes were significantly downregulated. The largest fold increase (5.02) was 2-hydroxy-3-oxopropionate reductase (*garR*) and the largest fold decrease (-2.21) was murein transglycosylase (*mltA*) (Table 5.2). PANTHER analysis revealed groups of genes that had altered expression in the furanone C30 exposed isolate. These were genes involved in purine synthesis such as *purH* (1.43), and *purE* (1.31) (Table 5.2), genes involved in cellular transport systems such as *dppD* (1.9) and *dppF* (1.19) were upregulated and *secY* (-1.4) (Table 5.2) was downregulated. Genes associated with 50S Ribosomal subunit L20 *(rplT*), L23 (*rplW*), and L4 (*rplD*) were downregulated (-1.08, -1.33, and -1.45 respectively).

5.5.2.7 F-DPD Following F-DPD exposure 86 genes were significantly ($p<0.05$) upregulated and 181 genes were significantly downregulated. The largest fold increase (2.76) was 2-hydroxy-3-oxopropionate reductase (*garR*) and the largest fold decrease (-4.76) was flagellin (*fliC*) (Table 5.2). PANTHER analysis revealed groups of genes that had altered expression in the F-DPD exposed isolate. These were genes involved in motility such as *fliA,D,F,G,H,I,J,K,L,M,N,O,P,S,T,Z* (-1.2 to -3.17) and *flgB,C,D,E,G,H,I,J,K,L,N* (-1.2 to -4.76). Antigen 43 (*ag43*) was downregulated (-1.2). Genes involved in adhesion such as *AfaC* and *afaD* increased expression (2.59 and 2.02 respectively). Genes involved in cell membrane synthesis such as *mepS* was upregulated (1.07) and *lysM* was downregulated (-1.26). Transporter *mdtE* was downregulated (-1.39).

	PHMB	Triclosan	BAC	Silver Nitrate	Cinnamaldehyde	Furanone C30	F-DPD	Associated Genes
MIC Fold Change	-5	260	2	2	-2	-2	No Change	*mltA* [249] *fabI* [80]
MBC Fold Change	-1.1	8	No Change	16	-2	-.1.5	No Change	*fadA* [185] *sufC* [250]
MBEC Fold Change	42.4	125	4	1.3	-4	-4	No Change	*mexE* [251]
Cross Resistance	No Change	Nitrofurantoin resistance	No Change	No Change	No Change	No Change	No Change	*potE* [252] *dnaX* [253]
Biofilm Formation (Plate)	No Change	Increase (p<0.0001)	Increase (p<0.0001)	No Change	Increase (p<0.001)	Increase (p=0.0124)	No Change	*bolA* [254] *wbbL* [255] *ag43* [256]
Biofilm Formation (Catheter)	Decrease (p=0.0069)	Decrease (p=0.0094)	No Change	No Change	No Change	Decrease (p=0.0056)	Decrease (p=0.0337)	*flg* [257] *fli* [257]
Pathogenicity	Decrease (p<0.001)	Decrease (p<0.001)	Decrease (p<0.001)	No Change	No Change	Decrease (p<0.001)	No Change	*wbbL* [255] *malF* [258] *secY* [259]
SMC Invasion	No Change	No Change	Increase (p=0.0006)	No Change	No Change	No Change	No Change	*purE,H,N* [260]

Table 5.2 Observed changes in MIC, MBC, MBEC, biofilm formation, cross resistance, pathogenicity, and cell invasion in EC958 after exposure to 7 antimicrobials. Where a change was observed, the p value is given. Genes whose expression was found to be affected by antimicrobial exposure and that are associated with the observed changes are also shown.

5.6.0 Discussion

There were certain mutations that occurred in all antimicrobial exposed EC958 isolates (Table 5.1). These indicate universal adaptation to antimicrobial stress. Genome sequencing revealed all isolates acquired mutations in the *recE1* gene. *RecE1* encodes exodeoxyribonuclease 8 which hydrolyses phosphodiester bonds in DNA and is mainly involved in homologous recombination and DNA damage repair [261]. Mutations in *recE* have been shown to abolish nuclease activity, which would likely impair DNA repair mechanisms [262]. Any functional deficits in EC958 in response to antimicrobial adaptation may be attributed to impaired DNA repair.

All EC958 isolates also acquired mutations in *yeeP* (Table 5.1). *yeeP* encodes 50S Ribosome binding GTPase. GTPases that are associated with ribosomes are essential to the function of the ribosome [263]. Mutations in *yeeP* have been previously associated with attenuated fitness in *E. coli* [264]. A similar GTPase (*era*) binds rRNA to the 30S ribosomal subunit, ensuring translation can take place [263]. A significant part of the bacterial stress response is impairment of translation and therefore protein synthesis [265], impacting cell division and fitness. Mutation in this GTPase may impair translation which could explain the reduction in pathogenicity seen in the PHMB, triclosan, BAC, and furanone C30 exposed isolates as a reduction in fitness would impair the bacteria's ability to grow and establish infection [266].

These mutations are deleterious (decreases fitness of the organism) and so are unlikely to be maintained after exposure to the antimicrobial is removed. These mutations are unlikely to be coincidental changes as they occurred in all seven exposured isolates so it is more likely that these functional deficits are universal adaptation to general antimicrobial challenge.

All isolates acquired multiple mutations in *entS* (Table 5.1). *EntS* encodes the EntS/YbdA MFS transporter. The transporter is mainly involved in efflux of enterobactin - one of the most effective ferric iron chelating compounds known in bacteria [267]. Enterobactin has been suggested to have another role - protection against oxidative stress [268]. As the molecule has exposed hydroxyl groups it would be an effective molecule to scavenge oxygen radicals [268]. Mutations in this gene may therefore potentially make bacteria more sensitive to oxidative stress. Cinnamaldehyde is known to exert oxidative stress on bacterial cells [194], and the cinnamaldehyde

exposed EC958 isolate showed increased susceptibility to cinnamaldehyde after exposure, suggesting a potential mechanism of increased susceptibility.

5.6.1 PHMB Exposure to PHMB induced an increase in susceptibility in planktonic EC958 (Table 5.2). RNA sequencing of the PHMB exposed isolate revealed a downregulation of murein transglycosylase (*mltA*). Peptidoglycan (murein) is integral to the structure and function of the bacterial cell wall and *mltA* is involved in peptidoglycan synthesis [249]. There was also an upregulation of peptidoglycan-binding protein *lysM*, these domain have multiple functions which include peptidoglycan degradation [269]. These impairments in peptidoglycan synthesis and an increase in degradation could drastically impair cell wall formation, the resulting loss of integrity increasing antimicrobial susceptibility.

The genes *gltA* (citrate synthase) and *fumC* (fumarate hydratase II) were both upregulated and are both involved in the TCA cycle. The TCA (tricarboxylic acid) /Krebs /citric acid cycle is a series of chemical reactions used by all aerobic organisms to generate energy (ATP) [270]. Citrate synthase catalyzes the condensation of oxaloacetate and acetyl coenzyme A to produce citrate plus coenzyme A [271]. Fumarate hydratase II catalyzes the stereospecific interconversion of fumarate to L-malate, *fumC* supplements *fumA* under conditions of iron limitation and oxidative stress [272]. PHMB is a decoupling agent and has been shown to play a role in disrupting respiration by altering the proton motive force (PMF) across the membrane [273]. Upregulation of the aforementioned genes could be a response of the bacteria to the limitation in respiration exerted by PHMB, by boosting the TCA cycle.

PHMB exposure led to a significant decrease in biofilm formation grown on urinary catheters (Table 5.2). RNA sequencing data analysis revealed downregulation of multiple genes associated with flagella structure and function. Flagella are an important factor in the initiation of bacterial biofilm formation [257] so loss of these structures would suggest that the ability of these isolates to form biofilms may be impaired. However the MBEC for this strain increased after PHMB exposure, possibly suggesting the presence of a small but persistent biofilm. RNA sequencing revealed an upregulation in the gene *bolA* which is a transcription factor that downregulates flagella synthesis and upregulates biofilm formation [254]. *BolA* was shown to repress *flhD* and *flhC* which are major regulators for flagella synthesis, and upregulate genes associated

with fimbriae (*yfcV*) and LPS biosynthesis which favours biofilm formation [254]. *BolA* also elevates expression of enzymes involved in the TCA cycle [254]. We see downregulation of *flhA*, upregulation of *yfcV* and *gltA* and *fumC* as mentioned earlier. This is likely occurring in response to the upregulation of transcription factor *bolA*. As this isolate is less motile this would affect initiation of biofilm growth on a catheter since motility is an important factor in the ability of bacteria to initiate biofilm development [257].

5.6.2 Triclosan Triclosan induced the largest frequency and magnitude of susceptibility decreases in MIC, MBC, and MBEC (Table 5.2). Mutations in the *fabI* gene found in the triclosan exposed isolate would explain the high levels of triclosan resistance as *fabI* encodes Enoyl-[acyl-carrier-protein] reductase which is a known target of triclosan [80]. Genome sequencing of the triclosan exposed mutant showed mutation in the *wbbL* gene, which encodes the enzyme rhamnosyltransferase which is involved in lipopolysacharide (LPS) and O antigen biogenesis. Mutation in *wbbL* has shown to impair O antigen biosynthesis, when O antigen is restored in *E.coli* the bacteria exhibit increased susceptibility to triclosan, decreased biofilm formation and increased virulence [255]. O antigen is important in maintaining the structure of the bacterial cell wall, and it has been shown that loss of O antigen increases cell permeability in *E.coli*, hence increasing antimicrobial susceptibility [274]. *FabI* is also involved in LPS synthesis [275] and because triclosan is a surfactant, the amount of LPS in the cell wall could have an effect on triclosan susceptibility.

Decreased pathogenicity was observed in the triclosan exposed isolate (Table 5.2). O antigen is an important virulence factor in UPEC [25] as it protects UPEC against phagocytosis by immune cells and complement mediated killing [276]. Therefore, a mutation in *wbbL* that inhibits O antigen synthesis may explain the decreased pathogenicity that was seen in this study. RNA sequencing showed downregulation of transporters *dcuC* and *malF*. *MalF* is a maltose transporter, knockout mutations of this gene caused *Vibrio spp.* to become less virulent by inhibiting the production and secretion of toxins and virulence factors [258]. This may also contribute to the decreased pathogenicity seen here in EC958 after triclosan exposure.

EC958 exhibited an increase in biofilm formation after triclosan exposure as well as an elevation in MBEC (Table 5.2). This could be explained by the mutation in *wbbL* that

was seen in the triclosan exposed isolate. As previously stated - O antigen synthesis decreases biofilm formation in *E.coli* so a mutation in *wbbL* leading to impaired O-antigen formation may increase biofilm formation [255].

The triclosan exposed isolate showed downregulation of *srlE* and *srlA* which are involved in the phosphoenolpyruvate-carbohydrate phosphotransferase system (PTS). In *Escherichia coli*, PTS is responsible for the transport and phosphorylation of sugars, such as glucose. PTS activity has a crucial role in the global signalling system that controls the preferential consumption of glucose over other carbon sources [277]. The enzyme IIC complex composed of *srlA*, *srlB* and *srlE* is involved in sorbitol transport, it can also transport D-mannitol [277]. Downregulation of this system could be a sign of reduced energy production which is common in a bacterial stress response [278].

5.6.3 BAC EC958 was observed to form increased biofilm biomass after BAC exposure and had a corresponding increase in MBEC (Table 5.2). The highest increase in gene expression after BAC exposure was antigen 43 (*ag43*). Antigen 43 is a self-recognizing adhesin that is associated with cell aggregation and biofilm formation in *E. coli* K-12 [256]. Such a large fold increase in this gene expression would undoubtedly cause increased biofilm production which is what we have observed.

After BAC exposure, multiple genes responsible for synthesis of flagella were down regulated. In fact, the gene with the highest fold decrease in expression was flagellin. Exposure to BAC decreasing motility of *E.coli* has been demonstrated previously [184]. As discussed earlier this decrease in motility would negatively impact the initiation of biofilm formation. The flagellar motor proteins *motA,B* and the chemotaxis proteins *cheA,R,W,Z* have been associated with biofilm initiation (attachment) [224] all were downregulated in the BAC exposed strain.

Exposure to BAC induced an increase in EC958 invasion in for SMC. Genes involved in purine biosynthesis: *purE*, *purH*, and *purN* were upregulated after BAC exposure. An upregulation of these genes could increase virulence by promoting increased survival inside the cell [260]. If the bacteria survive inside the cells they would survive until the end of the SMC invasion assay which would explain the increased SMC invasion observed for the BAC exposed isolate.

Increased expression of *dppD* and *dppF* which are involved in the Ntr (Nitrogen regulated) response was observed in this study, this was also seen after sublethal exposure to BAC in another UPEC isolate CFT073 [279]. It was hypothesised that biocide exposure depleted the bacteria of nitrogen and therefor mechanisms to scavenge nitrogen were upregulated.

5.6.4 Silver nitrate It was observed that EC958 decreased in silver nitrate susceptibility after long-term exposure (Table 5.2). Silver nitrate exposure induced a mutation in the *fadA* gene (3-ketoacyl-CoA-thiolase) which catalyses the final step of fatty acid oxidation. Silver-induced shortening of the acyl chain of fatty acids occurs mostly in the cell membrane and one effect of ionic silver is reducing the amount of unsaturated fatty acids in the cell wall [185]. *FadA* has been shown to be downregulated by ionic silver [185]. So an increase in the amount of fatty acids in the cell wall could be a potential mechanism of withstanding the effects of prolonged exposure to silver. RNA sequencing of the silver nitrate exposed isolate revealed *fadA* and *fadB* expression were upregulated which further corroborates this. The promotor region for the *fadBA* operon is located in *fadB* and the direction of transcription is *fadB* to *fadA* [280]. Therefore, it is highly unlikely that the mutation in *fadA* is responsible for the increased levels of transcription, so the increased expression of these genes may be more adaptive than mutational. One of the products of the final stage of fatty acid oxidation is acetyl-CoA [281] which is necessary for the TCA cycle (described above). Genes involved in the TCA cycle *gltA* (citrate synthase) and *fumC* (fumarate hydratase II) were also upregulated. Silver has been shown to depolarise the outer cell membrane and therefore inhibit respiration [282].The upregulation of all of these genes could be a response from the bacteria to the disruption of the TCA cycle by membrane depolarisation caused by silver.

Silver nitrate exposure led to no change in biofilm formation and a small magnitude increase in MBEC in EC958 (Table 5.2). The highest increase in gene expression for the silver nitrate exposed isolate was antigen 43 (*ag43*). Antigen 43 is a self-recognizing adhesin that is associated with cell aggregation and biofilm formation in *E. coli* K-12 [256]. This could explain the increase in MBEC observed in response to silver exposure.

5.6.5 Cinnamaldehyde Exposure to cinnamaldehyde induced an increase in susceptibility in planktonic EC958 (Table 5.2). RNA sequencing of the cinnamaldehyde

exposed isolate revealed a downregulation of murein transglycosylase (*mltA*). Peptidoglycan (murein) is integral to the structure and function of the bacterial cell wall and *mltA* is involved in peptidoglycan synthesis [249]. This impairment in peptidoglycan synthesis would drastically impair cell wall formation, the resulting loss of integrity increasing antimicrobial susceptibility. RNA sequencing also revealed a downregulation of *sufC* which is involved in iron-sulphur cluster synthesis [250]. Decreased activities of this enzyme have been shown to cause increased sensitivity to ROS and DNA damage in *S. aureus* [250]. As cinnamaldehyde's mechanism of action depends on generation of oxidative damage [194] this would explain the increase in sensitivity seen in this study. We also see that the largest fold decrease in gene expression after cinnamaldehyde exposure was *mexE* (efflux system). Multidrug efflux pumps have been shown to be able to transport AHL (QS molecules) out of the cell [251]. The mexEF operon is controlled by the global regulator MVAT which itself is activated by QS [283]. Constant inhibition of the QS signal may cause decreased expression of these transporters. With the cell less able to export antimicrobials, this could explain the increase in susceptibility.

In the cinnamaldehyde exposed isolate, a mutation in *proQ* was reported. *ProQ* encodes an RNA chaperone, which are proteins that aid in RNA folding, with significant RNA binding, strand exchange and duplexing activities [284]. RNA sequencing of EC958 indicated that *proQ* was downregulated after cinnamaldehyde exposure. *ProQ* has been shown to bind RNA to regulate transcription and prevent the degradation of mRNA, *proQ* deletion attenuated virulence in *Salmonella enterica* by disregulation of genes for chemotaxis, motility, and invasion [285]. We also observe downregulation of genes associated with chemotaxis (*cheA,R,W,Z*) and motility (flagella associated genes) in cinnamaldehyde exposed EC958.

Genome sequencing also revealed a mutation in *dnaX* (DNA polymerase III subunit tau). DNA polymerase III is a complex, multichain enzyme responsible for most of the replicative synthesis in bacteria [253]. *DnaX* is the promotor for *recR,* which encodes a protein involved in DNA repair [286] which was downregulated in EC958 after cinnamaldehyde exposure. The expression of *dnaK* (chaperone involved in DNA replication) was also downregulated. Furthermore, genes encoding proteins involved ribonucleotide and purine biosynthesis: uracil phosphoribosyltransferase (*upp*), CTP synthase (*pyrG*), carbamoyl-phosphate synthase (*carB*), adenylate kinase (*adk*) and

GMP synthase (*guaA*) were all downregulated. Each of the four antibiotics used in the cross resistance experiments act on DNA replication. As all of these genes are involved in DNA replication and synthesis, downregulation of these genes could confer resistance against these antibiotics because the active processes that the antibiotic is targeting is reduced. Cinnamaldehyde exposure induced 3 cases of antibiotic cross resistance although not in the EC958 isolate specifically so we cannot say for certain that this is a mechanism for antibiotic cross resistance in cinnamaldehyde exposed bacteria.

Cinnamaldehyde exposure induced a mutation in *ipd* which encodes dihydrolipoyl dehydrogenase. Dihydrolipoamide dehydrogenase is a bacterial enzyme that is part of the pyruvate dehydrogenase complex [287]. The pyruvate dehydrogenase complex converts pyruvate to acetyl-CoA to be used in the TCA cycle. Genes involved in the TCA cycle *gltA* (citrate synthase), *fumC* (fumarate hydratase II), and *sucA* (2-oxoglutarate dehydrogenase E1 component) were all upregulated. Cinnamaldehyde has been shown to interfere with the *E.coli* TCA cycle in previous studies [288] so the upregulation of these genes could be a response to this repression.

There was also a mutation in *tonB* which encodes the TONB protein. This is involved with the transport of iron-containing compounds and colicins into the cell and is a key virulence factor in UPEC [37]. RNA sequencing of the cinnamaldehyde exposed isolate revealed *tonB* expression was upregulated, the promoter region is located within the *tonB* gene [289] so it is possible that the mutation has affected the promotor region - causing the upregulation. Proteins associated with iron transport have been shown to be upregulated in cinnamaldehyde exposed *E.coli* previously [226]. It was hypothesised that induced uptake of iron would enhance microbial survival under stress conditions and contribute to microbial oxidative resistance (by sequestering free irons, which generate ROS). This study also reported decreased expression of genes associated with motility and biofilm formation [226]. We have also observed downregulation of flagella (*flgB,C,D,E,H,I,J,KL* and *fliA,D,F,G,H,J,K,L,M,N,P,S,T,Z)* in the cinnamaldehyde exposed isolate.

Biofilm formation in the cinnamaldehyde exposed strain increased when grown on a plastic surface (Table 5.2). Increased expression of *ag43*, as stated previously, would increase biofilm formation. Upregulation of *yfcV* was also observed in this isolate. *YfcV*

encodes a major fimbrial subunit and is an important virulence factor for UPEC [290]. Fimbriae are important for the initial formation of bacterial biofilms [291] so this could also explain an increase in biofilm formation.

The highest fold increase in expression was *garR* (2-hydroxy-3-oxopropionate reductase). This enzyme is involved in glyoxylate and dicarboxylate metabolism [292]. This increase in expression was also seen in the triclosan, furanone C30, and F-DPD exposed isolates. This means that in all of the QSI exposed strains *garR* had the highest increase in expression. As far as we are aware, there has been no reported between *garR* and quorum sensing.

In the cinnamaldehyde exposed isolate, 8 genes known to be controlled by AI-2 signaling [293] were shown to have altered expression. Genes that are upregulated by AI-2: *caiF* and *astD* were also upregulated after cinnamaldehyde exposure, and *motB* was downregulated after cinnamaldehyde exposure. Genes that are downregulated by AI-2: *cheW, fliP*, and *carB* were downregulated, but *uhpT* and *evgS* were upregulated after cinnamaldehyde exposure. It would be expected that inhibition of AI-2 signaling would upregulate expression of genes that would normally be downregulated by AI-2 and vice versa. This was seen in the cinnamaldehyde exposed isolate for some genes (*motB, uhpT*, and *evgS*) but we see the opposite in others (*caiF*, *astD*, *cheW*, *fliP*, and *carB*). *E.coli* do possess other QS pathways [294] so it could be that the genes that show the opposite of what we expected are also under the control of one of these pathways. Indeed, one of these genes, *astD* has been associated with being induced by indole signaling in *E.coli* [295]. *CheW* and *fliP* have also been shown to be downregulated by AI-2 inhibitors in previous studies [296].

5.6.6 Furanone C30 Exposure to furanone C30 induced high frequency of significant increases in susceptibility (Table 5.2). The highest fold decrease in gene expression for the furanone C30 exposed isolate was murein transglycosylase (*mltA*). Downregulation of this gene would lead to impaired cell wall formation, loss of integrity, difficulty in cell division [249]. This may cause increased susceptibility to antimicrobials.

The gene *secY* was downregulated after furanone C30 exposure. SECY supports the posttranslational translocation of proOmpA across the cytoplasmic membrane [297]. OmpA is also an important virulence factor in UPEC (it is an invasin and adhesin [259], and has been shown to be integral to IBC formation in bladder cells [298]). The

downregulation of ompA could explain the decreased pathogenicity observed in the furanone C30 exposed isolate (Table 5.2).

In the furanone C30 exposed isolate, 4 genes known to be controlled by AI-2 signaling [293] were shown to have altered expression. Genes that are upregulated by AI-2: *astD* were also upregulated after furanone C30 exposure. Genes that are downregulated by AI-2: *cspE*, *ivbL* and *carB* were downregulated after furanone C30 exposure. As previously stated, this is the opposite of what we would expect to observe during inhibition of AI-2 signaling. *AstD* is also controlled by indole signaling [295] but we couldn't find any literature that suggests the other genes are under the control of another quorum sensing system in *E.coli*.

5.6.7 F-DPD Exposure to F-DPD induced decreased biofilm formation for EC958 on catheter pieces (Table 5.2). We observed decreased expression of genes associated with flagella with the largest fold decrease in expression being flagellin, and there was downregulation of antigen 43 (*ag43*). All of these would explain the decrease in biofilm formation observed in EC958.

In the F-DPD exposed isolate, 4 genes known to be controlled by AI-2 signaling [293] were shown to have altered expression. Genes that are upregulated by AI-2: *motB* was downregulated after F-DPD exposure. Genes that are downregulated by AI-2: *cheW*, *fliP*, and *flgN* were downregulated after F-DPD exposure. *CheW*, *fliP*, and *flgN* have been shown to be downregulated by AI-2 inhibitors in previous studies [296]. In that study, it was postulated that the reduction of these motility associated genes explains the reduction in biofilm formation when AI-2 signaling is inhibited.

5.7.0 Conclusion

To understand the mechanisms of the phenotypic changes reported in previous chapters, one isolate (EC958) and the corresponding exposed strains, was subjected to genomic and transcriptomic analysis. This analysis has shown that long term exposure of UPEC to broad spectrum antimicrobials has an impact on UPEC resistance, virulence, motility, biofilm formation, and antibiotic resistance. Some of these changes can be beneficial in terms of a response to a catheter coating agent, whilst others could give cause for concern. It is important to fully understand and ellucidate these effects before developing a catheter coating for long-term catheterisation.

Chapter 6

General Discussion

6.1.0 Study Overview

Catheter associated urinary tract infections (CAUTIs) account for the highest proportion of hospital acquired infections (17.2%) [15] with between 43% and 56% of UTIs associated with an indwelling urethral catheter [15]. Uropathogenic *Escherichia coli* (UPEC) is reportedly responsible for 65% of complicated UTI cases [23]. CAUTI can lead to serious complications such as blood stream infections [14]. Currently *E. coli* is the leading cause of blood stream infection in the UK with 40,580 cases reported in 2016–17 and a mortality rate of 14.8% [17]. Of these cases, 21% are linked to the presence of an indwelling urinary catheter [17]. CAUTIs often show recalcitrance to antimicrobial treatment due to the formation of bacterial biofilms within the catheter in addition to the increasing prevalence of antibiotic resistance in uropathogens [3, 4].

In order to reduce the incidence of CAUTI approaches for the production of anti-infective catheter coatings have been developed including (i) surfaces containing antimicrobials that may be eluted into the surrounding environment [125] (ii) surfaces containing covalently bound antimicrobials [132] and (iii) surfaces coated in an anti-adhesive material to reduce bacterial attachment [118]. The advantage of using an anti-adhesive material is that it does not provide a selective pressure for antimicrobial resistant bacterial populations, however there are limited materials that can be effectively modified in this way and the non-specific deposition of host proteins during device insertion often provides sites for microbial attachment rendering the coating ineffective [119]. Covalently bound antimicrobials do not leach out over time, limiting cytotoxicity and reduces the creation of an antimicrobial gradient potentially selecting for resistance [132]. However, these coatings also become impaired due to host protein deposition and there are limitations in the number of antimicrobials that would have activity when covalently tethered to surfaces due to their structure. The controlled elution of antimicrobials is a currently considered strategy in preventing device associated infections as there is a wider availability of compounds that can be incorporated into coatings to be eluted out and avoid microbial colonisation [133].

Antimicrobial impregnated catheter coatings that are currently in clinical use include hydrogel silver alloy-coated latex catheters (CR Bard Inc.) and urethral catheters containing covalently bound nitrofurazone (Rochester Medical Corp) [114]. There have been numerous studies that have concluded the limited efficacy of these coated catheters

in preventing CAUTI, partially due to the emergence of insusceptible bacterial populations [113-115].

Biocides are often considered as anti-infective coating agents due to their broad-spectrum of antimicrobial activity and their multiple site-targeted mode of action [105], meaning the risk of selecting resistant microorganisms is comparatively low when compared to antibiotics. When biocide resistance does occur however, it has been associated with cross-resistance to third party agents such as other biocides and antibiotics [299]. Biocide exposure however often correlates with other functional deficits in bacteria such as impaired growth, reduced competitive fitness and pathogenicity [80] and even in some cases increased biocide susceptibility [73]. A novel approach in the production of anti-infective catheter coatings is to use quorum sensing inhibitors (QSIs). Quorum sensing (QS) is a process by which bacteria produce and detect signal molecules and thereby coordinate their behaviour in a cell density dependent manner [10]. The inhibition of quorum sensing as a strategy to prevent infection is a growing area of research but very little is known about the long term effects of QSIs in bacteria.

In this thesis, the long-term effects of biocide and QSI exposure were measured by subjecting clinical isolates and laboratory strains of UPEC (unexposed) to sustained antimicrobial challenge using a gradient plating system (exposed). This was done with each test antimicrobial. Control isolates, passaged in absence of antimicrobials, were also generated. After bacteria had undergone long-term antimicrobial exposure we evaluated a range of phenotypic effects. This included changes in antimicrobial susceptibility, biofilm formation and pathogenicity in a *Galleria mellonella* waxworm model.

After initial high- throughput screening of changes in biofilm formation via crystal violet assay we implemented a more realistic scenario whereby we determined changes in biofilm formation and biofilm metabolic activity on the surface of a urinary catheter. The capability of the bacterial isolates to invade human uroepithelial and bladder cell lines was also evaluated.

The project then focussed on developing polymer coatings containing antimicrobials and analysing the performance of these coatings in terms of antimicrobial efficacy and biocompatibility. The three coating candidates were Sol gel, Poly(ethylene glycol)

(PEG), and Poly(hydroxyethymethacrylate) (pHEMA). Once these coatings had been screened for their initial activity, the sol-gel coating was deemed the most effective, we then determined the antimicrobial activity of antimicrobial impregnated sol-gel coated urinary catheters in a Drip Flow Biofilm Reactor. The comprehensive screening of the test compounds and polymer coatings on UPEC in this study give a detailed overview of the suitability of these materials as anti-infective coatings for urinary catheters.

Following a detailed assessment of the phenotypic effects of biocide exposure, the final stage of the project was to investigate the underlying molecular mechanisms that govern such adaptations using full genome sequencing and RNA-sequencing in isolate EC958.

6.2.0 Changes in bacterial susceptibility, pathogenicity, and biofilm formation are induced after biocide and QSI exposure

Reduction in biocide susceptibility after bacterial exposure to antimicrobial agents such as biocides has become a growing concern especially considering the links to antibiotic cross-resistance [299]. In medical device coatings that contain biocides that a leachable into the surrounding environment this creates a gradient effect, which may expose the surrounding bacteria to sub-lethal biocide concentrations. This allows the bacteria to adapt to the presence of the antimicrobial which may induce insusceptibility in addition to other phenotypic changes. In this investigation, the changes in susceptibility of planktonic UPEC after long-term exposure to the test compounds were determined using MIC and MBC assays. PHMB exposure induced small magnitude (≤2-fold) increases in susceptibility in UPEC whilst triclosan induced a large frequency and magnitude of susceptibility decreases. Both BAC and silver nitrate only induced minor reductions in susceptibility. Exposure to cinnamaldehyde and furanone C30 induced high frequency of significant increases in susceptibility. For F-DPD, there was only one case of decreased susceptibility.

Genomic data can be utilised to identify potential mechanisms that contribute to our observed reductions in biocide susceptibility. Whole genome sequencing of the parent EC958 isolate and antimicrobial exposed isolates, revealed mutations in the triclosan target enzyme *fabI* that could be contributing to triclosan resistance [80]. The transcriptomic data also revealed possible mechanisms of increased susceptibility seen in the PHMB, cinnamaldehyde, and furanone C30 exposed isolates. The gene *mltA*

which is involved in peptidoglycan synthesis, was downregulated in the all of the aforementioned isolates which would lead to impairment of cell wall formation, the resulting loss of integrity may increase antimicrobial susceptibility. For the PHMB exposed isolate there was also an upregulation of peptidoglycan-binding protein *lysM*, these domain have multiple functions which include peptidoglycan degradation [269]. This would also contribute to loss of integrity of the cell wall increasing susceptibility.

It has been questioned whether bacteria can become resistant to QSI's and research has found that there are in fact numerous ways that bacteria can evolve to overcome QS inhibition such as: utilisation of multiple QS systems, efflux pumps, and mutation of QS system pathways [300]. There was only one case of increased resistance observed for F-DPD exposed EC34. RNA sequencing of F-DPD exposed EC958 revealed increased expression of *mepS*, a murein endopeptidase involved in peptidoglycan synthesis, and downregulation of *lysM* which would increase peptidoglycan synthesis and incorporation into the cell wall. The mechanism of F-DPD bactericidal activity is not currently know but common resistance mechanisms such as decreased cell wall permeability have been previously associated with reduced antimicrobial susceptibility and could explain the decreased susceptibility seen in this study.

Biofilm formation and susceptibility was assessed using crystal violet assay and MBEC assay. PHMB exposure led to a significant decrease in biofilm formation for two isolates which did not correspond with decreases in MBEC. All isolates that increased in biofilm formation after triclosan exposure also exhibited an elevation in MBEC. A high number of isolates were observed to form increased biofilm biomass after BAC exposure and 6 had a corresponding increase in MBEC. Silver nitrate exposure led to 1 increase in MBEC and 1 decrease, and 1 (non-corresponding) increase in biofilm formation. All isolates decreased in MBEC after cinnamaldehyde exposure which corresponded to 1/8 decreases in biofilm formation and 6/8 increased biofilm formation. For furanone C30 exposure, 6/8 decreased MBEC with 1 corresponding decrease in biofilm formation and a further 2 increases in biofilm formation. F-DPD did not induce any change in MBEC after exposure and induced only 1 increase in biofilm formation.

In terms of the underlying molecular mechanisms that govern our observed changes in biofilm formation, Antigen 43 (*ag43*) was upregulated after exposure to BAC and cinnamaldehyde which correlated with increased biofilm formation in these isolates.

Antigen 43 is a self-recognizing adhesin that is associated with cell aggregation and biofilm formation in *E. coli* K-12 [256]. An upregulation of this gene would likely confer increased biofilm formation to these isolates which is what we see here.

PHMB exposure induced significantly decreased relative pathogenicity in 3/8 isolates and a significant increase in pathogenicity for 1/8 in the *G. mellonella* model when compared to the respective control isolate (C12). When exposed to PHMB, 5/8 isolates showed an increase in SMC invasion. For HUEPC, exposure to PHMB induced increased invasion in 1/8 isolates. BAC exposure induced significantly decreased pathogenicity in 6/8 isolates and significantly increased pathogenicity in 1/8. Exposure to BAC induced an increase in invasion in 1/8 isolates for SMC and induced increases in HUEPC invasion for 2/8 isolates. Silver nitrate was the only biocide to only induce significant increases in pathogenicity which occurred in 2/8 isolates and 1/8 isolates showed increases in HUEPC invasion. Triclosan was the only biocide to induce only significant decreases in pathogenicity which occurred in 5/8 isolates. For HUEPC invasion, triclosan exposure induced increased invasion in 2/8 isolates. In the *G. mellonella* model cinnamaldehyde exposure induced significantly increased relative pathogenicity in 4/8 isolates and there was increased HUEPC invasion in 1/8 isolates. Furanone C30 was the only QSI to induce only significant decreases in pathogenicity in *G. mellonella* which occurred in 6/8 isolates. Furanone C30 exposure induced increased HUEPC invasion in EC34. F-DPD exposure induced significantly increased pathogenicity in 2/8 isolates and significantly decreased pathogenicity in 2/8 isolates in the *G. mellonella* model. F-DPD induced a decrease in SMC invasion in EC26 when compared to the respective control strain.

The decreased pathogenicity in the triclosan exposed isolate could be explained by the mutation in *wbbL* that is involved in O antigen biosynthesis which is an important virulence factor [255]. We did observe increase in expression of Type 1 fimbriae *fimA,C,D* in the triclosan exposed isolate EC958. Type 1 fimbriae are structures that are used by UPEC to attach and invade into cells [25]. So an increase in expression would be expected to potentially cause an increase in cell invasion, however, the EC958 isolate did not show increased invasion after triclosan exposure. In the cinnamaldehyde exposed strain EC958 there was an increased expression in *tonB* a key virulence factor [25]. Whilst it may be expected that this would correlate to increased pathogenicity,

EC958 did not increase in pathogenicity after cinnamaldehyde exposure. RNA sequencing of the furanone C30 exposed isolate revealed a decrease in expression of *secY*. *SecY* supports the posttranslational translocation of proOmpA across the cytoplasmic membrane [297]. OmpA is a very important UPEC virulence factor [298], it also acts as an adhesin and invasin [259] so this may explain the decreased pathogenicity seen after furanone C30 exposure.

When determining sensitivity to antibiotics there were 16 cases of antibiotic cross resistance observed. PHMB exposure induced 2 cases of cross resistance, triclosan induced 3, BAC induced 1, silver nitrate induced 1, cinnamaldehyde induced 3, furanone C30 induced 4, and F-DPD induced 2. Antimicrobial exposure induced increases in the transcription of numerous transporters including multidrug resistance transporters, *mdtE* in the PHMB exposed strain of EC958 and *marA* and *mdtN* for the cinnamaldehyde exposed strain of EC958. Out of the isolates that were sent for genetic sequencing, only the triclosan exposed strain EC958 acquired full cross resistance to an antibiotic (nitrofurantoin). Downregulation of *potE*, which has been shown to be involved in the uptake antibiotics into the cell [252], was observed in this isolate but this is not a resistance mechanism for this particular antibiotic.

On average, the QSI's induced more cases of cross-resistance than the biocides. Quorum sensing is thought to play a significant role in antibiotic tolerance of bacteria [301], inhibition of the AI-2 QS pathway by DPD analogues has been shown to increase rifampicin resistance by modulating LuxS mediated methylation of mutational hotspots [63]. In the RNA sequencing data downregulation of *aidB* (DNA alkylation response protein) was observed. Alkylation is another mechanism of DNA mutagenesis [302] so downregulation of this repair system could also possibly lead to cross resistance through increased mutation rate. In contrast, research by Brackman *et al.* [71] showed that use of QSI's increased the susceptibility of bacteria to antibiotics. However this was not long-term exposure but combination treatment and different quorum sensing systems were targeted (AHL and *agr* systems) so is not directly comparable to this study.

6.3.0 The effects of long term exposure to biocides and QSI's in a catheter biofilm model

When grown on a catheter surface, exposure to PHMB caused decreased biofilm formation in 4/8 isolates. When repeatedly exposed to BAC, 3/8 isolates demonstrated a significant decrease in biofilm formation. Silver Nitrate induced decreased biofilm formation in 3/8 isolates. Triclosan exposure decreased biofilm formation in 3/8 isolates and increased biofilm formation in 1/8 isolates. Biofilm formation in 2/8 isolates decreased when exposed to cinnamaldehyde and exposure to F-DPD induced decreased biofilm formation in 3/8 isolates. When exposed to furanone C30, 3/8 isolates showed a significant decrease in biofilm formation.

Impaired motility by downregulation of flagella associated genes occurred after exposure to PHMB, BAC, cinnamaldehyde and F-DPD. Flagella are an important factor in the initiation of bacterial biofilm formation [257] so loss of these structures would suggest that the ability of these isolates to form biofilms may be impaired.

The results for the biofilm formation on catheters differs from the biofilm formation experiments performed in 96 well plates (see above). The topography (the arrangement of physical features) of a surface has been shown to be an important factor in the ability of bacteria to attach to a surface and form biofilms [303]. In a study by Feng *et al.* *E.coli* were unable to form biofilms on surfaces with pores 15 - 25 nm in diameter [304]. The surface of a catheter would differ from a polystyrene plate which could explain the discrepancy in results. Another factor could be that the catheter pieces were transferred into fresh media after 24 hours. Thereby selecting the adhered bacterial populations and promoting biofilm growth, while the plate based assays were performed in batch culture. Having continuous supply of nutrients has been shown to significantly impact biofilm formation as opposed to limited nutrients, as traditionally found in batch culture [305].

6.4.0 Antimicrobial efficacy and biocompatibility of biocide and QSI containing polymer coatings for urinary catheters

Agar overlay and disc diffusion experiments were carried out to determine the overall biocompatibility of the antimicrobial agents when incorporated into three polymer coatings (sol gel, PEG, and pHEMA). On average, sol gel had the highest

biocompatibility values followed by PEG and pHEMA. Sol gel coatings are widely regarded as having a high degree of biocompatibility [233].

The order of cytotoxicity in relation to the compound concentration was silver nitrate > PHMB > F-DPD > BAC > cinnamaldehyde > triclosan > furanone C30. BI values for the eight isolates were averaged for each compound and the final ranked order of BI was PHMB > furanone C30 > cinnamaldehyde > triclosan > BAC > silver nitrate > F-DPD indicating the antiseptic potential of the compounds. When incorporated into the coatings these BI values changed to: furanone C30 > triclosan > silver nitrate > cinnamaldehyde > PHMB > BAC = F-DPD for sol gel, triclosan > cinnamaldehyde > PHMB > F-DPD > silver nitrate > BAC > furanone C30 for PEG, and triclosan > silver nitrate > BAC > PHMB = cinnamaldehyde = furanone C30 = F-DPD for pHEMA. This highlights the significant change in biocompatibility once the antimicrobials are changed from a planktonic suspension to a coated surface.

The polymer coatings will have a variety of physio-chemical properties (e.g. hydrophilicity or hydrophobicity, lubricity, smoothness, surface energy, wettability, surface roughness, swelling, electrostatic effects, solubility, degradability, thermal and mechanical stability [306]) that would all affect the biocompatibility of the coating even without the addition of the antimicrobial agents. How antimicrobials elute out of the coating would also make a difference. For example pHEMA hydrogels initially elute the majority of incorporated antimicrobial when first hydrated [220], whereas PEG and sol gel coatings both have a sustained release profile, sustained release is associated with higher biocompatibility, as you are not introducing a high concentration of antimicrobial in a short time frame [235]. As sol gel had the highest biocompatibility values of the three coatings, it was taken forward for further evaluation on the drip flow biofilm reactor.

The order of antimicrobial efficacy for the biofilm reactor in terms of reduction in biofilm growth was found to be PHMB > furanone C30 > silver nitrate > F-DPD > cinnamaldehyde > BAC > triclosan. This was intriguing as, up to this point, triclosan was performing as one of the most potent antimicrobials. It could be hypothesised that due to the fact that triclosan is a relatively small molecule that it eluted out of the sol gel in a short period of time and was washed away within the drip flow reactor, allowing any residual bacteria to repopulate. This highlights the importance of selecting a release strategy that complements the antimicrobial being incorporated.

It is well understood that as a biofilm matures antimicrobial susceptibility decreases. A previous study comparing biofilm eradication with antibiotics in 96 well plate and biofilm reactor conditions revealed that in biofilm reactor, bacteria were significantly more tolerant to antibiotics than in the well plate [305]. It was concluded that the main reason for this difference was the presence or absence of flow of nutrients to the biofilm [305]. Continuous fresh nutrients would allow the biofilm to continue to develop and would facilitate the removal of waste products. The fluid dynamics of our test systems may also have an effect: *P. aeruginosa* biofilms treated with cationic surfactant cetyltrimethylammonium bromide (CTAB) that were formed under laminar flow were more susceptible than those formed under turbulent flow [307]. Experiments with the drip flow biofilm reactor can produce varied data depending on environmental conditions e.g. biofilms of mono-culture grew in single layers whereas multi-species biofilms grew in multilayers [308]. It is clear that choosing the right experimental model with conditions closest to the clinical environment is incredibly important when evaluating anti-infective coatings for medical devices.

6.5.0 Future Directions

Although this study comprises a fairly comprehensive overview of the long term effects of the antimicrobial coatings tested, there is still much that could be explored. More detailed insight into the impact of antimicrobial exposure on bacteria could be obtained through proteomic analysis of the unexposed and exposed isolates selected for during this study. This would complement our transcriptional analysis and allow us to determine if the changes in gene expression that we observed translated into changes in protein expression. This would give information of the mechanisms that render the bacteria less susceptible towards an antimicrobial agent, but also of any other induced changes in the bacteria seen in this study. Similarly, there are a number of genes identified in this study that warrant further investigation. Notably the upregulation of antigen 43 in numerous biocide exposed isolates correlating to changes in biofilm formation is an interesting phenomenon. Antigen 43 has also been linked to increased virulence in UPEC [256]. A more detailed investigation of role of antigen 43 in antimicrobial adaptation and the consequence of this on bacterial virulence, potentially through use of site-directed mutagenesis, would be an area for future work.

Inductively coupled plasma mass spectrometry (ICP-MS) can be used to measure the elution of the antimicrobials out of the polymer coatings; this will provide valuable insight into the mechanism of elution and the antimicrobial lifespan of the coatings. By understanding the elution profiles of our antimicrobials we would be able to manipulate their release through changes in the sol-gel formulation and thereby maximise their activity.

Once the antimicrobial sol-gel coatings have been optimised, it would be interesting to more fully evaluate their anti-biofilm activity. Transfecting the UPEC isolates with a GFP plasmid would enable visualisation of the bacteria on the surface of coated catheter sections via confocal microscopy; this would give us more information about the efficacy of the coatings and their impact on biofilm architecture.

Comparing the potential synergistic activity of the biocides and QSIs could provide beneficial data. By incorporating both agents into the device surface we may be able to disrupt biofilm formation allowing eradication of any residual bacteria at relatively lower biocide concentrations, thus avoiding any cytotoxic effects of the biocides which may be observed at biofilm eradication concentrations.

The *in vivo* efficacy of any medically coated device would need to be evaluated, both in animal models and clinical trials, if the coating is to be used as a commercial product. *In vitro* susceptibility testing, whilst giving a good indication of bacterial response, is simplified and does not take into account the vast array of physiological conditions experienced during infection. Catheter infection models have already been developed in mice [309] so this would be something that could be taken further. Also, the experiments carried out in this study were carried out using only single isolates of UPEC and CAUTI is frequently associated with a mixed flora and may involve multiple interactions between microorganisms that cannot be accounted for in this type of assessment therefore experiments using mixed bacterial communities should be carried out.

6.6.0 Conclusion

Uropathogenic *E.coli* (UPEC) are the major causative agent of CAUTI which are becoming an increasing burden on healthcare providers due to antibiotic resistance and an aging population. Anti-infective coatings to prevent formation of bacterial biofilm on

the surface of the catheter are in clinical use but have limited effectiveness. The short-lived efficacy of these coatings are in part likely to be associated with the induction of biocide insusceptibility in bacterial pathogens. New coatings that display good antimicrobial efficacy and low cytotoxicity should be developed but the long-term impact of these coatings needs to be adequately assessed. The effects of long term exposure of UPEC to 7 antimicrobials (both biocides and QSIs) was determined. Multiple phenotypic adaptations were observed both in planktonic and biofilm growth and corroborated using genotypic and transcriptomic analysis. Furthermore, three polymers were evaluated for their potential as a catheter coating and evaluated using a biofilm reactor model.

Whilst reductions in antimicrobial susceptibility were evident, this was often coupled to other phenotypic effects including changes in biofilm formation and pathogenicity. This demonstrates the importance in both choosing appropriate methods to evaluate anti-infective coatings and highlights a need to take a multi-faceted approach to risk assessment when predicting their long-term consequence in patients.

Acknowledgements

Thank you to the BMRC for funding the project.

Thank you to my Director of Studies Dr Sarah Forbes for all of your help and advice. Your organisation and commitment to the project has been a real inspiration. I have really enjoyed my PhD and a lot of that is down to you. You have taught me that 'science has many colours'.

Thank you to my supervisors Dr Mel Lacey and Prof Tom Smith for your support and words of wisdom.

Thank you to the Microbiology Research Group for asking questions and answering them.

Thank you to the technical staff who have helped me in the lab too many times to count.

Thank you to my friends and colleagues at the BMRC, you have made these last few years amazing and an experience I will remember forever.

Thank you to my family, I would never have been able to do this without you.

References

1. **Abrams P, Cardozo L, Fall M, Griffiths D, Rosier P et al.** The standardisation of terminology of lower urinary tract function: report from the Standardisation Sub-committee of the International Continence Society. *Neurourology and urodynamics* 2002;21(2):167-178.
2. **Wilde MH, McMahon JM, McDonald MV, Tang W, Wang W et al.** Self-Management Intervention for Long-Term Indwelling Urinary Catheter Users: Randomized Clinical Trial. *Nurs Res* 2015;64(1):24-34.
3. **Colli J, Tojuola B, Patterson AL, Ledbetter C, Wake RW**. National trends in hospitalization from indwelling urinary catheter complications, 2001–2010. *International Urology and Nephrology* 2016;46(2):303-308.
4. **Renwick MJ, Brogan DM, Mossialos E**. A systematic review and critical assessment of incentive strategies for discovery and development of novel antibiotics. *The Journal of antibiotics* 2016;69(2):73-88.
5. **Bjarnsholt T, Denmark KUKN, Denmark KUKN**. The role of bacterial biofilms in chronic infections. *APMIS* 2016;121(s136):1-58.
6. **Balcazar JL, Subirats J, Borrego CM**. The role of biofilms as environmental reservoirs of antibiotic resistance. *Front Microbiol* 2015;6:1216.
7. **Paulus W**. *Microbicides for the protection of materials: yesterday, today, and tomorrow*. London: Elsevier Applied Science Publishers; 1991.
8. **Johnson JR, Kuskowski MA, Wilt TJ**. Systematic Review: Antimicrobial Urinary Catheters To Prevent Catheter-Associated Urinary Tract Infection in Hospitalized Patients. *Annals of Internal Medicine* 2016;144(2):116-126.
9. **Forbes S, Knight CG, Cowley NL, Amezquita A, McClure P et al.** Variable Effects of Exposure to Formulated Microbicides on Antibiotic Susceptibility in *Firmicutes* and *Proteobacteria*. *Applied and environmental microbiology* 2016;82(12):3591-3598.
10. **Brackman G, Coenye T**. Quorum sensing inhibitors as anti-biofilm agents. *Current pharmaceutical design* 2015;21(1):5-11.
11. **Stamm WE, Norrby SR**. Urinary tract infections: disease panorama and challenges. *J infect dis* 2001;183(1):S1-S4.
12. **The Medical Technology Group**. *NHS could slash emergency admission costs with better use of medical technology*. Leading medical practitioners, patient groups, and industry leaders join Virendra Sharma MP in call to Government to tackle issue. Media Release 2015. p. 1.
13. **Smyth ET, McIlvenny G, Enstone JE, Emmerson AM, Humphreys H et al.** Four country healthcare associated infection prevalence survey 2006: overview of the results. *J Hosp Infect* 2008;69(3):230-248.
14. **Gould CV, Umscheid CA, Agarwal RK, Kuntz G, Pegues DA**. Guideline for prevention of catheter-associated urinary tract infections 2009. *Infection control and hospital epidemiology* 2010;31(4):319-326.
15. **Plowman R, Graves N, Esquivel J, Roberts JA**. An economic model to assess the cost and benefits of the routine use of silver alloy coated urinary catheters to reduce the risk of urinary tract infections in catheterized patients. *J Hosp Infect* 2001;48(1):33-42.
16. **Loveday HP, Wilson JA, Pratt RJ, Golsorkhi M, Tingle A et al.** epic3: national evidence-based guidelines for preventing healthcare-associated infections in NHS hospitals in England. *J Hosp Infect* 2014;86 Suppl 1:S1-70.

17. **Jones LF, Meyrick, J., Bath, J., Dunham, O., McNulty, C.A.M.** Effectiveness of behavioural interventions to reduce urinary tract infections and *Escherichia coli* bacteraemia for older adults across all care settings: a systematic review. *J Hosp Infect* 2018.
18. **Getliffe K, Newton, T.** Catheter-associated urinary tract infection in primary and community health care. *Age Ageing* 2006;35(5):477-481.
19. **National Institute for Health and Care Excellence**. *NICE Quality Standard [QS90]*. Urinary tract infection in adults 2015.
20. **Dewar S, Reed LC, Koerner RJ**. Emerging clinical role of pivmecillinam in the treatment of urinary tract infection in the context of multidrug resistant bacteria. *J antimicrob chemother* 2013;69(2):303-308.
21. **Stapleton A**. Novel mechanism of p-fimbriated *Escherichia coli* virulence in pyelonephritis. *J am soc nephrol* 2005;16(12):3458-3460.
22. **Kucheria R, Dasgupta P, Sacks SH, Khan MS, Sheerin NS**. Urinary tract infections: new insights into a common problem. *Postgraduate medical journal* 2005;81(952):83-86.
23. **Flores-Mireles AL, Walker JN, Caparon M, Hultgren SJ**. Urinary tract infections: epidemiology, mechanisms of infection and treatment options. *Nature reviews Microbiology* 2015;13(5):269-284.
24. **Goering RV, Dockrell HM, Zuckerman M, Roitt IM, Chiodini PL**. *Mim's Medical Microbiology*, 5 ed. Edinburgh: Elsevier Saunders; 2013.
25. **Terlizzi ME, Gribaudo, G., Maffei, M.E.** UroPathogenic *Escherichia coli* (UPEC) Infections: Virulence Factors, Bladder Responses, Antibiotic, and Non-antibiotic Antimicrobial Strategies. *Front Microbiol* 2017;15(8).
26. **Greene SE, Hibbing ME, Janetka J, Chen SL, Hultgren SJ**. Human urine decreases function and expression of type 1 pili in uropathogenic *Escherichia coli*. *Mbio* 2015;6(4):1-9.
27. **Thanassi DG, Bliska JB, Christie PJ**. Surface organelles assembled by secretion systems of gram negative bacteria: diversity in structure and function. *Microbiol Rev* 2012;36:1046-1082.
28. **Dodson KW, Pinkner JS, Rose T, Magnusson G, Hultgren SJ et al.** Structural basis of the interaction of the pyelonephritic *E.coli* adhesion to its human kidney receptor.Structural basis of the interaction of the pyelonephritic *E.coli* adhesion to its human kidney receptor. *Cell* 2001;105(6):733-743.
29. **Kallenius G, Mollby R, Svenson SB, Helin I, Hultberg H et al.** Occurance of P-fimbriated *E.coli* in urinary tract infections. *Lancet* 1981;2:1369-1372.
30. **Taylor-Whiteley TR, Le Maitre, C.L., Duce, J.A., Dalton, C.F., Smith, D.P.** Recapitulating Parkinson's disease pathology in a three-dimensional human neural cell culture model. *Dis Model Mech* 2019;12(4).
31. **Barnhart MM, Chapman, M.R.** Curli biogenesis and function. *Annu Rev Microbiol* 2006;60:131-147.
32. **Wright KJ, Seed, P.C., Hultgren, S.J.** Uropathogenic *Escherichia coli* flagella aid in efficient urinary tract colonization. *Infect Immun* 2005;73(11):7657-7668.
33. **Aguiniga LM, Yaggie, R.E., Schaeffer, A.J., Klumpp, D.J.** Lipopolysaccharide Domains Modulate Urovirulence. *Infect Immun* 2016;84(11):3131-3140.
34. **Ellis TN, Kuehn, M.J.** Virulence and immunomodulatory roles of bacterial outer membrane vesicles. *Microbiol Mol Biol Rev* 2010;74(1):81-94.
35. **Wiles TJ, Kulesus, R.R., Mulvey, M.A.** Origins and Virulence Mechanisms of Uropathogenic *Escherichia coli*. *Exp Mol Pathol* 2008;85(1):11-19.

36. **Skaar EP**. The battle for iron between bacterial pathogens and their vertebrate hosts. *PLoS pathogens* 2010;6(8):e1000949.
37. **Torres AG, Redford, P., Welch, R.A., Payne, S.M.** TonB-dependent systems of uropathogenic *Escherichia coli*: aerobactin and heme transport and TonB are required for virulence in the mouse. *Infect Immun* 2001;69(10):6179-6185.
38. **Klausen M, Aaes-Jorgensen A, Molin S, Tolker-Nielsen T**. Involvement of bacterial migration in the development of complex multicellular structures in *Pseudomonas aeruginosa* biofilms. *Molecular microbiology* 2003;50(1):61-68.
39. **Klausen M, Heydorn A, Ragas P, Lambertsen L, Aaes-Jorgensen A et al.** Biofilm formation by *Pseudomonas aeruginosa* wild type, flagella and type IV pili mutants. *Molecular microbiology* 2003;48(6):1511-1524.
40. **Gonzalez MJ, Robino L, Iribarnegaray V, Zunino P, Scavone P**. Effect of different antibiotics on biofilm produced by uropathogenic *Escherichia coli* isolated from children with urinary tract infection. *Pathogens and disease* 2017;75(4).
41. **Anderson GG, Palermo JJ, Schilling JD, Roth R, Heuser J et al.** Intracellular bacterial biofilm-like pods in urinary tract infections. *Science (New York, NY)* 2003;301(5629):105-107.
42. **Manefield M, Turner SL**. Quorum sensing in context: out of molecular biology and into microbial ecology. *Microbiology (Reading, England)* 2002;148(Pt 12):3762-3764.
43. **Papenfort K, Bassler, B.** Quorum-Sensing Signal-Response Systems in Gram-Negative Bacteria. *Nature reviews Microbiology* 2016;14(9):576-588.
44. **Li Z, Nair, S.K.** Quorum sensing: How bacteria can coordinate activity and synchronize their response to external signals? *Protein Sci* 2012;21(10):1403-1417.
45. **Van Houdt R, Aertsen, A., Moons, P., Vanoirbeek, K., Michiels, C.W.** N-acyl-L-homoserine lactone signal interception by *Escherichia coli*. *FEMS Microbiol Lett* 2006;256(1):83-89.
46. **Kendall MM, Sperandio, V.** Cell-to-cell signaling in *E. coli* and *Salmonella*. *EcoSal Plus* 2014;6(1).
47. **Hardie KR, Heurlier K**. Establishing bacterial communities by 'word of mouth': LuxS and autoinducer 2 in biofilm development. *Nature reviews Microbiology series vol. 8)*. England 2008. pp. 635-643.
48. **Gonzalez Barrios AF, Zuo R, Hashimoto Y, Yang L, Bentley WE et al.** Autoinducer 2 controls biofilm formation in *Escherichia coli* through a novel motility quorum-sensing regulator (MqsR, B3022). *Journal of bacteriology* 2006;188(1):305-316.
49. **Pereira CS, Thompson JA, Xavier KB**. AI-2-mediated signalling in bacteria. *FEMS microbiology reviews* 2013;37(2):156-181.
50. **Safari M, Amache R, Esmaeilishirazifard E, Keshavarz T**. Microbial metabolism of quorum-sensing molecules acyl-homoserine lactones, gamma-heptalactone and other lactones. *Applied microbiology and biotechnology* 2014;98(8):3401-3412.
51. **Roberts ME, Stewart PS**. Modeling antibiotic tolerance in biofilms by accounting for nutrient limitation. *Antimicrob Agents Chemother* 2004;48(1):48-52.
52. **Borriello G, Werner E, Roe F, Kim AM, Ehrlich GD et al.** Oxygen limitation contributes to antibiotic tolerance of *Pseudomonas aeruginosa* in biofilms. *Antimicrob Agents Chemother* 2004;48(7):2659-2664.
53. **Donlan RM, Costerton JW**. Biofilms: survival mechanisms of clinically relevant microorganisms. *Clin Microbiol Rev* 2002;15(2):167-193.

54. **Walters MC, 3rd, Roe F, Bugnicourt A, Franklin MJ, Stewart PS**. Contributions of antibiotic penetration, oxygen limitation, and low metabolic activity to tolerance of *Pseudomonas aeruginosa* biofilms to ciprofloxacin and tobramycin. *Antimicrob Agents Chemother* 2003;47(1):317-323.
55. **Allesen-Holm M, Barken KB, Yang L, Klausen M, Webb JS et al.** A characterization of DNA release in *Pseudomonas aeruginosa* cultures and biofilms. *Molecular microbiology* 2006;59(4):1114-1128.
56. **Conibear TC, Collins SL, Webb JS**. Role of mutation in *Pseudomonas aeruginosa* biofilm development. *PloS one* 2009;4(7):e6289.
57. **Wood TK, Knabel, S.J., Kwan, B.W.** Bacterial Persister Cell Formation and Dormancy. *Applied and environmental microbiology* 2013;79(23):7116-7121.
58. **Lewis K**. Persister cells and the riddle of biofilm survival. *Biochemistry (Mosc)* 2005;70(2):267-274.
59. **Stickler DJ**. Bacterial biofilms in patients with indwelling urinary catheters. *Nature clinical practice Urology* 2008;5(11):598-608.
60. **Hentzer M, Givskov M**. Pharmacological inhibition of quorum sensing for the treatment of chronic bacterial infections. *The Journal of clinical investigation* 2003;112(9):1300-1307.
61. **Shen G, Rajan R, Zhu J, Bell CE, Pei D**. Design and synthesis of substrate and intermediate analogue inhibitors of S-ribosylhomocysteinase. *Journal of medicinal chemistry* 2006;49(10):3003-3011.
62. **Zhang M, Jiao XD, Hu YH, Sun L**. Attenuation of *Edwardsiella tarda* virulence by small peptides that interfere with LuxS/autoinducer type 2 quorum sensing. *Applied and environmental microbiology* 2009;75(12):3882-3890.
63. **Krasovec R, Belavkin RV, Aston JA, Channon A, Aston E et al.** Mutation rate plasticity in rifampicin resistance depends on *Escherichia coli* cell-cell interactions. *Nature communications* 2014;5:3742.
64. **Neiditch MB, Federle MJ, Miller ST, Bassler BL, Hughson FM**. Regulation of LuxPQ receptor activity by the quorum-sensing signal autoinducer-2. *Molecular cell* 2005;18(5):507-518.
65. **Roy V, Meyer MT, Smith JA, Gamby S, Sintim HO et al.** AI-2 analogs and antibiotics: a synergistic approach to reduce bacterial biofilms. *Applied microbiology and biotechnology* 2013;97(6):2627-2638.
66. **Manefield M, Rasmussen TB, Henzter M, Andersen JB, Steinberg P et al.** Halogenated furanones inhibit quorum sensing through accelerated LuxR turnover. *Microbiology (Reading, England)* 2002;148(Pt 4):1119-1127.
67. **Ren D SJ, Wood TK**. Inhibition of biofilm formation and swarming of *Escherichia coli* by (5Z)-4-bromo-5-(bromomethylene)-3-butyl-2(5H)-furanone. *Environ Microbiol* 2001;3(11):731-736.
68. **Vestby LK JK, Witsø IL, Habimana O, Scheie AA, Urdahl AM, Benneche T, Langsrud S, Nesse LL**. Synthetic brominated furanone F202 prevents biofilm formation by potentially human pathogenic *Escherichia coli* O103:H2 and *Salmonella ser. Agona* on abiotic surfaces. *Journal of applied microbiology* 2014;116(2):258-268.
69. **Ren D BL, Ye RW, Thomas SM, Wood TK**. Differential gene expression shows natural brominated furanones interfere with the autoinducer-2 bacterial signaling system of *Escherichia coli*. *Biotechnol Bioeng* 2004;88(5):630-642.
70. **Brackman G DT, Miyamoto C, Bossier P, Van Calenbergh S, Nelis H, Coenye T**. Cinnamaldehyde and cinnamaldehyde derivatives reduce virulence in *Vibrio spp*. by decreasing the DNA-binding activity of the quorum sensing response regulator LuxR. *BMC Microbiol* 2008;8:149.

71. **Brackman G, Cos P, Maes L, Nelis HJ, Coenye T**. Quorum sensing inhibitors increase the susceptibility of bacterial biofilms to antibiotics *in vitro* and *in vivo*. *Antimicrob Agents Chemother* 2011;55(6):2655-2661.
72. **Knapp L, Amezquita A, McClure P, Stewart S, Maillard JY**. Development of a protocol for predicting bacterial resistance to microbicides. *Applied and environmental microbiology* 2015;81(8):2652-2659.
73. **Moore LE, Ledder RG, Gilbert P, McBain AJ**. *In vitro* study of the effect of cationic biocides on bacterial population dynamics and susceptibility. *Applied and environmental microbiology* 2008;74(15):4825-4834.
74. **Gilbert P, Pemberton D, Wilkinson DE**. Synergism within polyhexamethylene biguanide biocide formulations. *The Journal of applied bacteriology* 1990;69(4):593-598.
75. **Gilbert P, Moore LE**. Cationic antiseptics: diversity of action under a common epithet. *Journal of applied microbiology* 2005;99(4):703-715.
76. **Gilbert P, Das JR, Jones MV, Allison DG**. Assessment of resistance towards biocides following the attachment of micro-organisms to, and growth on, surfaces. *Journal of applied microbiology* 2001;91(2):248-254.
77. **McDonnell G, Russell AD**. Antiseptics and disinfectants: activity, action, and resistance. *Clin Microbiol Rev* 1999;12(1):147-179.
78. **Regös J, Hitz, H.R.** Investigations on the mode of action of Triclosan, a broad spectrum antimicrobial agent. *Zentralbl Bakteriol Orig A* 1974;226(3):390-401.
79. **Heath RJ, Rubin JR, Holland DR, Zhang E, Snow ME et al.** Mechanism of triclosan inhibition of bacterial fatty acid synthesis. *The Journal of biological chemistry* 1999;274(16):11110-11114.
80. **Forbes S, Latimer J, Bazaid A, McBain AJ**. Altered Competitive Fitness, Antimicrobial Susceptibility, and Cellular Morphology in a Triclosan-Induced Small-Colony Variant of *Staphylococcus aureus*. *Antimicrob Agents Chemother* 2015;59(8):4809-4816.
81. **Levy CW, Roujeinikova A, Sedelnikova S, Baker PJ, Stuitje AR et al.** Molecular basis of triclosan activity. *Nature* 1999;398(6726):383-384.
82. **Phan TN, Marquis RE**. Triclosan inhibition of membrane enzymes and glycolysis of *Streptococcus mutans* in suspensions and biofilms. *Canadian journal of microbiology* 2006;52(10):977-983.
83. **McDonnell GE**. *Antisepsis, Disinfection, and Sterilization: Types, Action, and Resistance*. Washington, DC.: ASM Press; 2007.
84. **Gerba CP**. Quaternary Ammonium Biocides: Efficacy in Application. *Appl Environ Microbiol* 2015;81(2):464-469.
85. **Minnock A, Vernon DI, Schofield J, Griffiths J, Parish JH et al.** Mechanism of Uptake of a Cationic Water-Soluble Pyridinium Zinc Phthalocyanine across the Outer Membrane of *Escherichia coli*. *Antimicrob Agents Chemother series vol. 3)* 2000. pp. 522-527.
86. **Jung WK, Koo HC, Kim KW, Shin S, Kim SH et al.** Antibacterial Activity and Mechanism of Action of the Silver Ion in *Staphylococcus aureus* and *Escherichia coli*. *Applied and environmental microbiology* 2008;74(7).
87. **Bragg PD, Rainnie DJ**. The effect of silver ions on the respiratory chain of *Escherichia coli*. *Canadian journal of microbiology* 1974;20(6):883-889.
88. **Schreurs WJ, Rosenberg H**. Effect of silver ions on transport and retention of phosphate by *Escherichia coli*. *Journal of bacteriology* 1982;152(1):7-13.

89. **YakabeYoshikuni, SanoTakayuki, UshioHidetoshi, YasunagaTatsuya**. Kinetic studies of the interaction between silver ion and deoxyribonucleic acid. *Chemistry Letters*, research-article 2006;9(4):373-376.
90. **Prabhu S, Poulose, E.K.** Silver nanoparticles: mechanism of antimicrobial action, synthesis, medical applications, and toxicity effects. *Int nano lett* 2012;2(32).
91. **Furr JR, Russell AD, Turner TD, Andrews A**. Antibacterial activity of Actisorb Plus, Actisorb and silver nitrate. *J Hosp Infect* 1994;27(3):201-208.
92. **Maillard JY, Bloomfield S, Coelho JR, Collier P, Cookson B et al.** Does microbicide use in consumer products promote antimicrobial resistance? A critical review and recommendations for a cohesive approach to risk assessment. *Microbial drug resistance (Larchmont, NY)* 2013;19(5):344-354.
93. **Yu BJ, Kim JA, Ju HM, Choi SK, Hwang SJ et al.** Genome-wide enrichment screening reveals multiple targets and resistance genes for triclosan in *Escherichia coli*. *Journal of microbiology (Seoul, Korea)* 2012;50(5):785-791.
94. **Chuanchuen R, Beinlich K, Hoang TT, Becher A, Karkhoff-Schweizer RR et al.** Cross-Resistance between Triclosan and Antibiotics in*Pseudomonas aeruginosa* Is Mediated by Multidrug Efflux Pumps: Exposure of a Susceptible Mutant Strain to Triclosan Selects nfxB Mutants Overexpressing MexCD-OprJ. *Antimicrob agents chemother* 2001;4(2).
95. **Allen MJ, White GF, Morby AP**. The response of *Escherichia coli* to exposure to the biocide polyhexamethylene biguanide. *Microbiology (Reading, England)* 2006;152(Pt 4):989-1000.
96. **Forbes S, Cowley N, Humphreys G, Mistry H, Amezquita A et al.** Formulation of Biocides Increases Antimicrobial Potency and Mitigates the Enrichment of Nonsusceptible Bacteria in Multispecies Biofilms. *Applied and environmental microbiology* 2017;83(7).
97. **Bragg R, Jansen, A., Coetzee, M., van der Westhuizen, W., Boucher, C.** Bacterial resistance to Quaternary Ammonium Compounds (QAC) disinfectants. *Adv Exp Med Biol* 2014;808:1-13.
98. **Zou L, Meng, J., McDermott, P.F., Wang, F., Yang, Q., Cao, G., Hoffmann, M., Zhao, S.** Presence of disinfectant resistance genes in *Escherichia coli* isolated from retail meats in the USA. *J Antimicrob Chemother* 2014;69(10):2644-2649.
99. **Bore E, Hebraud M, Chafsey I, Chambon C, Skjaeret C et al.** Adapted tolerance to benzalkonium chloride in *Escherichia coli K-12* studied by transcriptome and proteome analyses. *Microbiology (Reading, England)* 2007;153(Pt 4):935-946.
100. **Mc Cay PH, Ocampo-Sosa, A.A., Fleming, G.T.** Effect of subinhibitory concentrations of benzalkonium chloride on the competitiveness of *Pseudomonas aeruginosa* grown in continuous culture. *Microbiology* 2010;156:30-38.
101. **Elkrewi E, Randall CP, Ooi N, Cottell JL, O'Neill AJ**. Cryptic silver resistance is prevalent and readily activated in certain Gram-negative pathogens. *J Antimicrob Chemother* 2017;72(11):3043-3046.
102. **Sutterlin S, Dahlo M, Tellgren-Roth C, Schaal W, Melhus A**. High frequency of silver resistance genes in invasive isolates of *Enterobacter* and *Klebsiella* species. *J Hosp Infect* 2017;96(3):256-261.
103. **Randall CP, Gupta A, Jackson N, Busse D, O'Neill AJ**. Silver resistance in Gram-negative bacteria: a dissection of endogenous and exogenous mechanisms. *J Antimicrob Chemother series vol. 4)* 2015. pp. 1037-1046.
104. **Latimer J, Forbes S, McBain AJ**. Attenuated virulence and biofilm formation in *Staphylococcus aureus* following sublethal exposure to triclosan. *Antimicrob Agents Chemother* 2012;56(6):3092-3100.

105. **Cowley NL, Forbes S, Amezquita A, McClure P, Humphreys GJ et al.** Effects of Formulation on Microbicide Potency and Mitigation of the Development of Bacterial Insusceptibility. *Applied and environmental microbiology* 2015;81(20):7330-7338.
106. **Grover N, Plaks JG, Summers SR, Chado GR, Schurr MJ et al.** Acylase-containing polyurethane coatings with anti-biofilm activity. *Biotechnol Bioeng* 2016;113(12):2535-2543.
107. **LaSarre B, Federle, M.J.** Exploiting quorum sensing to confuse bacterial pathogens. *Microbiol Mol Biol Rev* 2013;77(1):73-111.
108. **Gaonkar TA, Sampath LA, Modak SM**. Evaluation of the antimicrobial efficacy of urinary catheters impregnated with antiseptics in an *in vitro* urinary tract model. *Infection control and hospital epidemiology* 2003;24(7):506-513.
109. **Bayston R, Fisher LE, Weber K**. An antimicrobial modified silicone peritoneal catheter with activity against both Gram-positive and Gram-negative bacteria. *Biomaterials* 2009;30(18):3167-3173.
110. **Jones GL, Russell AD, Caliskan Z, Stickler DJ**. A strategy for the control of catheter blockage by crystalline *Proteus mirabilis* biofilm using the antibacterial agent triclosan. *European urology* 2005;48(5):838-845.
111. **Zodrow KR SJ, Elimelech M**. Biodegradable polymer (PLGA) coatings featuring cinnamaldehyde and carvacrol mitigate biofilm formation. *Langmuir* 2012;28(39):13993-13999.
112. **Nostro A SR, D'Arrigo M, Botta L, Filocamo A, Marino A, Bisignano G**. Study on carvacrol and cinnamaldehyde polymeric films: mechanical properties, release kinetics and antibacterial and antibiofilm activities. *Applied microbiology and biotechnology* 2012;96(4):1029-1038.
113. **Jacobsen SM, Stickler DJ, Mobley HLT, Shirtliff ME**. Complicated Catheter-Associated Urinary Tract Infections Due to *Escherichia coli* and *Proteus mirabilis*. *Clin Microbiol Rev series vol. 1)* 2008. pp. 26-59.
114. **Pickard R, Lam T, Maclennan G, Starr K, Kilonzo M et al.** Types of urethral catheter for reducing symptomatic urinary tract infections in hospitalised adults requiring short-term catheterisation: multicentre randomised controlled trial and economic evaluation of antimicrobial- and antiseptic-impregnated urethral catheters (the CATHETER trial). *Health technology assessment (Winchester, England)* 2012;16(47):1-197.
115. **Desai DG, Liao KS, Cevallos ME, Trautner BW**. Silver or Nitrofurazone Impregnation of Urinary Catheters Has a Minimal Effect on Uropathogen Adherence. *J Urol* 2010;184(6):2565-2571.
116. **Li XZ, Nikaido H, Williams KE**. Silver-resistant mutants of *Escherichia coli* display active efflux of Ag+ and are deficient in porins. *Journal of bacteriology* 1997;179(19):6127-6132.
117. **Darouiche R, Smith J, Hanna H, Dhabuwala C, Steiner M et al.** Efficacy of antimicrobial-impregnated bladder catheters in reducing catheter-associated bacteriuria: prospective, randomised, multicentre clinical trial. *Urology* 1999;54:976-981.
118. **Hetrick EM, Schoenfisch, M.H.** Reducing implant-related infections: active release strategies. *Chem Soc Rev* 2006;35(9):780-789.
119. **Kingshott P, Wei, J., Bagge-Ravn, D., Gadegaard, N., Gram, L.** Covalent Attachment of Poly(ethylene glycol) to Surfaces, Critical for Reducing Bacterial Adhesion. *Langmuir* 2003;19(17):6912-6921.
120. **Nejadnik MR, van der Mei, H.C., Norde, W., Busscher, H.J.** Bacterial adhesion and growth on a polymer brush-coating. *Biomaterials* 2008;29(30):4117-4121.

121. **Furno F, Morley, KS., Wong, B., Sharp, BL., Arnold, PL., Howdle, SM., Bayston, R., Brown, PD., Winship, PD., Reid, HJ.** Silver nanoparticles and polymeric medical devices: a new approach to prevention of infection? *J Antimicrob Chemother* 2004;54(6):1019-1024.
122. **Stigter M, Bezemer, J., de Groot, K., Layrolle, P.** Incorporation of different antibiotics into carbonated hydroxyapatite coatings on titanium implants, release and antibiotic efficacy. *J Control Release* 2004;99(1):127-137.
123. **Nablo B, Prichard, HL., Butler, RD., Klitzman, B., Schoenfisch, MH.** Inhibition of implant-associated infections via nitric oxide release. *Biomaterials* 2005;26(34):6984-6990.
124. **Rojas I, Slunt, JB., Grainger, DW.** Polyurethane coatings release bioactive antibodies to reduce bacterial adhesion. *J Control Release* 2000;63(1-2):175-189.
125. **Schierholz J, Steinhauser, H., Rump, AF., Berkels, R., Pulverer, G.** Controlled release of antibiotics from biomedical polyurethanes: morphological and structural features. *Biomaterials* 1997;18(12):839-844.
126. **Kwok C, Horbett, TA., Ratner, BD.** Design of infection-resistant antibiotic-releasing polymers. II. Controlled release of antibiotics through a plasma-deposited thin film barrier. *J Control Release* 1999;62(3):301-311.
127. **Yenice I, Caliş, S., Atilla, B., Kaş, HS., Ozalp, M., Ekizoğlu, M., Bilgili, H., Hincal, AA.** *In vitro*/*in vivo* evaluation of the efficiency of teicoplanin-loaded biodegradable microparticles formulated for implantation to infected bone defects. *J Microencapsul* 2003;20(6):705-717.
128. **Massè A, Bruno, A., Bosetti, M., Biasibetti, A., Cannas, M., Gallinaro, P.** Prevention of pin track infection in external fixation with silver coated pins: clinical and microbiological results. *J Biomed Mater Res* 2000;53(5):600-604.
129. **Yu D, Lin, WC., Yang, MC.** Surface modification of poly(L-lactic acid) membrane via layer-by-layer assembly of silver nanoparticle-embedded polyelectrolyte multilayer. *Bioconjug Chem* 2007;18(5):1521-1529.
130. **Dayyoub E, Frant, M., Pinnapireddy, SR., Liefeith, K., Bakowsky, U.** Antibacterial and anti-encrustation biodegradable polymer coating for urinary catheter. *Int J Pharm* 2017;531(1):205-214.
131. **Langmuir I**. The Arrangement of Electrons in Atoms and Molecules. *J Am Chem Soc* 1919;41(6):868–934.
132. **Chen C, Jing, RY., Wickstrom, E.** Covalent Attachment of Daptomycin to Ti6Al4V Alloy Surfaces by a Thioether Linkage to Inhibit Colonization by *Staphylococcus aureus*. *ACS Omega* 2017;2(4):1645-1652.
133. **Hume EB, Baveja, J., Muir, B., Schubert, T.L., Kumar, N., Kjelleberg, S., Griesser, H.J., Thissen, H., Read, R., Poole-Warren, L.A., Schindhelm, K., Willcox, M.D.** The control of *Staphylococcus epidermidis* biofilm formation and *in vivo* infection rates by covalently bound furanones. *Biomaterials* 2004;25(20):5023-5030.
134. **Anjum S, Singh, S., Benedicte, L., Roger, P., Panigrahi, M., Gupta, B.** Biomodification Strategies for the Development of Antimicrobial Urinary Catheters: Overview and Advances. *Global Challenges* 2018;2:1700068.
135. **Gottenbos B, van der Mei, HC., Klatter, F., Nieuwenhuis, P., Busscher, HJ.** *In vitro* and *in vivo* antimicrobial activity of covalently coupled quaternary ammonium silane coatings on silicone rubber. *Biomaterials* 2002;23(6):1417-1423.
136. **Johnson J, Berggren, T., Conway, AJ.** Activity of a nitrofurazone matrix urinary catheter against catheter-associated uropathogens. *Antimicrob Agents Chemother* 1993;37(9):2033-2036.

137. **Ahmed EM**. Hydrogel: Preparation, characterization, and applications: A review. *J Adv Res* 2015;6(2):105-121.
138. **Vimala K, Samba Sivudu, K., Murali Mohan, Y.,Sreedhar, B., Mohana Raju, K.** Controlled silver nanoparticles synthesis in semi-hydrogel networks of poly(acrylamide) and carbohydrates: A rational methodology for antibacterial application. *Carbohydr Polym* 2009;75(3):463-471.
139. **Mohan YM, Lee, K., Premkumar, T., Geckeler, K.E**. Hydrogel networks as nanoreactors: A novel approach to silver nanoparticles for antibacterial applications. *Polymer* 2007;48(1):158-164.
140. **Ahearn DG, Grace, D.T., Jennings, M.J., Borazjani, R.N., Boles, K.J., Rose, L.J., Simmons, R.B., Ahanotu, E.N.** Effects of hydrogel/silver coatings on *in vitro* adhesion to catheters of bacteria associated with urinary tract infections. *Current microbiology* 2000;41(2):120-125.
141. **Asmatulu R**. Nanocoatings for corrosion protection of aerospace alloys. *Corrosion Protection and Control Using Nanomaterials (Woodhead Publishing Series in Metals and Surface Engineering*: Woodhead Publishing; 2012. pp. 357-374.
142. **Wang D, Bierwagen, G.P.** Sol–gel coatings on metals for corrosion protection. *prog org coat* 2009;64(4):327-338.
143. **Nablo BJ, Rothrock, A.R., Schoenfisch, M.H.** Nitric oxide-releasing sol–gels as antibacterial coatings for orthopedic implants. *Biomaterials* 2005;26(8):917-924.
144. **Parker V, Giles M, Graham L, Suthers B, Watts W et al.** Avoiding inappropriate urinary catheter use and catheter-associated urinary tract infection (CAUTI): a pre-post control intervention study. *BMC Health Serv Res* 2017;17(314).
145. **Sharma G, Sharma S, Sharma P, Chandola D, Dang S et al.** *Escherichia coli* biofilm: development and therapeutic strategies. *Journal of applied microbiology* 2016;121(2):309-319.
146. **Lewis K**. Multidrug tolerance of biofilms and persister cells. *Current topics in microbiology and immunology* 2008;322:107-131.
147. **Wazait HD, Patel HR, Veer V, Kelsey M, Van Der Meulen JH et al.** Catheter-associated urinary tract infections: prevalence of uropathogens and pattern of antimicrobial resistance in a UK hospital (1996-2001). *BJU international* 2003;91(9):806-809.
148. **Forbes S, Dobson CB, Humphreys GJ, McBain AJ**. Transient and sustained bacterial adaptation following repeated sublethal exposure to microbicides and a novel human antimicrobial peptide. *Antimicrob Agents Chemother* 2014;58(10):5809-5817.
149. **Lu J, Jin M, Nguyen SH, Mao L, Li J et al.** Non-antibiotic antimicrobial triclosan induces multiple antibiotic resistance through genetic mutation. *Environment international* 2018;118:257-265.
150. **McMurry LM, Oethinger M, Levy SB**. Overexpression of marA, soxS, or acrAB produces resistance to triclosan in laboratory and clinical strains of *Escherichia coli*. *FEMS Microbiol Lett* 1998;166(2):305-309.
151. **Muller G, Kramer A**. Biocompatibility index of antiseptic agents by parallel assessment of antimicrobial activity and cellular cytotoxicity. *J Antimicrob Chemother* 2008;61(6):1281-1287.
152. **McBain AJ, Ledder RG, Moore LE, Catrenich CE, Gilbert P**. Effects of Quaternary-Ammonium-Based Formulations on Bacterial Community Dynamics and Antimicrobial Susceptibility. *Applied and environmental microbiology* 2004;70(6):3449-3456.

153. **Peleg AY, Monga D, Pillai S, Mylonakis E, Moellering RC, Jr. et al.** Reduced susceptibility to vancomycin influences pathogenicity in *Staphylococcus aureus* infection. *J Infect Dis* 2009;199(4):532-536.
154. **BSI**. *Chemical disinfectants and antiseptics. Quantitative suspension test for the evaluation of basic bactericidal activity of chemical disinfectants and antiseptics. Test method and requirements (phase 1).* BS EN 1040:2005: BSI; 16 January 2006.
155. **Andrews JM, BSAC Working Party on Susceptibility Testing ft**. BSAC standardized disc susceptibility testing method. *Journal of Antimicrobial Chemotherapy* 2017;48(suppl_1):43-57.
156. **Miller K, O'Neill AJ, Chopra I**. Response of *Escherichia coli* hypermutators to selection pressure with antimicrobial agents from different classes. *J Antimicrob Chemother* 2002;49(6):925-934.
157. **Lambert RJ, Joynson J, Forbes B**. The relationships and susceptibilities of some industrial, laboratory and clinical isolates of *Pseudomonas aeruginosa* to some antibiotics and biocides. *Journal of applied microbiology* 2001;91(6):972-984.
158. **Fraise AP**. Biocide abuse and antimicrobial resistance--a cause for concern? *J Antimicrob Chemother* 2002;49(1):11-12.
159. **McMurry LM, Oethinger M, Levy SB**. Triclosan targets lipid synthesis. *Nature* 1998;394(6693):531-532.
160. **Kim M HJ, Weigand MR, Krishnan R, Pavlostathis SG, Konstantinidis KT**. Genomic and Transcriptomic Insights into How Bacteria Withstand High Concentrations of Benzalkonium Chloride Biocides. *Applied and environmental microbiology* 2018;84(12).
161. **Choudhury RM, S.K.** Generic transcriptional response of *E. coli* to stress. *bioRxiv* 2015.
162. **Champlin FR, Ellison ML, Bullard JW, Conrad RS**. Effect of outer membrane permeabilisation on intrinsic resistance to low triclosan levels in *Pseudomonas aeruginosa*. *International journal of antimicrobial agents* 2005;26(2):159-164.
163. **Gaonkar TA, Caraos L, Modak S**. Efficacy of a silicone urinary catheter impregnated with chlorhexidine and triclosan against colonization with *Proteus mirabilis* and other uropathogens. *Infection control and hospital epidemiology* 2007;28(5):596-598.
164. **Poole K**. Bacterial stress responses as determinants of antimicrobial resistance. *J Antimicrob Chemother* 2012;67(9):2069-2089.
165. **Roberts ME, Stewart PS**. Modelling protection from antimicrobial agents in biofilms through the formation of persister cells. *Microbiology (Reading, England)* 2005;151(1):75-80.
166. **Machado I, Lopes SP, Sousa AM, Pereira MO**. Adaptive response of single and binary *Pseudomonas aeruginosa* and *Escherichia coli* biofilms to benzalkonium chloride. *Journal of basic microbiology* 2012;52(1):43-52.
167. **Niba ET, Naka Y, Nagase M, Mori H, Kitakawa M**. A genome-wide approach to identify the genes involved in biofilm formation in *E. coli*. *DNA research : an international journal for rapid publication of reports on genes and genomes* 2007;14(6):237-246.
168. **Curiao T, Marchi E, Viti C, Oggioni MR, Baquero F et al.** Polymorphic variation in susceptibility and metabolism of triclosan-resistant mutants of *Escherichia coli* and *Klebsiella pneumoniae* clinical strains obtained after exposure to biocides and antibiotics. *Antimicrob Agents Chemother* 2015;59(6):3413-3423.

169. **Gilbert P, Allison DG, McBain AJ**. Biofilms *in vitro* and *in vivo*: do singular mechanisms imply cross-resistance? *Symposium series (Society for Applied Microbiology)* 2002(31):98s-110s.
170. **Mulley G, Jenkins AT, Waterfield NR**. Inactivation of the antibacterial and cytotoxic properties of silver ions by biologically relevant compounds. *PloS one* 2014;9(4):e94409.
171. **Wei L, Tang J, Zhang Z, Chen Y, Zhou G et al.** Investigation of the cytotoxicity mechanism of silver nanoparticles *in vitro*. *Biomedical materials (Bristol, England)* 2010;5(4):044103.
172. **Singh RP, Ramarao P**. Cellular uptake, intracellular trafficking and cytotoxicity of silver nanoparticles. *Toxicology Letters* 2012;213(2):249-259.
173. **Rembe JD, Fromm-Dornieden C, Schafer N, Bohm JK, Stuermer EK**. Comparing two polymeric biguanides: chemical distinction, antiseptic efficacy and cytotoxicity of polyaminopropyl biguanide and polyhexamethylene biguanide. *Journal of medical microbiology* 2016;65(8):867-876.
174. **Deutschle T, Porkert U, Reiter R, Keck T, Riechelmann H**. *In vitro* genotoxicity and cytotoxicity of benzalkonium chloride. *Toxicology in vitro : an international journal published in association with BIBRA* 2006;20(8):1472-1477.
175. **Brinster S, Lamberet G, Staels B, Trieu-Cuot P, Gruss A et al.** Type II fatty acid synthesis is not a suitable antibiotic target for Gram-positive pathogens. *Nature* 2009;458(7234):83-86.
176. **Teplova VV, Belosludtsev KN, Kruglov AG**. Mechanism of triclosan toxicity: Mitochondrial dysfunction including complex II inhibition, superoxide release and uncoupling of oxidative phosphorylation. *Toxicology Letters* 2017;275:108-117.
177. **Zuckerbraun HL, Babich H, May R, Sinensky MC**. Triclosan: cytotoxicity, mode of action, and induction of apoptosis in human gingival cells in vitro. *European journal of oral sciences* 1998;106(2 Pt 1):628-636.
178. **Bazaid AS, Forbes S, Humphreys GJ, Ledder RG, O'Cualain R et al.** Fatty Acid Supplementation Reverses the Small Colony Variant Phenotype in Triclosan-Adapted *Staphylococcus aureus*: Genetic, Proteomic and Phenotypic Analyses. *Scientific reports* 2018;8(1):3876.
179. **Chew BH, Cadieux PA, Reid G, Denstedt JD**. *In-Vitro* Activity of Triclosan-Eluting Ureteral Stents against Common Bacterial Uropathogens. *Journal of Endourology*, research-article 2006;20(11):949-958.
180. **Melican K, Sandoval RM, Kader A, Josefsson L, Tanner GA et al.** Uropathogenic *Escherichia coli* P and Type 1 fimbriae act in synergy in a living host to facilitate renal colonization leading to nephron obstruction. *PLoS pathogens* 2011;7(2):e1001298.
181. **Vogt J, Schulz GE**. The structure of the outer membrane protein OmpX from *Escherichia coli* reveals possible mechanisms of virulence. *Structure (London, England : 1993)* 1999;7(10):1301-1309.
182. **Pagedar A, Singh J, Batish VK**. Adaptation to benzalkonium chloride and ciprofloxacin affects biofilm formation potential, efflux pump and haemolysin activity of *Escherichia coli* of dairy origin. *The Journal of dairy research* 2012;79(4):383-389.
183. **Dodson KW, Pinkner JS, Rose T, Magnusson G, Hultgren SJ et al.** Structural basis of the interaction of the pyelonephritic *E.coli* adhesion to its human kidney receptor. *Cell* 2001;105(6):733-743.
184. **Forbes S, Morgan, N., Humphreys, G.J., Amézquita, A., Mistry, H., McBain, A.J.** Loss of function in *Escherichia coli* exposed to environmentally relevant

concentrations of benzalkonium chloride. *Applied and environmental microbiology* 2019;85:e02417-02418.
185. **Saulou-Bérion C, Gonzalez, I., Enjalbert, B., Audinot, J.N., Fourquaux, I., Jamme, F., Cocaign-Bousquet, M., Mercier-Bonin, M., Girbal, L.** *Escherichia coli* under Ionic Silver Stress: An Integrative Approach to Explore Transcriptional, Physiological and Biochemical Responses. *PloS one* 2015;10(12).
186. **LeClerc JE LB, Payne WL, Cebula TA**. High mutation frequencies among *Escherichia coli* and *Salmonella* pathogens. *Science (New York, NY)* 1996;274(5290):1208-1211.
187. **MacIntyre CR, Bui, C.M.** Pandemics, public health emergencies and antimicrobial resistance - putting the threat in an epidemiologic and risk analysis context. *Arch Public Health* 2017;75(54).
188. **Firmino DF, Cavalcante, T.T.A., Gomes, G.A., Firmino, N.C.S., Rosa, L.D., de Carvalho, M.G., Catunda, F.E.A. Jr.** Antibacterial and Antibiofilm Activities of Cinnamomum Sp. Essential Oil and Cinnamaldehyde: Antimicrobial Activities. *ScientificWorldJournal* 2018:2018:7405736.
189. **Ren D, Bedzyk, L.A., Setlow, P., England, D.F., Kjelleberg, S., Thomas, S.M., Ye, R.W., Wood, T.K.** Differential gene expression to investigate the effect of (5Z)-4-bromo- 5-(bromomethylene)-3-butyl-2(5H)-furanone on *Bacillus subtilis*. *Applied and environmental microbiology* 2004;70(8):4941-4949.
190. **Amalaradjou MA NA, Baskaran SA, Venkitanarayanan K**. Antibiofilm effect of trans-cinnamaldehyde on uropathogenic *Escherichia coli*. *J Urol* 2010;184(1):358-363.
191. **Guo JL, Li, B.Z., Chen, W.M., Sun, P.H., Wang, Y.** Synthesis of Substituted 1H-Pyrrol-2(5H)-ones and 2(5H)-Furanones as Inhibitors of *P. aeruginosa* Biofilm. *Lett drug des discov* 2009;6(2).
192. **Kadirvel M FF, Forbes S, McBain A, Gardiner JM, Brown GD, Freeman S**. Inhibition of quorum sensing and biofilm formation in *Vibrio harveyi* by 4-fluoro-DPD; a novel potent inhibitor of signalling. *Chem Commun (Camb)* 2014;50(39):5000-5002.
193. **Henly E, Dowling, JAR., Maingay, JB., Lacey, MM., Smith TJ., Forbes, S.** Biocide Exposure Induces Changes in Susceptibility, Pathogenicity and Biofilm Formation in Uropathogenic *Escherichia coli*. *Antimicrob Agents Chemother* 2019;63(3).
194. **He TF WL, Niu DB, Wen QH, Zeng XA**. Cinnamaldehyde inhibit *Escherichia coli* associated with membrane disruption and oxidative damage. *Arch Microbiol* 2018.
195. **He TF ZZ, Zeng XA, Wang LH, Brennan CS**. Determination of membrane disruption and genomic DNA binding of cinnamaldehyde to *Escherichia coli* by use of microbiological and spectroscopic techniques. *J Photochem Photobiol B* 2018;178:623-630.
196. **Worthington RJ, Richards, J.J., Melander, C.** Small molecule control of bacterial biofilms. *Org Biomol Chem* 2012;10(37):7457-7474.
197. **Visvalingam J H-DJ, Holley RA**. Examination of the genome-wide transcriptional response of *Escherichia coli O157:H7* to cinnamaldehyde exposure. *Applied and environmental microbiology* 2013;79(3):942-950.
198. **Defoirdt T MC, Wood TK, Meighen EA, Sorgeloos P, Verstraete W, Bossier P**. The natural furanone (5Z)-4-bromo-5-(bromomethylene)-3-butyl-2(5H)-furanone disrupts quorum sensing-regulated gene expression in *Vibrio harveyi* by decreasing the DNA-binding activity of the transcriptional regulator protein luxR. *Environ Microbiol* 2007;9(10):2486-2495.

199. **Zhao J CW, He X, Liu Y, Li J, Sun J, Li J, Wang F, Gao Y**. Association of furanone C-30 with biofilm formation & antibiotic resistance in *Pseudomonas aeruginosa*. *Indian J Med Res* 2018;147(4):400-406.
200. **Lu Lv TJ, Shenghua Zhang, Xin Yu**. Exposure to Mutagenic Disinfection Byproducts Leads to Increase of Antibiotic Resistance in *Pseudomonas aeruginosa*. *Environ Sci Technol* 2014;48(14):8188-8195.
201. **Roy V MM, Smith JA, Gamby S, Sintim HO, Ghodssi R, Bentley WE**. AI-2 analogs and antibiotics: a synergistic approach to reduce bacterial biofilms. *Appl Microbiol Biotechnol* 2013;97(6):2627-2638.
202. **Ahmed NA, Petersen, F.C., Scheie, A.A.** AI-2 quorum sensing affects antibiotic susceptibility in *Streptococcus anginosus*. *J Antimicrob Chemother* 2007;60(1):49-53.
203. **Zhang JH, Liu, L.Q., He, Y.L., Kong, W.J., Huang S.A.** Cytotoxic effect of trans-cinnamaldehyde on human leukemia K562 cells. *Acta Pharmacol Sin* 2010;31(7):861-866.
204. **Ueda S, Masutani, H., Nakamura, H., Tanaka, T., Ueno, M., Yodoi, J.** Redox control of cell death. *Antioxid Redox Signal* 2002;4(3):405-414.
205. **K. Murakami MH, T. Makino, M. Yoshino**. Prooxidant action of furanone compounds: Implication of reactive oxygen species in the metal-dependent strand breaks and the formation of 8-hydroxy-2′-deoxyguanosine in DNA. *Food Chem Toxicol* 2007;45(7):1258-1262.
206. **Antunes LC, Ferreira, R.B., Buckner, M.M., Finlay, B.B.** Quorum sensing in bacterial virulence. *Microbiology (Reading, England)* 2010;156(2271-82).
207. **Hentzer M, Wu H, Andersen JB, Riedel K, Rasmussen TB et al.** Attenuation of *Pseudomonas aeruginosa* virulence by quorum sensing inhibitors. *The EMBO journal* 2003;22(15):3803-3815.
208. **Defoirdt T CR, Wood TK, Sorgeloos P, Verstraete W, Bossier P**. Quorum sensing-disrupting brominated furanones protect the gnotobiotic brine shrimp *Artemia franciscana* from pathogenic *Vibrio harveyi*, *Vibrio campbellii*, and *Vibrio parahaemolyticus* isolates. *Applied and environmental microbiology* 2006;72(9):6419-6423.
209. **Defoirdt T, Bossier, P., Sorgeloos, P., Verstraete, W.** The impact of mutations in the quorum sensing systems of *Aeromonas hydrophila*, *Vibrio anguillarum* and *Vibrio harveyi* on their virulence towards gnotobiotically cultured *Artemia franciscana*. *Environ Microbiol* 2005;7(8):1239-1247.
210. **Duan K DC, Stein J, Rabin H, Surette MG**. Modulation of *Pseudomonas aeruginosa* gene expression by host microflora through interspecies communication. *Molecular microbiology* 2003;50(5):1477-1491.
211. **Amalaradjou MA, Narayanan A, Venkitanarayanan K**. Trans-cinnamaldehyde decreases attachment and invasion of uropathogenic *Escherichia coli* in urinary tract epithelial cells by modulating virulence gene expression. *J Urol* 2011;185(4):1526-1531.
212. **Schwartz K, Stephenson, R., Hernandez, M., Jambang, N., Boles, B.R.** The use of drip flow and rotating disk reactors for *Staphylococcus aureus* biofilm analysis. *J Vis Exp* 2010(46):pii: 2470.
213. **Goeres DM, Hamilton, M.A., Beck, N.A., Buckingham-Meyer, K., Hilyard, J.D., Loetterle, L.R., Lorenz, L.A., Walker, D.K., Stewart, P.S.** A method for growing a biofilm under low shear at the air-liquid interface using the drip flow biofilm reactor. *Nat Protoc* 2009;4(5):783-788.

214. **Nweze EI, Ghannoum A, Chandra J, Ghannoum MA, Mukherjee PK**. Development of a 96-well catheter-based microdilution method to test antifungal susceptibility of *Candida* biofilms. *J Antimicrob Chemother* 2012;67(1):149-153.
215. **International Organisation for Standardisation**. *Biological evaluation of medical devices*. Part 5: Tests for *in vitro* cytotoxicity2010.
216. **Brooks T, Keevil, CW.** A simple artificial urine for the growth of urinary pathogens. *Letters in applied microbiology* 1997;24(3):203-206.
217. **Plowman R**. The socioeconomic burden of hospital acquired infection. *Euro surveill* 1999;5(4):4.
218. **Johnson JR, Johnston BD, Kuskowski MA, Pitout J**. *In vitro* activity of available antimicrobial coated Foley catheters against *Escherichia coli*, including strains resistant to extended spectrum cephalosporins. *J Urol* 2010;184(6):2572-2577.
219. **Lin CC, Anseth, K.S.** PEG hydrogels for the controlled release of biomolecules in regenerative medicine. *Pharm Res* 2009;26(3):631-643.
220. **Anderson EM, Noble, M.L., Garty, S., Ma, H., Bryers, J.D., Shen, T.T., Ratner, B.D.** Sustained release of antibiotic from poly(2-hydroxyethyl methacrylate) to prevent blinding infections after cataract surgery. *Biomaterials* 2009;30(29):5675.
221. **Czarnobaj K**. Preparation and Characterization of Silica Xerogels as Carriers for Drugs. *Drug Delivery* 2008;15(8):485-492.
222. **Eduok U, Suleiman, R., Gittens, J., Khaled, M., Smith, T.J., Akid, R., Alia, B.E., Khalil, A.** Anticorrosion/antifouling properties of bacterial spore-loaded sol–gel type coating for mild steel in saline marine condition: a case of thermophilic strain of *Bacillus licheniformis*. *RSC Advances* 2015;5(114).
223. **Bedran TB, Grignon, L., Spolidorio, D.P., Grenier, D.** Subinhibitory concentrations of triclosan promote *Streptococcus mutans* biofilm formation and adherence to oral epithelial cells. *PloS one* 2014;9(2):e89059.
224. **Suchanek VM**. *Role of Motility and its Regulation in Escherichia coli Biofilm formation*. University of Heidelberg; 2017.
225. **Singh N, Paknikar, K.M., Rajwade, J.** RNA-sequencing reveals a multitude of effects of silver nanoparticles on *Pseudomonas aeruginosa* biofilms. *Environ sci nano* 2019(6):1812-1828.
226. **Yuan WS, Z.J. Kohli, G.S. Yang, L. Yuk, H.G.** Stress Resistance Development and Genome-Wide Transcriptional Response of *Escherichia coli O157:H7* Adapted to Sublethal Thymol, Carvacrol, and trans-Cinnamaldehyde. *Applied and environmental microbiology* 2018;84(22):e01616-01618.
227. **Tavender TJ, Halliday, N.M., Hardie, K.R., Winzer, K.** LuxS-independent formation of AI-2 from ribulose-5-phosphate. *BMC Microbiol* 2008;8:98.
228. **Altman F**. Tetrazolium salts and formazans. *Prog Histochem Cytochem* 1976;9(3):1-56.
229. **Williams GJ SD**. Effect of triclosan on the formation of crystalline biofilms by mixed communities of urinary tract pathogens on urinary catheters. *Journal of medical microbiology* 2008;57(9):1135-1140.
230. **Jones GL MC, O'Reilly M, Stickler DJ**. Effect of triclosan on the development of bacterial biofilms by urinary tract pathogens on urinary catheters. *J Antimicrob Chemother* 2006;57(3):266-272.
231. **Lenahan M SÁ, Morris D, Duffy G, Fanning S, Burgess CM**. Transcriptomic analysis of triclosan-susceptible and -tolerant *Escherichia coli O157:H19* in response to triclosan exposure. *Microbial drug resistance (Larchmont, NY)* 2014;20(2):91-103.
232. **Russell AD, Hugo, W.B.** Antimicrobial activity and action of silver. *Prog Med Chem* 1994;31:351-370.

233. **Owens GJ, Singh, R.K., Foroutan, F., Alqaysi, M., Han, C.M., Mahapatra, C., Kim, H.W., Knowles, J.C.** Sol–gel based materials for biomedical applications. *Prog Mater Sci* 2016;77:1-79.
234. **Caló E, Khutoryanskiy, V.V.** Biomedical applications of hydrogels: A review of patents and commercial products. *Eur Polym J* 2015;65:252-267.
235. **Zhang P, Han, F., Li, Y., Chen, J., Chen, T., Zhi, Y., Jiang, J., Lin, C., Chen, S., Zhao, P.** Local delivery of controlled-release simvastatin to improve the biocompatibility of polyethylene terephthalate artificial ligaments for reconstruction of the anterior cruciate ligament. *Int J Nanomedicine* 2016;11:465-478.
236. **Kohane DS, Langer, R.** Biocompatibility and drug delivery systems. *Chem Sci* 2010;1:441-446.
237. **Cyphert EL, von Recum, H.A.** Emerging technologies for long-term antimicrobial device coatings: advantages and limitations. *Exp Biol Med (Maywood)* 2017;242(8):788-798.
238. **Zhang Q, Xia, Y.F., Hong, J.M.** Mechanism and toxicity research of benzalkonium chloride oxidation in aqueous solution by H2O2/Fe(2+) process. *Environ Sci Pollut Res Int* 2016;23(17):17822-17830.
239. **Zanini S, Polissi, A., Maccagni, E.A., Dell'Orto, E.C., Liberatore, C., Riccardi, C.** Development of antibacterial quaternary ammonium silane coatings on polyurethane catheters. *J Colloid Interface Sci* 2015;451:78-84.
240. **Baveja JK, Willcox, M.D., Hume, E.B., Kumar, N., Odell, R., Poole-Warren, L.A.** Furanones as potential anti-bacterial coatings on biomaterials. *Biomaterials* 2004;25(20):5003-5012.
241. **Zhi ZS, Y., Xi, Y., Tian, L., Xu, M., Wang, Q., Pandidan., Padidan, S., Li, P., Huang, W.** Dual-Functional Polyethylene Glycol-b-polyhexanide Surface Coating with *in Vitro* and *in Vivo* Antimicrobial and Antifouling Activities. *ACS Appl Mater Interfaces* 2017;9(12):10383-10397.
242. **Nicolle LE**. Catheter associated urinary tract infections. *Antimicrob Resist Infect Control* 2014;3:23.
243. **Forde BM, Ben Zakour, N.L., Stanton-Cook, M., Phan, M.D., Totsika, M., Peters, K.M., Chan, K.G., Schembri, M.A., Upton, M., Beatson, S.A.** The complete genome sequence of *Escherichia coli* EC958: a high quality reference sequence for the globally disseminated multidrug resistant *E. coli O25b:H4-ST131* clone. *PLoS One* 2014;9(8):e104400.
244. **Petty NK, Ben Zakour, N.L., Stanton-Cook, M., Skippington, E., Totsika, M., Forde, B.M., Phan, M.D., Gomes Moriel, D., Peters, K.M., Davies, M., Rogers, B.A., Dougan, G., Rodriguez-Baño, J., Pascual, A., Pitout, J.D., Upton, M., Paterson, D.L., Walsh, T.R., Schembri, M.A., Beatson, S.A.** Global dissemination of a multidrug resistant *Escherichia coli clone*. *Proc Natl Acad Sci U S A* 2014;111(15):5694-5699.
245. **Bolger AM, Lohse, M., Usadel, B.** Trimmomatic: a flexible trimmer for Illumina sequence data. *Bioinformatics* 2014;30(15):2114-2120.
246. **Bankevich A, Nurk, S., Antipov, D., Gurevich, A.A., Dvorkin, M., Kulikov, A.S., Lesin, V.M., Nikolenko, S., Pham, S., Prjibelski, A.D., Pyshkin, A.V., Sirotkin, A.V., Vyahhi, N., Tesler, G., Alekseyev, M.A., Pevzner, P.A.** SPAdes: a new genome assembly algorithm and its applications to single-cell sequencing. *J Comput Biol* 2012;19(5):455-477.
247. **Seemann T**. Prokka: rapid prokaryotic genome annotation. *Bioinformatics* 2014;30(14):2068-2069.

248. **Mi H, Muruganujan, A., Ebert, D., Huang, X., Thomas, P.D**. PANTHER version 14: more genomes, a new PANTHER GO-slim and improvements in enrichment analysis tools. *Nucleic Acids Res* 2019;47(D1):D419-D426.
249. **van Straaten KE, Dijkstra, B.W., Vollmer, W., Thunnissen, A.M.** Crystal structure of MltA from *Escherichia coli* reveals a unique lytic transglycosylase fold. *J Mol Biol* 2005;352(5):1068-1080.
250. **Roberts CA, Al-Tameemi, H.M., Mashruwala, A.A., Rosario-Cruz, Z., Chauhan, U., Sause, W.E., Torres, V.J., Belden, W.J., Boyd, J.M.** The Suf Iron-Sulfur Cluster Biosynthetic System Is Essential in *Staphylococcus aureus*, and Decreased Suf Function Results in Global Metabolic Defects and Reduced Survival in Human Neutrophils. *Infect Immun* 2017;85(6):e00100-00117.
251. **Yang S, Lopez, C.R., Zechiedrich, E.L.** Quorum sensing and multidrug transporters in *Escherichia coli*. *Proceedings of the National Academy of Sciences of the United States of America* 2006;103(7):2386-2391.
252. **Ibacache-Quiroga C, Oliveros, J.C., Couce, A., Blázquez, J.** Parallel Evolution of High-Level Aminoglycoside Resistance in *Escherichia coli* Under Low and High Mutation Supply Rates. *Front Microbiol* 2018;9:427.
253. **Chen KS, Saxena, P., Walker, J.R.** Expression of the *Escherichia coli* dnaX gene. *J Bacteriol* 1993;175(20):6663–6670.
254. **Dressaire C, Moreira, R.N., Barahona, S., Alves de Matos, A.P., Arraiano, C.M.** BolA is a transcriptional switch that turns off motility and turns on biofilm development. *mBio* 2015;6(1):e02352-02314.
255. **Browning DF, Wells, T.J., Franca, F.L.S., Morris, F.C., Sevastsyanovich, Y.R., Bryant, J.A., Johnson, M.D., Lund, P.A., Cunningham, A.F., Hobman, J.L., May, R.C., Webber, M.A., Henderson, I.R.** Laboratory adapted *Escherichia coli K-12* becomes a pathogen of *Caenorhabditis elegans* upon restoration of O antigen biosynthesis. *Mol Microbiol* 2013;87(5):939-950.
256. **Ulett GC, Valle, J., Beloin, C., Sherlock, O., Ghigo, J.M., Schembri, M.A.** Functional analysis of antigen 43 in uropathogenic *Escherichia coli* reveals a role in long-term persistence in the urinary tract. *Infect Immun* 2007;75(7):3233-3244.
257. **Domka J, Lee, J., Bansal, T., Wood, T.K.** Temporal gene-expression in *Escherichia coli K-12* biofilms. *Environ Microbiol* 2007;9(2):332-346.
258. **Lång H, Jonson, G., Holmgren, J., Palva, E.T.** The maltose regulon of *Vibrio cholerae* affects production and secretion of virulence factors. *Infect Immun* 1994;62(11):4781-4788.
259. **Smith SG, Mahon, V., Lambert, M.A., Fagan, R.P.** A molecular Swiss army knife: OmpA structure, function and expression. *FEMS Microbiol Lett* 2007;273-(1):1-11.
260. **Shaffer CL, Zhang, E.W., Dudley, A.G., Dixon, B.R.E.A., Guckes, K.R., Breland, E.J., Floyd, K.A., Casella, D.P., Algood, H.M.S., Clayton, D.B., Hadjifrangiskou, M.** Purine Biosynthesis Metabolically Constrains Intracellular Survival of Uropathogenic *Escherichia coli*. *Infect Immun* 2016;85(1):e00471-00416.
261. **Clark AJ, Satin, L., Chu, C.C.** Transcription of the *Escherichia coli* recE gene from a promoter in Tn5 and IS50. *Journal of bacteriology* 1994;176(22):7024-7031.
262. **Krasin F, Hutchinson, F.** Repair of DNA double-strand breaks in *Escherichia coli*, which requires recA function and the presence of a duplicate genome. *J Mol Biol* 1977;116(1):81-98.
263. **Sharma MR, Barat, C., Wilson, D.N., Booth, T.M., Kawazoe, M., Hori-Takemoto, C., Shirouzu, M., Yokoyama, S., Fucini, P., Agrawal, R.K.** Interaction of

Era with the 30S ribosomal subunit implications for 30S subunit assembly. *Molecular cell* 2005;18(3):319-329.
264. **Buckles EL, Luterbach, C.L., Wang, X., Lockatell, C.V.** Signature-tagged mutagenesis and co-infection studies demonstrate the importance of P fimbriae in a murine model of urinary tract infection. *Pathog dis* 2015;73(4):ftv014.
265. **Starosta AL, Lassak, J., Jung, K., Wilson, D.N.** The bacterial translation stress response. *FEMS microbiology reviews* 2014;38(6):1172-1201.
266. **Alteri CJ, Smith, S.N., Mobley, H.L.** Fitness of *Escherichia coli* during urinary tract infection requires gluconeogenesis and the TCA cycle. *PLoS Pathog* 2009;5(5):e1000448.
267. **Bleuel C, Große, C., Taudte, N., Scherer, J., Wesenberg, D., Krauß, G.J., Nies, D.H., Grass, G.** TolC Is Involved in Enterobactin Efflux across the Outer Membrane of *Escherichia coli*. *Journal of bacteriology* 2005;187(19):6701-6707.
268. **Adler C, Corbalan, N.S., Peralta, D.R., Pomares, M.F., de Cristóbal, R.E., Vincent, P.A.** The alternative role of enterobactin as an oxidative stress protector allows *Escherichia coli* colony development. *PloS one* 2014;9(1):e84734.
269. **Bateman A, Bycroft, M.** The structure of a LysM domain from *E. coli* membrane-bound lytic murein transglycosylase D (MltD). *J Mol Biol* 2000;299(4):1113-1119.
270. **Theodosiou E, Frick, O., Bühler, B., Schmid, A.** Metabolic network capacity of *Escherichia coli* for Krebs cycle-dependent proline hydroxylation. *Microb Cell Fact* 2015;14:108.
271. **Park SJ, McCabe, J., Turna, J., Gunsalus, R.P.** Regulation of the citrate synthase (gltA) gene of *Escherichia coli* in response to anaerobiosis and carbon supply: role of the arcA gene product. *Journal of bacteriology* 1994;176(16):5086-5092.
272. **Park SJ, Gunsalus, R.P.** Oxygen, iron, carbon, and superoxide control of the fumarase fumA and fumC genes of *Escherichia coli*: role of the arcA, fnr, and soxR gene products. *Journal of bacteriology* 1995;177(21):6255-6262.
273. **Broxton P WP, Gilbert P**. Injury and recovery of *Escherichia coli ATCC 8739* from treatment with some polyhexamethylene biguanides. *Microbios* 1984;40(161-162):187-193.
274. **Kulikov EE, Majewska, J., Prokhorov, N.S., Golomidova, A.K., Tatarskiy, E.V., Letarov, A.V.** Effect of O-acetylation of O antigen of *Escherichia coli* lipopolysaccharide on the nonspecific barrier function of the outer membrane. *Microbiology* 2017;86(3):310-316.
275. **Thomanek N, Arends, J., Lindemann, C., Barkovits, K., Meyer, H.E., Marcus, K., Narberhaus, F.** Intricate Crosstalk Between Lipopolysaccharide, Phospholipid and Fatty Acid Metabolism in *Escherichia coli* Modulates Proteolysis of LpxC. *Front Microbiol* 2018;9:3285.
276. **Sarkar S, Ulett, G.C., Totsika, M., Phan, M-D., Schembri, M.A.** Role of Capsule and O Antigen in the Virulence of Uropathogenic *Escherichia coli*. *PLoS One* 2014;9(4):e94786.
277. **Escalante A, Salinas Cervantes, A., Gosset, G., Bolívar, F.** Current knowledge of the *Escherichia coli* phosphoenolpyruvate-carbohydrate phosphotransferase system: peculiarities of regulation and impact on growth and product formation. *Applied microbiology and biotechnology* 2012;94(6):1483-1494.
278. **Jozefczuk S, Klie, S., Catchpole, G., Szymanski, J., Cuadros-Inostroza, A., Steinhauser, D., Selbig, J., Willmitzer, L.** Metabolomic and transcriptomic stress response of *Escherichia coli*. *Mol Syst Biol* 2010;6:364.

279. **Ligowska-Marzęta M, Hancock, V., Ingmer, H., M Aarestrup, F.** Comparison of Gene Expression Profiles of Uropathogenic *Escherichia Coli* CFT073 after Prolonged Exposure to Subinhibitory Concentrations of Different Biocides. *Antibiotics (Basel)* 2019;8(4):E167.
280. **DiRusso CC**. Primary sequence of the *Escherichia coli* fadBA operon, encoding the fatty acid-oxidizing multienzyme complex, indicates a high degree of homology to eucaryotic enzymes. *Journal of bacteriology* 1990;172(11):6459-6468.
281. **Campbell JW, Morgan-Kiss, R.M., Cronan, J.E. Jr**. A new *Escherichia coli* metabolic competency: growth on fatty acids by a novel anaerobic beta-oxidation pathway. *Molecular microbiology* 2003;47(3):793-805.
282. **Bondarenko OM, Sihtmäe,M., Kuzmičiova, J., Ragelienė, L., Kahru, A., Daugelavičius, R.** Plasma membrane is the target of rapid antibacterial action of silver nanoparticles in *Escherichia coli* and *Pseudomonas aeruginosa*. *Int J Nanomedicine* 2018;13:6779–6790.
283. **Fernández L, Hancock, R.E.** Adaptive and mutational resistance: role of porins and efflux pumps in drug resistance. *Clin Microbiol Rev* 2012;25(4):661-681.
284. **Sheidy DT, Zielke, R.A.** Analysis and expansion of the role of the *Escherichia coli* protein ProQ. *PloS one* 2013;8(10):e79656.
285. **Westermann AJ, Venturini, E., Sellin, M.E., Förstner, K.U., Hardt, W-D., Vogel, J.** The major RNA-binding protein ProQ impacts virulence gene expression in *Salmonella enterica serovar Typhimurium*. *mBio* 2019;10:e02504-02518.
286. **Kuzminov A**. Recombinational Repair of DNA Damage in *Escherichia coli* and Bacteriophage λ. *Microbiol Mol Biol Rev* 1999;63(4):751–813.
287. **Schmincke-Ott E, Bisswanger, H.** Dihydrolipoamide dehydrogenase component of the pyruvate dehydrogenase complex from *Escherichia coli K12*. Comparative characterization of the free and the complex-bound component. *Eur J Biochem* 1981;114(2):413-420.
288. **Mousavi F, Bojko, B., Bessonneau, V., Pawliszyn, J.** Cinnamaldehyde Characterization as an Antibacterial Agent toward *E. coli* Metabolic Profile Using 96-Blade Solid-Phase Microextraction Coupled to Liquid Chromatography–Mass Spectrometry. *J Proteome Res* 2016;15(3):963-975.
289. **Postle K, Good, R.F.** DNA sequence of the *Escherichia coli* tonB gene. *Proceedings of the National Academy of Sciences of the United States of America* 1983;80(17):5235–5239.
290. **Spurbeck RR, Dinh, Jr. P.C., Walk, S.T., Stapleton, A.E., Hooton, T.M., Nolan, L.K., Kim, K.S., Johnson, J.R., Mobley, H.L.T.** *Escherichia coli* Isolates That Carry vat, fyuA, chuA, and yfcV Efficiently Colonize the Urinary Tract. *Infect Immun* 2012;80(12):4115–4122.
291. **Ren Y, Palusiak, A., Wang, W., Wang, Y., Li, X., Wei, H., Kong, Q., Rozalski, A., Yao, Z., Wang, Q.** A High-resolution Typing Assay for Uropathogenic *Escherichia coli* Based on Fimbrial Diversity. *Front Microbiol* 2016;7:623.
292. **Gotto AM, Kornberg, H.L.** The metabolism of C2 compounds in micro-organisms. 7. Preparation and properties of crystalline tartronic semialdehyde reductase. *Biochem J* 1961;81:273-284.
293. **DeLisa MP, Wu, C.F., Wang, L., Valdes, J.J., Bentley, W.E.** DNA microarray-based identification of genes controlled by autoinducer 2-stimulated quorum sensing in *Escherichia coli*. *Journal of bacteriology* 2001;183(18):5239-5247.
294. **Koul S, Prakash, J., Mishra, A., Kalia, V.C.** Potential Emergence of Multi-quorum Sensing Inhibitor Resistant (MQSIR) Bacteria. *Indian J Microbiol* 2016;56(1):1-18.

295. **Ryan RP, Dow, J.M.** Diffusible signals and interspecies communication in bacteria. *Microbiology* 2008;154:1845-1858.
296. **Helmy YA, Deblais, L., Kassem, I.I., Kathayat, D., Rajashekara, G.** Novel small molecule modulators of quorum sensing in avian pathogenic *Escherichia coli* (APEC). *Virulence* 2018;9(1):1640-1657.
297. **Bacallao R, Crooke, E., Shiba, K., Wickner, W., Ito, K.** The secY protein can act post-translationally to promote bacterial protein export. *The Journal of biological chemistry* 1986;261(27):12907-12910.
298. **Nicholson TF, Watts, K.M., Hunstad, D.A.** OmpA of uropathogenic *Escherichia coli* promotes postinvasion pathogenesis of cystitis. *Infect Immun* 2009;77(12):5245-5251.
299. **Maillard JY**. Resistance of Bacteria to Biocides. *Microbiol Spectr* 2018;6(2).
300. **Kalia VC, Wood, T.K., Kumar, P.** Evolution of resistance to quorum-sensing inhibitors. *Microb Ecol* 2014;68(1):13-23.
301. **Hall CW, Mah, T.F.** Molecular mechanisms of biofilm-based antibiotic resistance and tolerance in pathogenic bacteria. *FEMS microbiology reviews* 2017;41(3):276-301.
302. **Mielecki D, Grzesiuk, E.** Ada response – a strategy for repair of alkylated DNA in bacteria. *FEMS Microbiol Lett* 2014;355(1):1-11.
303. **Hsu LC, Fang, J., Borca-Tasciuc, D.A., Worobo, R.W., Moraru, C.I.** Effect of micro- and nanoscale topography on the adhesion of bacterial cells to solid surfaces. *Applied and environmental microbiology* 2013;79(8):2703-2712.
304. **Feng G, Cheng, Y., Wang, A-Y., Borca-Tasciuc, D.A., Worobo,R.W., Moraru, C.I.** Bacterial attachment and biofilm formation on surfaces are reduced by small-diameter nanoscale pores: how small is small enough? *NPJ Biofilms Microbiomes* 2015;1.
305. **Manner S, Goeres, D.M., Skogman, M., Vuorela, P., Fallarero, A.** Prevention of *Staphylococcus aureus* biofilm formation by antibiotics in 96-Microtiter Well Plates and Drip Flow Reactors: critical factors influencing outcomes. *Scientific reports* 2017;7:43854.
306. **Bernard M, Jubeli, E., Pungente, M.D., Yagoubi, N.** Biocompatibility of polymer-based biomaterials and medical devices - regulations, *in vitro* screening and risk-management. *Biomater Sci* 2018;6(8):2025-2053.
307. **Simões MP, M.O., Vieira, M.J.** Action of a cationic surfactant on the activity and removal of bacterial biofilms formed under different flow regimes. *Water Res* 2005;39(2-3):478-486.
308. **Alvarado-Gomez E, Perez-Diaz, M., Valdez-Perez, D., Ruiz-Garcia, J., Magaña-Aquino, M., Martinez-Castañon, G., Martinez-Gutierrez, F.** Adhesion forces of biofilms developed *in vitro* from clinical strains of skin wounds. *Mater Sci Eng C Mater Biol Appl* 2018;82:336-344.
309. **Mandakhalikar KD, Wang, R., Rahmat, J.N., Chiong, E., Neoh, K.G., Tambyah, P.A.** Restriction of *in vivo* infection by antifouling coating on urinary catheter with controllable and sustained silver release: a proof of concept study. *BMC Infectious Diseases* 2018;18.

Appendices

Gene name	Gene Size (bp)	Location of SNP (bp)						
		PHMB	**Triclosan**	**BAC**	**Silver Nitrate**	**Cinnamaldehyde**	**Furanone C30**	**F-DPD**
recE1	2601	175, 535, 536, 830	535, 536, 830	535, 536, 830	175, 535, 536, 830	535, 536, 830	535, 536, 830	175, 535, 536, 830
yeeP	864	222, 292, 595, 610, 822	222, 292, 595, 610, 822	222, 292, 595, 610, 822	222, 292, 595, 610, 822	222, 292, 595, 610, 822	222, 292, 595, 610, 822	222, 292, 595, 610, 822
tnpA	1263	828	828	828	828	828	828	828
entS	1251	448, 870, 961	448, 870, 961	961	448, 870, 961	448, 870, 961	448, 870, 961, 1164	448, 870, 961
insB	504	136, 323	136, 323	136, 323	136, 323	136, 323	136, 323	136, 323
iss	294	144, 229	144, 229		144, 229	144, 229	144, 229	144, 229
yeeD	228	3, 10	3, 10		3, 10	3, 10	3, 10	
alpA	213	7, 101	7, 101	7, 101	7, 101	7, 101	7, 101	7, 101
fabI	789		604					
wbbL	795		121					
murJ	1536		806					
cspE	210			187				
ldrD2	108			86				
ldrD3	108							86
fadA	1164				743			
gadB	1401		370, 526, 539, 589, 655		370, 526, 539, 589, 655	370, 526, 539, 589, 655	370, 526, 539, 589, 655	370, 526, 539, 589, 655
proQ	699					328		
lpd	1425					39		
dnaX	1932					1564		
tonB	720					110		
mntP	567						427	
rsxC	2223							1883
yfhH	849							361
flu	389	134, 182, 191, 333, 364	134, 182, 191, 333, 364	134, 182, 191, 333, 364	134, 182, 191, 333, 364	134, 182, 191, 333, 364	134, 182, 191, 333, 364	134, 182, 191, 333, 364

Table 9.1 Position of single nucleotide polymorphisms identified in the full genome sequencing of seven exposed isolates of EC958 compared to the unexposed control.

Gene Product	Gene Name	PHMB	Triclosan	BAC	Silver nitrate	Cinnamaldehyde	Furanone C30	F-DPD
[citrate (pro-3S)-lyase] ligase	*citC*					1.16809445		
1-(5-phosphoribosyl)-5-[(5-phosphoribosylamino)methylideneamino]imidazole-4-carboxamide isomerase	*hisA*			-1.44642				
1,4-dihydroxy-2-naphthoyl-CoA synthase	*menB*			-1.00867				
10 kDa chaperonin	*groES*					-2.310612923		
1-pyrroline dehydrogenase		1.444561	1.038662		1.403760771			
2,3-bisphosphoglycerate-independent phosphoglycerate mutase	*gpmI*	-1.21346			-1.522463598	-1.233188273		
2,5-diketo-D-gluconate reductase A	*dkgA*	1.420137						
23S rRNA pseudouridine synthase E	*rluE*					-1.351049065		
23S rRNA pseudouridylate synthase B	*rluB*						-1.116090514	
2'-5' RNA ligase		1.714171	1.578466					
2-C-methyl-D-erythritol 2,4-cyclodiphosphate synthase	*ispF*			-1.24897		-1.063203493		
2-C-methyl-D-erythritol 4-phosphate cytidylyltransferase	*ispD*					1.009354875		
2-Cys peroxiredoxin	*tpx*					1.159104772		
2-dehydro-3-deoxy-6-phosphogalactonate aldolase	*dgoA*	2.874909	1.5404	2.236014	1.972597734	1.4771281	2.689877369	
2-deoxyribose-5-phosphate aldolase	*deoC*						1.100350819	
2-hydroxy-3-oxopropionate reductase	*garR*	-3.23155	5.484397	3.964862	-3.131713076	-1.86660665	-1.786009102	
2-hydroxy-3-oxopropionate reductase	*glxR*				2.941784872	4.643161487	5.018143166	2.75739
2-methylcitrate dehydratase	*prpD; mmgE*		-1.12799					-1.01523
2-oxoglutarate dehydrogenase subunit E1	*sucA*				1.198951029	1.14293087		
2-succinyl-5-enolpyruvyl-6-hydroxy-3- cyclohexene-1-carboxylic-acid synthase	*menD*			-1.09244				
2-succinylbenzoate-CoA ligase	*menE*			-1.10516				
30S ribosomal protein	*rpsV*	1.831126						

30S ribosomal protein S1	*rpsA*						-1.19196478	
30S ribosomal protein S11	*rpsK*			-1.47585			-1.429954085	
30S ribosomal protein S13	*rpsM*			-1.12972			-1.180682361	
30S ribosomal protein S14	*rpsN*			-1.14466		-1.030232607	-1.082494456	
30S ribosomal protein S15	*rpsO*				-1.001262476		-1.005409204	
30S ribosomal protein S17	*rpsQ*		-1.21567	-1.43211			-1.666356626	
30S ribosomal protein S18	*rpsR*			-1.22592		-1.33652143	-1.213549098	
30S ribosomal protein S19	*rpsS*			-1.74934		-1.159559291	-1.532937506	
30S ribosomal protein S2	*rpsB*						-1.293329798	
30S ribosomal protein S20	*rpsT*				-1.180615927			
30S ribosomal protein S3	*rpsC*			-1.73253			-1.620294829	
30S ribosomal protein S4	*rpsD*			-1.27738			-1.224962074	
30S ribosomal protein S5	*rpsE*			-1.54199		-1.135784995	-1.252538051	
30S ribosomal protein S6	*rpsF*			-1.18541		-1.556098676	-1.076156616	
30S ribosomal protein S8	*rpsH*			-1.17307		-1.110666739	-1.095071297	
30S ribosomal protein S9	*rpsI*						-1.310800278	
3-deoxy-manno-octulosonate cytidylyltransferase	*kdsB*	-1.00144		-1.40791		-1.311342939	-1.000112264	
3-ketoacyl-CoA thiolase	*fadA*				1.134335176			
3-oxoacyl-ACP synthase I	*fadB*		-1.17539					
4-alpha-glucanotransferase	*malQ*	-1.51841	-1.36164		-1.864476168			
4-amino-4-deoxy-L-arabinose lipid A transferase	*arnT*			-1.03045				
4-aminobutyrate aminotransferase	*gabT*	1.826855	1.33875		2.120603342	-1.314105035		-1.61882
4-deoxy-4-formamido-L-arabinose- phosphoundecaprenol deformylase ArnD	*arnD*			-1.49571				
5-(carboxyamino)imidazole ribonucleotide synthase	*purK*		1.227298	1.464015	2.127298466		1.254656717	
50S ribosomal protein L1	*rplA*						-1.028064134	
50S ribosomal protein L15	*rplO*		-1.46824	-2.04566		-1.086026821	-1.626519973	-1.44876

50S ribosomal protein L16	*rplP*		-1.01205	-1.65238			-1.653473007	
50S ribosomal protein L17	*rplQ*			-1.04097	-1.028106502		-1.349466308	
50S ribosomal protein L18	*rplR*			-1.58002		-1.237951548	-1.450589297	
50S ribosomal protein L2	*rplB*			-1.92057		-1.200612652	-1.65122741	
50S ribosomal protein L20	*rplT*						-1.078353557	
50S ribosomal protein L22	*rplV*		-1.0069	-1.9257		-1.220454975	-1.697205488	
50S ribosomal protein L23	*rplW*			-1.64564		-1.050394094	-1.33320688	
50S ribosomal protein L25	*rplY*				-1.628564893	-1.377747225		
50S ribosomal protein L28	*rpmB*				-1.155478457		-1.041489705	
50S ribosomal protein L29	*rpmC*		-1.28014	-1.47482			-1.711052068	
50S ribosomal protein L3	*rplC*			-1.30582			-1.223458411	
50S ribosomal protein L30	*rpmD*		-1.22959	-1.79843		-1.118659501	-1.513073683	
50S ribosomal protein L31 type B	*ykgM*					1.935360576	1.015600104	
50S ribosomal protein L4	*rplD*			-1.67878		-1.143041125	-1.454587806	
50S ribosomal protein L5	*rplE*			-1.1121			-1.081241426	
50S ribosomal protein L6	*rplF*			-1.29644		-1.147790715	-1.229610554	
50S ribosomal protein L9	*rplI*			-1.35484		-1.224486129	-1.44226617	
5-hydroxyisourate hydrolase	*hiuH*					1.146347076		
5-keto-4-deoxy-D-glucarate aldolase	*garL*	-2.75964			-2.931733744	-2.008820976	-1.104624822	
6-phosphogluconolactonase	*pgl*			-1.05628				
7-alpha-hydroxysteroid dehydrogenase	*hdhA*	1.336381			1.040030273		1.308030441	
7-cyano-7-deazaguanine synthase	*queC*		-1.20112					
ABC transporter ATP-binding protein	*sufC*	1.341158	1.254164			-1.374102694		
ABC transporter ATP-binding protein						-1.190839498		
ABC transporter permease		1.871876	1.116964	-1.77753	1.737642908	-1.372355102	1.198658616	
ABC transporter substrate-binding protein		1.142414		-1.1976	1.209524574	1.645268116	1.995362659	-1.01297
ABC transporter substrate-binding protein		1.066338		1.548703	2.330193863		1.286461683	

ABC transporter substrate-binding protein		2.951338			1.608735498			
ABC transporter substrate-binding protein		2.017172						
acetoacetate metabolism regulatory protein AtoC	*atoC*					1.308087919	1.329818347	
acetyl-CoA--acetoacetyl-CoA transferase subunit alpha	*atoD*			1.405937				
acetyl-coenzyme A synthetase	*acs*	2.247153	2.296064	1.12442	2.440046655	1.508443584	1.063430789	
acetylesterase	*aes*					1.076036214		
acetylglutamate kinase	*argB*		1.103282	-1.11514				
acetylornithine aminotransferase	*argD*	1.834893	1.600074	1.067413	1.959973467			
acetyltransferase					1.068414864			
acid stress chaperone HdeB	*hdeB*	2.477095		-2.71022	1.038579085	-1.015538793		-1.65106
acid stress protein IbaG	*ibaG*					-1.127971925		
acid-resistance protein HdeA	*hdeA*	2.266714		-2.89704	1.035602689	-1.369620592		-1.7355
acid-resistance protein HdeD	*hdeD*	1.658105		-3.29673		-2.297380649		-2.26446
acid-shock protein						1.149192399		
ACP phosphodiesterase	*acpH*					-1.131024505		
acrEF/envCD operon repressor	*envR*			1.102309				
acyl-coenzyme A dehydrogenase	*fadE*	1.020996				1.211244424		
adenosine deaminase	*add*		-1.13726	-1.41387	-1.098748079	-1.407062204		
adenosylcobinamide-GDP ribazoletransferase	*cobS*		-1.32791					
adenylate kinase	*adk*					-1.28779872		
adenylyl-sulfate kinase	*cysC*	1.449152		1.364652		2.111373905	1.105314339	
aerotaxis receptor					1.163153694			-1.02587
AfaC protein	*afaC*		-2.8207			1.43468877		2.591368
AfaE protein	*afaE*					1.355883772		1.004838
alanine racemase	*alr*				1.094049557			
alcohol dehydrogenase						1.025708304		
aldehyde dehydrogenase		1.306282			1.027312398	1.044629625		-1.35885

aldehyde dehydrogenase						1.125533382		
aldehyde dehydrogenase						-2.147439647		
aldehyde reductase Ahr	*ahr*		1.029725	-1.47058		-3.385406615		-1.80015
aldose isomerase		1.168262	-2.30442	-1.57799				
alkyl hydroperoxide reductase subunit C	*ahpC*				-1.191743323			
allantoin permease	*allP*	3.8272	4.783063	3.190361	3.63888144	4.418254293	4.766017366	1.808667
alpha/beta hydrolase						1.335109425		
alpha-amylase	*malS*	-1.73299		-1.45695	-1.817010463	-3.921428013		-1.94561
alpha-glycosidase	*aglB*	-1.92397	-1.19357		-1.719947721		-1.206456678	
alpha-ketoglutarate transporter					1.077564254			
altronate hydrolase	*uxaA*					1.312644974		
amidophosphoribosyltransferase	*purF*			1.236614	1.676717484		1.140688513	
amino acid ABC transporter permease		1.163996					1.009576433	
amino acid ABC transporter permease		1.235737						
amino acid ABC transporter substrate-binding protein		1.249931			1.683464379	1.095464849		
amino acid ABC transporter substrate-binding protein		1.138493	1.163659		1.030154159			
amino acid permease		1.86934			1.595100469			
amino acid permease		1.081148						
amino acid transporter		1.341336	1.668109	1.046651	1.608289332	1.370168232		
aminopeptidase PepB	*pepB*			-1.117				
ammonium transporter	*amtB*					1.437101475		
anaerobic C4-dicarboxylate transporter DcuB	*dcuB*	-1.96738	-1.87326		-3.082431438			
anaerobic C4-dicarboxylate transporter DcuC	*dcuC*		-1.11558		-1.550365413			
anaerobic glycerol-3-phosphate dehydrogenase subunit B	*glpB*					1.412832318		
anaerobic sulfatase maturase				1.341162		2.182842477		
anaerobic sulfatase maturase							2.214274875	
anti-adapter protein IraD	*iraD*					1.556798714		

antigen 43	*flu*			4.47401	4.803497926	1.135426671		-1.20156
antiporter				-2.54033	1.953678198	-1.710649992	1.072925758	-2.16105
antiporter				-1.18131	-1.73031499			
antiporter	*uhpT*					1.05004768		
antitoxin				1.055057				
antitoxin ChpS	*chpS*	1.209175				1.085214294		
antitoxin PrlF	*prlF*			1.05521	-1.248050736			
apo-citrate lyase phosphoribosyl-dephospho-CoA transferase	*citX*	-2.21409	-1.71036	-1.55414	-2.039623371	-1.278711792		
arabinose ABC transporter substrate-binding protein	*araF*		-1.03576			1.189737742		
AraC family transcriptional regulator						1.434049946		-1.13859
AraC family transcriptional regulator						-1.258937216		
AraC family transcriptional regulator						1.554699817		
arginine ABC transporter ATP-binding protein		1.367328						
arginine ABC transporter permease ArtQ	*artQ*					-1.000386038		
arginine decarboxylase						-1.028336407		
arginine N-succinyltransferase	*astA*	1.815495	1.534846	1.084137	2.034019267	1.184467202		
arginine transport ATP-binding protein ArtP	*artP*				1.062400873			
arginine:agmatine antiporter	*adiC*	-1.20646		-1.00099	-1.355293522	-1.020229521		
asparagine synthetase A	*asnA*				1.363531516			
aspartate carbamoyltransferase catalytic subunit	*pyrB*	-1.06494	-1.06963		-1.222767917			
aspartate carbamoyltransferase regulatory subunit	*pyrI*		-1.04631					
aspartate-semialdehyde dehydrogenase	*asd*		-1.18773					
aspartate--tRNA ligase	*aspS*					-1.142620767		
ATP-binding protein						-1.724693301		-1.26511
ATP-dependent RNA helicase						-1.170145595		
ATP-dependent RNA helicase RhlE	*rhlE*					-1.714668148		

ATP-dependent RNA helicase SrmB	*srmB*					-1.127056998		
ATP-independent periplasmic protein-refolding chaperone	*spy*		1.737543	1.352764				
autonomous glycyl radical cofactor GrcA	*grcA*		-1.63167		-1.098330934			
bacterioferritin	*bfr*	1.672041			1.122509556	-2.542938475	1.012768593	-1.50697
bacterioferritin-associated ferredoxin	*bfd*			1.058145				
barnase inhibitor	*yhcO*					-1.302293212		
baseplate assembly protein						-1.059862019		
baseplate assembly protein						-1.13200352		
baseplate protein							-1.220229697	
beta-glucuronidase	*uidA*	1.485712			1.169642002		1.047702579	
beta-hydroxydecanoyl-ACP dehydratase	*fabA*	-1.21934					-1.0930889	
bifunctional glucose-1-phosphatase/inositol phosphatase	*agp*					1.110304254		
bifunctional imidazole glycerol-phosphate dehydratase/histidinol phosphatase	*hisB*			-1.2281				
bifunctional isocitrate dehydrogenase kinase/phosphatase	*aceK*	1.34082	1.205086		1.967817577			
bifunctional phosphoribosylaminoimidazolecarboxamide formyltransferase/inosine monophosphate cyclohydrolase	*purH*		1.108741	1.486147	1.342942298		1.425663559	
bifunctional protein PutA	*putA*	1.343935	1.314752		2.499074033			
bifunctional UDP-glucuronic acid oxidase/UDP-4-amino-4-deoxy-L-arabinose formyltransferase				-1.73362				
biofilm regulator BssR	*bssR*	1.514282			1.298997828	2.283179479		
biopolymer transporter ExbB	*exbB*	-1.0595						
bis(5'-nucleosyl)-tetraphosphatase (symmetrical)	*apaH*					-1.20289525		
BlaEC family class C beta-lactamase					-1.016028515			
branched chain amino acid ABC transporter substrate-binding protein			1.130094		1.109597307			

branched chain amino acid ABC transporter substrate-binding protein			1.747837					
C4-dicarboxylate ABC transporter		1.171995			1.654275289			
C4-dicarboxylate ABC transporter permease		1.389984				1.18835249		
C4-dicarboxylate ABC transporter permease						1.09091475	1.22748116	
C4-dicarboxylate ABC transporter substrate-binding protein		1.033891			1.040680952	1.119262408		
C4-dicarboxylate ABC transporter substrate-binding protein		1.011859				1.383305389		
C4-dicarboxylate ABC transporter substrate-binding protein		1.160715						
carbamate kinase	*arcC*	1.402666				1.084518789		
carbamoyl-phosphate synthase large chain	*carB*	-2.46304	-1.19064	-2.24938	-2.852347288	-2.543090814	-2.673487858	
carbamoyl-phosphate synthase small subunit	*carA*	-2.2989		-2.03899	-2.510304109	-2.409288058	-2.197759504	
carbohydrate kinase	*lyx*			-2.3361		1.389227366		
carbon starvation induced protein		2.52098	1.031843		3.126593706	-1.161642353	1.095717455	-1.33747
carbon starvation protein A	*yjiY*	1.14129			1.708920647	1.854916762		
carboxymethylenebutenolidase					1.010945887			
carnitinyl-CoA dehydratase	*caiD*			-1.4426			-1.304482445	-1.25623
catalase HPII	*katE*	1.361509			1.039827739	-1.224465247		-1.06304
catalase peroxidase	*katG*			-1.05596				
cation acetate symporter	*actP*	1.017613			1.58829928			
cell division protein FtsL	*ftsL*					1.041154951		
cell division protein ZapB	*zapB*					1.15268834		
cell envelope biogenesis protein TonB	*tonB*					1.130527202		
cell filamentation protein Fic	*fic*					-1.535593392		-1.22583
chaperone modulatory protein CbpM	*cbpM*			-1.36464				
chaperone protein ClpB	*clpB*					-1.170660507		

chemotaxis protein CheA	*cheA*			-3.60171		-2.752982718		-3.75748
chemotaxis protein CheR	*cheR*			-3.58826		-2.137465152		-2.68669
chemotaxis protein CheW	*cheW*			-3.21408		-2.310815515		-2.91761
chemotaxis response regulator protein-glutamate methylesterase	*cheB*			-3.13862		-1.619025951		-2.94924
chlorohydrolase/aminohydrolase	*ssnA*	1.379886						
chromate reductase	*chrR6*			-1.29943				
citrate (Si)-synthase	*gltA*	1.257167			1.245182695	1.001889529		
citrate lyase ACP	*citD*	-3.4082	-2.26325	-1.04895	-2.437856098	-2.274517176		-1.29501
citrate lyase subunit alpha	*citF*	-2.51412	-1.68348	-1.48412	-3.383296213	-2.144341319		
citrate lyase subunit beta	*citE*	-2.36379	-1.66913	-1.67948	-2.508339596	-2.1344036		
class II aldolase					1.296287066			
class II fumarate hydratase	*fumC*	1.128007			1.074988488	1.356843161		
cold-shock protein		-1.39145		1.878404	-1.196464431			
cold-shock protein				1.665492			-1.666331042	
cold-shock protein CspD	*cspD*	1.253809			1.024647882	2.368019732		
cold-shock protein CspE	*cspE*	-1.00681					-1.121094496	
cold-shock protein CspG	*cspG*		1.783565	3.63428	-1.020701041		-1.018064208	1.214205
cold-shock protein CspH	*cspH*			2.231032				1.070326
colicin V production protein	*cvpA*			1.251708	1.641981206	1.444337727		
copper homeostasis protein CutC	*cutC*					1.127885781		
crossover junction endodeoxyribonuclease RuvA	*ruvA*					-1.140152678		
crossover junction endodeoxyribonuclease RuvC	*ruvC*	-1.03979						
Crp/Fnr family transcriptional regulator						1.072237187		
CTP synthase	*pyrG*					-1.177882954		
c-type cytochrome biogenesis protein CcmF	*ccmF*		-2.98523	-1.09124				
curli production assembly/transport component CsgE	*csgE*					1.118975628		

cyclic amidohydrolase		3.772421	3.895695	2.366878	4.04417938	3.674727214	4.322204141	1.339718
cyclic di-GMP phosphodiesterase				1.033999		1.066877555		
cyclic-guanylate-specific phosphodiesterase				-3.61174		-2.778750569		-3.76161
cyd operon protein YbgE	*ybgE*		-1.09213					
cysteine desulfurase		1.035085	1.276611			-1.053722693		
cysteine desulfuration protein SufE	*sufE*	1.189079	1.218943					
cysteine synthase A	*cysK*					1.781142774		
cysteine synthase B	*cysM*		1.024106					
cysteine/O-acetylserine efflux protein	*eamB*				-1.086798899			
cytochrome bd oxidase subunit I				-1.01743		-1.348195708		
cytochrome bd-I ubiquinol oxidase subunit 1	*cydA*		-1.16457					
cytochrome bd-I ubiquinol oxidase subunit 2	*cydB*		-1.13893					
cytochrome bd-I ubiquinol oxidase subunit X	*cydX*		-1.21438					
cytochrome bo(3) ubiquinol oxidase subunit 3	*cyoC*				1.117706284			
cytochrome c nitrite reductase Fe-S protein						1.256565748		
cytochrome C nitrite reductase pentaheme subunit	*nrfB*					1.008054035	1.09030139	
cytochrome c nitrite reductase subunit NrfD	*nrfD*					1.238316792		
cytochrome c-type biogenesis protein CcmE	*ccmE*		-2.08492					
cytochrome c-type biogenesis protein CcmH	*ccmH*		-2.41762		-1.052621066			
cytochrome c-type protein NapC	*napC*		-2.89464					
cytochrome o ubiquinol oxidase subunit IV					1.001055686			
cytochrome ubiquinol oxidase subunit I					1.297980385			
cytochrome ubiquinol oxidase subunit II					1.185581474			
cytochrome-c peroxidase						1.755665482		
D-alanyl-D-alanine carboxypeptidase	*dacD*			-1.17813				-1.04937
D-amino acid dehydrogenase small subunit		1.093984			1.735825869	1.205829588		
DEAD/DEAH box family ATP-dependent RNA helicase						-1.096299571	-1.148671314	

dehydratase						1.429403113		
dethiobiotin synthase	*bioD*				-1.281803834			
D-galactarate dehydratase	*garD*	-2.44282		1.240067	-2.396151897			
dienelactone hydrolase				-1.0651		-1.150420384		-1.14432
diguanylate phosphodiesterase	*yhjH*		1.48369					
dihydrodipicolinate synthase family protein		1.493167				1.247962322		
dihydrolipoamide succinyltransferase	*sucB*		1.055291					
dihydrolipoyllysine-residue acetyltransferase component of pyruvate dehydrogenase complex	*aceF*	-1.38858	-1.55078	-2.10756	-1.628558172	-1.136276565	-1.581398695	-1.10527
dihydroorotase	*pyrC*					-1.055110241		
dihydropyrimidine dehydrogenase subunit A	*preA*		-1.0114	-1.25188		1.212241122		
dihydropyrimidine dehydrogenase subunit B	*preT*		-1.17019	-1.38855		1.350152221		
dihydroxyacetone kinase subunit DhaK	*dhaK*					1.091863232	1.042566592	
dihydroxyacetone kinase subunit DhaL	*dhaL*					1.107321778	1.012549766	
dihydroxyacetone kinase subunit DhaM	*dhaM*					1.234198049		
dimethylsulfoxide reductase		1.22579			1.08527203			
dimethylsulfoxide reductase subunit A					-1.361289092			
dipeptide transport ATP-binding protein DppF	*dppF*	2.170213	2.443573	1.184617	1.841355913		1.194537493	
DNA alkylation response protein		1.319103		-1.34063	1.193018568	-1.276221876		-1.63113
DNA cytosine methyltransferase						-1.167483738		
DNA cytosine methyltransferase						1.07931475		
DNA gyrase inhibitor								-1.20678
DNA replication protein DnaC	*dnaC*					-1.246271281		
DNA-binding protein				1.222387				1.093105
DNA-binding response regulator			-1.01673			-1.257981199		
DNA-binding response regulator						1.050156978		
DNA-binding response regulator						-1.140963115		

DNA-binding transcriptional activator,3HPP-binding						1.151767329		-1.17397
DNA-binding transcriptional regulator DsdC	*dsdC*					1.280278822		
DNA-binding transcriptional regulator KdgR	*kdgR*		-1.34876					
DNA-directed RNA polymerase subunit alpha	*rpoA*			-1.22566			-1.367012584	
DNA-directed RNA polymerase subunit beta	*rpoB*			-1.57035		-1.462335803	-1.005579127	
DNA-directed RNA polymerase subunit beta'			-1.17885	-1.76741		-1.158398573	-1.259022844	
DNA-invertase					-1.080803659			
D-ribose ABC transporter substrate-binding protein		1.014619				1.16819799		
D-ribose pyranase	*rbsD*					1.676995359		
D-ribose transporter ATP-binding protein	*rbsA*					2.371816418		
D-serine/D-alanine/glycine transporter	*cycA*		1.235808		1.351380396	1.226726629		
dTDP-4-dehydrorhamnose 3,5-epimerase	*rfbC*			-1.62216				
dTDP-glucose 4,6-dehydratase	*rmlB*					-1.269313279		
DUF1107 domain-containing protein						1.060128475		
DUF1198 domain-containing protein				1.017456				
DUF1338 domain-containing protein					1.050410444	-1.585753967		-1.45669
DUF2542 domain-containing protein						1.136701274		
DUF2810 domain-containing protein		-1.03537			-1.059478815			
DUF883 domain-containing protein				-2.3966		-3.803982618		-2.67494
DUF903 domain-containing protein			1.153178					
D-xylose ABC transporter ATP-binding protein		1.004002				2.476900936		
ECF RNA polymerase sigma-E factor	*rpoE*	-1.0213						
electron transport complex subunit A				1.020664				1.07132
electron transport complex subunit D	*rnfD*					-1.230107239		
electron transport complex subunit G						-1.20821718		
elongation factor 4	*lepA*					-1.077270531		
elongation factor G	*fusA*						-1.023832359	

elongation factor P-like protein YeiP	*yeiP*					-1.262986945		
elongation factor Ts	*tsf*						-1.269146834	
endopeptidase			4.687891					
entericidin A	*ecnA*							1.006408
entericidin B	*ecnB*	1.321201			1.279626158	-3.255248342		-1.06293
ethanolamine ammonia-lyase heavy chain	*eutB*			-1.17646				-1.29825
ethanolamine ammonia-lyase small subunit	*eutC*			-1.19147				-1.10137
ethanolamine utilization protein EutA	*eutA*			-1.06665				
ethanolamine utilization protein EutP	*eutP*					1.35403825		
exclusion suppressor FxsA	*fxsA*	-1.74969				-1.262649609		
exodeoxyribonuclease VII large subunit	*xseA*					-1.14149151		
FAD-binding protein	*ydiJ*		1.331557		1.001349126			
fatty acid oxidation complex subunit alpha	*fadB*	1.337796			1.572931993			
Fe(2+) transport protein A	*feoA*				-1.423248504			
Fe(3+) dicitrate transport ATP-binding protein FecE	*fecE*					-1.299491398		
fe(3+) dicitrate transporter fecA	*fecA*		1.105877			-1.189995838		
ferredoxin			-2.6313	2.056382			1.01868493	1.304731
ferredoxin				1.427208				
ferredoxin-type protein NapG	*napG*		-4.05857					
ferredoxin-type protein NapH	*napH*		-4.37382					
ferric iron reductase involved in ferric hydroximate transport	*fhuF*			1.481058		2.083685832		1.145405
ferrichrome outer membrane transporter	*fhuA*			1.032519		1.201332944		
ferrous iron permease EfeU	*efeU*				1.211491178	1.126186226		
ferrous iron transporter C						1.01798874		
Fe-S cluster assembly protein SufB	*sufB*	1.374202	1.143138			-1.208143693	1.032355199	-1.18302
FeS cluster assembly protein SufD	*sufD*		1.07896			-1.510962201		-1.5207

fimbrial adhesin protein						1.227415705		
fimbrial chaperone protein FimC	*fimC*				-1.460495477			
fimbrial outer membrane usher protein						1.016962381		
fimbrial protein				1.147297				
fimbrial protein FimD	*fimD*		1.252401					
fimbrial protein Type 1, A chain	*fimA*		2.151372					
fimbrial yfcV	*yfcV*	1.21276	1.02406			1.827668275		
FKBP-type peptidyl-prolyl cis-trans isomerase	*fkpA*	-1.00537						
flagella synthesis chaperone protein FlgN	*flgN*			-1.06725				-1.22551
flagellar assembly protein H	*fliH*	-1.42356		-1.47985		-1.464887285		-1.62078
flagellar basal body L-ring protein	*flgH*	-1.00094		-1.15809		-1.09647634		-1.44769
flagellar basal body rod modification protein FlgD	*flgD*	-2.07152		-2.99159		-2.421987203		-2.78106
flagellar basal body rod protein FlgB	*flgB*	-1.35681				-1.124573106		-1.30909
flagellar basal body rod protein FlgC	*flgC*	-2.35356		-3.83487		-2.641818714		-2.31754
flagellar basal body rod protein FlgG	*flgG*	-1.25593		-1.24453				-1.67164
flagellar basal-body rod protein FlgF	*flgF*	-1.08496						
flagellar biosynthesis protein FlhA	*flhA*	-1.25666		-1.01842				-1.07308
flagellar biosynthesis protein FlhB	*flhB*			-1.389		-1.558100008		-1.19904
flagellar biosynthesis protein FliO	*fliO*	-1.53125		-1.92901				-1.47052
flagellar biosynthesis protein FliR	*fliR*			1.070856				
flagellar biosynthetic protein FliP	*fliP*	-1.09792		-1.70571		-1.588900631		-1.20238
flagellar brake protein YcgR	*ycgR*			-1.86587		-1.738706246		-1.69259
flagellar capping protein	*fliD*			-3.24274		-2.75086122		-3.16955
flagellar export chaperone FliS	*fliS*			-2.79478		-1.553995241		-2.32108
flagellar hook protein FlgE	*flgE*	-1.29363		-1.56139		-1.792255711		-1.70643
flagellar hook-associated protein 3	*flgL*			-1.87658		-1.179462861		-1.74504
flagellar hook-associated protein FlgK	*flgK*			-3.19052		-2.017976073		-2.65516

flagellar hook-length control protein FliK	*fliK*	-1.78451		-2.49466		-2.432154514		-2.46499
flagellar motor protein MotA	*motA*			-2.97271		-2.246027311		-3.09566
flagellar motor switch protein FliG	*fliG*	-1.12248		-1.67689		-1.23526912		-1.58122
flagellar motor switch protein FliM	*fliM*	-1.6174		-2.08467		-1.997080898		-1.74744
flagellar motor switch protein FliN	*fliN*	-2.11177		-2.9028		-2.281867819		-2.11771
flagellar M-ring protein FliF	*fliF*	-2.54583		-2.40843		-1.964029496		-1.51139
flagellar P-ring protein	*flgI*	-1.15992		-1.5013		-1.093739287		-1.2037
flagellar protein fliJ	*fliJ*	-1.61916		-3.0546		-2.344725922		-2.56522
flagellar protein fliL	*fliL*	-1.91266		-2.19794		-1.987716366		-1.90897
flagellar protein FliT	*fliT*			-1.39665		-1.683921962		-1.5181
flagellar regulatory protein FliZ	*fliZ*			-1.88889		-1.493573615		-1.75954
flagellin	*fliC*			-6.48211		-2.28560547		-4.75505
flagellum-specific ATP synthase	*fliI*	-1.29987		-1.30719				-1.58307
flavohemoprotein	*hmp*	1.451416				1.198232011	1.168902229	
Fml fimbriae subunit	*fmlA*	-1.41202		-1.30109	-1.220985034		-1.089303994	
FMN-binding protein MioC	*mioC*			1.225233				
formate acetyltransferase	*pflB*		-1.4879		-1.288073411			
formate dehydrogenase-N subunit alpha	*fdnG*	-1.07216		-1.05222	-1.054218764	-1.548641123		
fructose 1,6-bisphosphatase		-1.01867			-1.029124298	1.647247854		
fructose-bisphosphate aldolase		1.560542	1.023154		1.265661466	-1.857051453		
fructose-bisphosphate aldolase	*gatY*					2.606781815		-1.46132
fructuronate reductase	*uxuB*		1.146524					
fuculose phosphate aldolase	*fucA*					1.146592349		
fumarate hydratase	*fumC*	1.180062	-1.34245		1.478118839	-1.403356758		
fumarate hydratase		-1.77265			-2.869453902			
fumarate reductase flavoprotein subunit	*frdA*	-1.27133			-1.918520696			
fumarate reductase iron-sulfur subunit	*frdB*	-1.09306			-1.675131255			

fumarate reductase subunit C	*frdC*	-1.0103			-1.524198093			
fumarate reductase subunit D	*frdD*	-1.13539			-1.381625913			
GABA permease	*gabP*	2.2354			2.769278781			
galactonate oxidoreductase	*lgoD*	1.451892	1.326875		1.379041012			
galactonate transporter		-2.61609		1.73194	-2.562229226	-1.780845992		
galactose ABC transporter substrate-binding protein	*mglB*				1.70243694			
galactose/methyl galactoside import ATP-binding protein MglA	*mglA*	1.309831			1.584908819	1.631405468		
galactose-proton symporter	*galP*		1.067409					
galactoside ABC transporter permease MglC	*mglC*				1.07073029	1.186792869		
GalU regulator GalF	*galF*					-1.218276615		
gamma-glutamyltransferase	*ggt*					-2.395410552		-1.55164
geranyltranstransferase	*ispA*					-1.093936892		
GlcNAc-PI de-N-acetylase			2.563262					
glucans biosynthesis protein C	*opgC; mdoC*							1.088962
glucarate dehydratase	*gudD*	-2.61433		-1.24798	-2.442871659	-2.005785742	-1.675264389	
glucarate dehydratase		-2.54197			-2.153823809	-1.481383449	-1.243312362	
glucarate transporter	*gudP*	-2.3014		1.139103	-1.800540053	-1.255322256		
glucitol operon activator protein	*gutM*		-1.04084					
glucohydrolase		-3.98138	-1.48517		-4.813904768			
glucose-1-phosphate thymidylyltransferase 2	*rffH*			-1.382		-1.484963768		
glucuronide uptake porin UidC	*uidC*		1.047674					
glutamate ABC transporter permease					1.206203888	1.182056801		
glutamate ABC transporter permease					1.236403263			
glutamate decarboxylase alpha	*gadA*	2.062303		-2.15394	1.409579891	-1.616993947		-1.56334
glutamate decarboxylase beta	*gadB*	2.30645		-3.28715	1.749649747	-2.860443165		-2.32593
glutamate--cysteine ligase	*gshA*	1.274822				-1.692661684		

glutamate--tRNA ligase	*gltX*					-1.214263668		
glutaminase 1	*glsA1*	2.074415		-1.834	1.69770846	-3.109992398	1.080811343	-2.21477
glutamine ABC transporter permease	*glnP*							1.272332
glutamine amidotransferase			1.282822			-2.382913019		
glutamine amidotransferase								-1.39347
glutamine synthetase	*glnA*							1.219407
glutamine--tRNA ligase	*glnS*					-1.053463536		
glutamyl-tRNA amidotransferase		1.776669						1.032959
glutathione ABC transporter permease				1.263066				
glutathione-dependent reductase		1.291179			1.071903695			
glutathione-regulated potassium-efflux system ancillary protein KefF	*kefF*					-1.154056521		
glutathione-regulated potassium-efflux system ancillary protein KefG	*kefG*					1.228491047		
glutathione-regulated potassium-efflux system protein KefC	*kefC*							-1.08731
glycerate kinase		-2.63081			-2.278301975			
glycerol-3-phosphate transporter permease	*glpT*	1.843262			2.342955678		1.235007201	
glycerophosphoryl diester phosphodiesterase	*glpQ*					1.3523036		
glycine cleavage system protein H	*gcvH*					1.100117705		
glycine--tRNA ligase subunit alpha	*glyQ*					-1.335470953		
glycogen synthase	*glgA*	1.759589			1.223112427	2.611079807	1.066388737	
glycolate oxidase iron-sulfur subunit	*glcF*	1.087464	1.323866		1.307560987	1.231130591		
glycolate oxidase subunit GlcE	*glcE*	1.373988	1.163797		1.801281332	1.660825282		
glycolate permease GlcA	*glcA*	1.710411	1.636938		2.242751762	2.22574605	1.121604711	
glycoporin						1.372531709		
glycosyl transferase				-1.1636				
glycosyl transferase family 2				-1.04157				

glycosyltransferase			1.046937					
glyoxylate carboligase	*gcl*		4.931055	3.255242	1.486417226	2.020715432	3.623064643	1.90583
GMP synthetase	*guaA*			-1.01431		-1.320587245		
GTP cyclohydrolase II	*ribA*	-1.02904			-1.207414158			
GTPase ObgE/CgtA	*obgE*			-1.30115		-1.160265437		-1.14212
GTPase-activating protein						-1.391013536		
GTP-binding protein						-1.069911482	-1.109551908	
head protein			-1.01061	-1.37779		-1.265942152		
heat-inducible protein				1.095443				
heat-shock protein Hsp15	*hslR*					-1.640454223		
heat-shock protein IbpB	*ibpB*							1.117633
helix-turn-helix transcriptional regulator	*hqeH*	1.957311	1.715264	-1.59326	1.551642582		1.222529616	-1.10969
heme ABC exporter ATP-binding protein CcmA	*ccmA*		-2.244					
heme ABC transporter ATP-binding protein				1.294371		1.095399982		
heme ABC transporter permease			-2.4106					
heme exporter protein CcmB	*ccmB*		-2.2822					
heme exporter protein D	*ccmD*		-2.52825					
hemolysin expression-modulating protein Hha	*hha*			1.051953				
high-affinity branched-chain amino acid transport ATP-binding protein	*livF*	1.078275						
histidine phosphatase family protein								1.212996
histidine transport ATP-binding protein HisP	*hisP*					1.003349021		
homoserine O-succinyltransferase	*metAS*				1.240101386			
HslU--HslV peptidase ATPase subunit	*hslU*			-1.16066		-2.090489844		
HslU--HslV peptidase proteolytic subunit	*hslV*	-1.17135				-2.18856508		
HTH-type transcriptional regulator cbl	*cbl*	1.198536				1.777132238		
hydrogenase		-1.08931		-2.26266	-1.867476883	-1.964026057		

hydrogenase 1 b-type cytochrome subunit	*hyaC*			-1.72006		-1.231905742		
hydrogenase 1 maturation protease	*hyaD*			-1.32219				
hydrogenase 2 large subunit	*hybC*			-1.67134		-1.579009334		
hydrogenase 2 small subunit	*hybO*	-1.38966			-2.107617561			
hydrogenase assembly protein HypC	*hypC*	-1.01461			-1.456426411			
hydrogenase formation protein HypD	*hypD*				-1.001217229			
hydrogenase isoenzymes nickel incorporation protein HypB	*hypB*	-1.21494			-1.683166123			
hydrogenase-1 operon protein HyaE	*hyaE*			-1.2412				
hydrogenase-1 operon protein HyaF	*hyaF*			-1.35607		-1.010380502		
hydrogenase-2 large chain			-1.12095					
hydrolase		1.816713			1.26201084	-3.069928832		-1.49237
hydroxyethylthiazole kinase	*thiM*	1.340028						
hydroxyglutarate oxidase		1.84152	1.583003		2.121406606	-1.419152255		-1.30871
hydroxylamine reductase	*hcp*	1.048176				1.07455264	1.44500107	
hydroxymethylpyrimidine/phosphomethylpyrimidine kinase	*thiD*	1.425156						
hydroxypyruvate isomerase	*hyi*	1.893045	5.482994	3.759037	2.085082273	3.720873885	4.49907396	2.476193
IlvB leader peptide	*ivbL*	-1.07917	-1.5763				-1.379438518	
IlvGMEDA operon leader peptide			-1.29563		-1.510469714			
imidazole glycerol phosphate synthase subunit HisH	*hisH*			-1.39534				
IMP dehydrogenase	*guaB*					-1.227369456		
inhibitor of glucose transporter						1.164742522		
inner membrane protein YhjD	*yhjD*					-1.917781763		
inner membrane transport permease YhhJ	*yhhJ*	1.438155					1.07112344	
inositol monophosphatase	*suhB*					-1.025098258		1.279002
iron-siderophore ABC transporter permease						-1.065671994		

isochorismate synthase EntC	*entC*					1.418858109		
isocitrate lyase	*aceA*	2.161842	1.638174		3.461174061		1.170482645	
isomerase						1.069898224		
ketodeoxygluconokinase		-1.25728						
KHG/KDPG aldolase	*eda*	-1.21502	-1.205	-1.20684				
knotted carbamoyltransferase YgeW	*ygeW*		-1.06374		-1.305628328			
L+-tartrate dehydratase subunit beta	*ttdB*	-1.258	-1.95835	-1.62162	-2.233886878		-1.066621202	
lactose permease	*lacY*					1.376150841		
L-arabinose isomerase	*araA*			1.031682		1.187055744		
L-arabinose transport system permease protein AraH	*araH*					1.468387143		
L-asparaginase 2	*ansB*		-1.08919			1.118277667		
leu operon leader peptide	*leuL*	-1.01231	-1.12579		-1.887961074		-1.047786262	
LexA-regulated protein, CopB family	*ybfE*			1.058498				1.064692
L-fucose mutarotase	*fucU*	1.1157				1.02441738		
L-fuculokinase	*fucK*	1.078496						
L-fuculose-phosphate aldolase	*fucA*					1.118791418		
L-galactonate-5-dehydrogenase	*lgoD*			1.073072		1.271221682		
ligand-gated channel protein						1.282359797		
lipid A biosynthesis palmitoleoyl acyltransferase	*lpxP*			1.223499				
lipid kinase YegS	*yegS*					-2.165688885		-1.05206
lipoprotein			-1.18405		-1.382550002	1.0615249		
L-lactate dehydrogenase	*lldD*	-1.21068					-1.241692461	
L-lactate permease				2.528416				
LPS O-antigen length regulator								1.073316
L-ribulose-5-phosphate 4-epimerase	*araD*			1.160669		1.214129005	1.108658385	
L-serine ammonia-lyase					1.029333842			
L-serine dehydratase			-1.41126		-1.064661055			

lysine decarboxylase CadA	*cadA*					-1.116363421		
lysine--tRNA ligase heat inducible	*lysS*				-1.039761021			
lysogenic protein						1.432100092		
lysozyme inhibitor			1.399339	1.657795				
LysR family transcriptional regulator		1.146253		1.154994		1.240848912		
LysR family transcriptional regulator		1.094233		1.405305		1.344589365		
lytic transglycosylase F				1.013336				
magnesium transporter ATPase	*mgtA*	1.50589		-3.26288		-2.329508518		-1.79006
major curlin subunit	*csgA*					1.148072191		
major pilus subunit operon regulatory protein	*papI*	1.115487				1.773977687	1.035428005	
malate dehydrogenase	*mdh*					1.287524343		
malate synthase A	*aceB*	1.421364	1.504013		2.344922927			
malate synthase G	*glcB*		1.026546					
malonyl CoA-ACP transacylase	*fabD*			-1.04462				
maltodextrin phosphorylase	*malP*	-1.75764	-1.6447		-2.346055504			
maltoporin	*lamB*	-1.84977	-1.85237		-1.995522823			
maltose ABC transporter substrate-binding protein MalE	*malE*	-2.71742	-2.05282		-2.989503128			
maltose operon protein MalM	*malM*	-3.65351			-3.910585532			
maltose transporter membrane protein	*malF*	-3.65994	-1.5958		-3.895893802			
maltose/maltodextrin import ATP-binding protein MalK	*malK*	-2.34439	-1.49114		-2.588821827			
maltose/maltodextrin transport system permease protein	*malG*	-2.8487	-1.70804		-3.007863584			
manganese efflux pump MntP	*mntP*			1.55864				1.369305
mannose permease IID component		-1.2462	-1.25046					
mannosyl-3-phosphoglycerate phosphatase	*yedP*				1.17642063	-1.631005238	1.270392517	
MBL fold metallo-hydrolase			1.100794			1.188051395		
MDR efflux pump AcrAB transcriptional activator MarA	*marA*					1.500353974		
membrane protein insertion efficiency factor YidD	*yidD*					-1.590634901		

metal-binding protein ZinT	*zinT*	1.408427				2.045431579	1.187961699	
methyl-accepting chemotaxis protein	*tsr*			-2.22331		-1.421798759		-2.27934
methyl-accepting chemotaxis protein II	*tar*			-4.48519		-2.395715707		-3.80001
methylglyoxal synthase	*mgsA*					1.581130436		
methylisocitrate lyase	*prpB*		-1.83938	-1.2346		-2.20777103		-2.51048
methyltransferase						-1.24702984		
MexE family multidrug efflux RND transporter periplasmic adaptor subunit						-5.743801507		
MFS transporter		-1.19122			-1.210640826			
microcompartment protein EutL	*eutL*			-1.09646				
minor capsid protein E			-1.29158	-1.03609			-1.341038577	
molecular chaperone DnaK	*dnaK*	-1.08156				-2.347897757		
molecular chaperone FimC	*fimC*		2.20865					
molecular chaperone GroEL	*groEL*					-2.027025467		
molecular chaperone HscC	*hscC*					1.071986831		
molecular chaperone Hsp31 and glyoxalase 3		1.34866						
molecular chaperone Hsp33	*hslO*					-1.939414913		
molecular chaperone HtpG	*htpG*					-1.388566311		
molecular chaperone TorD	*torD*	1.073508						
molybdopterin biosynthesis protein MoeB	*moeB*	2.105819			1.478168031			
mononuclear molybdenum enzyme YedY	*yedY*					-1.201176485		
monooxygenase						1.393186557		
motility protein B	*motB*			-3.38021	1.068528485	-2.036618344		-2.6389
multidrug ABC transporter permease/ATP-binding protein	*mdlA*				1.152629045	1.002891525		
multidrug efflux RND transporter permease subunit		1.586454		-1.60512		-4.585115772		-1.31656
multidrug efflux RND transporter permease subunit						-1.872861133		

multidrug export protein EmrA	*emrA*					-1.073751655		
multidrug resistance protein MdtE	*mdtE*	1.720385		-1.89824		-2.728744088		-1.39371
multidrug resistance protein MdtH	*mdtH*		-1.05956					
multidrug resistance protein MdtN	*mdtN*					1.873964488		
multidrug transporter subunit MdtL	*mdtL*			1.411614				
multiphosphoryl transfer protein		-1.04389	-1.20911		-1.106079174			
murein DD-endopeptidase MepS/Murein LD-carboxypeptidase	*spr; yeiV*							1.065486
murein transglycosylase	*mltA*	-1.19502	-1.21739		-1.837771345		-2.209907403	
murein transglycosylase B	*mltB*					-1.02412571		
N5-carboxyaminoimidazole ribonucleotide mutase	*purE*		1.363896	2.155122	1.337089327		1.305578705	
N-acetyl-D-glucosamine kinase	*nagK*					-1.191096066		
N-acetylgalactosamine permease IIC component 1	*agaC*	1.144704	-1.45181	-1.20715	1.400427811	1.066671478		
N-acetylgalactosamine-specific phosphotransferase enzyme IIB component 1	*agaB*	1.305456	-2.51578	-1.69656	1.60074701	1.220144309		
N-acetylglucosamine-6-phosphate deacetylase	*nagA*		-1.88499	-1.51774		1.416986245		
N-acetylmannosamine kinase	*nanK*					1.113070821		
N-acetylmannosamine-6-P epimerase							1.202138269	
N-acetylneuraminate epimerase	*nanM*			-1.12113				
N-acetyltransferase			-1.26774					
NAD(P) transhydrogenase subunit alpha	*pntA*		-1.26693	-1.40155				
NAD(P)-dependent oxidoreductase		-1.24731			-1.28162501			
NAD(P)H dehydrogenase (quinone)	*wrbA*			-1.61166		-1.332632619		-1.3569
NAD-dependent deacylase	*cobB*					-1.166391742		
NAD-dependent succinate-semialdehyde dehydrogenase	*gabD*	1.65585	1.381397	-1.21345	1.921715629	-1.760195736		-1.72651
NADH dehydrogenase	*ndh*		-1.25625	-1.00062				
NADH:flavorubredoxin oxidoreductase						1.151502144		

NADH-dependent flavin oxidoreductase						2.082674585		
NADH-quinone oxidoreductase subunit F	*nuoF*			-1.19389				
negative regulator of flagellin synthesis	*flgM*			-1.08619		-1.290015867		-1.44226
Ni/Fe-hydrogenase b-type cytochrome subunit					-1.158416567			
nickel ABC transporter, nickel/metallophore periplasmic binding protein					-1.210945538			
nitrate reductase			-2.56281	2.604453			1.293311756	
nitrate reductase A subunit beta	*narH*		2.171319			-1.782916547		
nitrate reductase catalytic subunit			-3.29377	1.248517			1.106665526	
nitrate reductase molybdenum cofactor assembly chaperone NarJ	*narJ*	1.005426	1.9279	-1.5409	1.165775294	-1.780213285		-1.71218
nitrate reductase molybdenum cofactor assembly chaperone NarJ	*narJ*					-2.757549449		
nitrate reductase subunit alpha	*narZ*		2.408206	-2.30304	1.005817494	-1.573224801		-1.70311
nitrate reductase subunit alpha	*narZ*					-2.856319514		
nitrate reductase subunit beta	*narH*			-2.34683		-2.901841624		-1.88093
nitrate/nitrite transporter NarK	*narK*	-1.53228	1.140004	1.045364	-1.37036816	-1.549252635		
nitrite extrusion protein 2	*narU*	1.051608		-2.44289	1.104326426	-3.281023732		-1.42838
nitrite reductase (cytochrome; ammonia-forming) c552 subunit	*nrfA*					1.05355534	1.035252102	
nitrite reductase large subunit	*nirB*	-1.15432		1.034864	-1.045286514		1.085822959	
nitrite reductase small subunit	*nirD*			1.134389			1.298247425	
nitrite transporter NirC	*nirC*			1.925257			1.917414204	1.342738
nitrogen regulatory protein P-II 2	*glnK*	1.446277		2.043794	1.459188481	2.672575924	1.606476419	1.09413
non-canonical purine NTP pyrophosphatase						-1.219535786		
non-heme ferritin	*ftnA*	1.30668	-1.16197			2.224089817		
NrdH-redoxin		1.638894			1.682646781		1.62925904	
N-succinylglutamate 5-semialdehyde dehydrogenase	*astD*	2.102714	1.542596	1.442752	2.044775709	1.161774224	1.119555249	

nucleoid-associated protein			2.482541	-1.07064		-1.653685137		
nucleoside permease				1.023637		1.327281891	1.623917825	
nucleoside permease						1.965854532		
nucleoside recognition pore and gate family inner membrane transporter	*yjiH*					1.661124133		
nucleoside triphosphatase	*nudI*			1.083008		1.004656813		
nucleotide exchange factor GrpE	*grpE*	-1.26098						
NUDIX hydrolase						-1.057512269		
octanoyltransferase	*lipB*		-1.03101					
oligopeptide ABC transporter substrate-binding protein OppA	*oppA*		1.005154			1.083752678		
ornithine decarboxylase	*speC/F*		-1.03564					
osmoprotectant uptake system permease					1.145863758	-1.636571895		
osmoprotectant uptake system substrate-binding protein				-1.06936		-2.769750871		-1.16128
osmotically-inducible lipoprotein B	*osmB*		2.526407	2.514519				
osmotically-inducible protein Y	*osmY*	1.688076	1.742297	-1.24166	1.512569469	-3.044958711		-1.67963
o-succinylbenzoate synthase	*menC*			-1.42715			-1.196857424	
outer membrane integrity lipoprotein						-1.034178973		
outer membrane integrity lipoprotein								-1.12233
outer membrane protein assembly factor BamB	*bamB*						-1.005831077	
outer membrane protein slp	*slp*	1.794826		-1.75972				-1.33313
outer membrane protein W	*ompW*		-1.18392					
oxidoreductase		1.0758	-1.56693	-1.39018	1.018312413			
oxidoreductase FeS-binding subunit		-1.09558			-1.304173575			
oxidoreductase FixC	*fixC*					1.06112056		
PAS domain-containing sensor histidine kinase	*phoR*	1.086235				1.101716247		
peptidase			1.223884		-1.214760946	1.210830663		

peptidase E	*pepE*	-1.47052	-1.00789		-1.61658609			
peptidase M37						-1.112179745		
peptide ABC transporter ATP-binding protein	*dppD*	2.752686	3.339171	1.530426	2.585338291		1.902923284	
peptide ABC transporter permease		2.771301	3.102961	1.937968	3.102405113		2.164611771	
peptide ABC transporter permease		2.80573	3.413521	2.761191	3.380545132		2.789842286	
peptide chain release factor 2	*prfB*					-1.008969609		
peptidoglycan hydrolase FlgJ	*flgJ*			-1.86839		-1.281698054		-1.8209
peptidoglycan-binding protein LysM	*lysM*	1.212193				-1.150404662		-1.26425
periplasmic dipeptide transporter	*dppA*	1.817551	3.502534	1.19989	1.787953476		2.09251152	
periplasmic nitrate reductase, electron transfer subunit	*napB*		-4.26939					
periplasmic protein CpxP	*cpxP*			1.338223				
periplasmic trehalase	*treA*			-1.03856		-2.677415903		
periplasmic trehalase	*treA*							-1.57981
permease		1.09385	1.722223	2.691906	2.105746044	2.196843252	2.81638144	
permease		3.166126			1.008138888			
peroxiredoxin OsmC	*osmC*	1.141894				-1.409689976		-1.01386
phage antitermination protein			-1.41915				-1.454177035	
phage encoded cell division inhibitor protein				-2.42178		1.584977656		
phage major tail tube protein					-1.016622941			
phage protein			1.037037					
phage recombination protein Bet	*bet*			-1.31088				
phage Tail Collar domain protein				1.428296				
phage tail protein						1.212611354		
phage-shock protein	*pspG*			1.121886		1.09326646		
phenylalanine--tRNA ligase subunit beta	*pheT*			-1.09626				
pheromone autoinducer 2 transporter								-1.11547
phosphate acetyltransferase	*pta*					-1.038210631		

phosphate acetyltransferase	*pta*					1.370883926		
phosphate starvation-inducible protein PsiE	*psiE*		1.116247					
phosphate starvation-inducible protein PsiF	*psiF*	1.224139						
phosphoadenosine phosphosulfate reductase	*cysH*	1.449919	3.597341	1.670915		1.868481043		
phosphoadenosine phosphosulfate reductase	*cysH*		1.3325					
phosphoanhydride phosphorylase	*appA*					-1.015018536		
phosphogluconate dehydratase	*edd*	-1.22081		-1.3335	-1.372350884	-1.004607413		-1.2474
phosphogluconate dehydrogenase (NADP(+)-dependent, decarboxylating)			-1.26884					
phosphoglycolate phosphatase	*gph*			-1.11185		-1.114957383		
phosphomethylpyrimidine synthase ThiC	*thiC*	2.658962			1.353916389			
phosphonate metabolism protein PhnP	*phnP*		1.051612					
phosphoporin protein E		1.594362			1.704085691			
phosphoribosylamine--glycine ligase	*purD*				1.157156024			
phosphoribosylaminoimidazolesuccinocarboxamide synthase	*purC*				1.349215882		1.094066791	
phosphoribosylformylglycinamidine cyclo-ligase	*purM*			1.112934	2.14080823		1.238333929	
phosphoribosylformylglycinamidine synthase	*purL*		1.117734	1.125461	1.398915693		1.221188626	
phosphoribosylglycinamide formyltransferase	*purN*			1.139568	1.104443106			
phosphoribosylglycinamide formyltransferase 2	*purT*			1.843347	2.196907365		1.728999603	
phosphotriesterase						1.242095981		
plasmid partition protein	*parA*						-1.258236521	
poly(A) polymerase	*pcnB*					-1.04158127		
polyamine ABC transporter ATP-binding protein		1.767649			1.691155213	-2.458348947	1.41340634	-1.12539
poly-beta-1,6-N-acetyl-D-glucosamine biosynthesis protein PgaD	*pgaD*					1.084102326		
Poly-beta-1,6-N-acetyl-D-glucosamine N-deacetylase	*pgaB*			-1.0074				
polysaccharide production threonine-rich protein				1.514398		1.367270386		

polysialic acid capsule synthesis protein KpsS	*kpsS*					1.385160218		
polysialic acid transport ATP-binding protein KpsT	*kpsT*	1.096318				1.161547794		
polysialic acid transporter	*kpsD*			-1.05567		-1.024628604		
polysialic acid transporter KpsM	*kpsM*	1.496602			1.163389028	1.966510022	1.356072468	
porin		1.281174				1.254394078	1.215796299	
porin						1.070898024		
primosomal protein 1	*dnaT*					-1.180608891		
primosomal replication protein N	*priB*			-1.33689		-1.524813897	-1.272629592	
PrkA family serine protein kinase		1.523657			1.150160015	-2.534518243	1.206781412	-1.54322
probable cadaverine/lysine antiporter	*cadB*			1.76682				1.506767
proline/betaine transporter	*proP*					-1.579176691		
propionate catabolism operon regulatory protein PrpR	*prpR*	1.680333	1.218814		1.796650523			
propionate/acetate kinase			-1.07613		-1.039404012	1.080578567		
protease					-1.198916883			
protease 7		1.431444		1.510351		1.294853378	1.697419786	
protease modulator HflK	*hflK*					-1.184968488		
protein AaeX	*aaeX*							1.023228
protein AfaD	*afaD*		-2.57638		-1.338895434	1.11970708		2.021172
protein BolA	*bolA*	1.238158						
protein ElaB	*elaB*					-2.42307918		-1.22945
protein GlcG	*glcG*		1.049112		1.051962552	1.048494083		
protein GnsA	*gnsA*			1.274167				
protein HypA	*hypA*	-1.02667			-2.202763432			
protein MtfA	*mtfA*					1.145887734		
protein NrdI	*nrdI*				2.067069127			
protein PhnO	*phnO*					-1.33920729		
protein phosphatase CheZ	*cheZ*	-1.22369		-3.99691		-2.614266398		-2.89054

protein SufA	*sufA*	1.167004				-1.804852172		-1.3133
protein Syd	*syd*	-1.03618				-1.013757497		
protein translocase subunit SecF	*secF*		-1.0187				-1.207155053	
protein translocase subunit SecY	*secY*			-1.1407			-1.40410035	
protein transporter HofC	*hofC*	1.036451	1.026246					
protein TsgA	*tsgA*		1.257335	1.148054				1.270565
protein TusB	*tusB*					-1.186904657		
protein UmuD	*umuD*					1.06598021		
protein-export membrane protein SecG	*secG*			1.006063				1.166305
protoheme IX farnesyltransferase	*cyoE*				1.069578098			
pseudouridine kinase	*psuK*			1.193383		1.451442634		
pseudouridine-5'-phosphate glycosidase	*psuG*					1.427061224		
PTS fructose transporter subunit EIIBC	*fruA*					1.040476913		
PTS fructose transporter subunit IIC		1.560703				1.755047435		
PTS galactitol transporter subunit IIC	*gatC*	1.540763		1.119385	1.088015824	1.847141952	1.09718785	
PTS glucose EIICB component	*ptsG*	-1.18447				-1.229689862		
PTS mannose transporter subunit EIIAB	*manX*	-1.10577	-1.11641		-1.039656313			
PTS mannose/fructose/sorbose transporter subunit IIC	*sorA*	-1.1922	-1.40269					
PTS N-acetylgalactosamine transporter subunit IIA			-2.77395	-2.21776	1.154729775	1.388000589		
PTS N-acetylgalactosamine transporter subunit IIB			-2.76798	-1.57568		1.19999167		
PTS N-acetylgalactosamine transporter subunit IIC		1.248252	-2.23891	-1.35454		1.536529368	1.037708752	
PTS N-acetylgalactosamine transporter subunit IID			-2.1401	-1.61204	1.151985262	1.349950671		
PTS N-acetylglucosamine transporter subunit IIABC						1.352720754		
PTS sorbitol transporter subunit IIA			-2.28129	-1.30809				
PTS sugar transporter subunit IIA		1.00079				1.521447255		
PTS sugar transporter subunit IIB	*glvC*					1.045812819		
PTS sugar transporter subunit IIB	*glvC*					1.221192195		

PTS system glucitol/sorbitol-specific EIIB component	*srlE*		-2.07868	-1.13222				
PTS system glucitol/sorbitol-specific EIIC component	*srlA*		-2.02715					
PTS trehalose transporter subunit IIBC	*treB*	-4.93242	-2.24455		-5.428954376		-1.015039719	
PulS_OutS family protein				1.137398				
purine-nucleoside phosphorylase				1.393126		1.923018426		
putative cation transport regulator ChaB	*chaB*					-1.646149657		
putrescine transport ATP-binding protein PotG	*potG*				1.023333358			
putrescine-ornithine antiporter	*potE*		-1.66241	-1.19387				
pyrBI operon leader peptide			-1.11102				-1.222739725	
pyridine nucleotide-disulfide oxidoreductase		1.071955		-1.22884		-1.327052095		-1.59003
pyrimidine utilization protein A				1.158778		1.248184642		
pyruvate dehydrogenase				-1.15848		-3.621986746		-1.64227
pyruvate dehydrogenase E1 component	*aceE*	-1.31552	-1.3458	-1.95774	-1.686989034	-1.368089345	-1.38919925	
racemase								-1.22815
reactive intermediate/imine deaminase			-2.22273	-1.41699	-1.432581401			
recombination protein RecR	*recR*	-1.16536				-1.617314055		
regulator of sigma D	*rsd*				1.082992114			
regulatory protein AriR	*ariR*	1.288055			1.20520338	1.237259558		
respiratory nitrate reductase subunit gamma	*narI*		1.241906			-1.918836457		
restriction endonuclease					-1.019561566			
Rha family transcriptional regulator	*rha*					1.018604304		
ribokinase	*rbsK*	1.165683		1.136679		1.206359262	1.324412867	
ribokinase	*rbsK*					1.178143107		
ribokinase RbsK	*rbsK*	1.241417				1.787017265	1.367908326	
ribonuclease HII	*rnhB*					-1.174549119		
ribonuclease P protein component	*rnpA*					-1.396474658		
ribonuclease PH	*rph*					-1.356906552		

ribonuclease T	*rnt*							1.023681
ribonucleoside hydrolase RihC	*rihC*					1.04716315		
ribonucleotide-diphosphate reductase subunit beta	*nrdB*	1.207312			1.18857136		1.259252253	
ribose ABC transporter permease	*rbsC*	1.223409						
ribosomal-protein-alanine N-acetyltransferase RimI	*rimI*					-1.299786334		
ribosome modulation factor	*rmf*		-1.60422	-1.1141		1.109433124		-1.08613
ribosome-associated inhibitor A	*raiA*					1.507080953		
ribosome-binding factor A	*rbfA*			-1.53691			-1.221477238	
RNA chaperone ProQ	*proQ*					-1.443494525		
RNA polymerase sigma factor FliA	*fliA*			-3.40407		-1.929735414		-3.14584
RNA polymerase sigma factor RpoD	*rpoD*			-1.08857		-1.171647218		
RNA-binding protein						1.270682942		
RNase II stability modulator	*yciR*			-1.10388		-2.139629733		-1.06317
RpoE-regulated lipoprotein	*yfeY*	-1.29099						
S-adenosyl-L-methionine (SAM)-dependent methyltransferase PhcB	*phcB*			1.146464				
SCP-2 sterol transfer family protein			-1.09193	-1.00647				
SDR family oxidoreductase				-1.79511				
secretion pathway protein				1.277401				
SecY/SecA suppressor protein				-1.17834		-1.975221225		-1.35109
serine endoprotease		-1.27053		-1.18272			-1.116152455	
serine hydroxymethyltransferase	*glyA*			1.083968	1.317505732			
serine/threonine dehydratase			-1.15339			1.522328363	1.145186056	
serine/threonine protein phosphatase	*pphA*		1.022703		1.052530705			
serine/threonine transporter				1.139312				
serine/threonine transporter SstT	*sstT*		2.056471	1.260339	1.026735346	1.274056578		
short-chain dehydrogenase				-1.89887				

short-chain fatty acids transporter	*atoE*					1.197922033		
sialic acid transporter	*nanT*					1.120019011		
sigma-54-dependent Fis family transcriptional regulator		1.52722		1.030652		1.042785686	1.311285249	
sigma-54-dependent Fis family transcriptional regulator						1.503121588		
sn-glycerol 3-phosphate ABC transporter permease		1.696391	1.088209		2.007354756			
sn-glycerol-3-phosphate ABC transporter substrate-binding protein		1.286202			1.474165048	-1.063357423		-1.26576
sn-glycerol-3-phosphate dehydrogenase subunit A	*glpA*	-2.77367	-1.49989	-1.01124	-1.855418535		-1.124941685	
sodium:proline symporter	*putP*				1.312446753			
sodium:solute symporter						1.116090939		
soluble cytochrome b562	*cybC*	1.033565						
sorbitol 6-phosphate dehydrogenase	*srlD*		-2.11007	-1.24914				
SoxR reducing system protein RseC	*rseC*					-1.384306919		
spermidine/putrescine ABC transporter permease	*potB*	1.422584			1.422311622	-1.261390927		
spermidine/putrescine ABC transporter substrate-binding protein	*potA*	1.149556		-1.20279	1.354995255	-3.002350209		-1.86918
spermidine/putrescine ABC transporter substrate-binding protein PotF	*potF*				1.36839352			
spermidine/putrescine-binding periplasmic protein	*potD*			-1.08759				
SpoVR family protein		1.552021				-2.49132886		-1.6394
SprT family protein	*sprT*			1.05379				
stationary phase inducible protein CsiE	*csiE*			-1.25634		-1.664742545		-1.28276
succinate dehydrogenase cytochrome b556 subunit	*sdhC*				1.264012289			
succinate dehydrogenase flavoprotein subunit	*sdhA*	1.241619			1.587673202			
succinate dehydrogenase hydrophobic membrane anchor subunit	*sdhD*				1.600173297			
succinate dehydrogenase iron-sulfur subunit	*sdhB*	1.19216			1.705804283	1.153837927		
succinate-semialdehyde dehydrogenase	*gabD*					1.081105388		

succinylarginine dihydrolase	*astB*	1.76255	1.55444	1.173933	2.124027725	1.044097995		
succinyl-CoA ligase subunit alpha	*sucD*	1.049996	1.333022	1.12211	1.303270696			
succinyl-CoA ligase subunit beta	*sucC*		1.142977		1.341142867			
succinyl-CoA--3-ketoacid-CoA transferase							1.634668879	
succinylglutamate desuccinylase	*astE*	1.875302	1.136489	1.086593	2.200411475	1.128240147		
sucrose porin	*scrY*		-1.17137					1.113427
sugar ABC transporter		1.005131				4.021609596	1.240311984	
sugar ABC transporter						1.468575294		
sugar ABC transporter ATP-binding protein		1.810212		-2.01984	1.296119177		1.038866003	
sugar ABC transporter permease		1.468875			1.340025819	2.72349871		
sugar ABC transporter permease		1.464831			1.342687446			
sugar ABC transporter substrate-binding protein						1.290030748		
sugar fermentation stimulation protein SfsA	*sfsA*					1.132352518		
sugar kinase				-1.12567		2.22564744		
sugar phosphatase SupH	*supH*			-1.13073				
sulfatase		1.436516				1.885457585	1.130344923	
sulfate ABC transporter permease	*cysW*	1.575508	1.434139	1.013468	1.010861954	2.255189892	1.037395993	
sulfate ABC transporter substrate-binding protein	*cysP*	-1.24083			-1.1499416	-1.565417532		
sulfate adenylyltransferase	*cysN*	1.646004	1.416276	1.196107		2.212346795	1.406671551	
sulfate adenylyltransferase subunit 2	*cysD*	2.061822	1.423871			2.447675979		-1.06805
sulfate transporter subunit				1.350803		2.354229735	1.116350239	
sulfate/thiosulfate import ATP-binding protein CysA	*cysA*	1.94393	2.016911	1.486323	1.380738952	2.540173541	1.298600392	
sulfate/thiosulfate transporter subunit		1.581931	1.240398		1.044046491	2.489202019	1.031759974	
sulfite reductase subunit alpha	*cysJ*	1.113527	1.460377			1.44540612		
sulfite reductase subunit beta	*cysI*	1.35802	1.750679			1.713668188	1.019341732	
superoxide dismutase	*sodA/B*					1.366447244		
symporter YdjN	*ydjN*					1.339002184		

tagatose-1,6-bisphosphate aldolase	*kbaY; agaY*	1.225515	-2.36568	-1.81058	1.233612272			
tagatose-bisphosphate aldolase			-2.17514	-1.55282				
tail fiber assembly protein		1.059036						
tartrate dehydratase subunit alpha	*ttdA*	-1.09246	-1.64391	-1.20276	-2.27500166			
taurine ABC transporter substrate-binding protein	*tauA*					1.311560616		
taurine dioxygenase	*tauD*					1.029793969		
TDP-4-oxo-6-deoxy-D-glucose aminotransferase						-1.155776826		
TDP-fucosamine acetyltransferase	*wecD*					-1.154585877		
terminase				-1.4742				
thiamine biosynthesis lipoprotein ApbE	*apbE*					-1.277418744		
thiamine biosynthesis protein ThiH	*thiH*	2.517461			1.803326034			
thiamine biosynthesis protein ThiS	*thiS*	2.123782			1.353771869			
thiamine phosphate synthase	*thiE*	1.822024			1.234644112			
thiamine transporter substrate binding subunit	*tbpA*	1.032237						
thiamine-monophosphate kinase	*thiL*					-1.082308196		
thiazole synthase	*thiG*	2.157706			1.436401473			
thiol:disulfide interchange protein		-1.21559	-2.68829	-1.36587				
thiosulfate reductase cytochrome B	*ydhU*					1.545303622		
thiosulfate sulfurtransferase PspE	*pspE*					1.126928275		
thiosulfate transporter subunit		2.122218	1.115237			2.524452331		
threonine/serine transporter TdcC	*tdcC*		-1.73728			1.167515658		
thymidine phosphorylase	*deoA*						1.143402383	
thymidylate kinase	*tmk*					-1.039181099		
toxin B								-1.37667
toxin YhaV	*yhaV*				-1.111996589			
trans-aconitate 2-methyltransferase	*tam*	1.257216				-2.449996195	1.007995726	-1.22777
transaldolase A	*talA*	1.015437				-1.463223301		-1.12286

transcriptional activator TtdR	*ttdR*		-1.63853		-1.481315885			
transcriptional activatory protein CaiF	*caiF*		-1.0887		-1.608327234	1.299025615		
transcriptional regulator				1.442941			1.327073377	-1.02569
transcriptional regulator							2.505910105	-1.21307
transcriptional regulator								-1.52499
transcriptional regulator GadE	*gadE*	2.03063		-2.21011		-1.970638408	1.186404037	-1.2399
transcriptional regulatory protein RcsA	*rcsA*		1.88301	1.14251				
transferase			1.436867					
transketolase				-2.92578		-1.357423802		-1.29002
transketolase				-2.5855		-1.396903992		-1.02589
transketolase				-1.16743		-1.514085749		-1.42455
translation initiation factor IF-2	*infB*			-1.85332			-1.392507584	-1.20562
translation initiation factor Sui1	*sui1*				-1.006639983			
transpeptidase				1.096626		-1.22227393		
transporter					1.297115721	1.245747431		-1.03291
trehalose-phosphatase			1.20642			-2.723223004		-1.56329
tRNA (cytosine(34)-2'-O)-methyltransferase TrmL	*trmL*					-1.251788627		
tRNA (guanine-N(1)-)-methyltransferase	*trmD*						-1.049077397	
tRNA methyltransferase						-1.199916424		
tRNA pseudouridine synthase TruC	*truC*					-1.183873782		
tRNA pseudouridine(55) synthase TruB	*truB*			-1.26451			-1.127574733	
tRNA threonylcarbamoyladenosine biosynthesis protein TsaB	*tsaB*					-1.123028424		
tRNA(5-methylaminomethyl-2-thiouridine)-methyltransferase	*mnmA*					-1.307125876		
tRNA-dihydrouridine synthase A	*dusA*					-1.107138313		
tryptophan permease		1.235346		1.710155		2.432953266	1.592353488	1.429317

tryptophanase leader peptide	*tnaL*					1.266236825		
two-component sensor histidine kinase		1.069499				1.34145907		
two-component system response regulator				-3.10894		-2.215299104		-2.91895
two-component system sensor histidine kinase EvgS	*evgS*					1.511039324		
type I glyceraldehyde-3-phosphate dehydrogenase		1.812072			1.027235574	-1.573207257	1.135309891	-1.06349
type II secretion system protein GspC	*gspC*		1.459332			1.341070361		
type II secretion system protein GspH	*gspH*					-1.105624339		
U32 family peptidase		-1.18468			-1.018926049			
UDP-N-acetylglucosamine 1-carboxyvinyltransferase	*murA*					-1.103828495		
undecaprenyl-phosphate 4-deoxy-4-formamido-L-arabinose transferase	*arnC*			-1.01791				
universal stress protein A	*uspA*					1.510536466		
universal stress protein B	*uspB*							-1.13852
universal stress protein C	*uspC*		-1.14602			1.084658836		
universal stress protein D	*uspD*			-1.03338				
universal stress protein F	*uspF*					1.343585569		
universal stress protein G	*uspG*					1.079043682		
uracil phosphoribosyltransferase	*upp*					-1.311194658		
uracil/xanthine transporter	*ybbY*	-1.54153	-1.44752	-1.62589	-1.533717503	-1.300243417	-1.812818122	
uronate isomerase	*uxaC*						1.147731464	
xanthine permease XanP	*xanP*	1.586574	1.994395	3.575241	3.127456164	1.838939164	2.432877787	1.58842
xylose ABC transporter substrate-binding protein	*xylF*	1.088153				1.827009653		
xylose isomerase	*xylA*					1.057099522		
xylulokinase	*xylB*			1.163497		1.128319359		
YggU family protein						-1.087659942		
YggW family oxidoreductase						-1.076099647		
zinc resistance-associated protein	*zraP*					1.038744457		

zinc-binding dehydrogenase				-1.01453		-1.861249039		-1.53388
zinc-dependent alcohol dehydrogenase	*adhP; adhA*		1.213187	-1.63077		-2.88922666		-1.52167
Zn-dependent oxidoreductase	*rspB*							-1.38513

Table 9.2 Significantly differentiated genes identified from RNA sequencing of seven exposed isolates of EC958 compared with control isolate. Genes discussed in Chapter 5 are highlighted in **bold**.